

MILAN STATE UNIVERSITY  
DOCTORATE SCHOOL IN CHEMICAL SCIENCE AND TECHNOLOGIES

DEPARTMENT OF CHEMISTRY  
CHEMICAL SCIENCE XXVI CYCLE  
CHIM/03

SYNTHESIS, CHARACTERIZATION AND CATALYTIC  
ACTIVITY OF  
IRON, RUTHENIUM AND COBALT PORPHYRIN COMPLEXES

DOCTORATE THESIS OF:  
Daniela Intrieri  
Matr. R09026

TUTOR: Prof.ssa Emma Gallo

CO-TUTOR: Dott. Alessandro Caselli

CO-ORDINATOR: Prof.ssa Emanuela Licandro

ACADEMIC YEAR 2012/2013

# Index

1. Introduction .....	3
1.1. The Porphyrin Ring .....	4
1.1.1. Chemical Characteristics of the Porphyrin Ligands .....	4
1.1.2. Synthesis of Porphyrin Ligands .....	5
1.2. Porphyrin Complexes .....	7
1.2.1. Synthesis of Metal Porphyrin Complexes .....	7
1.3. Porphyrins with Enhanced Bio-Mimetic and Catalytic Features .....	11
1.4. Asymmetric Porphyrins and Porphyrin Complexes .....	15
1.3.2. Bis-Strapped Porphyrins .....	20
1.5. Metallo Porphyrin-Catalysed Amination Reactions .....	23
1.5.1. ArI=NR as nitrene sources .....	24
1.5.2. Chloramine-T and bromamine-T as nitrene sources .....	31
1.5.4. Organic azides as nitrene sources .....	33
1.6. The Metallo Porphyrin-Catalysed Cyclopropanation Reactions .....	39
1.6.1 Rhodium-catalysed reactions .....	40
1.6.2. Cobalt-Catalysed Reactions .....	47
1.6.3. Iridium-Catalysed Reactions .....	55
1.6.4. Iron Porphyrin Complexes .....	56
2. Results and Discussion .....	57
2.1. Intermolecular Benzylic Amination .....	58
2.1.1. Kinetic Study of the Ruthenium-Catalyzed Benzylic Amination .....	63
2.2. Intramolecular Benzylic Amination .....	66
2.3. Allylic Amination .....	72
2.3.1. Kinetics Study of the Allylic Amination .....	82
2.4. Cyclopropanation Reactions .....	88
3. Experimental Section .....	95
3.1. General .....	96
3.2. Synthesis of Ruthenium Source .....	97
3.3. Synthesis of chiral binaphthyl derivatives .....	98
3.4. Synthesis of Porphyrins Ligands .....	99
3.5. Synthesis of Metal-Porphyrin Complexes .....	105
3.6. Synthesis of Aryl Azides .....	117
3.7. Synthesis of 2-Amino Biaryls .....	121
3.8. Synthesis of 2-Azido Biaryls .....	127
3.9. Intermolecular Benzylic Amination .....	134

3.9.1. General procedure for catalytic reactions .....	134
3.9.19. General procedure for kinetic measurements .....	144
3.10. Intramolecular Benzylic Amination.....	146
3.11. Allylic Amination.....	152
3.11.1. General procedure for catalytic reactions .....	152
3.11.2. General procedure for kinetic measurements.....	166
3.12. Cyclopropanation Reactions .....	169
3.12.1. Catalytic procedures .....	169
3.12.2. Recycle of Catalyst 119Fe. ....	169

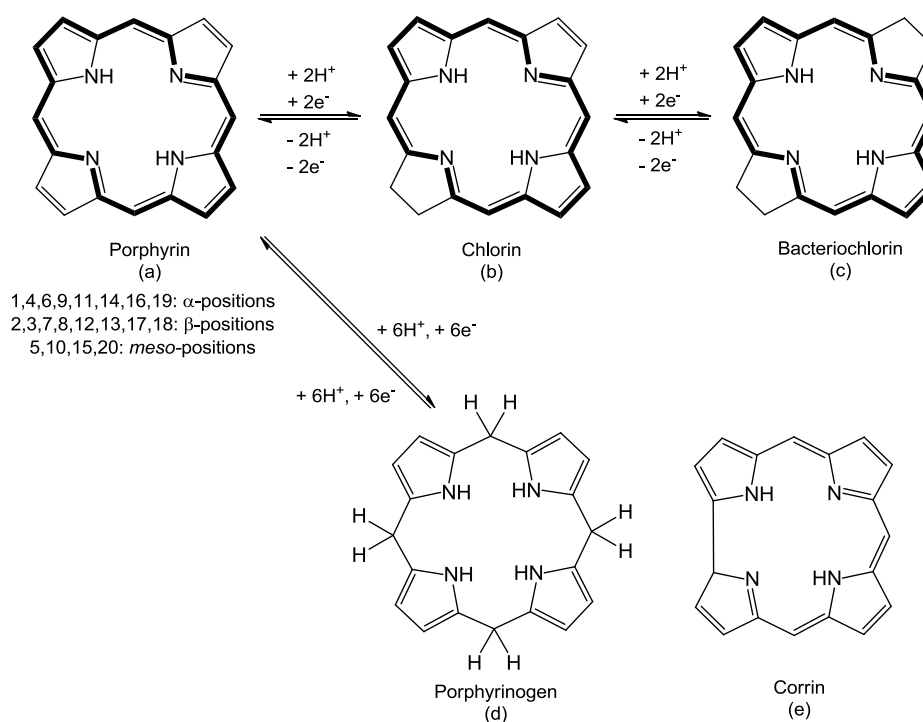
# 1. Introduction

## 1.1. The Porphyrin Ring

### 1.1.1. Chemical Characteristics of the Porphyrin Ligands

The porphyrin ligand is an aromatic macrocycle constituted of four pyrrolic rings joined at the 2 and 5 positions by methane groups, thus having 11 conjugate double bonds and fulfilling the Hückel  $4n+2$  rule. The parent macrocycle, once formally known as porphine but now, according to the IUPAC nomenclature,<sup>1</sup> simply called porphyrin, is depicted in Scheme 1.1 (figure a), together with other related tetrapyrrolic macrocycles. The classification of the porphyrin carbon atoms as  $\alpha$ ,  $\beta$  and *meso* carbons are also illustrated in scheme 1.1 (figure a). In its neutral form, two of the pyrrolic nitrogen atoms are protonated, and the porphyrin is called “free-base porphyrin” or simply “free-base” (this last terminology will be extensively employed in the following).

Porphyrin ligands are fundamental molecules for all organisms as well as their related reduced-aromatic forms chlorins (Scheme 1.1, figure b) and bacteriochlorins (Scheme 1.1, figure c),<sup>2,3</sup> their acyclic congeners phytocyanins and other tetrapyrrolic macrocycles. For example, vitamin B<sub>12</sub>, a cobalt complex based on a corrin macrocycle (Scheme 1.1, figure e),<sup>4</sup> serves as a cofactor for a wide variety of biochemical processes. These highly colored ligands, due to their fundamental biological importance, have been named “the pigments of life”.<sup>5</sup>



**Scheme 1.1.** Tetrapyrrolic macrocycles

In Scheme 1.1 (figure d) is reported the reduced-not aromatic tetrapyrrolic derivative called “porphyrinogen” which represents the synthetic precursor of the porphyrin ligand.

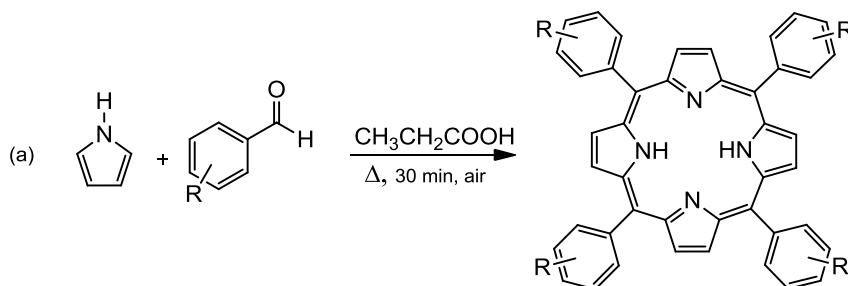
### 1.1.2. Synthesis of Porphyrin Ligands

Considering that the isolation of porphyrins from natural sources in pure and significant amounts<sup>6,7</sup> often required time-consuming synthesis or extensive purifications, many efforts have been concentrated over the years on modeling these ligands by constructing synthetic analogues.

In 1926 Hans Fisher and Bruno Walach reported the first synthesis of a porphyrin.<sup>8</sup> In the following decades studies concerning their preparations and characterization started to play a prominent role both in biochemistry and chemistry.<sup>9-11</sup> Up to now, more than sixty thousand papers and books regarding synthesis and uses of porphyrins have been published.<sup>12</sup>

After the preliminary work of Fisher and Walach, in the years between 1930 and 1950 different and continuously improved routes for the preparation of *meso*-tetraphenyl and *meso*-substituted porphyrins have been reported, in particular due to the work of Rothermund.<sup>13-19</sup> In subsequent years, various porphyrins were also structurally characterized, affording a deep comprehension of their chemistry and physical properties.<sup>20-24</sup>

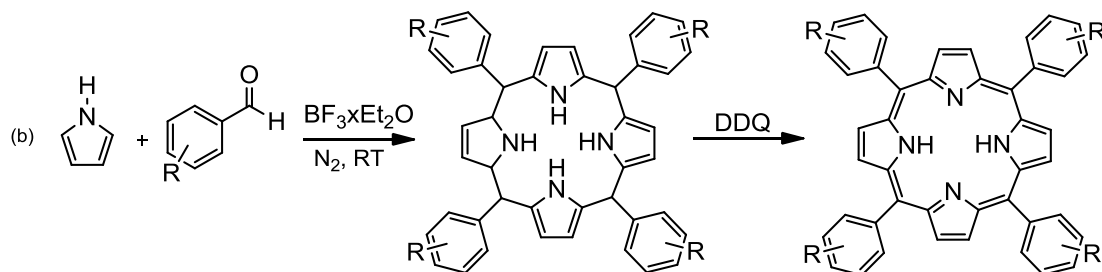
Alder and Longo improved the existing methodologies by reacting pyrrole with a variety of benzaldehydes in refluxing propionic acid (bp > 140°C) for 30 minutes in air (Scheme 1.2).<sup>25-27</sup>



**Scheme 1.2.** The one pot open air synthesis for *meso*-substituted tetraphenylporphyrin

This reaction has allowed (and allows) a wide selection of substituted benzaldehydes to be converted into the corresponding porphyrins in yields up to 20%. Although the reported procedure does not represent the conditions for the preparation of a porphyrin with the highest yield, it constitutes the most convenient method for rapidly obtain large amounts of crystalline and relatively high pure material. In fact, this process has been reported to be efficient for 70 different aldehydes in multi-gram quantities. Adler's methodology is though beset with certain problems. First of all, the harsh reaction conditions do not allow the synthesis of porphyrin bearing sensitive functional group. In this optic, minor modifications of this synthesis have been reported regarding the reaction media: acetic acid (bp 115 °C) and mixture of acetic acid and nitrobenzene have in fact also been widely employed. Moreover, the high level of the produced tar causes purification problems and provides a rather poor batch-to-batch reproducibility.<sup>28, 29</sup> In recent years it has been shown that condensations of pyrrole with substituted benzaldehydes may be performed following the Alder route under microwave irradiation.<sup>30-33</sup> Although, in many cases the presence of large amounts of side-products renders very difficult the isolation of the desired porphyrin. In the eighties Lindsey and co-workers reported a two steps milder variant of this one-pot porphyrin synthesis in which a pyrrole and an aromatic aldehyde

react at room temperature in dichloromethane under anaerobic conditions in the presence of catalytic amounts of  $\text{BF}_3 \cdot \text{Et}_2\text{O}$ . The so-obtained porphyrinogen intermediate can be directly aromatized by refluxing the reaction mixture in the presence of a quinone as the oxidant (2,3-dichloro-5,6-dicyano-1,4-benzoquinone or 2,3,5,6-tetrachloro-1,4-benzoquinone, see Scheme 1.3)<sup>34</sup>.



**Scheme 1.3.** Synthetic method reported by Lindsey in 1987

In the paper where this preparation was reported for the first time,<sup>35</sup> almost 20 different aldehydes have been used, affording yields up to 55%. This mild, relatively low temperature, two-step one-pot procedure, that is henceforth referred as the Lindsey synthesis, has recently been deep revisited and reviewed.<sup>36-42</sup>

By tuning the reaction conditions depending on the characteristic of the pyrrole and aromatic aldehyde employed,<sup>43</sup> Adler and/or Lindsey methods open the route to the preparation of porphyrin macrocycles with a large variety of substituents on the  $\beta$ -pyrrolic and/or *meso*-positions. This synthetic flexibility of the reported methodology permits the preparation of a large number of porphyrin complexes with a plethora of possible structural and electronic properties. In fact, different substituted tetrapyrrolic systems and/or improved preparation of already reported ligands have been published during the years<sup>44-63</sup> either by using Adler's or Lindsey's approach or by changing the nature of the macrocycle after its synthesis,

## 1.2. Porphyrin Complexes.

Porphyrins occupy a prominent role both in chemistry and biology. They indeed are present as ligands in many molecules active in different fundamental biological processes. Furthermore, due to their rigid and highly stable macrocyclic structure, porphyrins constitute a unique class of ligands, able to provide to a coordinated metal distinctive chemical characteristics. Due to the importance of metal-porphyrin species and the interest in both bio-mimetic studies and chemical applications, chemists have always been interested in their study. Nowadays, much is known about their synthesis, characteristic and applicability in different fields.

### 1.2.1. Synthesis of Metal Porphyrin Complexes

When the two internal protons of the free-base porphyrin are removed, the porphyrin becomes a tetradentate chelating dianion capable to coordinate a metal ion in the central cavity. The four pyrrolic nitrogen atoms define an equatorial plane with four fold symmetry (Figure 1.1). So far, porphyrin ligands have been reported to form complexes with all the transition metals, all the lanthanides, several of actinides and some of the main group metals.<sup>64</sup> Metal fragments bonded to porphyrin species can exist in a large range of oxidation states (-2 to 6), d electron configurations ( $d^0$  to  $d^{10}$ ), spin states ( $S=0$  to  $S=5/2$ ) and coordination numbers (from 4, if the porphyrin is the only ligand, to 8). Thus, porphyrins offer a great versatility and a very wide applicability as ligands. Due to this great diversity, a great control over the coordination environment of the central metal can be achieved. In general, the metal coordinated to porphyrin ligands are constrained to have two mutually *trans*-coordination sites (figure 1.1).

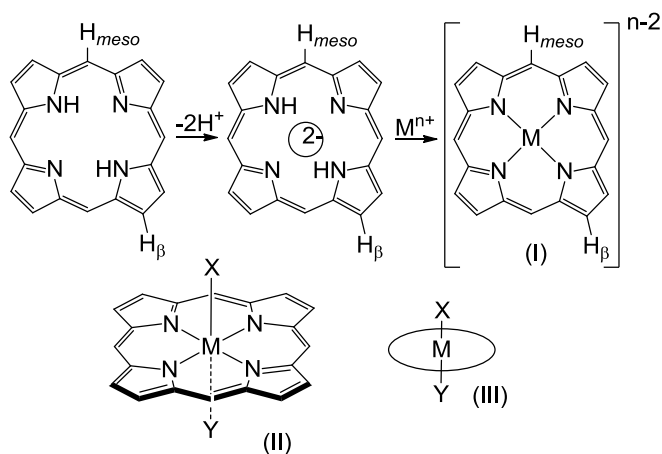


**Figure 1.1.** A schematic illustration of a metallo porphyrin complex which presents a tetracoordinated metal in the tetrapyrrolic core (I) and a metal with two axial ligands in *trans*-coordination one each other (II and, in a simplified representation, III)

Steric and electronic factors can be tailored by adjusting the peripheral substitution of the porphyrin but rearrangements or stereoisomerism of the meridional or facial type are not possible. The rich inorganic, organic and organometallic chemistry of metallo-porphyrin species and the opportunity to synthesize

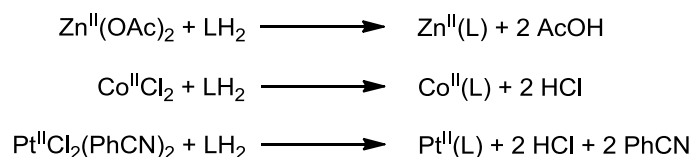


complexes with virtually all the metals (and not only), can allow the design of a virtually unlimited class of different compounds. Porphyrin complexes have led to a large number of important discoveries and continue to be an extremely active area of chemical research.

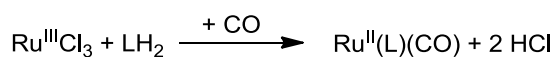
Different routes have been employed for the insertion of a metal or a M-L<sub>n</sub> fragment into a porphyrin ring, mostly depending on the nature of the metal source, while for the same metal the experimental conditions are generally exploitable on different free bases. In Scheme 1.4 some examples of metal insertions are reported. Depending on the previous oxidation state of the metal, the reaction may involve coordination, reduction or oxidation of the metal center. In the last case the oxidation of the metal may be achieved spontaneously thanks to the reaction conditions. In some cases an external oxidant has to be furnished for the reaction reaches completion.

**A) Coordination of a metal from a MX<sub>2</sub> salt** (Scheme 1.4, entry A). For this reaction the main problem lies on the difficulty of getting both the free-base and the metallic reagent simultaneously into the same solution under reactive conditions. This is due to the fact that good solvents for porphyrins in their neutral forms are generally poor solvents for simple metallic ions and vice versa. Adler and co-workers have investigated a number of solvents as possible reaction media which would give reasonable solubility for both the porphyrin and metal ion under the reaction conditions.<sup>65</sup> Among a lot of solvents tested, *N,N*-dimethylformamide (DMF) proved to be an useful reaction medium, offering a number of advantages for synthetic purposes for both a large variety of porphyrins and metals. The synthetic procedure simply consists of allowing the free-base and a divalent metal salt to react in refluxing DMF. The desired M(porphyrin) complex is obtained in short reaction times with good to excellent yields for a number of metals (Zn, Co, Cu, Ni, Fe, Cr, Mn, Pb, Pd, Hg, Cd etc.). The addition of a weak Brønsted base promotes the reaction rate removing the two pyrrolic protons of the free base.

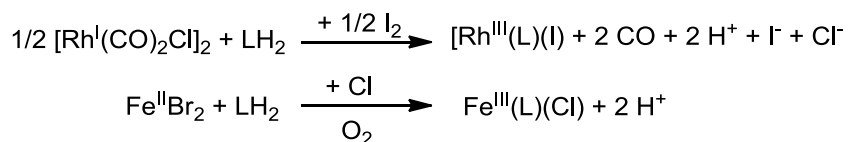
**A) Coordination of a metal:**



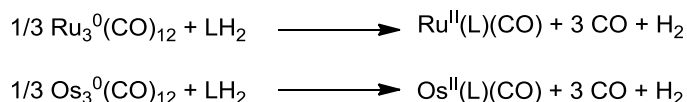
**B) Reduction of the metal center:**



**C) Oxidation by an external oxidant:**



#### D) Spontaneous oxidation:

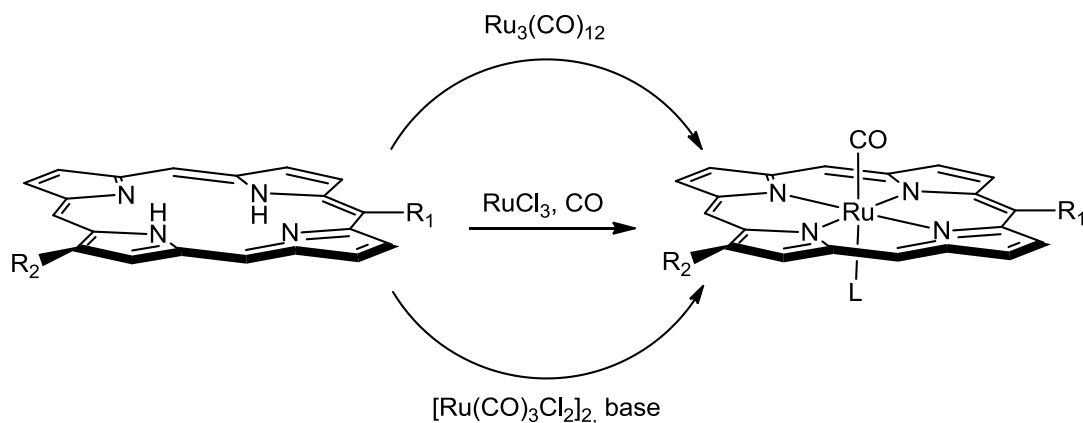


**Scheme 1.4.** Reaction conditions for the insertion of a metal center into a porphyrin ring.

**B) Reduction of a metal salt** (Scheme 1.4, entry B). In 1984 Collman and James independently reported an insertion of a Ru-CO moiety starting from  $\text{RuCl}_3$  under a carbon monoxide atmosphere in 2-(2-methoxyethoxy)ethanol as the reaction solvent.<sup>66, 67</sup> In this case, carbon monoxide itself acts both as the reductant and the ligand to complete the coordination sphere of the metal in the produced metallo porphyrin. A complete and satisfactory stoichiometry for this reaction has not been reported, partially due to the fact that competing side reactions may take place during the reaction. Nonetheless, this methodology for the insertion of ruthenium in a free base porphyrin seems not to be different from just an “in situ” formation of  $\text{Ru}_3(\text{CO})_{12}$  followed by a reaction between this cluster and the ligand (see entry D).

**C) Oxidation with an external oxidant** (Scheme 1.4, entry C). In other cases, an oxidant has to be added to the reaction mixture to promote the variation of the oxidation state of the metal center in order to have an isolable and stable product. In the case of iron, the intermediate  $\text{Fe}(\text{II})(\text{P})$  initially formed is oxidized to  $\text{Fe}(\text{III})$  during the work-up runs in air and in the presence of donor ligand (for example  $\text{Cl}^-$  from an aqueous  $\text{HCl}/\text{NaCl}$  mixture). For other metals stronger oxidants are necessary to promote the formation of the product: i.e., the insertion of rhodium as  $\text{Rh}(\text{III})$  in a porphyrin, starting from a carbonylic complex of  $\text{Rh}(\text{I})$  ( $[\text{Rh}(\text{CO})_2\text{Cl}]_2$ ), is accomplished in the presence of molecular iodine as the oxidant.

**D) Spontaneous oxidant of the metal starting from  $M(0)$  cluster** (Scheme 1.4, entry D). The more extensively reported way for the preparation of ruthenium-CO<sup>68, 69</sup> and osmium-CO porphyrin<sup>70</sup> complexes involves the reaction between the free-base and the neutral cluster  $\text{M}_3(\text{CO})_{12}$  in a high boiling point solvent, such as for example decahydronaphthalene (for Ru) and diethylen glycol monomethyl ether (for Os). In these cases the oxidation of the two protons displaced from the free-base into molecular hydrogen. Differently from what stated above in the case of reactions between  $\text{MX}_2$  inorganic salts and free-base porphyrins, for this synthetic procedure the complete solubility of the two reactants in the reaction media is not a determining and fundamental factor for the success of the insertion of the metal into the porphyrin core. Nevertheless, a number of different solvents have been used, depending on the stability of the free-base at high temperature and on its conformation in solution.<sup>67, 71-73</sup>



**Scheme 1.5.**

Whichever are the source of ruthenium employed, the nature of the porphyrin ligand (for simplicity in Scheme 1.5 are reported only one *meso*- and  $\beta$ - substituents) and the conditions used for the reaction, the direct insertion of ruthenium in a free-base porphyrin usually brings to the formation of ruthenium(II) CO porphyrin species. The same compound has been reported to result also from the reaction of  $\text{TPPH}_2$  with  $[\text{Ru}^{\text{II}}(\text{CO})_3\text{Cl}_2]_2$  in the presence of a base.<sup>74</sup>

The sixth axial ligand, when it was not unambiguously detected by X-ray diffraction or spectroscopic analyses, has been simply supposed to be the more coordinating ligand used in the course of the reaction's work-up due to the strong tendency of ruthenium to reversibly binds a sixth ligand to complete its coordination sphere.

### 1.3. Porphyrins with Enhanced Bio-Mimetic and Catalytic Features

The most abundant natural occurring metalloporphyrin is the complex iron protoporphyrin IX (Figure 1.2), known as heme. This iron complex is peripherally substituted by eight alkyl and alkenyl residue, as occurs for most natural occurring species. Heme is the prosthetic group for a large number of biological active proteins (that are indeed named heme proteins or hemoproteins) which at first sight appear to have diverse and unrelated functions. Among of the most interesting and the most widely studied heme proteins a prominent role is occupied by cytochromes P-450,<sup>75-92</sup> so called for the strong UV-vis absorption that they exhibit at 450 nm when they are reversibly inhibited by the coordination of CO to the metal centre. These compounds are responsible of the oxidation of unactivated carbon-hydrogen bonds in living systems.

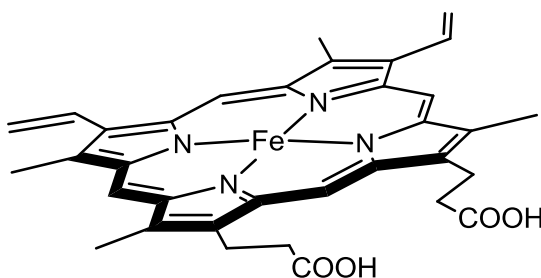
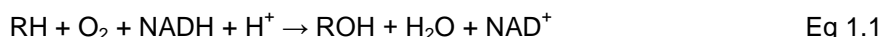


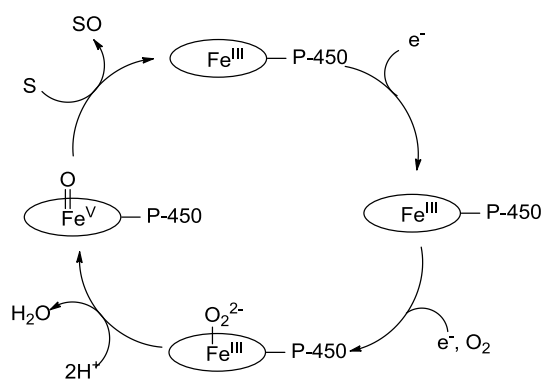
Figure 1.2. Heme

P-450 containing enzymes are able to activate molecular  $O_2$  and incorporate an oxygen atom into organic substrates with the simultaneous reduction of the other oxygen of  $O_2$  into water (equation 1.1). A unique feature of these enzymes is to cleave heterolytically O-O bonds of iron (III) hydroperoxide porphyrin, forming high valent iron-oxo intermediates, putatively  $[Fe^V(P)O]$  or  $[Fe^{IV}(P^{\cdot})O]^+$ .<sup>71-73</sup> It should be noted that recent studies have suggested the possibility of an existing competition between heterolytic and homolytic cleavage of the O-O bond depending on the nature of the terminal oxidant used ( $H_2O_2$ , ROOH, peracids etc.).<sup>93-96</sup>



The mechanism of the oxygen activation and transfer by cytochrome P-450 has been widely investigated. Although several aspects of the catalytic cycle are still controversial, the process represented in the outer cycle of Scheme 1.6 is supported by experimental data recorded with several substrates. The exact nature of the species responsible for the oxygen insertion is still a matter of debate, but an oxo-iron species such as  $[Fe^V(P)O]$  is mostly accepted. Recently, Meunier published a review dealing with the mechanistic aspects of this cycle.<sup>91</sup>

Considering that exogenous oxygen donors (ROOH,  $IO^4$ , PhIO) are the effective oxygen donors for this mechanism, this transformation has been adopted for biomimetic investigations.



**Scheme 1.6.** Main accepted feature of cytochrome P-450 catalytic cycle (external cycle) and peroxide shunt pathway (inner cycle).

Studies concerning the mechanism of heme proteins and related biological active systems suggest that both the intrinsic reactivity and lability of the cited high-valent iron-oxo complex are related to the presence of the protein chains around the active site. Since the chemistry (the breaking and making of bonds) take place at the metal centre of the porphyrinic prosthetic group, chemists and biomimetic chemists have studied metalloporphyrins models that present superstructure similar to the biological one.

Inspired by the extraordinary catalytic capabilities of heme-containing enzymes in nature, metalloporphyrins have been recognized as an important class of synthetic catalysts for oxo and related atom/group transfer reactions on account of their unique ligand environment and metal coordination mode. The fact that cytochrome P-450 enzymes in biological systems bear iron porphyrin active sites makes iron porphyrin unique candidate for model compounds of these enzymes. Numerous efforts have been directed to oxo-iron porphyrins and their oxygen atom transfer reactions with alkenes or alkanes to afford epoxidation or C-H insertion (i.e. hydroxylation) products,<sup>75, 97-99</sup> mainly to mimic the corresponding hydrocarbon oxidation reactivity of the putative oxo-iron species of cytochrome P-450 enzymes.

Among these artificial counterparts, simple ligands as  $\beta$ -octaethylporphyrin (OEPH<sub>2</sub>) and *meso*-tetraphenylporphyrin (TPPH<sub>2</sub>) were firstly employed as models of the biological systems (Figure 1.3-I and – II).

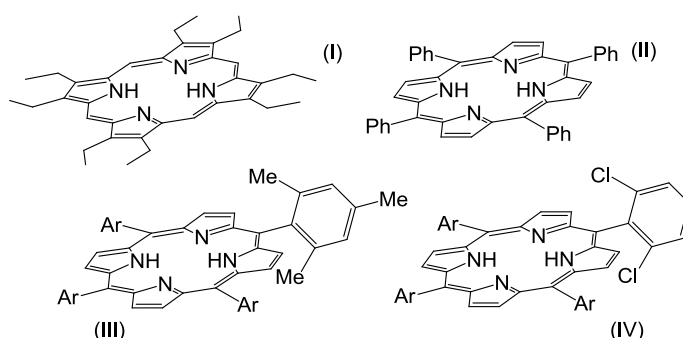
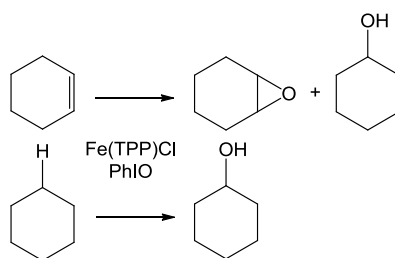


**Figure 1.3.** Schematic representation of  $\beta$ - or 2,3,7,8,12,13,17,18-octaethylporphyrin (OEPH<sub>2</sub>, I), *meso*- or 5,10,15,20-tetraphenylporphyrin (TPPH<sub>2</sub>, II), *meso*- or 5,10,15,20-tetramesitylporphyrin (TMPH<sub>2</sub>, III) and

*meso*- or 5,10,15,20-tetra(2,6-dichlorophenyl)porphyrin (2,6-Cl<sub>2</sub>TPPH<sub>2</sub>, IV), among the first systems studied in metalloporphyrins applications.

While the OEPH<sub>2</sub> structure is closely related to the macrocycle of protoporphyrin, the structure of (TPPH<sub>2</sub>) is less similar but this porphyrin was extensively employed with the scope of having a more rigid backbone in order to sterically protect the tetrapyrrolic planar ring. By using one of these simple systems, Fe<sup>III</sup>(TPP)Cl, Groves *et al.* first reported in 1979 its use as catalyst for olefins epoxidation and alkanes hydroxylation by using PhIO as the oxygen donor (Scheme 1.7)<sup>100</sup>.



**Scheme 1.7.** First oxidation reported by using a synthetic metalloporphyrin complex as catalyst.

In their studies it was shown that cyclohexene was converted into the corresponding epoxide and cyclohexane to cyclohexanol in 55% and 8% yield, respectively.<sup>101, 102</sup> However, the catalytic activity of these first-generation catalysts rapidly decreased because of the extensive destruction of the active form of the metalloporphyrin. These data were in accord to studies of Collman and co-workers in which they showed that synthetic iron-porphyrins, which are not sterically protected on both faces, easily afford inert  $\mu$ -oxo dimers.<sup>103</sup>

While *meso*-tetraarylporphyrins are electronically similar to their  $\beta$ -octaalkyl counterparts, they are sterically quite different, being the four aryl groups essentially orthogonal to the plane of the 22 $\pi$ -aromatic porphyrin macrocycle. This structural feature can be used as a backbone to sterically protect the faces of the porphyrin. For example, simple *ortho*-substitution of the *meso*-aromatic rings bring sterically protected and more robust systems. *Meso*-tetramesitylporphyrin (TMPH<sub>2</sub>) and *meso*-tetra(2',6'-dichloro)phenylporphyrin (2,6-Cl<sub>2</sub>TPPH<sub>2</sub>) (Figure 1.3-III and IV respectively) were developed with the purpose to improve the stability of both the porphyrin itself and its metal complex.

In fact, the so named "second-generation catalyst" such as iron(III) *meso*-tetramesitylporphyrin chloride (Fe<sup>III</sup>(TMP)Cl) and iron(III) *meso*-(2,6-dichlorophenyl)porphyrin chloride (Fe<sup>III</sup>(2,6-Cl<sub>2</sub>TPP)Cl) were found to be unusually robust (for example, 10<sup>4</sup> TON for the epoxidation of norbornene in the case of Fe<sup>III</sup>(2,6-Cl<sub>2</sub>TPP)Cl as catalyst).<sup>104</sup> In this kind of tetrapyrrolic ligands the large substituents present in the *ortho*-position of *meso*-aromatic groups prevent the  $\mu$ -oxo dimerization described by Collman, thus enhancing the stability of the catalyst.

Even if more common system in mammalian biochemistry utilise hemoproteins (and so iron-porphyrins) for oxygen activation, many others transition-metal system can be involved in these reactions. In the 80's indeed metalloporphyrins with different metals (including Cr, Mn and Ru) were also shown to catalyzed both epoxidation of olefins and hydroxylation of unactivated hydrocarbons.

Among these various species ruthenium complexes present different advantages and peculiar characteristics. Interest in ruthenium porphyrins originally stemmed, at least in part, from attempts to model certain aspects of cytochrome P-450 systems. Interest in ruthenium porphyrins chemistry stems also in the intriguing possibility to have species in oxidation state ranging from -II to +VI, though some of them (-II and 0) not isolable and generable only in situ.

The first ruthenium porphyrin complex was described in 1969,<sup>105</sup> although a corrected formulation of this species as  $\text{Ru}^{\text{II}}(\text{TPP})(\text{EtOH})(\text{CO})$  on the basis of elemental analysis and mass spectra results was published two years later.<sup>74</sup> In the same year the description of a series of new ruthenium(II) carbonyl complexes appeared in the literature,<sup>106, 107</sup> and in the following decade a number of papers have been published that involve structural and chemical characterizations of these complexes.<sup>108-117</sup> Early investigations into chemistry of ruthenium porphyrins and most of their applications in different fields, were initially restricted to carbonyl complexes  $\text{Ru}^{\text{II}}(\text{P})(\text{CO})$ , common products of direct insertion of ruthenium into free-base porphyrin.<sup>118-126</sup> The CO ligand is a strong  $\pi$ -acid and it strongly bound to the metal centre. Some ruthenium complexes have been found to undergo "true" biomimetic reactions, as shown for the first time by Groves and Quinn,<sup>123</sup> who found that sterically hindered dioxo-ruthenium(VI) porphyrin( $\text{Ru}^{\text{VI}}(\text{TMP})(\text{O})_2$ ) species, can catalyzed the aerobic epoxidation of alkenes. It is worth of noting that, approximately half of the papers appearing in literature concerning ruthenium porphyrins deal with olefin epoxidation.<sup>127, 128</sup> Epoxides are found in natural occurring compounds,<sup>129, 130</sup> and they are important intermediates inorganic synthesis. In the case of asymmetric epoxidation, stereospecific ring-opening of the epoxide brings to chiral alcohols.<sup>131</sup>

After preliminary results reported in the 80's by Groves and Quinn, several high valent dioxo-ruthenium(VI)porphyrin complexes have been isolated and found to be excellent catalysts for hydrocarbon oxidations. Furthermore, while the mechanism relative to iron porphyrin complexes is still not well understood, more is known regarding the corresponding ruthenium species. In fact, ruthenium porphyrin complexes not only are potent oxidant of organic hydrocarbons, but they are more inert than their first-row congeners and should be good model systems for mechanistic investigations of oxygen-atom transfer reactions.

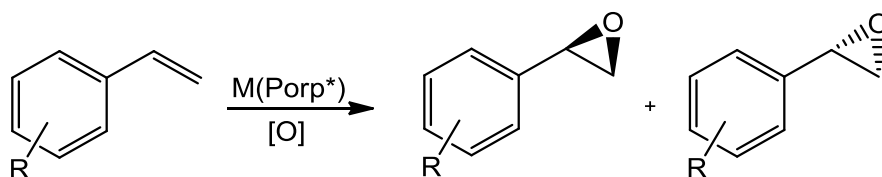
Ruthenium porphyrin species, initially developed with the role of analogous synthetics of the natural iron counterparts, have demonstrated high activity and selectivity in different fields. Thanks to their periodic relationship with iron, the relative easy feasibility of their preparation, their stability and versatility are nowadays a central argument in the field of metallo porphyrin chemistry. For these reasons they still play a prominent role in the metalloporphyrin-catalyzed hydrocarbon-functionalization of non activated molecules.

Ruthenium-porphyrin species have been found to potentially be effective catalysts non only for the described reaction of epoxidation of unfunctionalized olefins, but they are also active in alkane hydroxylation,<sup>75, 92</sup> in the oxidation of different organic molecules,<sup>89</sup> as tioetjers, amines, phosphines, phosphites, arsine, stibines. In additionan to that metallo-porphyrins are competent catalysts of cyclopropanation<sup>127, 128, 132-134</sup> and amination reactions. Obviously, the appealing opportunity to have a unique catalyst active in different applications, had brought to a huge interest for ruthenium porphyrin complexes.

## 1.4. Asymmetric Porphyrins and Porphyrin Complexes

The design and synthesis of molecules which display structural analogies to biological active sites can be a key step in biomimetic chemistry. Bio-active molecules often present chiral moieties (i.e. the proteic chain in active metallo-enzymes) which at the same time stabilise the compound surrounding the active centre in the living system and promote its biological activity. Consequently, a useful strategy for the elaboration of the porphyrin backbone may be the insertion in it of asymmetric moieties. During the last two decades various methods have been reported to achieve elaborated superstructure of porphyrin ligands,<sup>135-140</sup> able to play the role that in Nature is accomplished by protein chains. For example, the design of artificial systems analogous to hemoproteins must take care of the chemical structure near the metal centre because in natural systems groups in the vicinity of the metal centre are able to control the access to the active site and consequently the biological activity of the whole system.

Furthermore, a synthetic chiral porphyrin derivative may have enantioselective applications. Numerous chiral porphyrin structures appeared during the last twenty-five years, and most of them have been at first used as iron(III) or manganese(III) complexes to catalyze enantioselective epoxidation reactions<sup>141-145</sup> such as the epoxidation of styrene derivatives (Scheme 1.8). Currently, the scientific interest in their catalytic use developed in a continuously growing number of applications and to extend the utility of metallo porphyrin species, a wide variety of chiral porphyrins have been developed over the years.



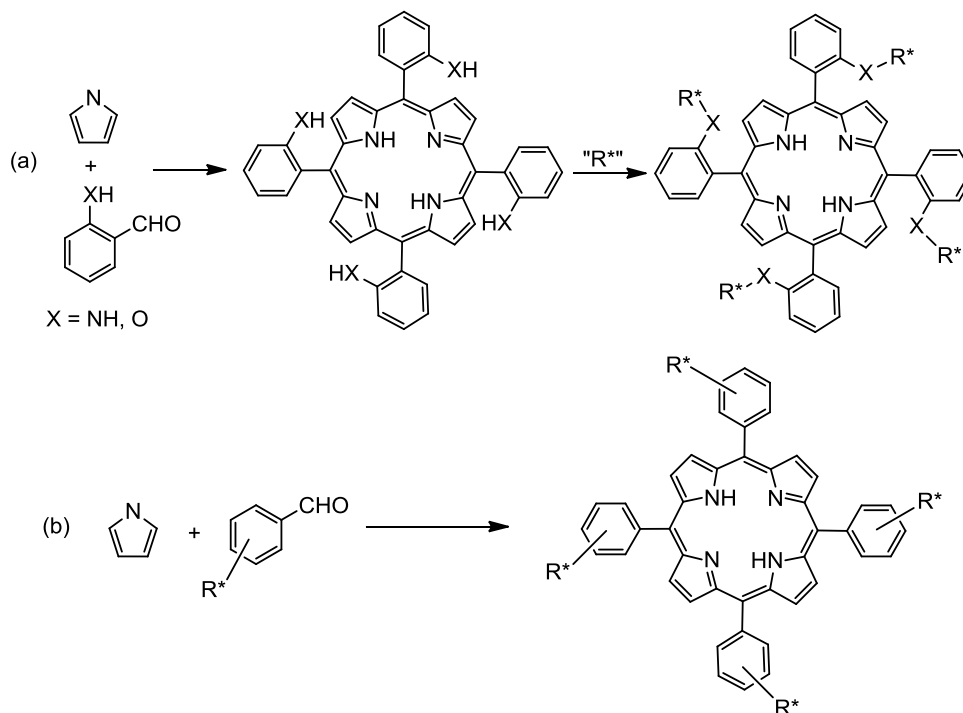
**Scheme 1.8.** Epoxidation of styrene derivatives, an useful strategy for the evaluation of activity and selectivity of a metalloporphyrin catalysts.

Chiral porphyrins have been mainly prepared in three different ways. The most common approach, first used by Groves and Meyers,<sup>102</sup> involves the attachment of chiral units to preformed porphyrins such as tetra(hydroxy-) or tetra(amino-) 2-substituted or 2,2'-disubstituted TPP species (Scheme 1.9-a). O'Malley and Kodadek<sup>146</sup> showed that chiral substituents can be introduced at the porphyrin-forming step by allowing a chiral aldehyde to condense with pyrrole through a classic Lindsey procedure (Scheme 1.9-b).

It is worth mentioning here that while tetra(2,2'-disubstituted)phenyl porphyrins can exist only in one possible conformation, tetra(2-monosubstituted)phenylporphyrin present four different isomers, named atropisomers, which differ for the orientation of the substituents with respect to the mean-plane of the tetrapyrrolic macrocycle (Figure 1.4). Synthesis of this class of porphyrins from pyrroles and the related 2-substituted benzaldehyde brings to the statistical mixture of the four possible products. The concept of biphenyl-type atropisomerism in *ortho*-substituted *meso*-tetraphenylporphyrins was first demonstrated by Ullman<sup>147</sup> separating the four atropisomers of *meso*-tetra(2-hydroxyphenyl)porphyrin. In these molecules phenyl groups are oriented nearly perpendicularly to the porphyrin plane, projecting in this way the *ortho*



substituents above or below the tetrapyrrolic plane. In such cases the four atropisomers depicted in Figure 1.4 can be interconverted and this equilibrating process gives a statistical ratios of abundance. The possibility of the interconversion and the temperature at which the equilibration becomes rapid depend on the bulkiness of the *ortho*-substituents. For X = NH (tetra(*o*-aminophenylporphyrin)) and X = O (tetra(*o*-hydroxyphenylporphyrin)), the two most widely used porphyrins as backbone for chiral superstructures, the interconversion is possible even at room temperature, and becomes very rapid over 70-80 °C.



**Scheme 1.9.** Strategies for the construction of chiral tetraphenylporphyrins: linkage of chiral groups to pre-constructed macrocycles (a) or Lindsey condensation of chiral aldehydes with pyrroles (b).

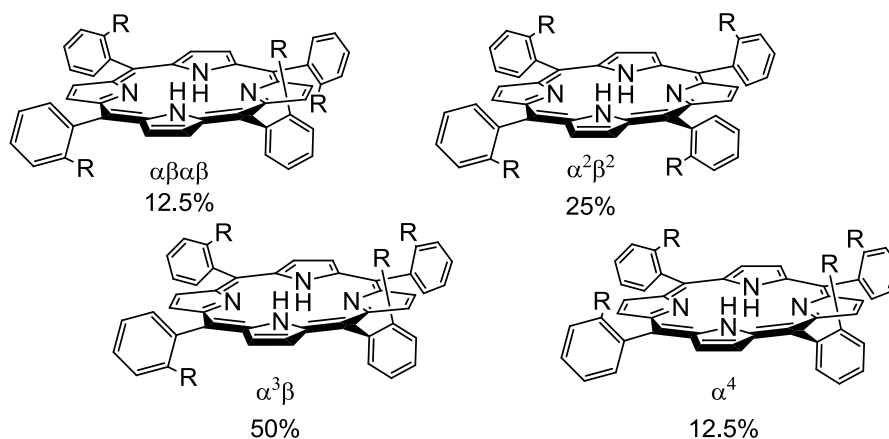


**Figure 1.4.** Possible atropisomers and statistical percentage for *meso*-(2-substituted)TPP

The first typology of studied ligands was called “single-face” protected porphyrins and particular examples of this class are picket fence porphyrins schematically represented in Figure 1.5-a. Some natural-occurring species have this geometry, with the open face protected from a protein chain. Synthetic single-face chiral systems were firstly reported in the early seventies in order to inhibit the described  $\mu$ -oxo dimerization reactions that are responsible for the deactivation of the active form of species.<sup>148</sup> Afterward, Collman and co-workers contributed most significantly to the development of new macrocyclic chiral ligands.<sup>103</sup> In particular, they reported a chiral “picnic basket” porphyrin,<sup>97</sup> having isophthalate moieties. A schematic representation of this kind of system is depicted in Figure 1.5-b, while a specific example, bearing an isophthalate amide loops and a binaphthyl linker is shown in detail in Figure 1.5-c. These porphyrins, and subsequently some related flexible threitol porphyrins<sup>149</sup> were firstly used as catalysts for epoxidation of alkenes as manganese complexes,  $Mn^{III}(P)Cl$ . Anyway, these systems have not found widespread applications as catalysts, since to avoid the approach of the substrate only on the open achiral face (that prevent a stereoselectivity), it is necessary to firmly coordinate a strong bulky (and maybe very expensive and/or extremely difficult to prepare) anionic ligand to the metal centre on its “non-selective” side. Nevertheless, they represent basic building blocks for models of hemoprotein active sites,<sup>150-154</sup> and they have also found relevance in the field of cation binding applications.<sup>155, 156</sup> Similar porphyrins have been prepared for the discrimination of  $O_2$  with respect to  $CO$ .<sup>103, 157</sup>

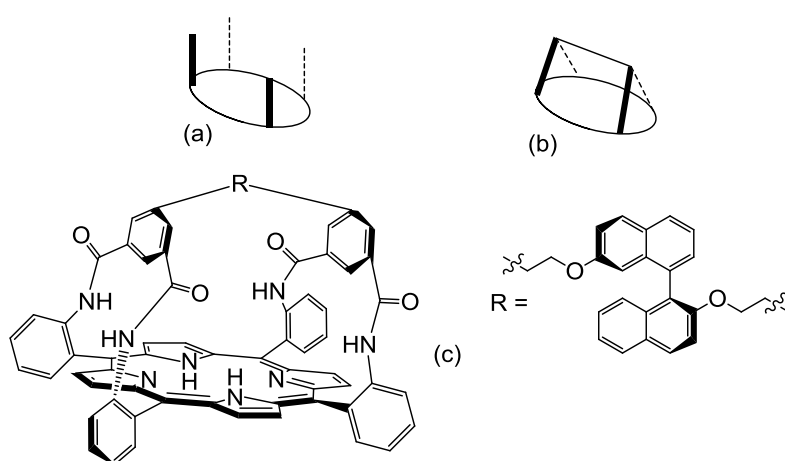


**Figure 1.5.** Schematic representation of the single-face protected picket fence (a) and picnic basket (b). Picnic basket porphyrin, bearing isophthalate amide loops and a binaphthyl diether linker (c)

Double faced picket porphyrins can be achieved both starting from 2,2'-disubstituted or  $\alpha,\beta,\alpha,\beta$ -atropisomers of 2-substituted *meso*-tetra(amino)- or *meso*-tetra(hydroxy)- phenylporphyrin. A range of different porphyrins of this kind have been reported in the literature,<sup>158-163</sup> and in many cases interesting results have been obtained in term of both yields and enantioselectivity in oxidation catalysis using iron and/or manganese complexes. On the other hand, Paolesse *et al.* ascribed these failures due to the difficult access of substrates to the catalytic centre in such encumbered systems.<sup>158</sup> This observation was then confirmed using “picket-fence” double faces protected systems obtained by coupling porphyrin bearing different aryl substituted groups on meso positions (figure 1.6) with Mosher’s reagent<sup>164</sup> ( $\alpha$ -methoxy- $\alpha$ -

(trifluoromethyl)phenyl-acetyl chloride, mtpa). Rose and co-workers, using iron(III)-chloride complexes of this family of chiral ligands for the epoxidation of styrene, showed that, nonetheless an intrinsic general low selectivity, the “least bad” *ee* was obtained with the least crowded derivative with only one chiral group (Figure 1.6).<sup>145, 156</sup> In particular, they used a mixed porphyrin backbone constructed through Lindsey condensation of pyrrole with pentafluorobenzaldehyde and 2,6-dinitro-4-*tert*-butylbenzaldehyde. The pentafluorobenzaldehyde was used to improve the stability of the resulting porphyrin, while the substituted *tert*-butylbenzaldehyde was chosen in order to increase the solubility of the catalyst. With no one of the resulting mixed catalysts good results in term of yields or *ee* were obtained. Anyway, the “less bad” result was obtained with the less crowded system A reported in Figure 1.6 demonstrating that free access to the catalytic centre is a determining factor to increase both efficiency and selectivity of enantioselective reactions.

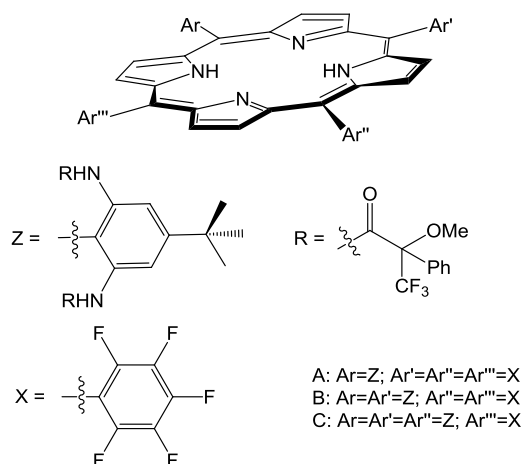


**Figure 1.6.** Chiral porphyrins bearing Mosher's pickets on a mixed scaffold.

On a related geometry, Simonneaux and co-workers in 1991 described a family of porphyrins obtained by coupling the four atropisomers of *meso*-(2-aminophenyl)porphyrin with Mosher's reagent. Among the four products, the two double faces protected isomers  $\alpha,\beta,\alpha,\beta$  and  $\alpha,\alpha,\beta,\beta$  were employed as chiral ligands (Figure 1.7).<sup>72, 73, 89</sup>

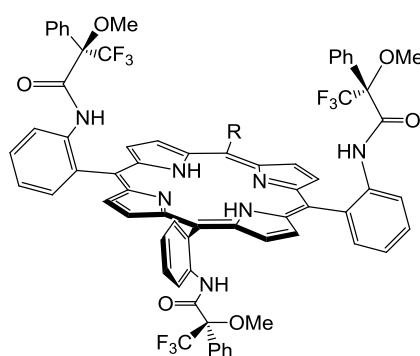


**Figure 1.7.** Double-faced protected chiral porphyrins: the Mosher's reagent was used as a chiral source on a TAPPH<sub>2</sub> scaffold.

Using double face protected  $\alpha,\beta,\alpha,\beta$ -tetra[(R)-1,1'-binaphth-2-yl]porphyrins (“chiral walls”, not represented here), Kodadek *et al.*<sup>146</sup> obtained good results in term of yield, selectivity and TON for the epoxidation of styrenes catalyzed by manganese complexes. These *meso*-binaphthyl substituted porphyrins were easily obtained by Lindsey condensation of pyrrole and optically pure (R)-binaphthaldehydes following a synthetic pathway firstly reported by Meyers.<sup>165</sup> A further increase in the dimension of the “chirality-provider” *meso*-substituents brought to worst results both in terms of yields and selectivities, thus confirming the observation that, a certain degree of the steric constrain is necessary to achieve selectivity but systems too hindered may easily result less efficient.<sup>166</sup> Recently, Salvadori and co-workers reported a modification of the chiral walls system of Kodadek demonstrating that the simply introduction of a methoxy group into the 2' position of each binaphthyl moiety improves the activity of the system. In the same paper they also compared the activity of the various possible atropisomers of their system to conclude that the  $\alpha,\beta,\alpha,\beta$  C<sub>2</sub> isomer shows the best catalytic efficiency.<sup>167</sup>

A different family of double faced porphyrins is that of the D<sub>4</sub>-symmetric porphyrins, that were firstly developed by Halterman (Figure 1.8).<sup>168, 169</sup> Epoxidation of styrenes using these ligands both as complex of iron and manganese immediately brought to very good results in term of yields, TON and *ee*. Nowadays these kind of chiral ligands are extensively employed with different metals and for various catalytic applications. In particular the groups of Che and Berkessel have utilized ruthenium and manganese complexes of the simplest porphyrin of this family (X = H, Figure 1.8) for stoichiometric and catalytic reactions of oxidation,<sup>127, 128, 132-134</sup> cyclopropanation<sup>134, 170-172</sup> and amination<sup>173-175</sup> of unfunctionalized hydrocarbons, always reaching good to very good results in term of yields.<sup>134, 168</sup> A modified anthracene-9-carboxaldehyde was then prepared in order to achieved better results but the synthesis of the corresponding porphyrin is very tedious.

Recently, Brekessel and co-workers have published the synthesis of different 10-substituted derivatives of this aldehyde and of the related porphyrins (Figure 1.8-A, with X = OMe, Me or CF<sub>3</sub>),<sup>176, 177</sup> and a supported version of this catalyst has also been reported, by directly linking the tetra-10-vinyl substituted analogous of this porphyrin to macroporous polymers.<sup>178</sup> Closely related and more crowded systems have also been developed (Figure 1.8-B) with the aim to improve the selectivity by increasing steric constrains. Anyway, this modified chiral moieties usually required very tedious synthetic preparations.

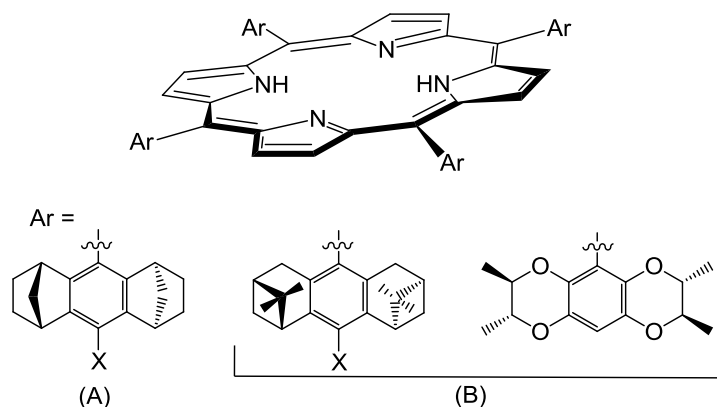
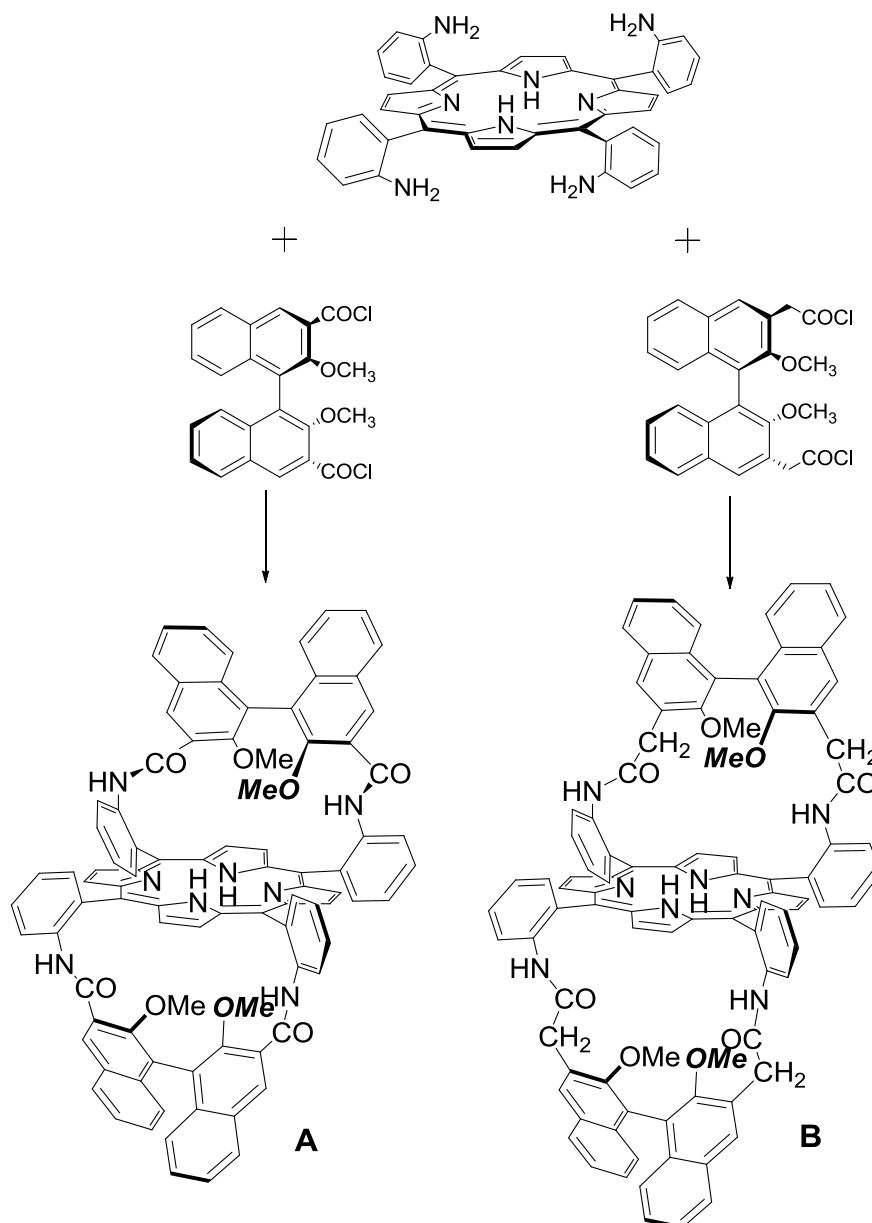


**Figure 1.8.** D<sub>4</sub>-symmetric systems developed by Halterman and their possible modifications.

### 1.3.2. Bis-Strapped Porphyrins.

An important breakthrough in this field was achieved with the so called “bis-strapped” porphyrins. These systems are characterized by the presence of chiral binaphthyl (BINAP) groups attached on the  $\alpha,\alpha,\beta,\beta$  atropisomer of TAPPH<sub>2</sub> or on the more robust and soluble 5,10-pentafluorophenyl-15,20-(2,6-diamino-4-*tert*-butylphenyl)porphyrin.<sup>145, 179-183</sup> An important feature of this kind of ligands is that they provide free access to the metal centre for the substrate and at the same time they are characterised from a significant steric bulk in the vicinity of the active site. These feature contribute to high catalytic activity and selectivity.



**Scheme 1.10.** Condensation between  $\alpha,\alpha,\beta,\beta$ -TAPPH<sub>2</sub> and a chiral binaphthyl moiety, to give A 1999<sup>179</sup> and B 2003.<sup>183</sup> Proximal methoxy groups are depicted in bold-italic (see text).

As stated before, during the development of different chiral metalloporphyrin complexes and their applications in various enantioselective catalysis it has been found that fine-tuning of the steric bulk of the chiral substituents dramatically influences both yield and *ee* values. In many cases, the most crowded system induced the lowest enantioselectivities, and vice versa better *ee* values were obtained by using less bulky arrangements. For example, groups of Collman and Rose reported the synthesis of  $C_2$ -symmetric bis-binaphthyl chiral porphyrin from condensation of  $\alpha,\alpha,\beta,\beta$  atropisomer of TAPP $H_2$  with two equivalents of 2,2'-dimethoxy-1,1'-binaphthyl-3,3'-diacetylchloride (Scheme 1.10-A).

This chiral system is generally referred as “C1” Bis-strapped porphyrin, for the presence of only one carbon atom in the bridge that connects the porphyrin scaffold and the BINAP moiety. Using Fe(III)Cl complex of this species the best results, were obtained for the epoxidation of some styrene derivatives both for yields and *ee* using PhIO as the terminal oxidant.<sup>179</sup> Later, the good versatility of this iron complex was demonstrated by employing it as a catalyst for different reactions.<sup>180</sup> According to the idea that the efficiency of the system would be improved by providing more access to the metal centre, Rose *et al.* few years later also prepared the so called “homologated” system, by elongating the binaphthyl moiety of one methylenic unit (Scheme 1.10-B). The resulting “C2” binaphthyl bis strapped porphyrin as Fe(III)(P)Cl complex (Figure 1.9), gave even better results with respect to the shorted system in terms of yields and *ee* (some other results are reported in table 1.1) and it also appeared very stable. In fact a TON of 16000 was reached without highly affecting the *ee*.<sup>183</sup> An important feature of this class of ligands is that due to the rigidity of the structure, the methoxy groups are different among them. Two OCH<sub>3</sub> groups point toward the tetrapyrrolic core, and are thus defined as “proximal”, while the other two OCH<sub>3</sub> groups point outward and are called “distal” (Scheme 1.10), the proximal groups are written in bold-italic.

In the following we will see how this distinction is a practical tool for NMR studies of this species and their metallo-complexes. In fact, while the <sup>1</sup>H NMR signals of distal methoxy group are only slightly upfielded with respect to characteristic values of aromatic OCH<sub>3</sub> groups (respectively, 2.96 ppm and 1.95 ppm in CDCl<sub>3</sub> for **A** and **B**), proximal methoxy groups resonate at very higher fields (respectively, -0.63 ppm and -0.51 ppm in CDCl<sub>3</sub> for **A** and **B**). This phenomenon is directly related to the close proximity of these groups to the core of the porphyrin. The extended aromaticity of the macrocycle in fact generates a strong “ring current”, a magnetic field that may strongly affect <sup>1</sup>H NMR signals. This trend is quite common for porphyrin and metal-porphyrin species.

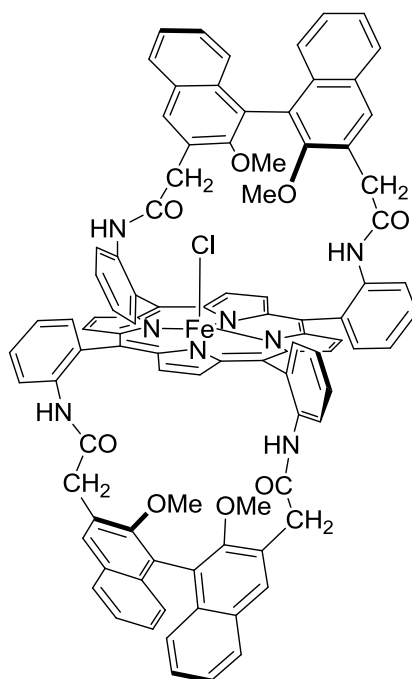


**Figure 1.9.** Iron complex of the C2 bis-strapped porphyrin.

**Table 1.1.** Catalytic epoxidation of styrenes by using the complex shown in Figure 1.9.

Olefin	Yield %	ee %
styrene	96	97
pentafluorostyrene	80	96
3-fluorostyrene	87	93
3-chlorostyrene	90	88
4-chlorostyrene	75	84
3-nitrostyrene	84	90

Reaction conditions:  $\text{Fe}^{\text{III}}(\text{C2-porphyrin})(\text{Cl})$  as the catalyst, PhIO as the terminal oxidant. Molar ratios catalyst/oxidant/olefin 1:100:1000. Reaction performed in dichloromethane at RT (see ref <sup>183</sup>).

## 1.5. Metallo Porphyrin-Catalysed Amination Reactions

The biological and pharmaceutical activities of organonitrogen compounds prompted the scientific community to develop new methods for the direct and selective C–N bond formation. The choice of the appropriate nitrogen source to introduce into the organic frameworks, the aza-functionality represents a key point to synthesize useful fine chemicals in an economical fashion and using environmentally benign technologies. Recently, the use of nitrene precursors for the introduction of a “NR” moiety into an organic molecule received special attention and many reviews have been published on this subject.<sup>184-190</sup>

Nitrenes are the nitrogen analogues of carbenes and their reactivity is due to the presence of four non-bonding electrons. In a singlet electrophilic nitrene the electrons are arranged as two lone pairs, whereas, if the electrons are present in three orbitals, one filled and two semi-filled, the corresponding nitrene is in a triplet state and shows a diradical behaviour (Figure. 1.10). In both cases, nitrenes are not stable as free molecules and react very easily with a great variety of organic substrates.

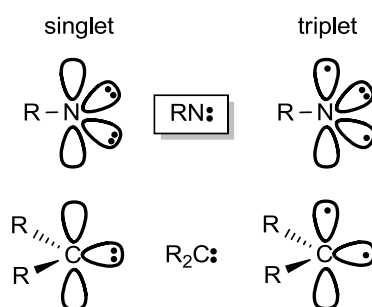


**Figure 1.10.** Singlet and triplet states for nitrenes and carbenes.

Typical nitrene sources used for the synthesis of nitrogen-containing molecules are reported in Figure 1.11. The most commonly employed nitrene source for amination reactions is  $\text{PhI}=\text{NR}$  that can be also formed *in situ* by the reaction of the corresponding amine,  $\text{RNH}_2$ , with an oxidant such as  $\text{PhI}(\text{OAc})_2$  or  $\text{PhIO}$ . As indicated below, iminophenylidines suffer from several drawbacks, therefore alternative nitrogen sources such as chloramine-T ( $\text{TsN}(\text{Cl})\text{Na}$ ) ( $\text{Ts}=\text{tosyl}$ ), bromamine-T ( $\text{TsN}(\text{Br})\text{Na}$ ) and organic azides ( $\text{RN}_3$ ) were more recently investigated.

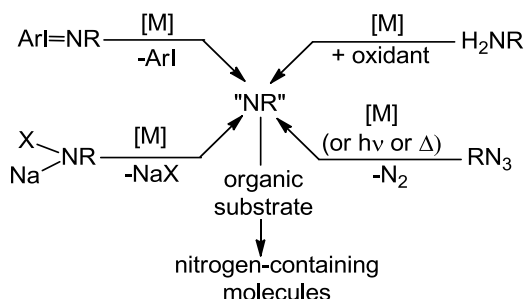


**Figure 1.11.** General scheme for the nitrene formation and transfer.

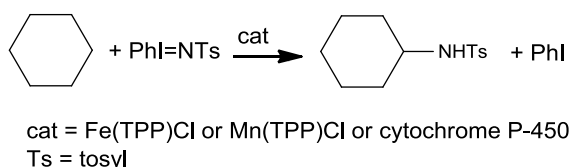


The formation of the “RN” moiety is promoted by transition metals that can also selectively drive the nitrene transfer towards organic molecules. Transition metal complexes of porphyrins were shown to be very efficient in both stoichiometric and catalytic nitrene transfer reactions.

In this introduction, we want to examine a selection of papers concerning the activity of metalloporphyrins in several nitrene transfer reactions. Each nitrene source will be discussed separately to give an overview on the potentiality and limits of these methodologies to synthesize nitrogen containing compounds even in an enantioselective way. Moreover, since the proper choice of the metal catalyst and/or the reaction substrate allows the chemoselective addition of the nitrene to either an alkene, forming an aziridine, or to a C–H bond, to yield an amine, a further distinction has been introduced.

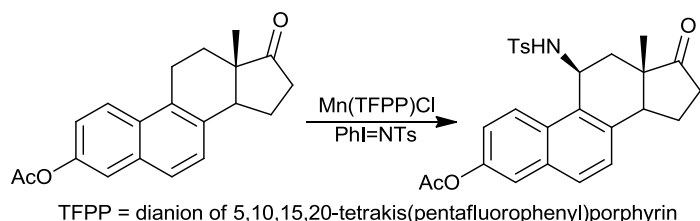
### 1.5.1. ArI=NR as nitrene sources

The synthesis of a new type of iodine-nitrogen ylide, *N*-tosylimino aryl iodine together with a study of its reactivity was reported by Yamada in 1975<sup>191</sup> but it was the group of Evans to develop the nitrene transfer to olefins by PhI=NTs into a synthetically useful method.<sup>192-194</sup> Breslow and Gellman<sup>195</sup> in 1982 demonstrated that PhI=NTs, the tosylimido analogue of iodosobenzene, is active in the M(TPP)Cl (M = Mn(III) or Fe(III) and TPP = dianion of tetraphenylporphyrin) catalyzed C–H amidation of cyclohexane (Scheme 1.11). The fact that even cytochrome P-450 is catalytically active indicated that this reaction can be considered a nitrogen version of the hydroxylation of C–H bonds performed by Nature.



**Scheme 1.11.** C–H amidation of cyclohexene.

Unfortunately the recovered yield of the aminated product was only of 3–8%. It is worth noting that since publication of that paper, several efforts were devoted to improve the efficiency of the amination of alkanes, reagents that generally show low chemical reactivity. Nitrene insertion reactions occur more easily into activated C–H bonds such as allylic and benzylic ones.<sup>196</sup> In fact, the synthesis of allylic and benzylic amines was efficiently catalyzed by manganese porphyrin complexes also when using natural products such as cholesterol<sup>175</sup> or equilenin acetate<sup>197</sup> (Scheme 1.12) as starting materials.



**Scheme 1.12.** C–H amidation of equilenin acetate.

To cope with the increasing demand for enantiomerically pure compounds, Che and co-workers investigated the use of chiral manganese porphyrin complexes to achieve optically pure aminated products.<sup>173-175</sup> Using the manganese complex of 5,10,15,20-tetrakis- $\{(1S,4R,5R,8S)\}$ -1,2,3,4,5,6,7,8-octahydro-1,4:5,8-dimethanoanthracene-9-ylporphyrin (**1**) (Figure 1.12), benzylic and allylic amines were obtained with enantioselectivities up to 54%.<sup>174</sup>

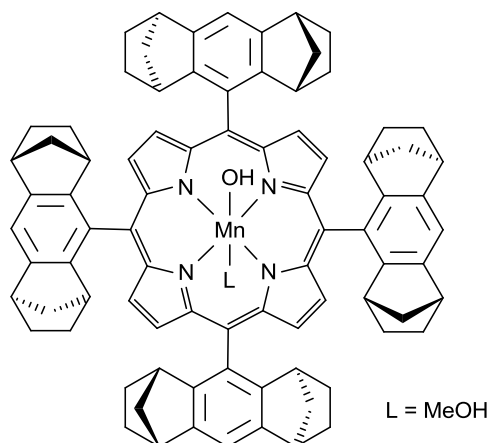
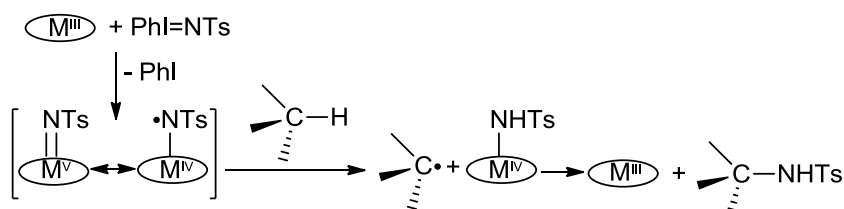


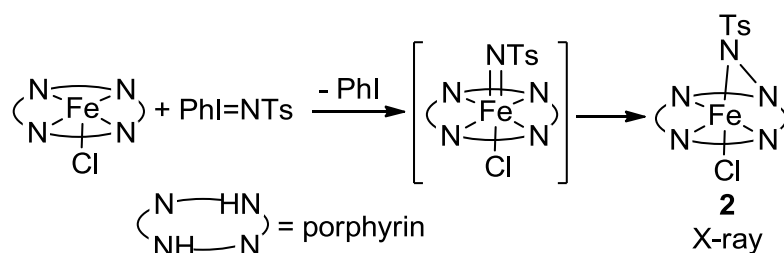
**Figure 1.12.** Structure of  $\text{Mn}(\text{P}^*)(\text{OH})(\text{MeOH})$  (**1**).

A mechanism for this reaction was initially proposed by Mansuy and co-workers (Scheme 1.13)<sup>196, 198</sup>.



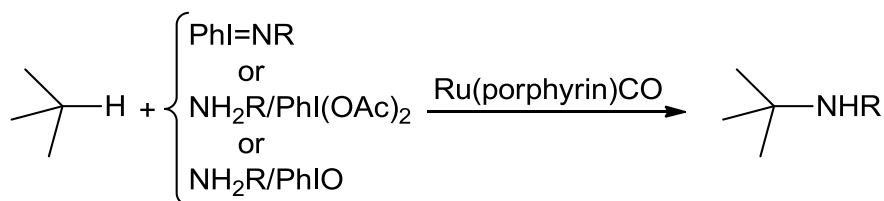
**Scheme 1.13.** Proposed mechanism for the tosyl amidation of alkanes, catalyzed by  $\text{M}(\text{porphyrin})\text{Cl}$  ( $\text{M} = \text{MnIII}$  or  $\text{FeIII}$ ) complexes.

As shown in Scheme 1.13, the insertion of the “NR” moiety into the C–H bond should occur through a hydrogen atom abstraction by a metallo-nitrene intermediate complex. The formation of an active imido intermediate was suggested on the basis of the analogy with the C–H hydroxylation, in which a high valent metal-oxo compound is responsible for the oxidation reaction. The possible existence of iron imido intermediates was supported by the isolation and characterization of complex **2** (Scheme 1.14) in which a nitrene functionality is bridging the metal centre and a nitrogen atom of the porphyrin ligand. Mansuy and co-workers proposed that **2** was formed by an insertion of the tosylimido moiety into the iron-pyrrolic nitrogen bond of the unstable terminal imido porphyrin complex (Scheme 1.14).<sup>199, 200</sup>



**Scheme 1.14.** Synthesis of the bridged iron nitrene porphyrin complex **2**.

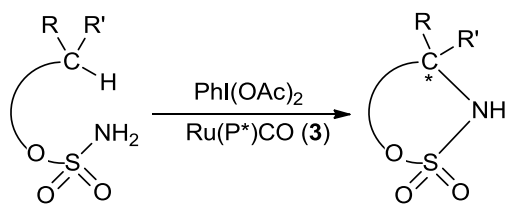
Complex **2** did not transfer the nitrene functionality to hydrocarbons in stoichiometric reactions but it was able to generate the catalytic active specie if used in place of Fe(TPP)Cl. Unfortunately, a deeper mechanistic investigation of the C–H nitrene insertion catalyzed by iron porphyrin complexes was hampered by the high instability of the catalytic intermediates. Significant progress in understanding the mechanism of the reaction was achieved by using ruthenium in place of iron and this substitution also allowed to improve the efficiency of the catalytic systems<sup>174, 175, 201</sup>. Nitrene transfer reactions were carried out with pre-isolated PhI=NR or with iminoiodinanes formed *in situ* by an oxidative reaction of the commercially available RNH<sub>2</sub> (Scheme 1.15).



**Scheme 1.15.** General procedure for amination reactions catalyzed by ruthenium porphyrin complexes.

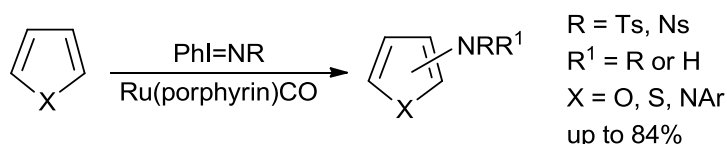
The amination with RNH<sub>2</sub>/PhI(OAc)<sub>2</sub> or RNH<sub>2</sub>/PhIO gave in the majority of cases results as good as to those obtained with PhI=NR.<sup>201</sup> Up to that point, the pre-formation of PhI=NR species limited the variety of R groups available for the synthesis of aza-derivatives whereas, the *in situ* formation of iminoiodinanes allowed to widen the scope of the reaction. In fact, besides *N*-aryl sulfonyl groups (*N*-(SO<sub>2</sub>-*p*-C<sub>6</sub>H<sub>4</sub>R<sup>1</sup>)) also *N*-SO<sub>2</sub>Me and *N*-COCF<sub>3</sub>, whose corresponding iminoiodinanes are not stable, were inserted into C–H bonds.

The chiral ligand reported in Figure 1.12 was also used for the synthesis of the ruthenium catalyst Ru(P<sup>\*</sup>)CO (**3**) but, unfortunately, its use in intermolecular asymmetric amidations of hydrocarbons occurred with moderate enantiomeric excess.<sup>174, 175</sup> On the other hand, high diastereo- and enantioselectivity values were obtained in intramolecular amidations of a great variety of sulfamate esters (–OSO<sub>2</sub>NH<sub>2</sub>)<sup>202-204</sup> and several heterocycles were synthesized with *ee* values up to 88% (Scheme 1.16).



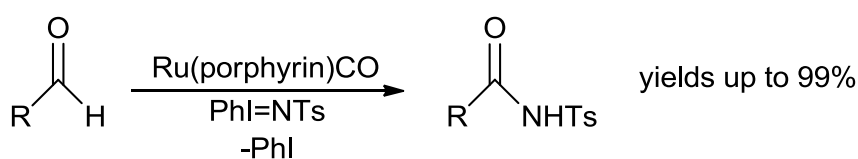
**Scheme 1.16.** General procedure for enantioselective intramolecular amidation reactions catalyzed by Ru(P\*)CO (**3**).

To extend the scope of the methodology, the amidation of  $sp^2$  C–H bonds was explored. Aromatic heterocycles were amidated by PhI=NR in the presence of ruthenium porphyrin catalysts (Scheme 1.17) to give amino-functionalized five-membered heterocycles<sup>205</sup>.



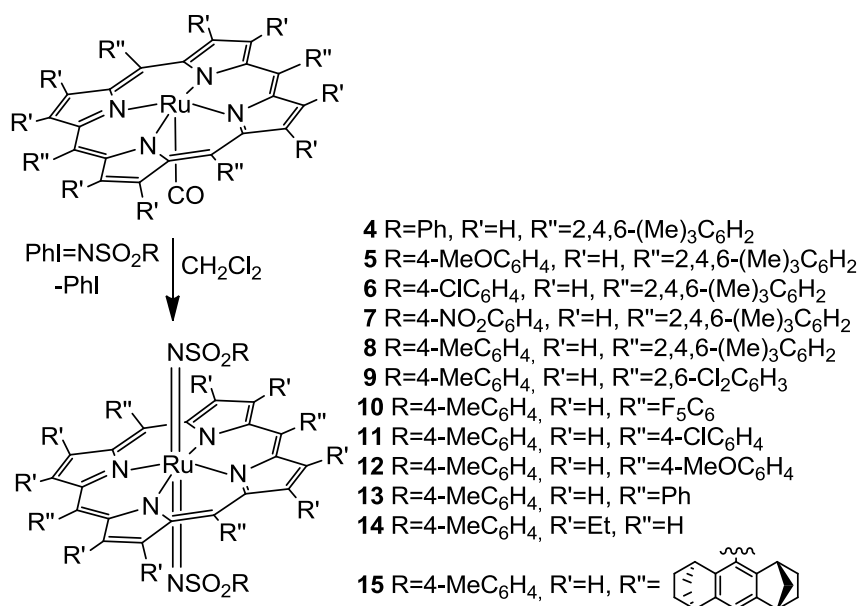
**Scheme 1.17.** Ruthenium porphyrins catalyzed amidation of five-membered heterocycles with PhI=NR (R = Ts, Ns).

More recently, the nitrene transfer insertion into the  $sp^2$  C–H bonds of aldehydes was exploited to synthesize amides. The ruthenium porphyrin/PhI=NR protocol turned out to be very efficient for the amidation of a wide range of aldehydes, also to obtain bioactive compounds.<sup>206</sup> The general procedure is shown in Scheme 1.18.



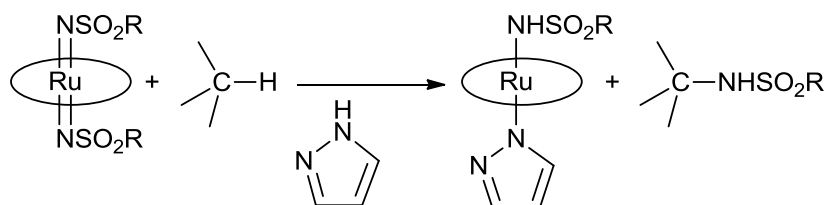
**Scheme 1.18.** Ruthenium porphyrins catalyzed amidation of aldehydes.

To look into the mechanism of the ruthenium catalyzed C–H amination, the reaction between ruthenium(II) porphyrin catalysts and the nitrene source PhI=NSO<sub>2</sub>R was investigated. Notably, numerous Ru(porphyrin)(NSO<sub>2</sub>R)<sub>2</sub> were isolated, but unfortunately their extreme instability prevented, up to now, X-ray characterization.<sup>174, 175, 207-210</sup> The general synthesis of ruthenium bis-tosylimido complexes<sup>187, 197</sup> is reported in Scheme 1.19.



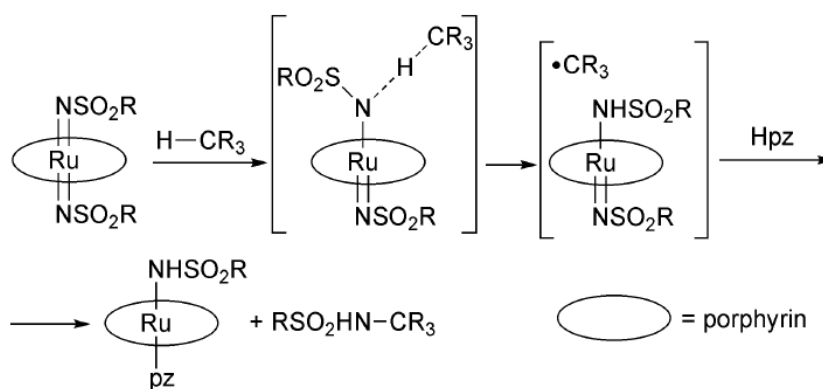
**Scheme 1.19.** Synthesis of ruthenium bis-tosylimido porphyrin complexes.

Ruthenium bis-imido porphyrin complexes are stable for a few days at -15 °C in the solid state, whereas when left standing in dichloromethane solution, a degradation process occurs. The nitrene functionalities present in complexes **4–15** are all transferable to hydrocarbons affording the corresponding aminated species and uncharacterized ruthenium products. If the reaction was run in the presence of pyrazole, amido ruthenium porphyrin complexes were isolated and fully characterized (Scheme 1.20)<sup>207, 208, 210</sup>.



**Scheme 1.20.** Nitrene transfer reaction from the bis-imido ruthenium complex to a hydrocarbon with the concomitant formation of Ru(porphyrin)(NHSO<sub>2</sub>R)(pz) complex.

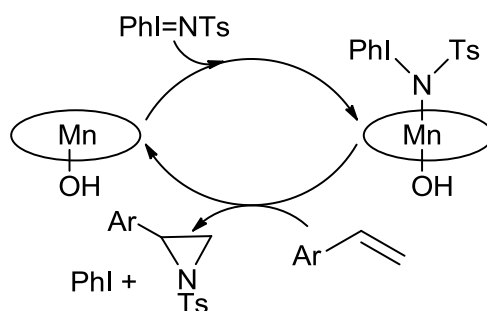
The nitrene transfer reaction reported in Scheme 1.20 was studied in detail by Che and co-workers and all collected data indicated the mechanism illustrated in Scheme 1.21.<sup>208, 210</sup>



**Scheme 1.21.** Proposed mechanism for the nitrene transfer reaction to hydrocarbons.

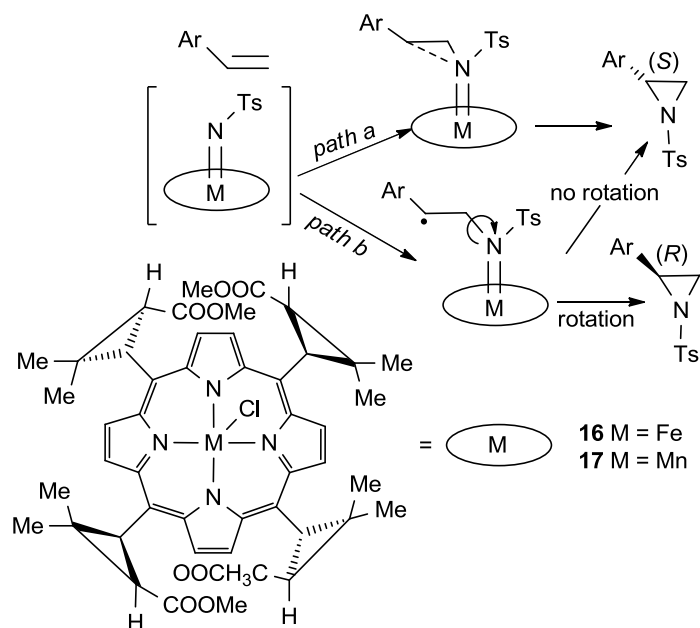
The authors suggested that the amidation reaction proceeds *via* carboradical intermediates. A hydrogen atom abstraction by the ruthenium imido complex should occur on the periphery of the complex, since the imido moiety is bound to the coordinatively and electronically saturated ruthenium centre. Then, the radicals produced are efficiently scavenged by the ruthenium porphyrin.

N-tosylimido compounds can be also employed to synthesize aziridines. This class of molecules<sup>211</sup> show various biological properties and they represent useful building blocks in organic synthesis for the high reactivity of the three membered ring. Aziridines can be considered nitrogen analogues of epoxides. However, up to now their chemistry was less explored. The first metallo-porphyrin catalyzed synthesis of aziridines by a nitrene transfer reaction from iminoiodinanes was performed in the presence of iron and manganese complexes.<sup>212, 213</sup> The chiral manganese complex reported in Scheme 1.22<sup>173</sup> was employed to catalyze the aziridination of styrene-type substrates with enantiomeric excesses up to 68%. Moreover, spectroscopic studies indicated a mechanism (Scheme 1.22) in which a Mn-PhINTs adduct is implicated.



**Scheme 1.22.** Proposed mechanism for the 1-catalyzed aziridination of styrenes.

The absolute configuration of the aziridine depends on the mechanism involved in the ring formation. It is well known that a nitrene can react with an alkene in a concerted or in a two step mechanism<sup>211</sup> depending on the state, singlet or triplet, of the NR moiety. Marchon and co-workers<sup>214</sup> studied the catalytic activity of iron and manganese porphyrin complexes **16** and **17** (Scheme 1.23); ee up to 57% and opposite aziridine enantioselectivities for the two complexes were observed.

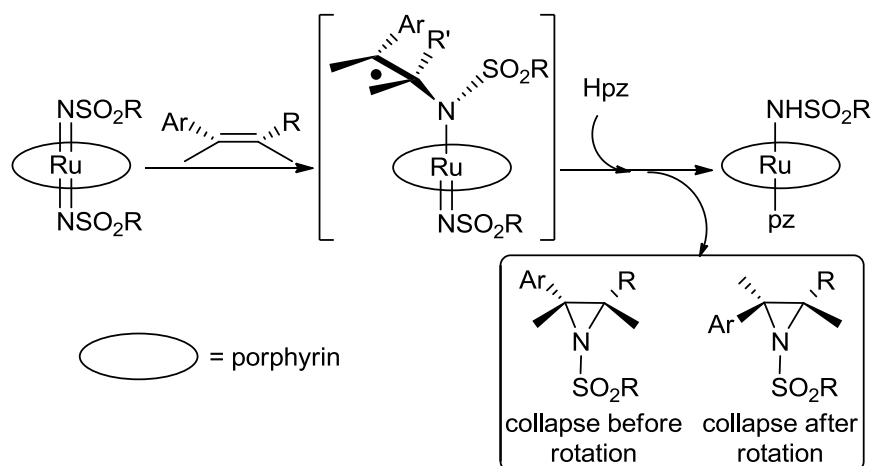


**Scheme 1.23.** Marchon mechanism for the **16** and **17**-catalyzed aziridination of styrenes.

The authors proposed that each metal centre favours only one of the two competing mechanisms illustrated in Scheme 1.23. Complex **16** induces a concerted mechanism (Scheme 1.23, path a) while in the case of **17** a two step radical process (Scheme 1.23, path b) allows an internal rearrangement.

Ruthenium porphyrins showed a very good catalytic activity in aziridination reaction with iminoiodinanes,<sup>207</sup> even in enantioselective reactions.<sup>175</sup> If the reaction is conducted using the  $\text{RNH}_2/\text{PhI}(\text{OAc})_2$  protocol, intramolecular aziridinations can also be performed.<sup>203</sup>

The aziridination is non-stereospecific with a partial loss of the alkene stereochemistry with the consequent formation of a mixture of *cis*- and *trans*-aziridines. Thanks to the isolation of several ruthenium imido complexes (Scheme 1.19), a very rigorous mechanistic study on the nitrene transfer reaction from an imido compound to an alkene was carried out.<sup>175, 208, 210</sup> Kinetic and spectroscopic investigations allowed to postulate that the alkene aziridination should occur through the rate-limiting formation of a carboradical intermediate<sup>208</sup> that can undergo C–C bond rotation prior to the ring closure to produce aziridines (Scheme 1.24).



**Scheme 1.24.** Stoichiometric aziridination of alkenes by ruthenium imido porphyrin complexes.

This mechanistic hypothesis is in accord with that already proposed for the manganese catalyzed aziridination.<sup>214</sup>

The stoichiometric reaction was run in the presence of pyrazole (Hpz) to isolate again the (porphyrin)Ru(NHSO<sub>2</sub>R)(pz) complex<sup>207</sup>. As previously described for the stoichiometric ruthenium porphyrin C–H amidation, in the absence of Hpz, several unidentified porphyrin species were formed.<sup>208 210</sup>

Che and co-workers have also studied the effect of the electronic properties of the imido ligand on the aziridination of styrene-type substrates.<sup>210</sup> Kinetic studies showed that better results are achieved employing very electron deficient imido complexes indicating an electrophilic nature of the nitrene functionality in the attack to the alkene.

### 1.5.2. Chloramine-T and bromamine-T as nitrene sources

In spite of the extensive use of iminoiodinanes, there are some limitations for a practical application of this class of reagents. Firstly, they are not commercially available and frequently their syntheses are not simple. Moreover, ArI=NR are not always soluble in common organic solvents and the stoichiometric side product of the reaction is ArI. To overcome these synthetic problems, other nitrene sources such as chloramine-T, the alkylammonium salt of chloramine-T, and bromamine-T have been explored (Figure 1.13).

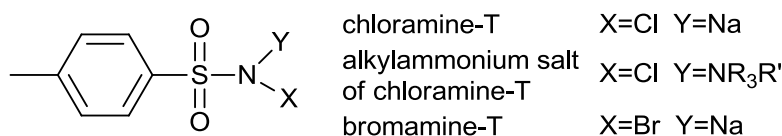
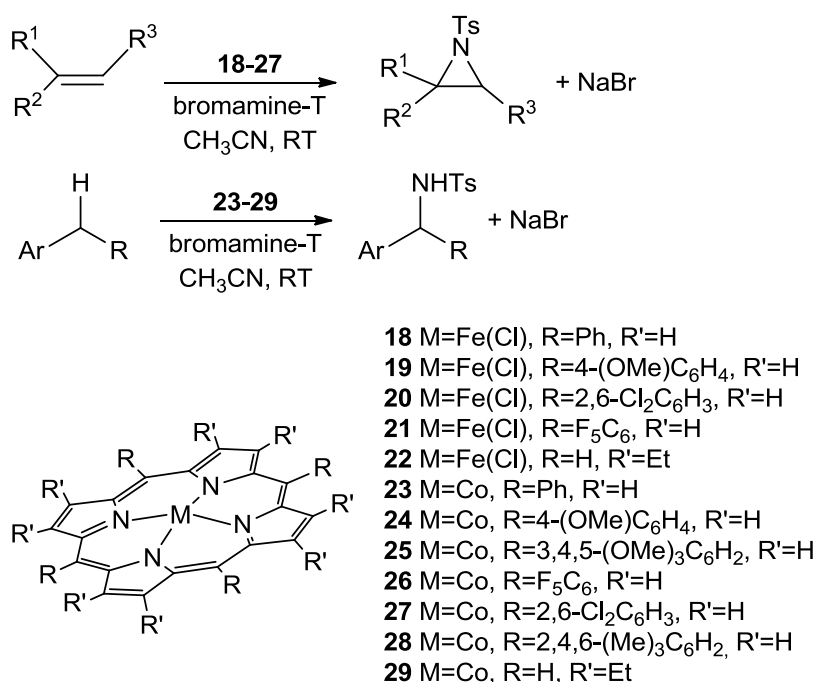


**Figure 1.13.** Chloramine-T, the alkylammonium salt of chloramine-T and bromamine-T.



In 1983<sup>215</sup> Barton and co-workers reported on the use of *in situ* generated ferrous chloride–chloramine-T complex for the amination and aziridination of several hydrocarbon substrates. Afterwards, chloramine-T has been employed in the presence of several catalytic systems.<sup>216-222</sup>

One inconvenience associated with the use of chloramine-T is its poor solubility in low polar solvents. To circumvent this problem some years ago Cenini and co-workers reported on the use of the alkylammonium salt of chloramine-T as aminating agent of cyclic olefins in the presence of iron or manganese porphyrin complexes in methylene chloride.<sup>223</sup> The corresponding allylic amines were obtained. On the other hand, by using a more polar reaction solvent such as CH<sub>3</sub>CN and bromamine-T as nitrene source, excellent results were achieved by Zhang's group (Scheme 1.25).<sup>224-226</sup>



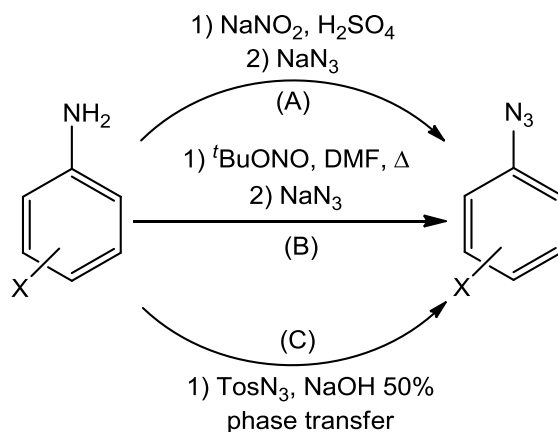
**Scheme 1.25.** Aziridination and C–H amidation with bromamine-T catalyzed by iron and cobalt porphyrin complexes.

Iron complexes **18–22** (Scheme 1.25) catalyzed the aziridination of aromatic, aliphatic, cyclic, and acyclic olefins, as well as  $\alpha,\beta$ -unsaturated esters. Using a 5 mol% catalyst loading and the hydrocarbon as the limiting agent,<sup>224</sup> yields up to 80% were obtained with NaBr as by-product. Unfortunately, the stereospecificity of the reaction was only moderate for 1,2-disubstituted olefins. Better catalytic results were achieved with cobalt complexes **23–27** (Scheme 1.25).<sup>225</sup> With a 5 mol% catalyst loading, aziridines yields up to 94% were obtained. Alpha and beta substituted styrenes, cyclic and linear olefins were aziridinated under mild conditions with alkenes as limiting agents. The same catalytic system was also used for the amination of  $sp^3$  C–H bonds<sup>226</sup> in the presence of catalytic amounts of **23–29** (Scheme 1.25). Benzylic amines were formed in good yields.

### 1.5.4. Organic azides as nitrene sources

The chemistry of organic azides,  $\text{RN}_3$ , as nitrogen sources have been explored to a large extent in the last few years due to the high synthetic versatility of this class of molecules.<sup>227, 228</sup> The lability of the  $\text{N}\alpha\text{-N}\beta$  bond of the  $\text{N}_3$  group allows the generation of a nitrene unit, "RN", with the eco-friendly molecular nitrogen being the only reaction side-product. Therefore, organic azides can be considered as atom-efficient nitrene transfer reagents.

The simplest route for their preparation involves diazotization of the corresponding anilines in acidic media followed by addition of sodium azide (Scheme 1.26, path A). This methodology, that will be adopted for the preparation of aryl azide used for this work, is easily carried out multi-gram scales. Depending on the feature of the functional group present in the starting aniline, also neutral (Scheme 1.26, path B) and basic (Scheme 1.26, path C) conditions are available for their synthesis.

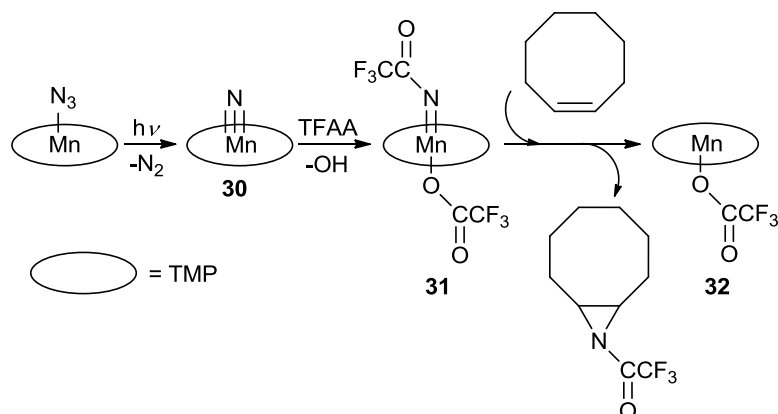


**Scheme 1.26.** Main synthetic routes for the preparation of aryl azides. Detailed examples by using path A will be described in the Experimental Section.

The nitrene transfer from  $\text{RN}_3$  to an organic substrate can be performed by thermal or photochemical activation,<sup>229, 230</sup> but drastic experimental conditions are required and very often the chemoselectivity of the reaction is not easily controlled. The best results have been achieved in intramolecular reactions that represent a useful methodology to lead to aza-heterocycles.<sup>231</sup> To improve the selectivity of intermolecular nitrene transfer reactions and to use milder reaction conditions, the presence of a transition metal catalyst is required. The first metal-catalysed nitrogen atom-transfer from organic azide was reported by Kwart and Kahn, who demonstrated that copper powder promoted the decomposition of benzenesulfonyl azide when heated in cyclohexene.<sup>232, 233</sup> More recently, organic azides as aminating agents were largely employed by Katsuki's group that reported in several papers the activity of ruthenium Schiff base complexes to catalyse aziridination and allylic C–H amination of olefins even with excellent enantioselectivity.<sup>234, 235</sup>

The first example of a nitrene transfer reaction from an imido porphyrin metal complex to olefins to give aziridines was due to Groves and Takahashi.<sup>236</sup> They reacted  $\text{Mn}(\text{TMP})(\text{N})$  (**30**) with trifluoroacetic anhydride

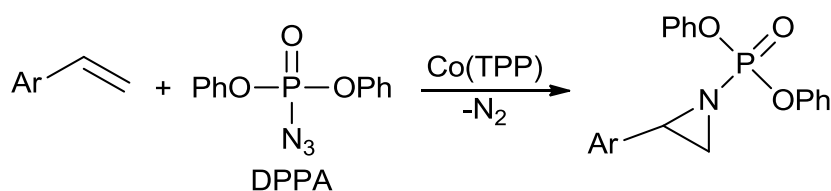
(TFAA) to give the imido complex (**31**). The addition of cyclooctene gave Mn(TMP)(TFA) (**32**) (TFA = trifluoroacetate) and the (trifluoroacetyl)aziridine of cyclooctene (Scheme 1.27).



**Scheme 1.27.** The stoichiometric formation of (trifluoroacetyl)aziridine of cyclooctene.

It is worth noting that the starting material for the aziridine formation was not an organic azide, but a metal-azido adduct that yielded by the photochemical activation of the metal-nitride complex **30**.

The stoichiometric reaction of the latter complex with TFAA was responsible for the synthesis of the imido complex **31**, the active species in the amination reaction of cyclooctene. The use of cobalt porphyrin complexes allowed performing aziridination of olefins in a catalytic way by using organic azides. Zhang and co-workers<sup>237</sup> reported on the use of diphenylphosphoryl azide (DPPA) as the nitrene source in the aziridination of styrenes by Co(TPP). The methodology allowed the synthesis of synthetically valuable *N*-phosphorylated aziridines in good yields (Scheme 1.28).

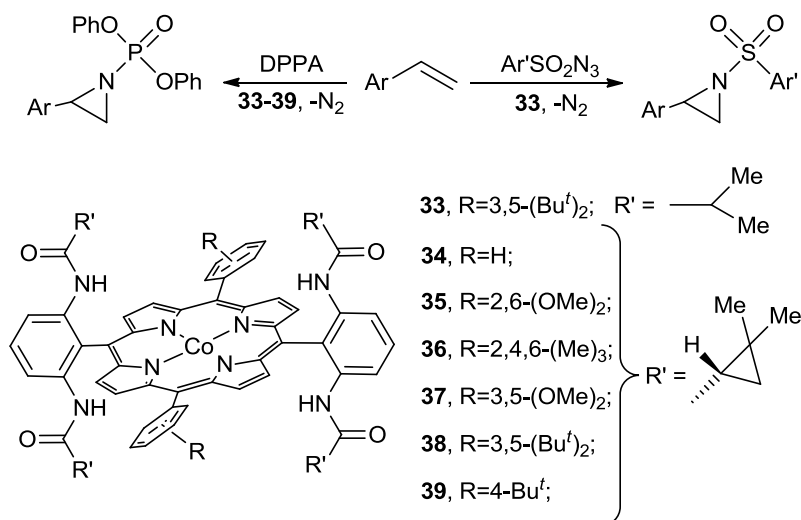


**Scheme 1.28.** Synthesis of *N*-phosphoryl aziridines.

It should be noted that *N*-phosphorylated aziridines offer advantages as synthetic building blocks because the protecting group can be easily displaced to yield non substituted aziridines.

Zhang and co-workers demonstrated that the efficiency of the Co(porphyrin)-based catalytic system is strictly correlated to the nature of the azide/catalyst couple. In fact, whilst arylsulfonyl azides did not react with olefins in the presence of Co(TPP), aziridines were efficiently formed if a different cobalt catalyst was employed. The authors synthesized the cobalt porphyrin complex **33** to block, by hydrogen-bonding interactions, the sulfonyl azide to the cobalt centre in the catalytic intermediate species.<sup>238</sup> The general

synthesis illustrated in Scheme 1.29 was efficient for the synthesis of several arylsulfonyl aziridines in yield up to 98%.



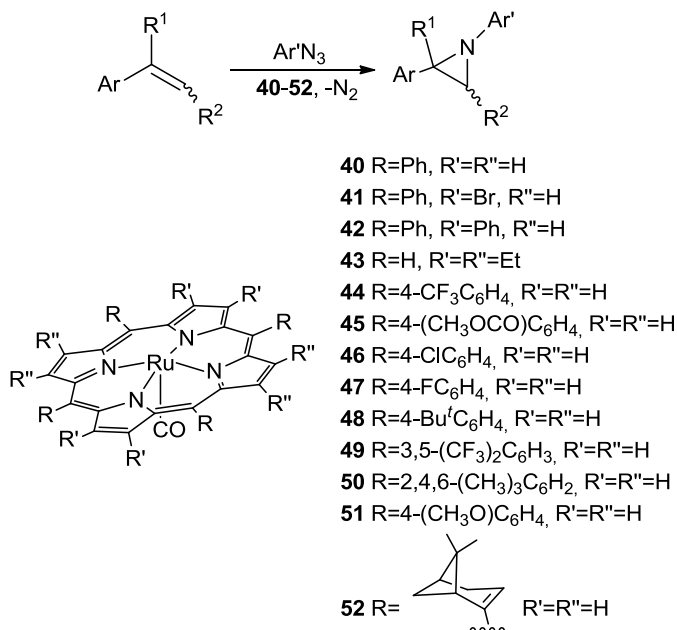
**Scheme 1.29.** Synthesis of *N*-arylsulfonyl and *N*-phosphoryl aziridines.

The modification of the skeleton of the porphyrin ligand of complex **33**, afforded the series of *D*<sub>2</sub>-symmetric chiral porphyrins **33–29** (Scheme 1.29).<sup>239</sup> The catalysts afforded *N*-phosphorylated aziridines in moderate to good yields with acceptable degree of asymmetric induction. The best ee, 71%, was reached using styrene as substrate and complex **38** as catalyst. Zhang and co-workers observed that the reaction performance strongly depends on the nature of the solvent and axial ligand employed. The reaction was inhibited by a coordinating solvent such as tetrahydrofuran and negative effect was also observed in the presence of nitrogen-based ligands with strong coordinating ability. Conversely, better results have been achieved using chlorobenzene as solvent and DMAP (4-dimethylamino pyridine) as additive. Organic azides are also active aminating agents in the presence of ruthenium porphyrin complexes.

As we shall see in the following our group exploited the activity of aryl azides as nitrene precursors. It should be noted that, contrary to phosphoryl and arylsulfonyl groups, the aryl group on the aziridine nitrogen should be considered part of the molecule, which can play an important role in further aziridine rearrangements rather than to be a protective group. Several aryl azides, olefins and Ru(porphyrin)CO complexes were tested to investigate the scope of the reaction. Quantitative yields and short reaction times have been achieved using terminal olefins and aryl azides bearing electron withdrawing groups on the aryl moiety.<sup>240</sup> The general route illustrate in Scheme 1.30 has been used for several olefins and azides employing catalysts **40–52**.

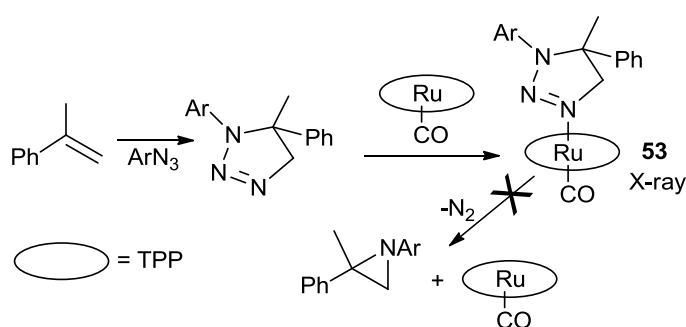
Using the commercially available catalyst Ru(TPP)CO (**40**) a very high TON (2300), for the amination of  $\alpha$ -methylstyrene by 4-nitrophenyl azide was obtained by our research group some years ago. Preliminary studies on enantioselective aziridination of styrenes by chiral ruthenium porphyrin complex **52** afforded low enantioselectivities.<sup>241</sup> We have also performed a kinetic study of the  $\alpha$ -methylstyrene aziridination. The reaction rate linearly increased with the olefin concentration up to a point where a decrease in rate was

observed upon further increase of the olefin amount. This behaviour was due to the competitive formation of a triazoline compound by the uncatalyzed cycloaddition of 4-nitrophenyl azide to  $\alpha$ -methylstyrene.



**Scheme 1.30.** General route for the synthesis of *N*-aryl aziridines.

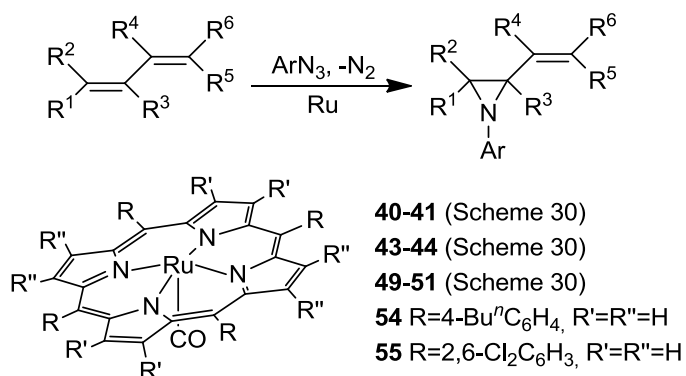
Triazoline molecules were often presented as intermediates in the aziridine formation<sup>242-244</sup> but it was demonstrated that it competes with the azide for the coordination to the metal centre inhibiting the catalytic process.<sup>245</sup> We have isolated and characterized by crystal diffraction analysis the catalytically inactive ruthenium complex **53** (Scheme 1.31) and shown that the axial ligand triazoline is never transformed into the corresponding aziridine even under forcing conditions.



**Scheme 1.31.** Synthesis of complex **53**.

To widen the scope of the methodology, was explored the Ru(CO)(porphyrin) complexes-catalyzed aziridination of conjugated dienes by aryl azides. This reaction allowed the synthesis of *N*-aryl-2-vinylaziridines, a class of very reactive organic building blocks thanks to the simultaneous presence of both

an aziridine ring and a double bond that easily induce ring-opening<sup>246, 247</sup> or ring-expansion<sup>248-251</sup> reactions. Several hydrocarbons and azides were tested and the protocol can provide *N*-aryl-2-vinylaziridines with excellent chemoselectivities (Scheme 1.32).<sup>252</sup>



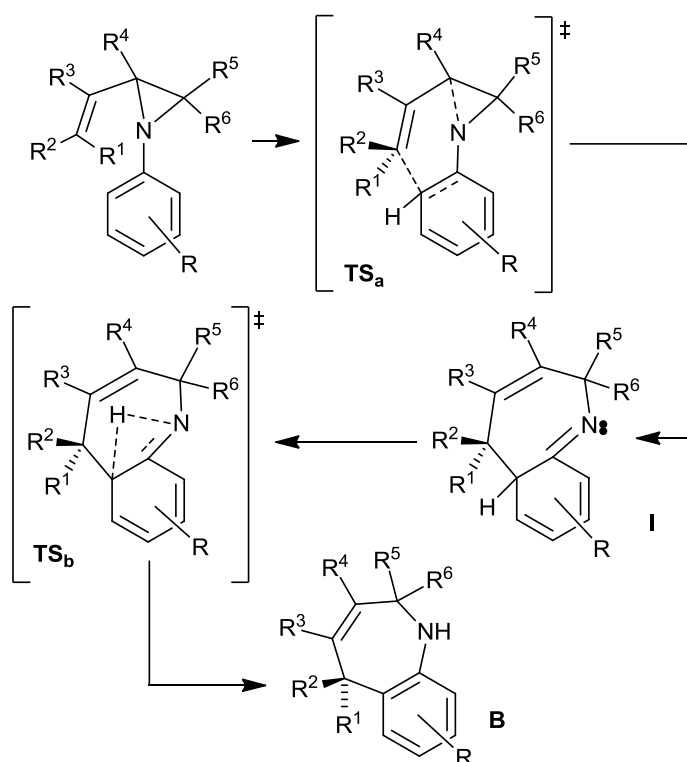
**Scheme 1.32.** Ruthenium-catalyzed synthesis of *N*-aryl-2-vinylaziridines.

The crucial step to obtain *N*-aryl-2-vinylaziridines is the purification procedure and a lowering of the yields can be observed during the chromatographic process even when using deactivated silica. We turned the great instability of *N*-aryl-2-vinylaziridines into an advantage promoting an isomerization processes, the Claisen rearrangement, to form 2,5-dihydro-1*H*-benzo[*b*]azepines (Scheme 1.33, **B**) in yield up to 65%. Moreover, to gain insight into the mechanism of the reaction, we carried out theoretical calculations using density functional theory methods (Scheme 1.33).<sup>253</sup>

Collected data indicated that this sigmatropic rearrangement would involve the attack of the vinyl group to the aryl ring with a concomitant C-N bond cleavage of the aziridine moiety leading to an imine intermediate **I**, followed by an aromatization with a concomitant proton shift from the aryl moiety to the nitrogen and a double bond shift from the imine to the aryl ring to yield the final benzazepine product **B**.

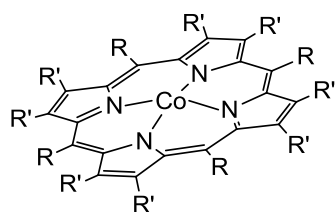
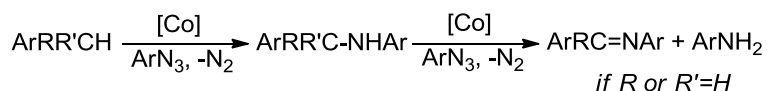
It should be noted that isomerization reactions of *N*-aryl-2-vinylaziridines can also afford dihydropyrroles depending on both the steric properties of the starting diene and the experimental conditions employed for the rearrangement.<sup>253</sup>

To prepare catalysts more stable, selective and easily recovered and recycled, we investigated the preparation and characterization of new catalytic polymeric membranes based on Hyflon AD60X polymer, entrapping Ru(4-(CF<sub>3</sub>)TPP)CO without any covalent bond formation.<sup>254</sup> The catalytic heterogeneous membranes afforded aziridines with 90–99% selectivities. In several cases the membrane was reused three times with a catalyst leaching ≤6%, but no decrease in selectivities upon recycle.<sup>255</sup>



**Scheme 1.33.** Proposed mechanism for the aza-[3,3]-Claisen rearrangement of *N*-aryl-2-vinylaziridines to benzoazepines **B**.

Organic azides can be largely employed as reagent for C-H aminations. A few years ago, Cenini's group published the first synthesis of benzylic amines and imines from hydrocarbons containing a benzylic group catalyzed by cobalt porphyrin complexes **56**–**59** (Scheme 1.34).<sup>256, 257</sup>



- 56** R=Ph, R'=H
- 57** R=4-(OMe)C<sub>6</sub>H<sub>4</sub>, R'=H
- 58** R=4-ClC<sub>6</sub>H<sub>4</sub>, R'=H
- 59** R=H, R'=Et

**Scheme 1.34.** Cobalt porphyrins catalyzed synthesis of benzylic amines and imines.

As illustrated in Scheme 1.34, arylazides reacted with the hydrocarbons to form the corresponding benzylic amines and, if R or R' was a hydrogen group, the reaction proceeded further to give the imine. The study of the reaction scope revealed that a wide range of aminated products can be achieved also because of the synthetic availability of aryl azides. The reaction proceeds in good yields when the aromatic azide bears electron-withdrawing substituents and the hydrocarbons are sterically non encumbered. The mechanism of the reaction was also investigated; kinetic and spectroscopic studies indicated that the first step of the amination reaction is a reversible coordination of the aryl azide to the cobalt atom to generate a

cobalt-azido adduct in which the  $\text{ArN}_3$  assumes a pocket conformation that prevents a too close approach of the incoming hydrocarbon (Figure 1.14).

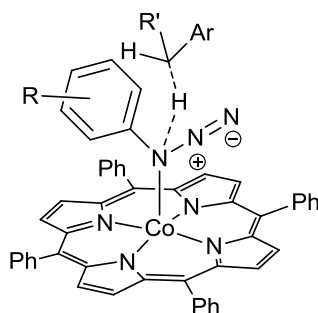
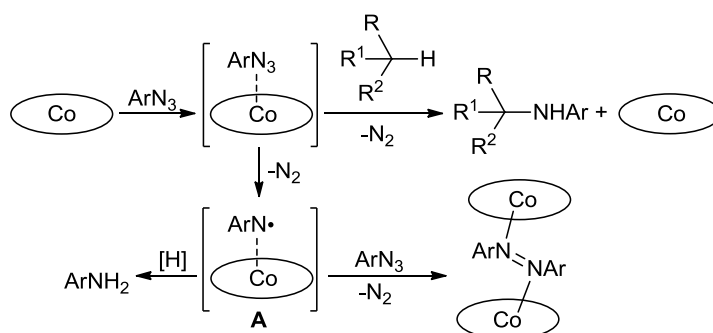


**Figure 1.14.** Proposed transition state for the C–H amination reaction with  $\text{ArN}_3$ .

The hypothesis formulated in Figure 1.14 was corroborated by the large isotopic effect observed when deuterated toluene was used instead of toluene as hydrocarbon substrate. The rate of the amination reaction of toluene was 14 times larger than the rate of the amination of deuterated toluene, indicating an isotopic tunnelling effect.<sup>258, 259</sup> Cobalt porphyrin complexes catalyzed as well C–H aminations of non-activated olefins<sup>260</sup> to form allylic amines in moderate to good yields. Kinetic and spectroscopic studies have shown that also in the present system the often postulated cobalt-imido complex was not the catalytic intermediate. It was also proposed that in the allylic C–H amination the occurrence of a reversible interaction between the cobalt porphyrin and the arylazide. This azido-adduct can either react with the hydrocarbon to yield the allylic amine, or lose molecular nitrogen in an uni-molecular reaction to afford an intermediate, formulated as a true imido complex **A**, responsible for the formation of by-products diazene and aniline (Scheme 1.35).



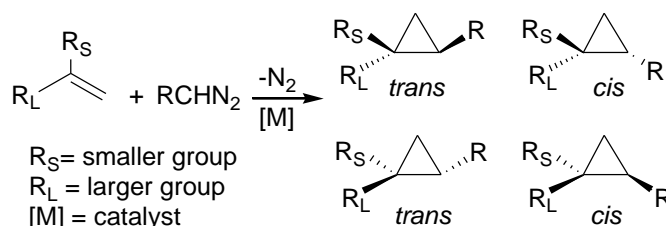
**Scheme 1.35.** Proposed mechanism for the allylic C–H amination.

## 1.6. The Metallo Porphyrin-Catalysed Cyclopropanation Reactions

Three-membered carbon rings, namely cyclopropanes, are an important class of molecules, both for their employment as building blocks in organic chemistry and for their presence in compounds presenting pharmaceutical properties.<sup>261, 262</sup> The scientific interest in developing new strategies for the synthesis of



cyclopropanes has steadily increased since Nozaki and Noyori reported the first copper-mediated enantioselective cyclopropanation.<sup>263</sup> Cyclopropanes can be obtained by a thermal or photochemical activation of a diazo compound,  $RR'CN_2$ , that transfers the carbene moiety  $[RR'C]$  to an unsaturated double bond. However, extreme experimental conditions are required and very often it is not possible to control the selectivity of the reaction because of the formation of free carbenes. To improve the selectivity of intermolecular carbene transfer reactions and to use milder reaction conditions, the presence of a transition metal catalyst is required.<sup>264</sup> The general reaction reported in Scheme 1.36 yields a mixture of two diastereoisomers (*cis* and *trans*), each of them exist as a pair of enantiomers.



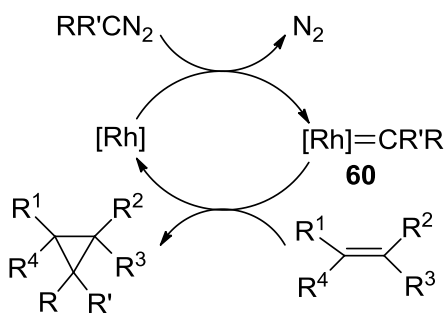
**Scheme 1.36.** Cyclopropanation of olefins by diazo compounds.

As a result of the requirement of the chemical industry for efficient syntheses of fine chemicals, one of the major challenges for chemists is the development of extremely selective reactions. In the field of cyclopropanation, it is essential to optimise the diastereoselectivity and/or the enantioselectivity of the reaction. Whilst enantioselective reactions have been successfully achieved by employing several catalytic systems, only a few catalysts capable of achieving high diastereoselectivities with a wide range of substrates are known.<sup>265</sup>

Among catalytic systems employed in cyclopropanations, those based on porphyrins surely play a prominent role.<sup>182, 266-272</sup> Herein we discuss some important examples that have resulted a significant progress in this field.

### 1.6.1 Rhodium-catalysed reactions

The catalytic competence of dirhodium(II) tetraacetate,  $Rh_2(OAc)_4$ , to promote the cyclopropanation of olefins by decomposition of diazo derivatives was reported several years ago.<sup>273-277</sup> Since then, several dirhodium compounds have been synthesised by replacement of acetates with other ligands, and very good results in both enantio- and diastereoselectivity have been achieved.<sup>278-283</sup> In the 1980s,<sup>274, 284</sup> the formation of a metal carbene intermediate for rhodium catalysed cyclopropanations was first proposed, and more recent theoretical papers have supported this hypothesis.<sup>285, 286</sup> According to the general catalytic cycle (Scheme 1.37),<sup>282</sup> the first step of the cyclopropanation is the formation of an electrophilic metal carbene intermediate (**60**) that transfers the carbene unit to the incoming olefin to yield the cyclopropane.



**Scheme 1.37.** General mechanism for olefin cyclopropanation catalysed by rhodium complexes.

Up to now, much evidence regarding the formation of complex **60** has been provided, but, to the best of our knowledge, the formation of a carbene complex from a dirhodium compound was never established by spectroscopic or analytical methods.

Assuming the catalytic intermediate to be a carbene complex, the diastereocontrol of carbene transfer to an olefin is modulated by the nature of the diazo compound and the ligands on rhodium.  $\text{Rh}_2(\text{OAc})_4$  is known to give good diastereoselectivities only when diazo compounds bearing bulky substituents are used, whereas the cyclopropanation of olefins by the simple and commercially available ethyl diazoacetate (EDA) occurs with moderate stereocontrol (*cis/trans* = 38:62).<sup>265</sup>

The influence of ligands on the activity of rhodium complexes to improve the *cis/trans*-cyclopropane ratio was initially reported by Callot et al. in a paper in which the catalytic activity of the rhodium porphyrin complex  $\text{Rh}(\text{TPP})\text{I}$  (TPP = dianion of tetraphenyl porphyrin) was established (Figure 1.15).<sup>287</sup>

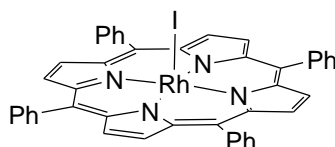


**Figure 1.15.** Molecular structure of  $\text{Rh}(\text{TPP})\text{I}$ .

The large steric effect of the porphyrin ligand on the catalytic activity of the metal centre can be exploited for a diastereoface discrimination yielding up to 87% of *cis*-cyclopropane with EDA as carbene source, *cis*-olefins and porphyrin catalysts with different bulkiness on the peripheral substituents. The authors proposed that the olefin can approach a putative carbene perpendicularly (Figure 1.16-a) or in parallel (Figure 1.16-b). For internal olefins, a perpendicular approach would be more favoured than the parallel for steric reasons. Conversely, a terminal olefin can react with the intermediate carbene in a parallel approach.

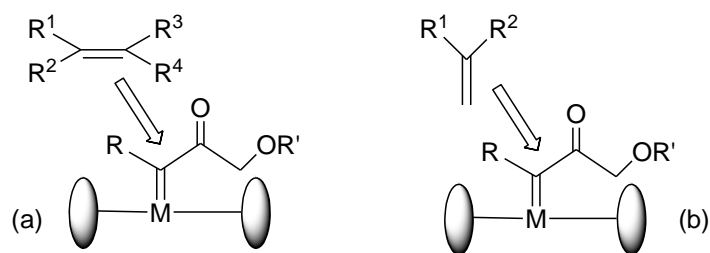
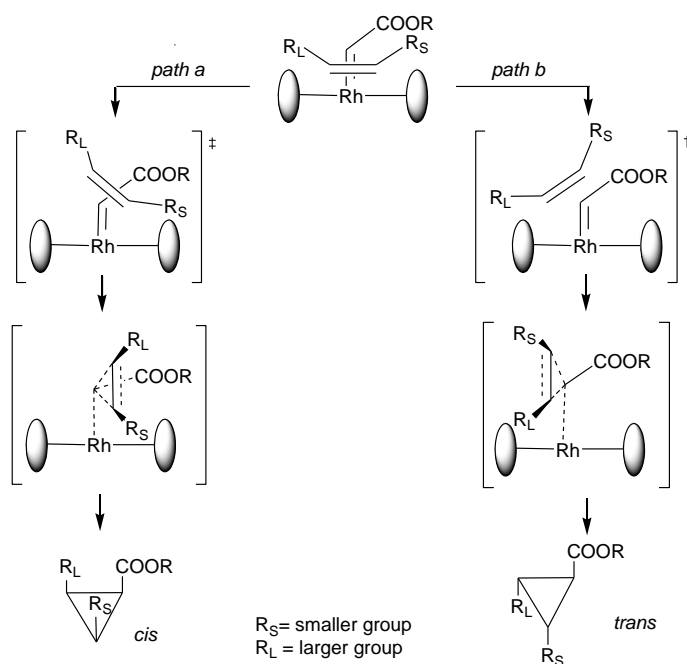


**Figure 1.16.** Perpendicular (a) and parallel (b) approach of an olefin to a putative carbene intermediate.

An explanation of the observed diastereoselectivity was proposed by Kodadek et al., who suggested that the cyclopropanation occurs with the concerted mechanism shown in Scheme 1.38.<sup>288</sup> According to Kodadek's proposal, the perpendicular approach of a *cis*-substituted olefin to the active carbene site pushes the larger group  $R_L$  as far away as possible from the ester group of the diazo fragment. In this scenario, there could be two possible pathways depending on the steric hindrance of the porphyrin ligand and the ester group of the carbene.

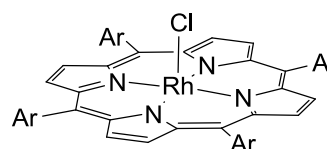


**Scheme 1.38.** Mechanistic hypothesis for the cyclopropanation of unsymmetrical olefins catalysed by rhodium porphyrin complexes. (The porphyrin is represented as a line and the *meso*-aryl groups as ovals).

When bulky *meso*-aryl substituents are present on the porphyrin skeleton, *path a* will be preferred to minimise  $R_L$ -porphyrin interactions. The resulting clockwise rotation of the olefin, on the axis orthogonal to the rhodium-carbon bond, causes the formation of the *cis* diastereoisomer. On the other hand, a very high steric hindrance of the ester group provokes a counterclockwise rotation (Scheme 1.38, *path b*) with the

consequent formation of the *trans*-cyclopropane. This mechanistic hypothesis can explain the high *cis/trans* diastereoselectivity observed by Callot with porphyrin catalysts bearing bulky *meso*-aryl groups.

The influence of the steric hindrance of the porphyrin ligand in controlling the diastereoisomeric ratio of cyclopropanations was also investigated by Tagliatesta et al.<sup>289</sup> The electronic and steric properties of porphyrins were modulated by introducing different groups to the *ortho*-positions of the *meso*-aryl rings and  $\beta$ -positions of pyrroles. Some results on the cyclopropanation of three olefins by EDA are shown in Figure 1.17.



	styrene		cyclohexene		norbornene	
	$\frac{cis}{trans}$	yield %	$\frac{cis}{trans}$	yield %	$\frac{cis}{trans}$	yield %
<b>61</b> : Ar = 2,6(OCH <sub>3</sub> ) <sub>2</sub> C <sub>6</sub> H <sub>3</sub>	0.4	88.8	0.9	59.1	1.5	55.6
<b>62</b> : Ar = 2,6(Cl) <sub>2</sub> C <sub>6</sub> H <sub>3</sub>	1.7	43.7	1.5	80.1	3.5	50.2

**Figure 1.17.** Cyclopropanation of styrene, cyclohexene and norbornene catalysed by rhodium catalysts **61** and **62**.

The *cis/trans* ratio of the reaction catalysed by **61** depends on the nature of the olefin. With styrene, the *trans* diastereoisomer becomes the major product, although the cyclopropanation of norbornene gives a reasonable yield of *cis*-cyclopropane. This experimental result can be due to the formation of a transition state in which the phenyl group of styrene is pushed far away from the ester group of the carbene intermediate already pointing towards the *orthomethoxy* groups of the aryl moieties.<sup>290</sup> According to the authors, this process is more difficult for norbornene because of its low flexibility, consequently the stereoselectivity of the reaction is controlled by the steric interactions between the olefin and the porphyrin, and a higher *cis/trans* ratio was obtained. This effect was enhanced when methoxy groups were replaced by chlorine to give complex **62**. The *cis*-selectivity observed with every olefin, when employing **62** as catalyst, indicated that the mechanism reported by Kodadek was operative.<sup>288</sup>

An inversion of the reaction diastereoselectivity was observed by replacing porphyrins with *N*-confused porphyrins. Rhodium complexes shown in Figure 1.18 exhibited very good catalytic activity, styrene was cyclopropanated in yields up to 93% and a *trans/cis* ratio of 98:2.<sup>291</sup>

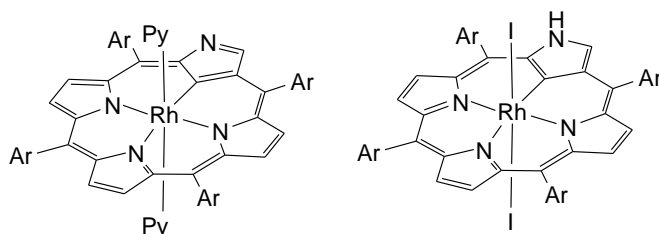
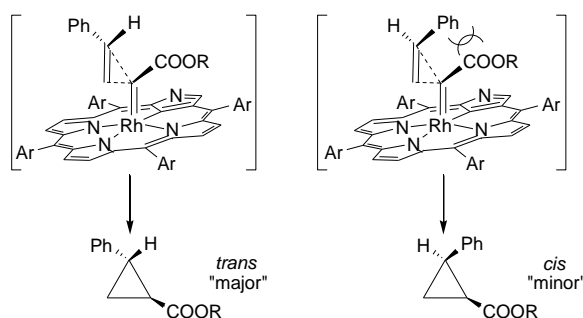


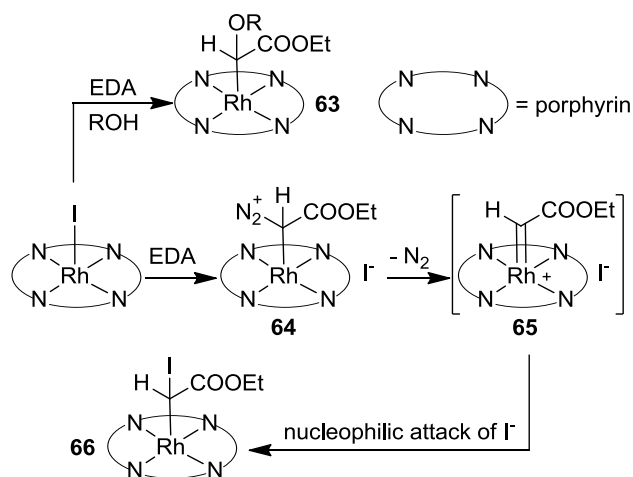
**Figure 1.18.** Cyclopropanation of styrene catalysed by rhodium *N*-confused porphyrins.

The best results were obtained by employing *tert*-butyl diazoacetate as the carbene source; however, the reaction of EDA with styrene gave the corresponding cyclopropanes in yields up to 92% and a *trans/cis* ratio of 91:9. According to the authors, the diastereoselectivity inversion, *trans/cis* ratio > 1, could be due to the electronic differences between the two classes of ligands. The authors suggested that the higher back-donating effect of rhodium *N*-confused porphyrins would stabilise the carbene intermediate with the consequent formation of a late transition state. In such a scheme the terminal olefin approaches the carbene moiety in a parallel fashion, and the stabilisation of the electrophilic carbene should allow the olefin to come much closer to the active site, which results in the preferred formation of the *trans* isomer (Scheme 1.39). Conversely, the perpendicular approach of the internal olefin and an early transition state (Scheme 1.38) proposed by Kodadek should favour the formation of *cis*-cyclopropane when the reaction is run in the presence of bulky rhodium porphyrins. The mechanism of the cyclopropanations mediated by rhodium *N*-confused porphyrins was not investigated in detail; therefore, in our opinion, further studies are necessary to confirm the mechanistic hypothesis reported above.



**Scheme 1.39.** Proposed transition state for the cyclopropanation of styrene catalyzed by rhodium *N*-confused porphyrins.

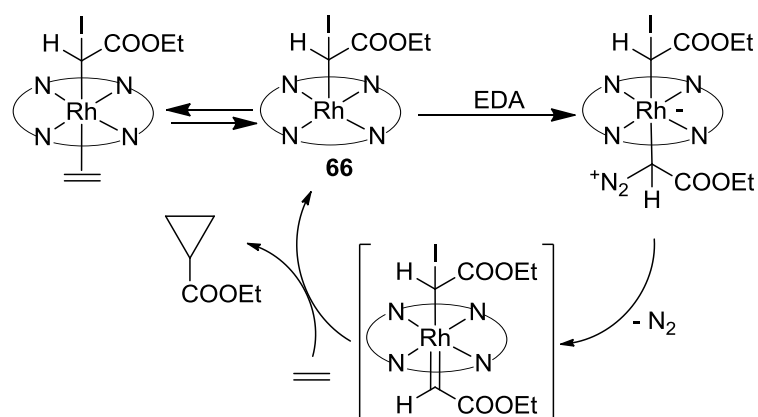
All data reported up to now indicates a strong dependence of the reaction stereoselectivity on the nature of the porphyrin skeleton. It is also clear that the design of the appropriate ligand is enabled by the comprehension of the reaction mechanism. With this idea in mind, the first study on the reactivity of rhodium(III) porphyrins towards diazo compounds was performed by Callot, who analysed the reaction of Rh(TPP)I with EDA in the presence of alcohols. It was suggested that the isolated alkylrhodium(III) porphyrin **63** (Scheme 1.40) should result from the addition of the alcohol to an intermediate carbene species.<sup>292</sup>



**Scheme 1.40.** Stoichiometric reaction of EDA with Rh(TPP)I in the absence of an olefin.

A more detailed study of the mechanism of cyclopropanation catalysed by rhodium porphyrins was then performed by Kodadek et al. in an interesting series of papers.<sup>293-295</sup> They demonstrated that the first step of the stoichiometric reaction between Rh(TPP)I and EDA was the coordination of the diazo compound to the metal centre to give complex **64** (Scheme 1.40). The following release of molecular nitrogen yielded a supposed carbene complex **65**, too reactive to be either isolated or spectroscopically identified. In the absence of an olefin, complex **65** yielded the rhodium alkyl species **66**, which was fully characterised by NMR spectroscopy.

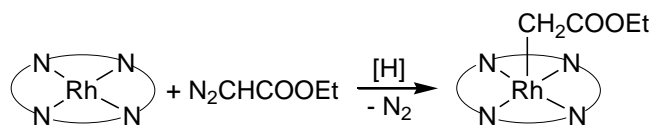
The formation of adduct **64** between rhodium porphyrin and EDA was detected at a low temperature of -40 °C by IR and NMR spectroscopy. By warming the reaction solution, complex **64** was transformed into **66** with the evolution of molecular nitrogen. Complex **65** was never identified, but a kinetic study supported the formation of such carbene intermediates. Complex **66** showed good catalytic activity. Scheme 1.41 reports a plausible catalytic cycle in which **66** is involved.<sup>295</sup>



**Scheme 1.41.** Proposed mechanism for the cyclopropanation of olefins catalysed by iodo-rhodium porphyrin.

The authors suggested that the olefin, in addition to being the substrate, can inhibit the reaction by competing with EDA for the coordination on the free axial position. The reversible coordination of olefins was

established by UV spectroscopy and can explain why different olefins react at different rates even though kinetics indicate carbene formation as the rate-determining step of the reaction. It should be noted that up to now every attempt to isolate a carbene complex from the reaction of rhodium(III) porphyrins with diazo compounds has failed. Even the reaction of rhodium(II) complexes with EDA yielded rhodium(III) porphyrin alkyl compounds by abstraction of a hydrogen atom from the diazo compound (Scheme 1.42).<sup>296</sup>



**Scheme 1.42.** Reaction between Rh<sup>II</sup>(porphyrin) complexes and EDA.

To improve the synthetic utility of cyclopropanations mediated by rhodium porphyrins, the use of diazo compounds, such as glycine ethyl ester, as precursors was also explored. By employing this methodology, several aromatic and aliphatic olefins were transformed into the corresponding cyclopropanes in good yields but unfortunately with low diastereoselectivity.<sup>297</sup>

Considering the high *cis*-selectivity of cyclopropanations mediated by rhodium porphyrins, some efforts have been made to fine-tune an enantioselective catalysis. Kodadek reported the synthesis of “chiral wall”<sup>298</sup> and “chiral fortress”<sup>166</sup> (compounds **67** and **68**, respectively) rhodium porphyrins that efficiently catalysed the cyclopropanation of different olefins with high turnover numbers. However, in spite of the good *cis/trans* diastereoselectivity observed in several cases, the enantiomeric excesses achieved were generally modest. Several years later, Che and co-authors reported *ee* values up to 68% by using the rhodium *D*<sub>4</sub>-porphyrin complex<sup>299</sup> **69**, but a common *trans*-diastereoselectivity was observed. The chiral complexes **67**, **68** and **69** are shown in Figure 1.19.

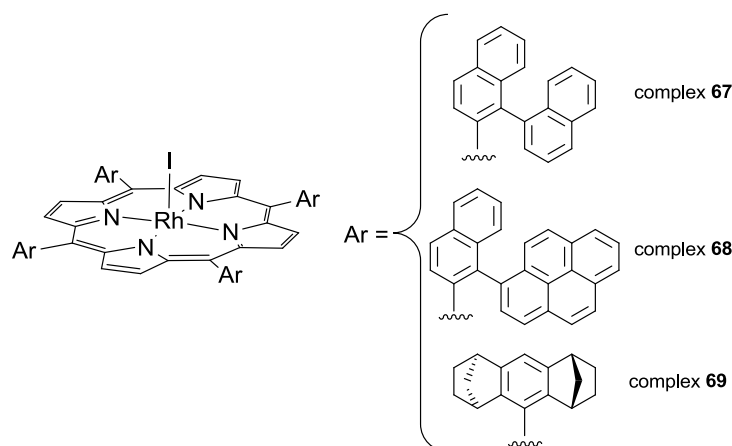


**Figure 1.19.** Molecular structures of complexes **67**, **68** and **69**.

In conclusion, all data reported up to now clearly indicate that to achieve a very high *cis*-stereochemical induction it is not sufficient to use porphyrin complexes bearing bulky groups. It is necessary to take into account other parameters such as steric properties of the diazo compounds and the olefins.

## 1.6.2. Cobalt-Catalysed Reactions

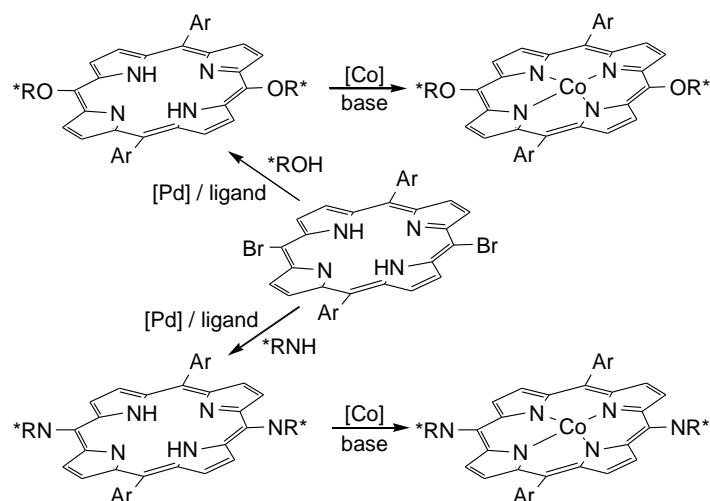
The catalytic activity of cobalt complexes in the stereoselective cyclopropanation of olefins was first established by Nakamura et al. by using cobalt(II) complexes of camphorquinonedioximes.<sup>300-302</sup> The reactions of several olefins with diazo compounds yielded the corresponding cyclopropanes with enantioselectivity up to 88% *ee*, but generally equal amounts of *cis* and *trans* isomers were obtained. Camphorderivative ligands were also employed by Jommi et al.<sup>303</sup> to synthesise cobalt(II) complexes that are active for the cyclopropanation of simple olefins such as 1-octene. The observed diastereoselectivity was low (*cis/trans* = 1:1.8) but the *trans* isomer reached 97% *ee*.

Both diastereo- and enantiocontrol in intermolecular cyclopropanations of olefins were independently reached by Katsuki and Yamada by using cobalt complexes of chiral Schiff bases and ketoiminato ligands, respectively.<sup>304</sup> Katsuki et al. demonstrated that the diastereoselectivity of the reaction can be driven towards the formation of the *trans* or the *cis* isomer by changing the oxidation state of the metal<sup>305-307</sup> and adjusting the steric and electronic properties of substituents on the C3(3') and C5(5') positions of the Schiff base.<sup>305, 308, 309</sup> For example, the reaction of styrene with  $\alpha$ -diazoacetate gave, in the presence of different cobalt catalysts, the corresponding *cis* and *trans* isomers with very high diastereo- and enantioselectivity. The *cis*-cyclopropane was obtained with 99% *dr* and 98% *ee*,<sup>310</sup> whereas the *trans* isomer was formed with 82% *dr* and 86% *ee*.<sup>311</sup>

Yamada et al. developed a catalytic system based on chiral ketoiminatocobalt(II) complexes to attain very good diastereo- and enantiomeric excesses.<sup>312</sup> The nature of the cobalt ligand promoted a *trans* selectivity; the cyclopropanation of styrene by EDA yielded 90% of the corresponding *trans*-cyclopropane with 96% *ee*.<sup>313</sup> The effect of the addition of a coordinating ligand, such as *N*-methylimidazole (NMI), to enhance the stereocontrol of cyclopropanation reactions was also investigated.<sup>314</sup> On the basis of theoretical analyses,<sup>315, 316</sup> it was suggested that the positive effect of a coordinating ligand is due to a reduction of the activation energy to form the cobalt-carbene intermediate, which results in a more efficient catalytic process.

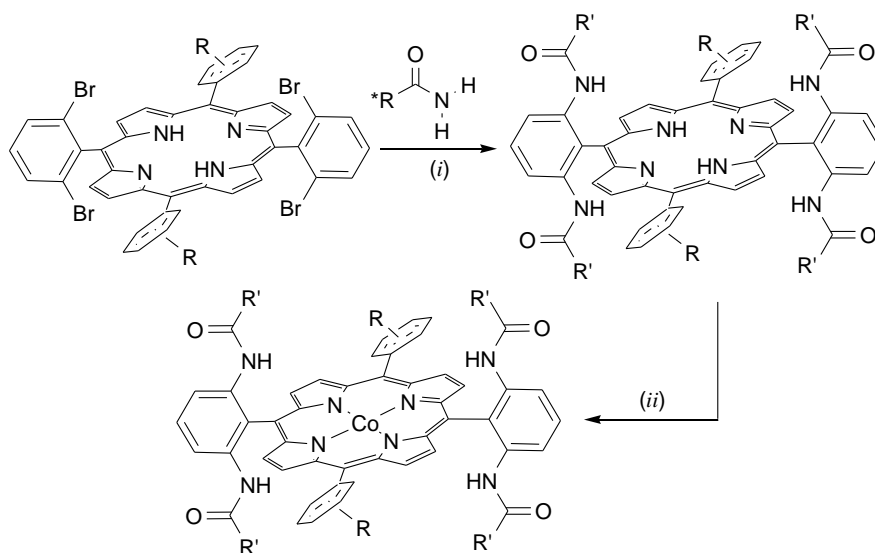
The catalytic activity of several cobalt complexes of modified Schiff bases,<sup>317-319</sup> terpyridines,<sup>320</sup> nitrogen macrocycles,<sup>321</sup> pincer ligands<sup>322</sup> and polyoxometallates<sup>323</sup> was also reported. However, porphyrin ligands represent, along with Schiff bases, the most frequently used class of ligands to synthesise cobalt cyclopropanation catalysts. The catalytic activity of achiral Co<sup>II</sup> porphyrin complexes in the cyclopropanation of olefins, independently reported by Zhang<sup>324</sup> and our group<sup>325</sup> in 2003, revealed a general *trans* selectivity and the absence of maleate and fumarate side products resulting from coupling reactions of EDA.<sup>326</sup> An enantiomeric version of cyclopropanations catalysed by cobalt porphyrins was then reported by Zhang et al. by using vitamin B<sub>12</sub><sup>327</sup> and *meso*-chiral porphyrin complexes<sup>328</sup> as catalysts. These last porphyrins were prepared by employing synthetic procedures reported in Scheme 1.43.





**Scheme 1.43.** Synthesis of *meso*-chiral cobalt porphyrin complexes.

The reaction of several olefins with EDA catalysed by vitamin B<sub>12</sub> afforded the *cis*-cyclopropane as the major isomer; the best recorded diastereo- and enantioselectivity were 67 and 78%, respectively. On the other hand, a *trans* selectivity was observed by running cyclopropanations in the presence of porphyrin complexes reported in Scheme 1.43, but unfortunately enantioselectivities were not satisfying. Since then, Zhang et al. developed the synthetic procedure<sup>329, 330</sup> shown in Scheme 1.44 by using bromoporphyrins as synthons, to reach a wide pool of chiral porphyrins with *D*<sub>2</sub> symmetry (Figure 1.20).



**Scheme 1.44.** Synthesis of chiral cobalt porphyrin complexes. (i) Pd(OAc)<sub>2</sub>/XantPhos, Cs<sub>2</sub>CO<sub>3</sub>; (ii) CoCl<sub>2</sub>, 2,6-lutidine.

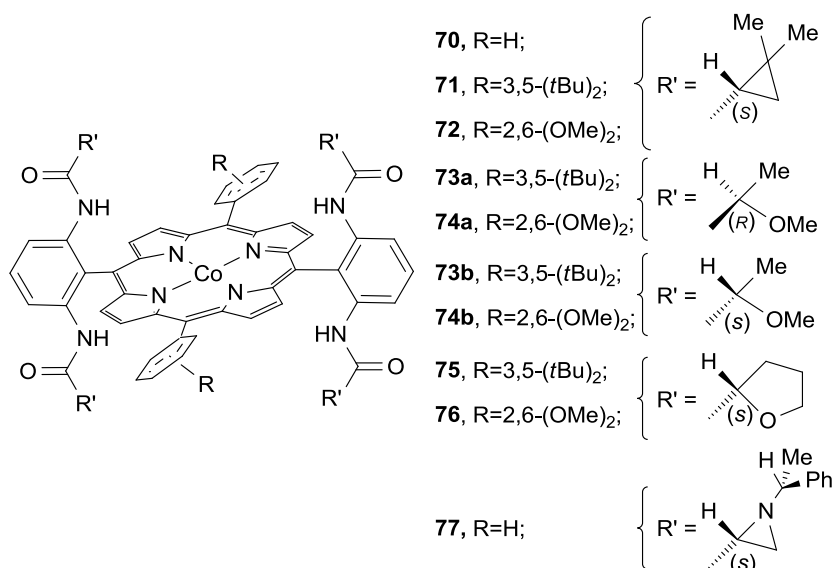
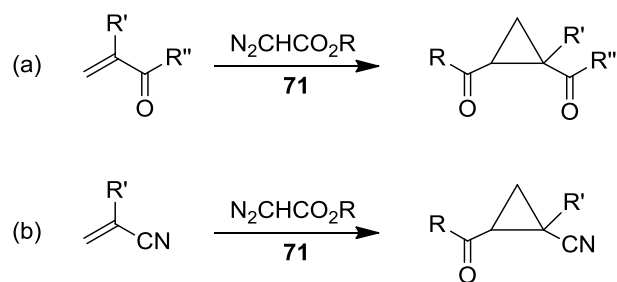


**Figure 1.20.** Chiral porphyrins used as cyclopropanation catalysts.

An initial screening of the catalytic activity of these porphyrins showed that both R and R' groups affect the reaction stereoselectivity, which can be strongly improved by adding a coordinating ligand.<sup>329</sup> The asymmetric cyclopropanation of styrene by *t*BDA (*tert*-butyldiazoacetate) run in the presence of 1% **71** and 0.5 equiv. [4-(dimethylamino)-pyridine] (DMAP) yielded cyclopropanes with a *trans/cis* ratio greater than 99:1 and 98% *ee*. The positive *trans* effect of DMAP was disclosed by studying the influence of several coordinating additives on the catalytic efficiency of the reaction.<sup>331</sup> It should be noted that DMAP must be used in a substoichiometric amount to avoid a partial inhibition of the reaction. Probably, when an excess of DMAP is employed, both axial coordinative sites of the metal centre can be occupied, with a resulting decrease in the catalytic activity of the cobalt porphyrin. With **71** as the catalyst and the synthetic protocol reported above, a broad range of styrene derivatives, bearing both electron-withdrawing and electron-donating substituents, were cyclopropanated in high yields and excellent diastereo- and enantiomeric excesses.<sup>332</sup> Complex **71** not only exhibited an exceptional catalytic activity in the cyclopropanation of electron-sufficient olefins, but it also was a competent catalyst for the cyclopropanation of electron-deficient olefins (Scheme 1.45)<sup>333</sup> Very high enantioselectivities (up to 97%) and diastereoselectivities (*trans/cis* ratio up to 99:1) were obtained. With this methodology, acrylates (Scheme 1.45 a, R' = H; R'' = OEt or *t*Bu), methacrylates (Scheme 1.45 a, R' = Me; R'' = OMe), acrylamide (Scheme 1.45 a, R' = H; R'' = NH<sub>2</sub>), its mono- (Scheme 1.45 a, R'=H; R''=NH/Pr) and disubstituted derivatives (Scheme 1.45 a, R' = H; R'' = NMe<sub>2</sub>), acryl ketones (Scheme 1.45 a, R' = H or Me; R'' = Et or Me or <sup>*n*</sup>Pe) and acrylonitriles (Scheme 1.45 b, R' = H, Me) were cyclopropanated.



**Scheme 1.45.** Cyclopropanation of electron-deficient olefins catalyzed by **71**.

To expand the scope of the reaction, several diazo compounds other than EDA or *t*BDA were tested. The catalytic system showed an excellent efficiency also with use of diazosulfones,<sup>330</sup>  $\alpha$ -nitrodiazoacetates,<sup>334</sup> succinimidyl diazoacetate<sup>335</sup> and  $\alpha$ -cyanodiazoacetate<sup>336</sup> (Figure 1.21).

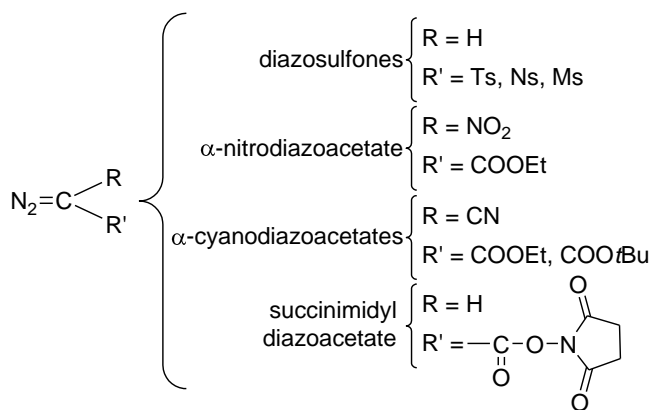


**Figure 1.21.** Diazo compounds employed in cyclopropanation reactions.

The synthesis of cyclopropanes bearing the different R and R' groups listed in Figure 1.21 represents an important synthetic result for several reasons. Firstly, acceptor/acceptor- substituted diazo compounds are not generally reactive in other catalytic systems; therefore, the synthesis of the corresponding cyclopropanes indicated the high efficiency of the methodology based on cobalt porphyrins. In addition, cyclopropanes bearing such R or R' groups can be further modified to yield biologically important cyclopropanes.

The exceptional enantioselectivity observed in cyclopropanation reactions catalysed by chiral cobalt(II) porphyrins<sup>337</sup> shown in Figure 1.20 can be due to a particular arrangement of their molecular structure in which chiral R\* units are forced toward the centre of the porphyrin. However, the electronic and steric behaviour of the putative cobalt–carbene derivative should be responsible for the outstanding diastereoselectivities.

To study the steric and conformational ligand requirements to obtain stereocontrol of the reaction, several years ago Cenini's synthesized the cobalt(II) complex<sup>241</sup> **78** (Figure 1.22) of the chiral porphyrin already reported by Marchon et al.<sup>338</sup>

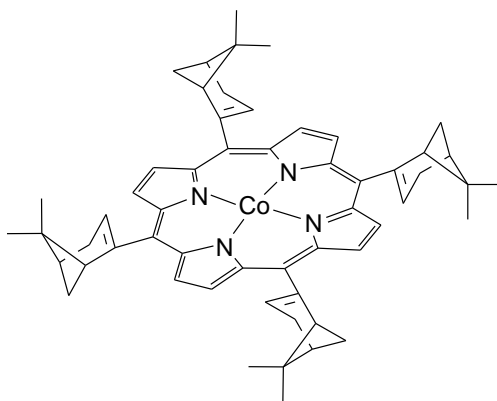


**Figure 1.22.** Structure of **78**.

The cyclopropanation of  $\alpha$ -methylstyrene by EDA catalyzed by **78** afforded the corresponding cyclopropanes with low diastereo- and enantioselectivity. The observed experimental results were justified by theoretical calculations, which disclosed the existence of **78** as a pool of interconverting atropisomers.

Better catalytic results by using the more rigid complexes **79**,<sup>339</sup> **80**<sup>145, 340</sup> and **81**<sup>341</sup> reported in Figure 1.23 were achieved

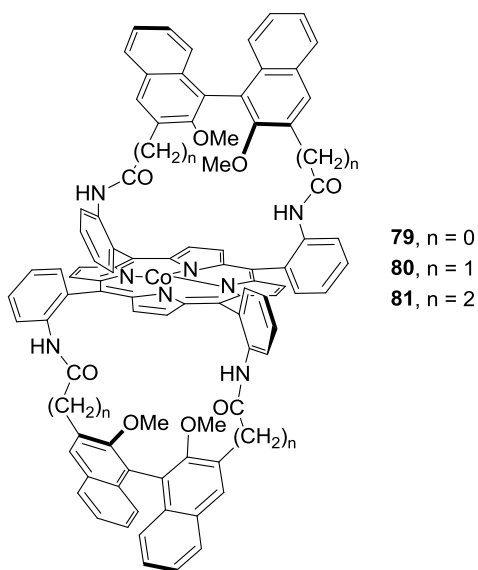
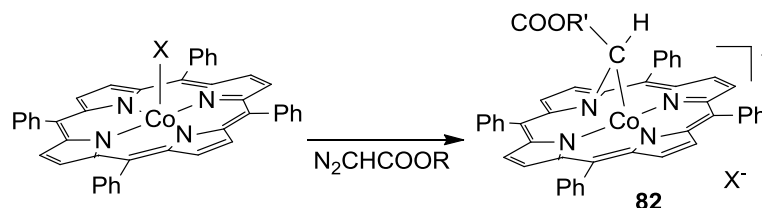


**Figure 1.23.** Structures of chiral cobalt bis(binaphthyl)porphyrins.

Among the cobalt(II) complexes of chiral bis(binaphthyl) porphyrins reported in Figure 1.23, complex **80** showed the best catalytic activity. Several olefins were tested in the reaction with EDA, and good yields as well as good enantioselectivities (up to 90% ee) were observed with *cis/trans* ratios reaching 11:89.

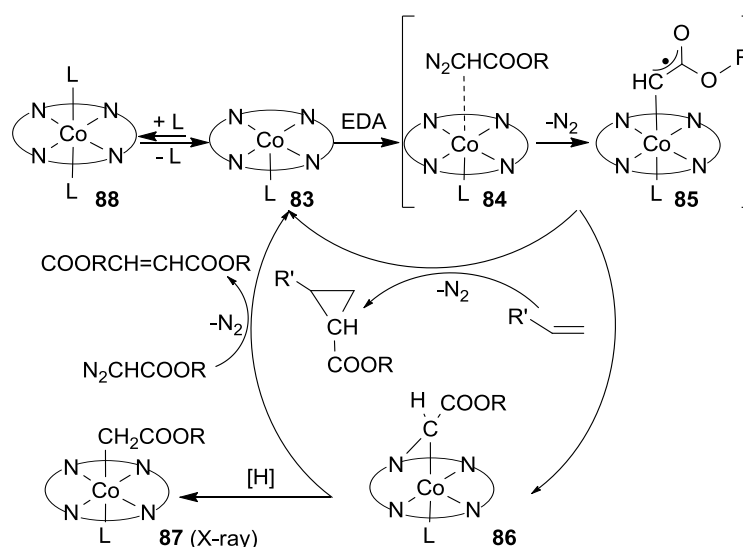
The strong dependence of the catalytic performance on the electronic and steric nature of the porphyrin ligand prompted the scientific community to clarify the reaction mechanism, in order to design new and more efficient catalysts. First, spectroscopic studies of the reaction between cobalt(III) porphyrins and diazoacetates suggested the insertion of the carbene unit into the bond between the cobalt and a porphyrin

nitrogen atom to give the cobalt(III)-bridged carbene complex **82**, whose catalytic activity was not further investigated (Scheme 1.46).<sup>342-344</sup> More recently, a *N*-bridged carbene cobalt(III) corrole was isolated and fully characterised.<sup>345</sup> A spectroscopic study revealed an equilibrium between a bridged carbene complex and an axial carbenoid compound, which was the only active species in the cyclopropane formation.



**Scheme 1.46.** Synthesis of the bridged carbene complex **82**.

A more complete mechanistic study of cyclopropanations catalysed by cobalt(II) porphyrins was undertaken a few years ago by Cenini's group. The reaction between EDA and  $\alpha$ -methylstyrene was studied in the presence of Co(TPP)<sup>325</sup> or complex **80**<sup>341</sup> and on the basis of spectroscopic reactions and kinetic data, we proposed the cycle shown in Scheme 1.47.



**Scheme 1.47.** Catalytic cycle for the Co(porphyrin)-catalysed cyclopropanation suggested on the basis of kinetic data and experimental studies.

The spectroscopic investigation of the reaction catalyzed by Co(TPP) revealed the formation of a bridged carbene complex, **86**<sup>346</sup> (L = none), which, instead of being the active species, could be responsible for the formation of maleate and fumarate both formed by a reaction with an additional EDA molecule when the olefin is present in very low concentrations. Conversely, with an excess of olefin, the catalytically active species (**84** or **85**) rapidly reacted with the unsaturated substrate to yield cyclopropanes, and the formation of

coupling compounds was not observed. Both of these reactions regenerate Co(TPP) (**83**, L = none). Alternatively, complex **86** can be transformed into the catalytically inactive Co<sup>III</sup>(TPP)(CH<sub>2</sub>COOR)L (R = Et; L = none) (**80**) by a hydrogen atom abstraction. Complex **87** was characterized by X-ray analysis.

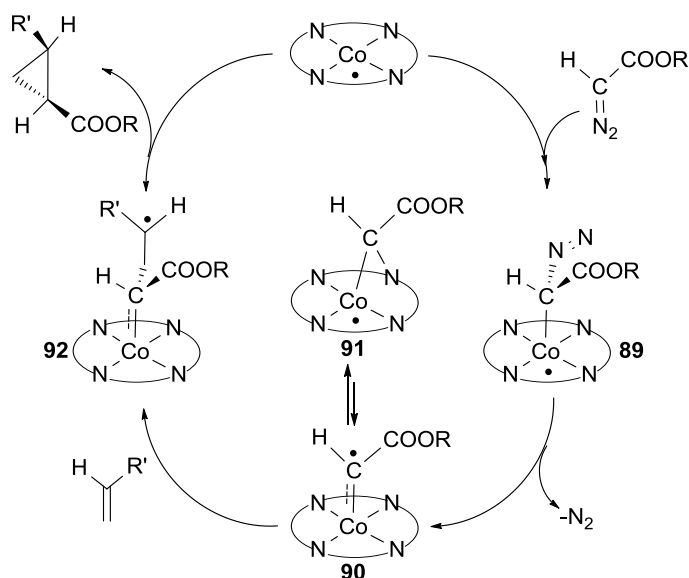
A similar mechanism was also suggested for the reaction catalysed by **80**. Was also studied the crucial role of NMI usually used as a promoter in this class of reaction. UV/Vis spectroscopic studies of the cyclopropanation of  $\alpha$ -methylstyrene showed an isosbestic point on both the Soret and the Q-bands for the reaction of **80** with NMI, which suggests the formation of **88** (L = NMI) without the accumulation of any long-lived intermediate. On the basis of the Soret band shift observed when EDA was added to **88**, we proposed that during the catalytic cycle one NMI ligand must be lost to allow the coordination of EDA to the metal centre and form either **84** or **85**; therefore, a high NMI concentration disfavours ligand replacement with a consequent inhibition of the catalytic reaction. Moreover, the modification of the catalyst induced by a coordinating ligand was also studied by NMR spectroscopy by exploiting the presence of methoxy groups in the skeleton of the porphyrin ligand in **80**.<sup>347</sup> The paramagnetism of the cobalt complexes prevented a direct NMR spectroscopic study, hence a zinc bis(binaphthyl) porphyrin was used instead.

The OCH<sub>3</sub> groups of the binaphthyl handles (Figure 1.23), being very close to the metal centre, were used as “NMR probes” to observe modifications of the porphyrin core. NMR spectroscopic data indicated a conformation change of the binaphthyl handles induced by NMI, and in our opinion this particular arrangement of the porphyrin skeleton was responsible for the enhancement of enantioselectivities observed in the reaction catalysed by **80** in the presence of NMI. Finally, the radical nature of the reaction mechanism was supported by the strong inhibiting effect of TEMPO (2,2,6,6-tetramethylpiperidine *N*-oxide) when added to the cyclopropanation of  $\alpha$ -methylstyrene catalysed by either Co(TPP) or **80**.

However, mechanistic investigations did not unequivocally indicate a catalytic cycle, and many aspects remained unsolved until exhaustive mechanistic surveys were carried out very recently by B. De Bruin and X. P. Zhang.<sup>348-350</sup> The key to the elucidation of the mechanism was a deep theoretical study that took into account experimental data on the nature of the catalytic intermediate. EPR spectroscopic and ESI-MS analyses of the reaction between complex **71** (Figure 1.20) and EDA disclosed the presence of both “bridging” and “terminal” carbene species, which are in equilibrium in solution.<sup>349</sup> DFT calculations indicated that the bridging carbene is a metal-centred radical whilst the terminal carbene is a carbon-centred radical (Scheme 1.48, complexes **91** and **90**, respectively). The energy difference among the two species is not so large, thus the possible existence of a dynamic equilibrium is confirmed. The DFT study identified the terminal carbene as the species that reacts with the olefin, which, according to the authors, approaches the carbene in a parallel way (Scheme 1.48). The reaction of **90** with the olefin yields a  $\gamma$ -carbon radical species **92** that collapses to form the cyclopropane and the Co(porphyrin) complex. This kind of reaction was also observed in the synthesis of several cyclopropanes from allylcobaloximes.

A radical species was responsible for the homolytic displacement of cobaloxime(II) from the allylcobaloxime(III) complex, and then a ring-closure reaction yielded the desired cyclopropane.<sup>351</sup>

The calculated TS energy barrier values for *cis*- and *trans*-cyclopropanations indicated that, probably for steric reasons, the *trans*-cyclopropanation is more favoured than the *cis*-cyclopropanation. The theoretical data was in agreement with the experimental results reported by Zhang in previous papers.<sup>330-336, 339</sup>



**Scheme 1.48.** Catalytic cycle for the Co(porphyrin)-catalysed cyclopropanation proposed on the basis of DFT and experimental studies.

It is worth noting that theoretical calculations indicated carbene complex **90** to be a “radical Fischer carbene” with a partial nucleophilic character, which explains its good catalytic activity in the cyclopropanation of electron-deficient olefins. This feature of **90** is due to the presence of a *redox-noninnocent carbene ligand*, which controls the progress of the reaction. Very recently, Woodcock et al.<sup>350</sup> theoretically described the electronics of **90**-like carbene species (Figure 1.24).

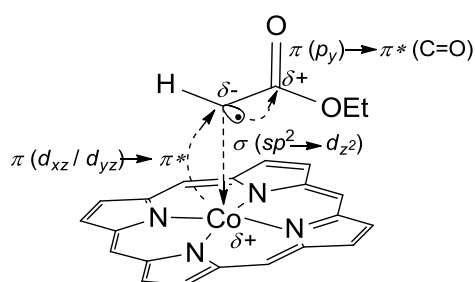
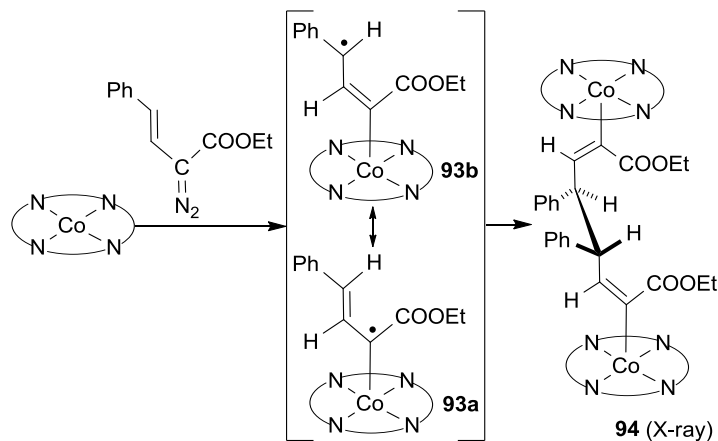


**Figure 1.24.** Formation of the cobalt–carbon bond in the radical carbene complex.

According to this study, the cobalt–carbon single bond is formed through a  $\sigma$  donation from the  $sp^2$  molecular orbital of the ligand to the singly occupied  $d_{z^2}$  atomic orbital on the metal centre, associated to a back-donation from the  $\pi$ -symmetry orbitals of the cobalt atom into the Co–C  $\pi^*$  molecular orbital. This process establishes an electron density  $\delta^-$  on the carbene carbon atom that is stabilized by back-donation into a  $\pi^*$  orbital of the acceptor C=O group.

As reported in Scheme 1.48, the radical carbene intermediate **90** should form the  $\gamma$ -radical species **92** by reaction with an olefin. Chemical evidence for the formation of such radical species was provided by Zhang and De Bruin who studied the reaction of Co(TPP) with ethyl styryldiazoacetate in the absence of any other olefin (Scheme 1.49).<sup>348</sup> The synthetic strategy reported in Scheme 1.49 has already been employed to trap iridium radical species.<sup>352</sup>



**Scheme 1.49.** Reaction of Co(TPP) with ethyl styryldiazoacetate to yield **94**.

The electronic nature of this diazo compound allows for the allylic radical resonance **93a** $\leftrightarrow$ **93b**. Then  $\gamma$ -radical species **93b**, instead of reacting with a hydrogen donor to form a cobalt(III) alkyl compound,<sup>325</sup> self-dimerises to yield compound **94**, which was isolated and fully characterized by X-ray analysis. DFT calculations indicated that the formation of **94** is preferred over a hydrogen-atom abstraction because of the higher energy barrier related to this latter reaction. It is important to point out that the isolation of **94** was fundamental in defining the mechanism illustrated in Scheme 1.48, initially supported on the basis of EPR spectroscopic, ESI-MS and DFT studies.

All results reported up to now highlight the excellent performance of cobalt porphyrins in catalysing the cyclopropanation of a wide range of olefins by different diazo derivatives. Moreover, the information accumulated by investigations on the mechanism of the cyclopropanation reaction has laid the foundation for new and more efficient catalytic systems.

### 1.6.3. Iridium-Catalysed Reactions

Although iridium Schiff bases have been used by Katsuki et al. as catalysts in cyclopropanations of olefins by diazo compounds,<sup>353-355</sup> to the best of our knowledge the catalytic efficiency of iridium porphyrins remains almost unexplored. The lack of iridium(II) porphyrin complexes as cyclopropanation catalysts may be due to their easy transformation, by reaction with simple olefins such as ethene, into iridium(III) porphyrin anionic radical species. The intramolecular electron-transfer reaction, from the Ir<sup>II</sup> centre to the porphyrin ligand, is responsible for the formation of a (P)<sup>-</sup>Ir<sup>III</sup>(CH<sub>2</sub>=CH<sub>2</sub>) radical species.<sup>356, 357</sup> The formation of such a species during cyclopropanation reactions can explain the low catalytic activity of iridium(II) porphyrins. The

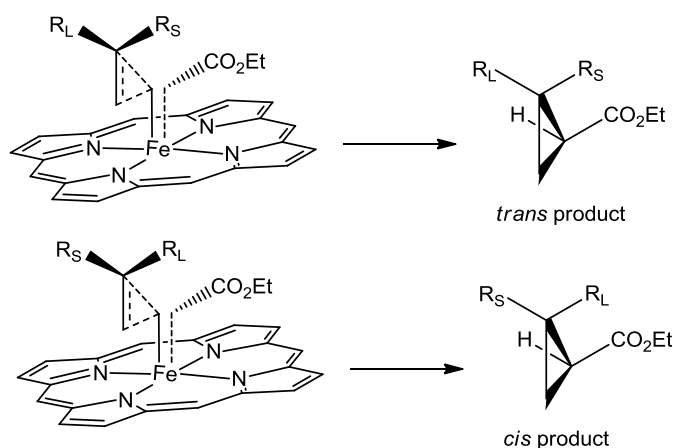


SciFinder database contains only an oral communication by Woo et al. on the employment of  $\text{CH}_3\text{-Ir}^{\text{III}}(\text{TTP})$  (TTP = dianion of tetratolylporphyrin) and  $\text{Ir}^{\text{III}}(\text{TTP})\text{X}(\text{CO})$  ( $\text{X} = \text{Cl}, \text{Br}$  and  $\text{I}$ ) as cyclopropanation catalysts. Surely the use of iridium(III) porphyrins in the field of catalytic carbene-transfer reactions will be a topic to explore in the near future.

#### 1.6.4. Iron Porphyrin Complexes

The carbon analogues of oxo-iron porphyrin, namely, iron porphyrin carbene complexes, have also received much attention. In 1977, Mansuy and co-workers<sup>358</sup> performed the reaction of 5,10,15,20-tetraphenylporphyrinatoiron(II)[(TPP)Fe<sup>II</sup>] with carbon tetrachloride in the presence of an excess of reducing agent leads to a complex having properties consistent with the carbene,  $:\text{CCl}_2$ , bound to Fe<sup>II</sup>; this is believed to be the first example of a carbene complex of a metalloporphyrin. However, the carbon atom transfer reactions of iron porphyrin carbene complexes with alkenes to form cyclopropanes are studied just in the last decade probably because of their air-sensitivity. Isolated iron(II) porphyrins are relatively easy handled only in an inert atmosphere and are generally not convenient reagent for organic synthesis.

In 1995, Kodedak, Woo and their co-workers reported that iron porphyrins are active catalysts for cyclopropanation of alkenes with ethyl diazoacetate. The active species in the catalytic carbon atom transfer reaction are assumed to be iron porphyrin carbene complexes (Scheme 1.50).<sup>290</sup>



**Scheme 1.50.** Proposed transition state for iron porphyrin-catalyzed cyclopropanation reactions. The porphyrin meso substituents were omitted for clarity. R<sub>L</sub> = large olefin substituent, R<sub>S</sub> = small olefin substituent.

In this work Kodedak and Woo demonstrated that iron porphyrins can efficiently catalyze the cyclopropanation of alkenes and high turnover numbers have been observed (TON = 4300). Shortly after, Suslick and co-workers demonstrated that photolysis of several halocarbene iron porphyrins gives free halocarbenes, which can be trapped by alkenes to form cyclopropanes.<sup>359</sup>

Despite the presence of a wide variety of chiral iron porphyrins, and their remarkable efficiency, few of these have been tested as cyclopropanation catalysts, in fact, chiral iron porphyrins were not used in asymmetric cyclopropanation until 1999.<sup>360</sup>

## **2. Results and Discussion**

## 2.1. Intermolecular Benzylic Amination

The development of new strategies for the synthesis in an economical way of aza-derivatives has a relevant scientific interest due to the importance such species have as precursors for biological and pharmaceutical compounds.<sup>361, 362</sup>

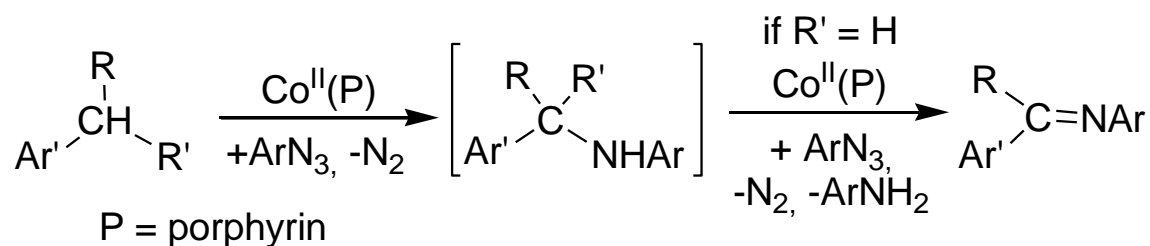
Nitrogen containing molecules can be efficiently obtained in one pot by a direct insertion of a nitrene functionality [RN] into an organic framework.<sup>184, 185, 189</sup> Among nitrogen sources available to perform amination reactions, organic azides (RN<sub>3</sub>) represent a versatile class of starting materials,<sup>228</sup> they are very reactive and in several cases they are easily formed from the corresponding amines.

Organic azides react with unsaturated or saturated hydrocarbons affording, with high chemo- and stereoselectivities, aziridines and amines respectively.<sup>227</sup> The reaction of saturated hydrocarbons with organic azides is responsible for the direct transformation of a C-H into a C-N bond, a research area of high impact and extreme synthetic utility. Some examples of intramolecular C-H aminations by organic azides, giving nitrogen-based heterocycles<sup>363</sup> such as carbazoles,<sup>364, 365</sup> pyrroles,<sup>364</sup> indoles,<sup>364, 366, 367</sup> indolines,<sup>368</sup> and benzimidazoles,<sup>369</sup> have already been reported.

As already discussed in the introduction, among the transition metal complexes employed as catalysts in these reactions, metallo-porphyrins exhibited a very good catalytic activity for the intramolecular C-H amination of organic sulfonyl or phosphoryl azides, forming benzosultams<sup>370</sup> and cyclophosphoramidates<sup>371</sup> respectively. On the other hand, to the best of our knowledge, there are few examples of intermolecular C-H aminations by organic azides catalysed by metal porphyrins.<sup>256, 257, 372</sup>

Among them the amination of benzylic substrates by arylazides catalysed by cobalt porphyrin complexes was reported by Gallo and co-workers some years ago.<sup>256, 257</sup> Aryl azides are very interesting nitrogen sources in aziridination reactions<sup>240, 252, 253, 255, 260</sup> because of their convenient reactivity/stability relationship and their easy synthesis starting from commercially available anilines.

The general path for the synthesis of benzylic amines and imines employing arylazides (ArN<sub>3</sub>) as aminating agents in the presence of cobalt porphyrins is shown in scheme 2.1.

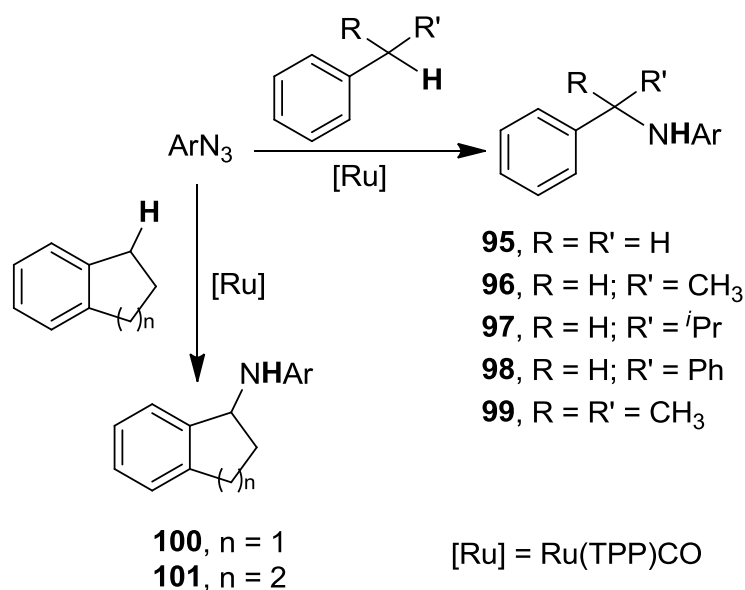


**Scheme 2.1.** Benzylic amination by arylazides catalysed by Co(porphyrin) complexes

The reaction of ArN<sub>3</sub> with hydrocarbons containing a benzylic group, Ar'RR<sup>1</sup>CH, initially produces the corresponding amines Ar'RR<sup>1</sup>C-NHAr. When either R or R' is hydrogen, the catalytic reaction always proceeds further giving the corresponding imine Ar'RC=NAr by reaction with another arylazide molecule. The

corresponding aniline is the by-products of the imine formation. A mechanistic study of the cobalt porphyrins catalysed reaction evidenced a reversible coordination of the arylazide to the metal, affording an unstable Co(II) adduct that reacts with the hydrocarbon forming the aminated product.<sup>257</sup> Kinetic and spectroscopic data excluded the formation of a “formal” cobalt imido complex, whereas imido intermediates are usually proposed for ruthenium porphyrins-catalysed amination reactions.<sup>207, 210, 373</sup>

In order to compare the chemoselectivity of the benzylic amination catalysed by Ru(TPP)CO with that catalysed by Co(porphyrin) complexes, several benzylic substrates were reacted at 100°C with arylazides employing the hydrocarbon as reaction solvent and the catalytic ratio Ru(TPP)CO/azide = 4:50 (scheme 2.2). Collected data is reported in table 2.1.



**Scheme 2.2.** Amination reaction of benzylic hydrocarbons by ArN<sub>3</sub> catalysed by Ru(TPP)CO

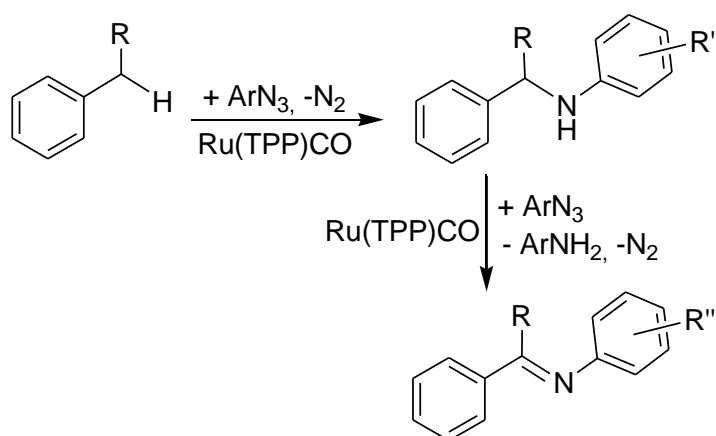
Benzylic substrates containing an exocyclic benzylic carbon (table 2.1, entries 95-99) were reacted with at least two different arylazides, 3,5(CF<sub>3</sub>)<sub>2</sub>C<sub>6</sub>H<sub>3</sub>N<sub>3</sub> and 4(NO<sub>2</sub>)C<sub>6</sub>H<sub>4</sub>N<sub>3</sub>. Data reported in table 2.1 reveals similar or even better yields but always longer reaction times for the reactions employing 4(NO<sub>2</sub>)C<sub>6</sub>H<sub>4</sub>N<sub>3</sub> as the aminating reagent. It is worth noting that only in the case of the amination of toluene (table 2.1, entry 1) was the formation of the imine, *N*-benzylidene-4-nitrobenzenamine or *N*-benzylidene-3,5-bis-trifluoromethylbenzenamine, deriving from the reaction of **95 a,b** with another molecule of azide, observed by GC-MS. In all other cases, the aniline deriving from the starting arylazide was the only by-product of the reactions. On the other hand, when a substituent was present on the benzylic position (table 2.1, entries 2, 3, 4) any further reaction of the benzylic amine with arylazide was inhibited by the increase in the steric hindrance on the benzylic hydrogen atom (scheme 2.3).

The formation of imine starting from isopropyl benzene is impossible due to the double substitution on the C-H benzylic bond, but the yield of amines **99a** and **99b** are not satisfactory because of the contemporary formation of the anilines deriving from the corresponding azides.

**Table 2.1.** Ru(TPP)CO-catalysed benzylic amination at 100°C<sup>a</sup>

entry	product	Ar	time (min) <sup>b</sup>	yield (%)
1		3,5(CF3)2C6H3, <b>95a</b>	50	14 <sup>c</sup>
		4(NO2)C6H4, <b>95b</b>	60	25 <sup>d</sup>
2		3,5(CF3)2C6H3, <b>96a</b>	60	31 <sup>c</sup>
		4(NO2)C6H4, <b>96b</b>	180	80 <sup>d</sup>
3		3,5(CF3)2C6H3, <b>97a</b>	30	67 <sup>c</sup>
		4(NO2)C6H4, <b>97b</b>	90	57 <sup>c</sup>
		4( <sup>t</sup> Bu)C6H4, <b>97c</b>	70	10 <sup>d</sup>
		2,6(NO2)2C6H3, <b>97d</b>	25	31 <sup>d</sup>
4		4-BrC6H4, <b>97e</b>	70	48 <sup>d</sup>
		3,5(CF3)2C6H3, <b>98a</b>	25	65 <sup>c</sup>
		4(NO2)C6H4, <b>98b</b>	60	55 <sup>d</sup>
5		3,5(CF3)2C6H3, <b>99a</b>	25	31 <sup>c</sup>
		4(NO2)C6H4, <b>99b</b>	50	41 <sup>d</sup>
6		3,5(CF3)2C6H3, <b>100a</b>	30	53 <sup>c</sup>
		4(NO2)C6H4, <b>100b</b>	90	54 <sup>c</sup>
7		3,5(CF3)2C6H3, <b>101a</b>	25	60 <sup>c</sup>
		4(NO2)C6H4, <b>101b</b>	120	50 <sup>c</sup>

<sup>a</sup>General procedure for catalytic reactions: Ru(TPP)CO (36 mg, 4.85×10<sup>-2</sup> mmol) in the hydrocarbon as the reaction solvent (30 mL) at 100°C; mol ratio Ru(TPP)CO/ArN<sub>3</sub> = 4:50. <sup>b</sup>Time required to reach complete conversion of the starting ArN<sub>3</sub>. <sup>c</sup>Isolated yield; <sup>d</sup>Determined by <sup>1</sup>H NMR employing 2,4-dinitrotoluene as the internal standard.

**Scheme 2.3.** Ru(TPP)CO catalysed benzylic imine formations

Isobutylbenzene was also aminated employing 4(<sup>t</sup>Bu)C<sub>6</sub>H<sub>4</sub>N<sub>3</sub>, 2,6(NO<sub>2</sub>)<sub>2</sub>C<sub>6</sub>H<sub>3</sub>N<sub>3</sub> and 4(Br)C<sub>6</sub>H<sub>4</sub>N<sub>3</sub> (table 2.1, entry 3). At the moment we do not have enough data to give a definite explanation for the observed

trends in the selectivity towards the benzylic amine, imine, or aniline product. However, the following arguments can account for the observed results.

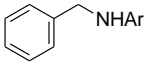
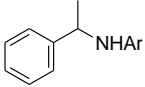
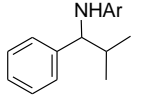
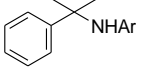
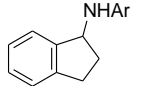
Previous studies on the cobalt-porphyrin catalyzed benzylic amination of hydrocarbons by arylazides<sup>257</sup> unequivocally showed that the activation of the C-H bond proceeds by an intermediate having a marked radical character on the benzylic carbon. Formation of such a radical is strongly accelerated by the presence of an amino group in the  $\alpha$  position. The cobalt catalyst is not very active and thus the reactive intermediate should be able to select the most reactive substrate in solution (the just formed amine) with respect to the less reactive one (the starting hydrocarbon) despite the latter is present in a much larger concentration, being the reaction solvent. Even a preliminary examination of the reaction rates shows the ruthenium-tetraphenylporphyrin catalyst to be much more active. This implies that the reactive intermediate will react with the first suitable substrate it will meet, most likely the hydrocarbon, allowing the accumulation of the amine in solution.

As for the cobalt catalysed reaction, the reaction is favoured by electronwithdrawing substituents on the azide aryl ring. In fact, the best yield was achieved performing the reaction with 3,5(CF<sub>3</sub>)<sub>2</sub>C<sub>6</sub>H<sub>3</sub>N<sub>3</sub> and only 10% of benzylic amine was obtained when a *tert*-butyl group was present in the *para* position of the aryl group of the azide. Conversely, steric hindrance disfavours the amination reaction and the reaction of isobutylbenzene with 2,6(NO<sub>2</sub>)<sub>2</sub>C<sub>6</sub>H<sub>3</sub>N<sub>3</sub> afforded the corresponding amine only in low yield. The rate of the amination reaction should not be confused with the rate of azide consumption, which is very high for the dinitro substituted azide. Indeed, formation of the active intermediate by reaction of the azide with the ruthenium porphyrin complex or hydrogen abstraction of the latter to generate aniline should be much less sensitive to steric effects than a coupling reaction to generate a new C-N bond. Thus the azide consumption rate remains high, but the main product is dinitroaniline.

Steric hindrance surely also affects the reaction of the initially formed benzylic amine with another azide molecule. Thus it is not surprising that the only case in which imine formation was detected with the ruthenium catalyst involves toluene as the substrate. The corresponding benzylic amines are the only ones to have a secondary benzylic carbon atom, whereas a tertiary benzylic carbon atom is formed in all other cases. The Ru(TPP)CO catalyst is also active for the amination of substrates containing an endocyclic benzylic C-H bond (table 2.1, entries 6 and 7) and the corresponding amines have been isolated in good yields. It must be underlined that compound **101b**, deriving from the reaction of tetrahydronaphthalene with 4(NO<sub>2</sub>)C<sub>6</sub>H<sub>4</sub>N<sub>3</sub>, has a pharmaceutical interest being a drug that, antagonising nicotinic acetylcholine receptors (nAChRs), is used to reduce the addiction of nicotine self-administration by negative allosteric modulation.<sup>374</sup>

In order to improve the catalytic efficiency, the hydrocarbon aminations were repeated lowering the catalytic ratio Ru(TPP)CO/azide from 4:50 to 1:50 and running the reactions at higher temperature. The reactions described in table 2.1 were performed in the refluxing hydrocarbon as the reaction solvent. The amination of diphenyl methane and 1,2,3,4-tetrahydronaphthalene were not carried out for the very high boiling points of those hydrocarbons (264°C and 207°C respectively). Data collected is reported in table 2.2.

**Table 2.2.** Ru(TPP)CO-catalysed benzylic amination in refluxing hydrocarbon<sup>a</sup>

entry	product	Ar	time (min) <sup>b</sup>	yield (%) <sup>c</sup>
1		3,5(CF <sub>3</sub> ) <sub>2</sub> C <sub>6</sub> H <sub>3</sub> , <b>95a</b>	60	66
		4(NO <sub>2</sub> )C <sub>6</sub> H <sub>4</sub> , <b>95b</b>	90	25
2		3,5(CF <sub>3</sub> ) <sub>2</sub> C <sub>6</sub> H <sub>3</sub> , <b>96a</b>	240	85
		4(NO <sub>2</sub> )C <sub>6</sub> H <sub>4</sub> , <b>96b</b>	300	20
3		3,5(CF <sub>3</sub> ) <sub>2</sub> C <sub>6</sub> H <sub>3</sub> , <b>97a</b>	60	75
		4(NO <sub>2</sub> )C <sub>6</sub> H <sub>4</sub> , <b>97b</b>	45	40
4		3,5(CF <sub>3</sub> ) <sub>2</sub> C <sub>6</sub> H <sub>3</sub> , <b>99a</b>	69	90
		4(NO <sub>2</sub> )C <sub>6</sub> H <sub>4</sub> , <b>99b</b>	75	30
5		3,5(CF <sub>3</sub> ) <sub>2</sub> C <sub>6</sub> H <sub>3</sub> , <b>100a</b>	25	80
		4(NO <sub>2</sub> )C <sub>6</sub> H <sub>4</sub> , <b>100b</b>	60	30

<sup>a</sup>General procedure for catalytic reactions: Ru(TPP)CO (10 mg, 1.35×10<sup>-2</sup> mmol) in refluxing hydrocarbon (30 mL); mol ratios Ru(TPP)CO/ArN<sub>3</sub> = 1:50. <sup>b</sup>Time required to reach complete conversion of the starting ArN<sub>3</sub>. <sup>c</sup>Determined by <sup>1</sup>H NMR (2,4-dinitrotoluene as the internal standard).

Comparing these data with those in table 2.1, an opposite behaviour was observed when employing 3,5(CF<sub>3</sub>)<sub>2</sub>C<sub>6</sub>H<sub>3</sub>N<sub>3</sub> or 4(NO<sub>2</sub>)C<sub>6</sub>H<sub>4</sub>N<sub>3</sub> as nitrene sources. The amination by 3,5(CF<sub>3</sub>)<sub>2</sub>C<sub>6</sub>H<sub>3</sub>N<sub>3</sub> occurred with a general improvement of the yields, however the reactions performed with 4(NO<sub>2</sub>)C<sub>6</sub>H<sub>4</sub>N<sub>3</sub> formed the corresponding benzylic amine in lower yields with respect to those reported in table 2.1. This result can be explained by the different thermal stability of these two aryl azides. Indeed, with the exception of toluene, the boiling points of all tested hydrocarbons is always higher than 130°C. The presence of two CF<sub>3</sub> groups on the aryl moiety of 3,5(CF<sub>3</sub>)<sub>2</sub>C<sub>6</sub>H<sub>3</sub>N<sub>3</sub> conferred it a better stability than that of 4(NO<sub>2</sub>)C<sub>6</sub>H<sub>4</sub>N<sub>3</sub> and a thermal decomposition of 3,5(CF<sub>3</sub>)<sub>2</sub>C<sub>6</sub>H<sub>3</sub>N<sub>3</sub> at T > 130°C is then avoided. Considering the different catalyst loading for the benzylic aminations of tables 2.1 and 2.2, a comparison between reaction times is impossible.

Imine compounds were never formed and, in all the cases investigated, the reaction by-product was the aniline deriving from the aryl azide decomposition.

For every amination by 3,5(CF<sub>3</sub>)<sub>2</sub>C<sub>6</sub>H<sub>3</sub>N<sub>3</sub> shown in table 2.2 the yield was higher than 66% showing that the positive effect of raising the temperature prevails on the lower catalyst loading. In fact, the best yield of 90% has been obtained employing isopropylbenzene, which has the highest boiling point among the tested hydrocarbons.

### 2.1.1. Kinetic Study of the Ruthenium-Catalyzed Benzylic Amination

To investigate the mechanism of the benzylic amination catalysed by Ru(TPP)CO, a kinetic study was undertaken employing 4-nitrophenylazide and toluene as substrates. The reaction was followed by IR spectroscopy, monitoring the intensity of the  $2120\text{ cm}^{-1}$  absorption of the arylazide. All kinetic experiments were run at  $75^\circ\text{C}$  to avoid boiling of benzene in those reaction in which it was present. The dependence of the reaction rate with respect toluene concentration has been investigated employing a catalytic ratio Ru(TPP)CO/arylazide = 4:50.

The reaction rate showed a first-order dependence on azide and [Ru(TPP)CO] concentrations. However, an irregular dependence on toluene concentration, the other solvent being benzene, was observed (Figure 2.1). The rate is approximately first order in toluene concentration up to a 7M concentration, but an inhibiting effect of higher toluene concentrations is evident.

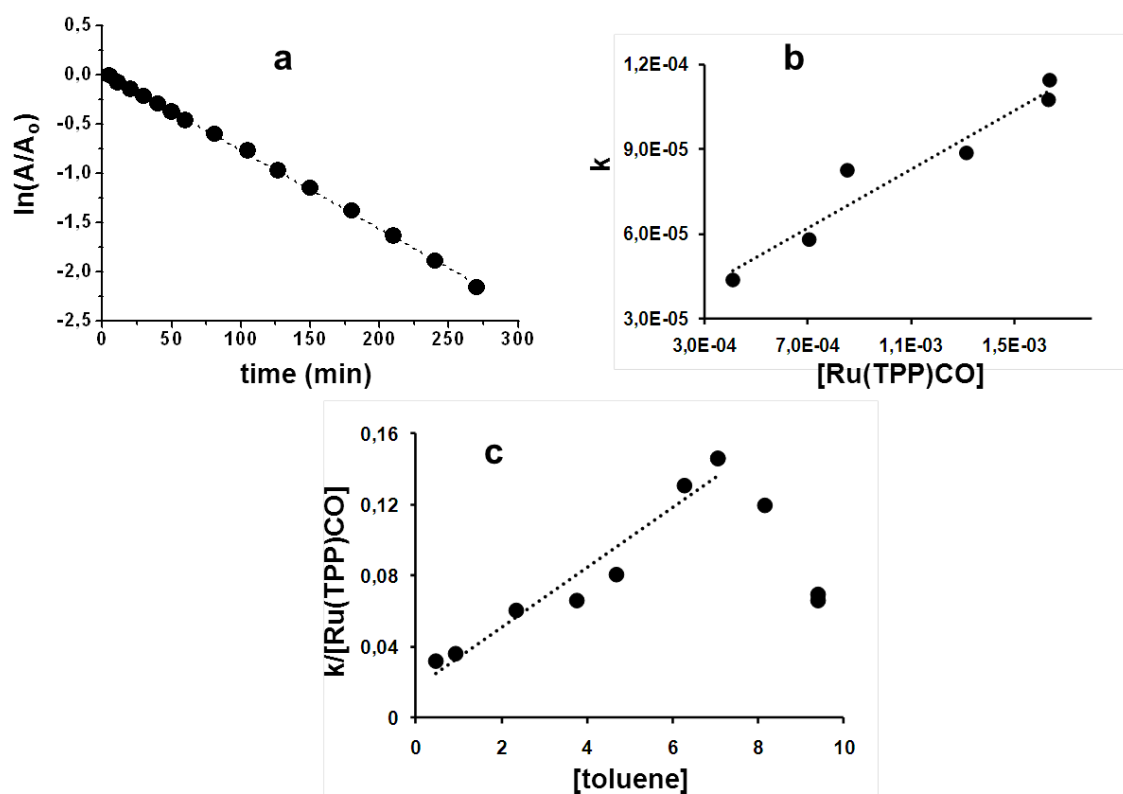


**Figure 2.1.** Kinetic dependence of the reaction rate with respect 4-nitro-phenylazide (a), Ru(TPP)CO (b) and toluene concentrations (c).

To better investigate the inhibition effect observed in the benzylic amination at high toluene concentrations we have repeated the reaction with benzene/toluene ratios of 75:25, 50:50 and neat toluene analysing the composition of the reaction mixture by GC-MS. As shown in figure 2.2, the raise in toluene concentration caused an increase in the imine/amine ratio.



The kinetic and selectivity data together indicate that the reaction pathway is complex and not exactly the same as for the corresponding allylic amination reaction. A more in depth study will be necessary to clarify all aspects of this interesting reaction. The presently available data is consistent with an active role of a ruthenium-imido intermediate, which is formed in a slow step by reaction of a ruthenium complex with the azide. However, the complex kinetic behaviour with respect to toluene concentration clearly indicates that more than one reaction pathway is available to this intermediate. The formation of the benzylic amine obviously requires the interaction of the intermediate with toluene and this process can account for the increasing branch of the rate vs. [toluene] plot (Figure 2.1, c). On the other hand, we must assume that a different type of interaction between the intermediate and toluene can also occur, which leads to a less catalytically active species. The formation of a less active species explains both the slower rate at high toluene concentration and the increased amount of imine formed under these conditions. Indeed, the same situation encountered with the less active cobalt-porphyrin catalysts and discussed above would result. A less reactive intermediate is more able to select the most reactive partner among those present in solution, even if the concentration of the benzylic amine is relatively low with respect to that of a less reactive partner such as the starting hydrocarbon. It should be noted that formation of a completely inactive complex would explain the rate drop, but not the change in selectivity. The available data are insufficient to identify this less active intermediate and speculating on its identity at this stage is premature. Attempts are in progress to isolate and characterise this complex, so that its reactivity and kinetic behaviour can be investigated.

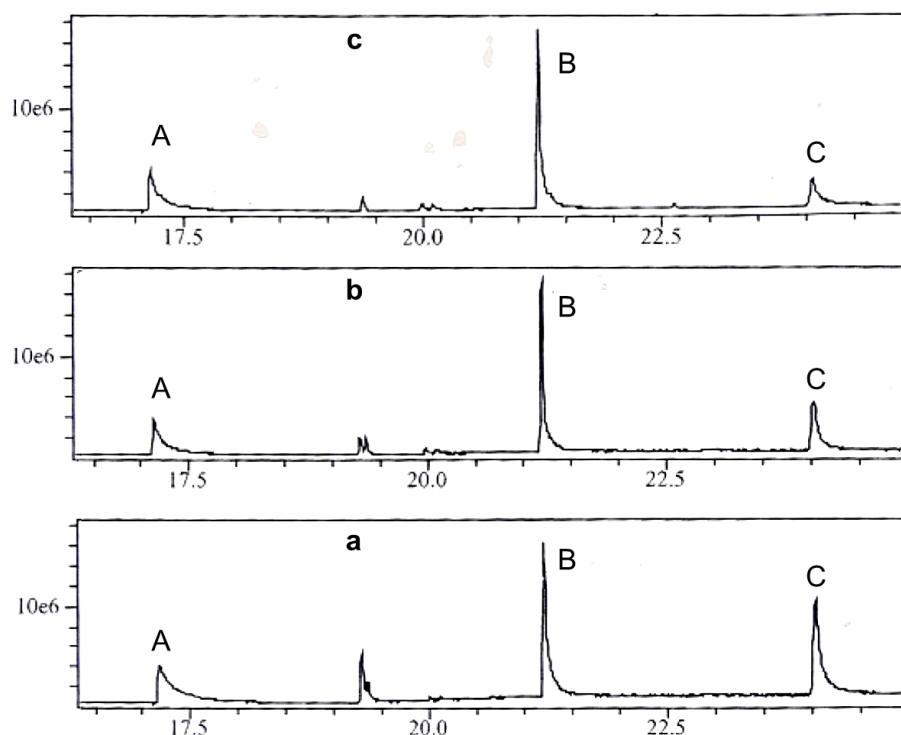


**Figure 2.2.** GC-MS spectra of reactions run with benzene/toluene ratios of 75:25 (a), 50:50 (b) and neat toluene (c). **A** =  $4(\text{NO}_2)\text{C}_6\text{H}_4\text{NH}_2$ , **B** =  $4(\text{NO}_2)\text{C}_6\text{H}_4\text{N}=\text{CHC}_6\text{H}_5$ , **C** =  $4(\text{NO}_2)\text{C}_6\text{H}_4\text{NH}-\text{CH}_2\text{C}_6\text{H}_5$

The catalytic activity of Ru(TPP)CO in the amination of benzylic substrates demonstrated that the treatment of the same benzylic substrate with an aromatic azide, in the presence of ruthenium or cobalt porphyrin complexes produces different products. Therefore these two methodologies are complementary because they can be alternately used depending on the desired aminated product.

Moreover, the preliminary mechanistic study performed indicates an important role of the hydrocarbon concentration to drive the chemoselectivity of the reaction.

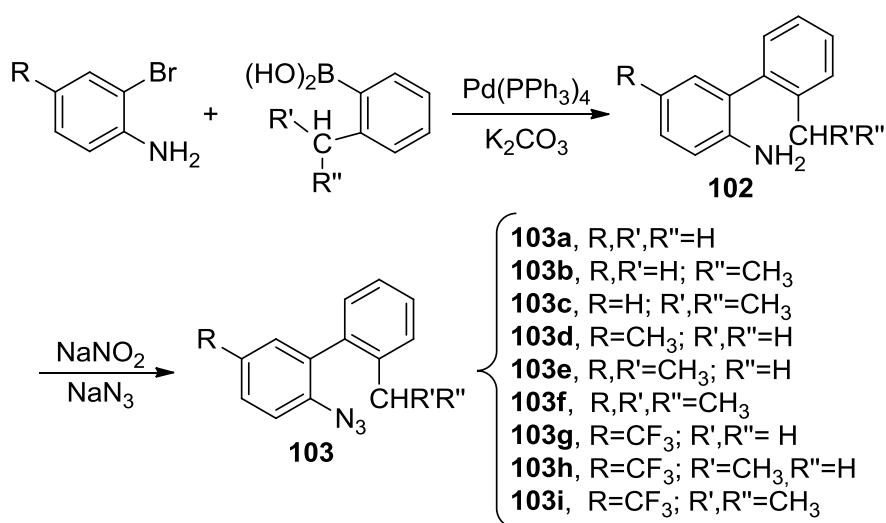
## 2.2. Intramolecular Benzylic Amination

The reaction scope of the benzylic amination has been then explored studying the intramolecular amination reaction of biphenyl azides containing benzylic C-H bonds

The scientific community is greatly interested in the development of new methodologies to synthesise *N*-heterocycles because of their pharmaceutical and biological properties. Many efforts have been made to develop efficient and clean procedures affording high added-value fine chemicals in a few steps and with good selectivity.<sup>375</sup> Intramolecular annulation reactions of organic azides could be a suitable strategy to respond to society's demand for environmentally benign *N*-heterocycles syntheses, because in the presence of a suitable catalytic system an intramolecular C-H amination occurs with excellent selectivity.<sup>376, 377</sup>

Recently, T. G. Driver and co-workers studied the intramolecular azide C-H aminations in depth and reached good to excellent reaction selectivities. Nitrogen-based heterocycles such as carbazoles,<sup>365</sup> pyrroles,<sup>364</sup> indoles,<sup>366, 367, 378, 379</sup> indolines,<sup>368</sup> and benzimidazoles<sup>369</sup> were synthesised employing various catalytic systems. Among the transition metal complexes employed as catalysts in these reactions, metalloporphyrins exhibited a very good catalytic activity for the intramolecular C-H amination of organic sulfonyl, phosphoryl, sulfamoyl azides, forming benzosultams,<sup>370</sup> cyclophosphoramidates<sup>371</sup> and 1,3 diamines<sup>380, 381</sup> respectively.

Phenanthridines and dihydrophenanthridines are important core structures of a large class of pharmaceutical compounds,<sup>382</sup> consequently several synthetic methods have been developed to prepare them.<sup>383-385</sup> Up to now, azides have not extensively been employed as starting material and only old papers<sup>386, 387</sup> have reported on the pyrolyses of biaryl azides yielding phenanthridine derivatives in low yields and selectivities. Therefore, we decided to study the synthesis of this class of *N*-heterocycles starting from 2-azido biaryls applying our expertise of intermolecular C-H aminations catalysed by ruthenium porphyrins.<sup>388-391</sup> We report herein the intramolecular aminations of several 2-azido biaryls (**103a-103i**) that have been prepared adapting the procedure already reported by Driver<sup>365</sup> (scheme 2.4).

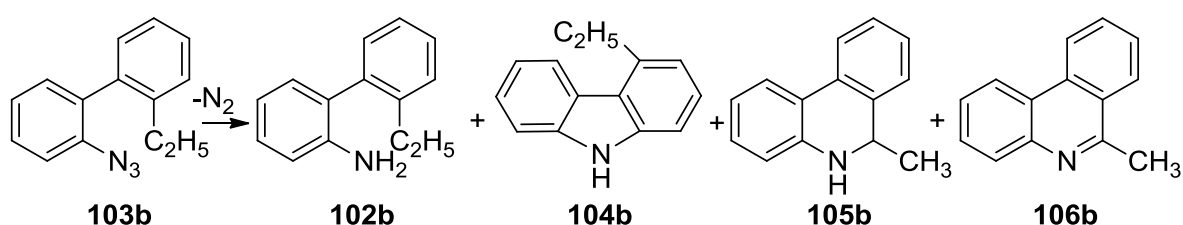


**Scheme 2.4.** Synthesis of 2-azido biaryl derivatives.

To test the catalytic activity of Ru(TPP)CO, the intramolecular amination of **103b** was run under dinitrogen using all the experimental conditions listed in table 2.3. We obtained a mixture of 2-amine biaryl (**102b**), carbazole (**104b**), dihydrophenanthridine (**105b**) and phenanthridine (**106b**) corresponding to **103b**. It should be noted that carbazole **104b**, usually obtained as the major compound using rhodium based catalysts,<sup>377</sup> was formed only as a by-product in the presence of the ruthenium catalyst.

As reported in table 2.3, the reaction times (compare entries 5 and 7) can be largely reduced by irradiating the reaction mixture with a 400 W halogen lamp; a contemporary decrease of the carbazole yield was observed. The employment of the lamp allowed the synthesis of equal yield for **105b/106b** mixture (77 vs 75%, compare entries 2 and 7) but at reduced reaction temperature (120 instead of 180 °C), cutting the time in half as well as the catalyst loading. The positive effect of a halogen lamp assumes practical importance in terms of low cost and availability.

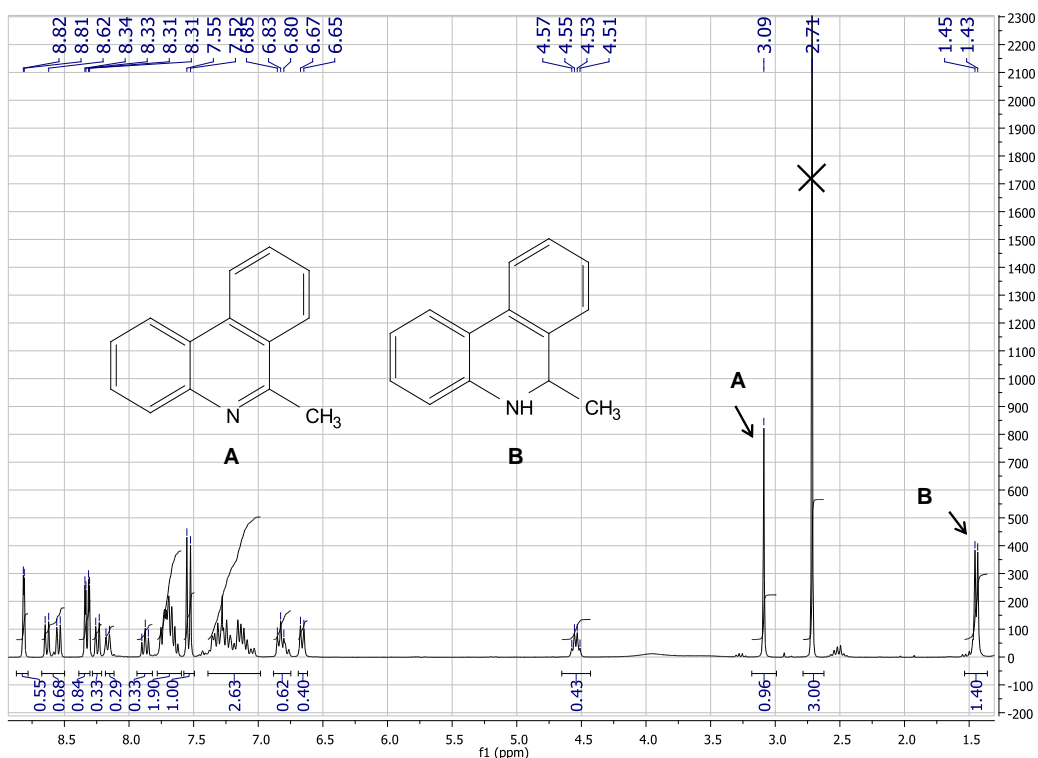
**Table 2.3.** Optimization of the intramolecular C-H amination of **103b**<sup>[a]</sup>



entry	Ru(TPP)CO%	T (°C)	time (h) <sup>[b]</sup>	yields % <sup>[c]</sup>			
				<b>102b</b>	<b>104b</b>	<b>105b</b>	<b>106b</b>
1	none	180	13	7	92	-	-
2	2	180	2	7	8	23	54
3	0.4	180	3	12	18	27	41
5	1	120	10	31	10	10	40
6 <sup>[d]</sup>	0.4	120	1.5	12	24	14	46
7 <sup>[d]</sup>	1	120	1	11	4	46	32
8 <sup>[d]</sup>	none	120	1.5	2	97	-	-

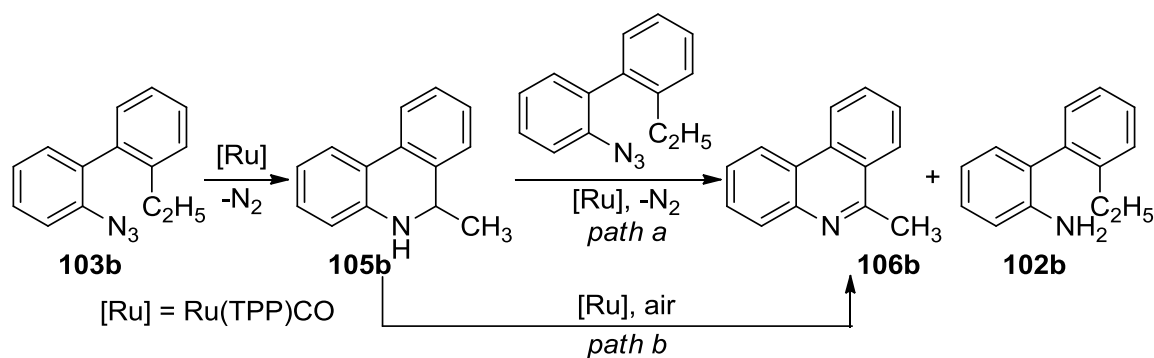
[a] General procedure: **103b** (60.0 mg,  $2.70 \times 10^{-4}$  mmol) was dissolved in 1,2 dichlorobenzene (20 mL) under dinitrogen. [b] Time required to reach complete conversion of **103b**. [c] Determined by <sup>1</sup>H NMR (2,4-dinitrotoluene as the internal standard). [d] The reaction mixture was irradiated with a 400 W halogen lamp.

Data collected up to now indicate 120 °C, 1 mol % catalyst coupled with a halogen lamp as the optimal conditions to perform intramolecular aminations. In fact, the use of lower catalyst loading (entry 6, table 2.3) was associated to the formation of a significant amount of carbazole by the competitive uncatalysed reaction. As shown in table 2.3, dihydrophenanthridine (**105b**) and phenanthridine (**106b**) are obtained in variable amounts depending on the experimental conditions and in every run the formation of the 2-amine biaryl (**102b**) was observed.



NMR spectrum of phenanthridine (**A**) and dihydrophenanthridine (**B**)

Previous study on the intermolecular benzylic amination of hydrocarbons by aryl azides<sup>257</sup> indicated that the first step of the C-H amination was the formation of a benzylic amine that yields the corresponding imine through a reaction with another azide molecule. The stoichiometric side-products of this second step is the aniline. If we envisage a similar mechanism for the intramolecular amination, we should obtain equal amounts of phenanthridine (**106b**) and 2-amino biaryl (**102b**) and, considering a complete azide conversion, the remainder of the material must be dihydrophenanthridine (**105b**). This hypothesis is not in accordance with experimental data (see entry 2 table 2.3 for example). Thus, the formation of **106b** must also be due to a competitive oxidation mechanism. Supposing that the oxidation of **105b** to **106b** could be promoted by Ru(TPP)CO, a catalytic mixture containing both heterocyclic compounds was left stirred at 120°C and directly exposed to local air for 2 hours. A complete conversion of **105b** to **106b** was observed. This experimental result indicates that the phenanthridine formation is probably due to the two mechanisms indicated in Scheme 2.5. We suggest that, being the **105b** dehydrogenation to **106b** a favourite process, it can start before the complete consumption of azide due to the presence of traces of air in the reaction mixture. Leaving the mixture exposed to air at 120 °C in the presence of the catalyst for another two hours concludes the oxidation process. To support the role of *path b* in the **106b** formation, we repeated the reaction leaving the mixture under nitrogen for 5 hours after the complete conversion of the starting azide. A complete transformation of **105b** into **106b** was not observed due to the lack of air.



**Scheme 2.5.** Suggested mechanism for the phenanthridine formation.

In order to favour the oxidation of **105b** into **106b**, we performed the intramolecular amination of **103b** using the experimental conditions described for entry 7 (table 2.3) but the reaction was exposed to air from the beginning. The  $^1H$  NMR spectrum of the crude registered after the complete consumption of the azide showed the presence of **106b** (17%), **105b** (66%), **102b** (10%) and **104b** (traces). Only if the reaction mixture was left stirred at  $120^\circ C$  for a further 2 hours, was **105b** completely transformed into **106b** to indicate that the oxidation is a slower process than the C-H amination. The decreasing of the **106b** yield (the yield decreased from 30% to 17% by running the reaction exposed to air instead than under  $N_2$ ), could be due to a different reaction rate of *path a* with respect to *path b* (scheme 2.5). As expected,<sup>257</sup> *path a* maybe even inhibited by dioxygen and therefore the formation of **106b** should be mainly due to *path b*.

The role of the ruthenium in the conversion of **105b** into **106b** was confirmed by stirring a ruthenium-free mixture of the two compounds exposed to air at  $120^\circ C$  for 7 hours. The  $^1H$  NMR spectra registered at the beginning and end of the reaction showed an unvaried product distribution indicating that the oxidation process of **105b** to **106b** requires a catalytic amount of  $Ru(TPP)CO$  to occur. It is worth noting that despite the fact the dehydrogenation of **105b** into **106b** is known to be a relatively easy process, to the best of our knowledge it doesn't take place in absence of an hydrogen acceptor<sup>392</sup> or strong oxidants.<sup>393</sup> On the other hand,  $Ru(TPP)CO$  catalyses this reaction employing atmosphere  $O_2$  as the oxidant species.

In order to study the scope of the reaction, we performed the C-H intramolecular amination of the 2-azido biaryls **103a-103i** (scheme 2.4) by using the optimal experimental conditions (entry 7, table 2.3). To follow the formation of heterocyclic compounds **105** and **106**, we first performed a  $^1H$  NMR analysis after the complete consumption of the azide and then another after stirring the reaction for an additional 2 hours exposed to air at  $120^\circ$  without irradiating with the halogen lamp. The experimental results listed in table 2.4 indicate that  $Ru(TPP)CO$  can be considered a competent catalyst for a *tandem reaction in which an intramolecular C-H amination is followed by an oxidation process*. This reaction afforded phenanthridine yields from good to excellent by using the  $Ru(TPP)CO$ /white light/ $O_2$  combination.

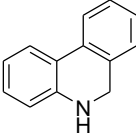
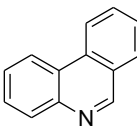
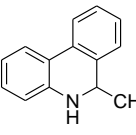
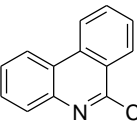
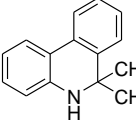
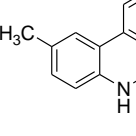
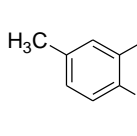
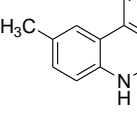
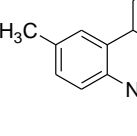
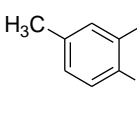
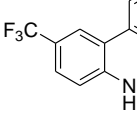
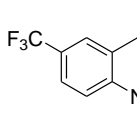
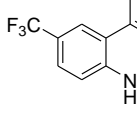
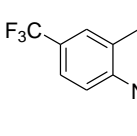
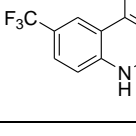
It should be noted that the annulation of the azide **103a** afforded phenanthridine **106a** in 47% yield (table 2.4, entry 1), whereas in the presence of a rhodium catalyst the corresponding carbazole<sup>365</sup> was the mayor reaction product. The presence of **105a** was not detected in the  $^1H$  NMR spectrum recorded under nitrogen after complete consumption of the azide. The  $^1H$  NMR spectrum revealed the presence of aniline **102a** and carbazole **104a** in 31 and 20% yield respectively. This result suggests that **103a** annulation should mainly

occur by *path a* (Scheme 2.5) in which the formed dihydrophenanthridine immediately reacts with the azide yielding equimolar amounts of **106a** and **102a**.<sup>257</sup> The fast dehydrogenation of **105a** is responsible for the formation of the rest of **106a** and explains the absence of **105a** in the reaction mixture. The same behaviour was observed for the annulation of **103d** evidencing, as expected, a favourable dehydrogenation process for dihydrophenanthridines bearing two hydrogen atoms on the 6 position. This trend is less marked if an electron withdrawing group is present on the 2 position of the starting **105** derivative (entry 7). Dihydrophenanthridine was obtained as the unique reaction product only when the dehydrogenation process was impossible (table 2.4, entries 3, 6 and 9). In all other cases a dihydrophenanthridine / phenanthridine mixture was initially obtained and the further oxidation process allowed the complete transformation of **105** into **106** (entries 2, 5, 7 and 8). The high **105h** yield obtained for the annulation of **103h** (table 2.4, entry 8) is probably due to a synergic effect of the CF<sub>3</sub> and CH<sub>3</sub> groups present on 2 and 6 positions respectively. In all runs reported in table 2.4 the rest of the material consisted of aniline and carbazole corresponding to the azide employed.

In conclusion, this is a convenient three steps methodology to form dihydrophenanthridines and phenanthridines starting from commercially available anilines and boronic acids. The reported methodology presents several practical advantages. Firstly, 1 mol % of commercially available Ru(TPP)CO catalyses an intramolecular C-H amination followed by an oxidation process in a tandem reaction. Then, the use of an ordinary halogen lamp speeds up the reaction and renders the procedure feasible in any laboratory and at a low cost. Finally, the formation of molecular nitrogen as the by-product associated with the use of molecular oxygen for the dihydrophenanthridine oxidation grants this method sustainable.

Considering that porphyrins are potent photosensitizers (PS) capable of transforming <sup>3</sup>O<sub>2</sub> into <sup>1</sup>O<sub>2</sub> by irradiation with visible light,<sup>394</sup> the influence of the catalyst/white light combination on the decomposition of the azide N<sub>3</sub> group deserves a more in depth investigation. Moreover, because of the great importance of the use of oxygen as a “green” oxidant species, further work will also be devoted to clarifying the mechanism of the dihydrophenanthridine oxidation.

**Table 2.4.** The Ru(TPP)CO (1%) catalysed C-H intramolecular amination of 2-azido biaryls (**103a-103i**)<sup>[a]</sup>

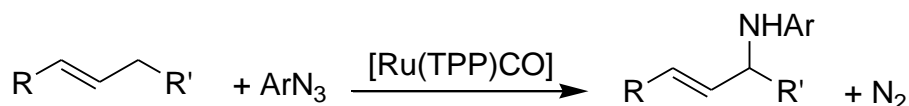
entry	time (h) <sup>[b]</sup>	Dihydrophenanthridine yield (%) <sup>[c]</sup>	phenanthridine yield (%)
1	1.5	 <b>105a</b> , -	 <b>106a</b> , 47 <sup>[c]</sup>
2	1	 <b>105b</b> , 46	 <b>106b</b> , 32 <sup>[c]</sup> (78) <sup>[d]</sup>
3	1	 <b>105c</b> , 85	-
4	1.5	 <b>105d</b> , -	 <b>106d</b> , 48 <sup>[c]</sup>
5 <sup>]</sup>	1	 <b>105e</b> , 38	 <b>106e</b> , 52 <sup>[c]</sup> (90) <sup>[d]</sup>
6 <sup>]</sup>	1.5	 <b>105f</b> , 85	-
7	2.5	 <b>105g</b> , 24	 <b>106g</b> , 48 <sup>[c]</sup> (72) <sup>[d]</sup>
8	3	 <b>105h</b> , 85	 <b>106h</b> , 10 <sup>[c]</sup> (95) <sup>[d]</sup>
9	1	 <b>105i</b> , 98	-

[a] General procedure for catalytic reactions: Ru(TPP)CO (2.0 mg,  $2.70 \times 10^{-6}$  mmol) in 1,2 dichlorobenzene (20 mL) at 120 °C under N<sub>2</sub> and 400 W halogen lamp irradiation; mol ratios cat/azide = 1:100. [b] Time required to reach complete conversion of azide. [c] Determined by <sup>1</sup>H NMR (2,4-dinitrotoluene as the internal standard) after the complete consumption of azide. [d] Determined by <sup>1</sup>H NMR (2,4-dinitrotoluene as the internal standard) after oxidation by atmospheric oxygen.



## 2.3. Allylic Amination

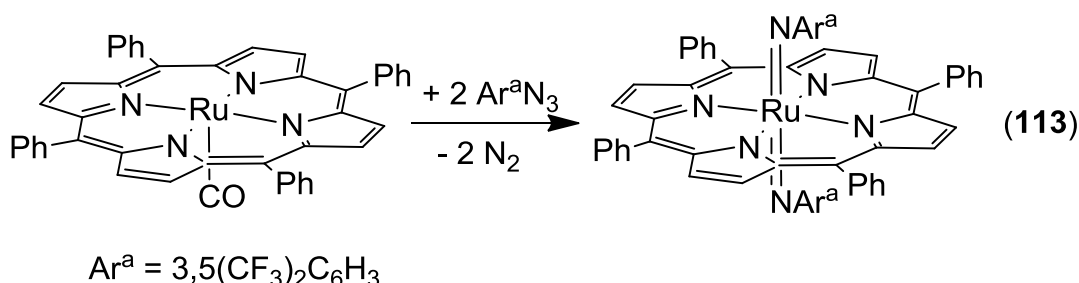
Since Ru(TPP)CO has demonstrated to be a good catalyst in benzylic amination reactions we have subsequently studied the activity of this catalyst in allylic amination reactions (scheme 2.6).



**Scheme 2.6.** Amination of allylic substrates catalysed by Ru(TPP)CO

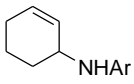
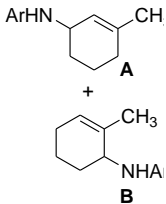
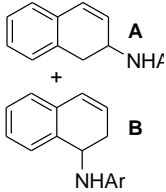
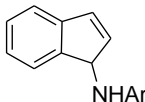
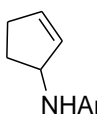
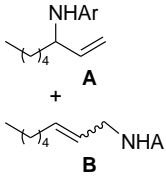
The synthesis of allylic amines reported in table 2.5 was firstly performed in refluxing benzene, employing mol ratios Ru(TPP)CO/ArN<sub>3</sub>/olefin = 1:50:250, and then running the reaction in the neat olefin as the solvent. Data reported in table 2.5 indicates that in using the latter methodology better yields are generally obtained. In particular, very high yields have been achieved in refluxing olefin for the allylic amination of cyclohexene by almost every azide (table 2.5, run 1). The low yield observed in the reaction of 4-OMeC<sub>6</sub>H<sub>4</sub>N<sub>3</sub> with cyclohexene (run 1, product **107h**) is probably due to the coordination of the methoxy group to the ruthenium atom that can partially inhibit the catalysis.<sup>240</sup> It should be noted that the reduced chemoselectivity of the amination of 1,2-dihydronaphthalene was due to the contemporary presence of both allylic and benzylic functionalities (run 3).<sup>389</sup> Finally, the amination of 1-octene occurred only to some extent due to the poor reactivity of this linear olefin (run 6). In all the reactions tested the secondary products recovered were the aryl diazene and aniline corresponding to the azide employed.

Believing that an important step for the improvement of the catalytic efficiency of the reported methodology is the comprehension of the reaction mechanism, we first studied the catalyst reactivity towards the components of a model reaction, cyclohexene and 3,5(CF<sub>3</sub>)<sub>2</sub>C<sub>6</sub>H<sub>3</sub>N<sub>3</sub>. No catalyst modification was observed by <sup>1</sup>H NMR when Ru(TPP)CO was suspended in cyclohexene and refluxed for a couple of hours. On the other hand, the reaction between Ru(TPP)CO and an Ar<sup>a</sup>N<sub>3</sub> excess (3 equiv.) (Ar<sup>a</sup> = 3,5(CF<sub>3</sub>)<sub>2</sub>C<sub>6</sub>H<sub>3</sub>) yielded the bis imido complex Ru(TPP)(NAr<sup>a</sup>)<sub>2</sub> (**113**) in 70% yield (scheme 2.7)



**Scheme 2.7.** Synthesis of Ru(TPP)(NAr<sup>a</sup>)<sub>2</sub> (Ar<sup>a</sup> = 3,5(CF<sub>3</sub>)<sub>2</sub>C<sub>6</sub>H<sub>3</sub>) (**113**)

**Table 2.5.** The Ru(TPP)CO-mediated allylic amination by ArN<sub>3</sub><sup>[a]</sup>

run	product <sup>[b]</sup>	Ar	yield (%) <sup>[b]</sup>	time (h) <sup>[c]</sup>
1		<b>107a</b> , 3,5(CF <sub>3</sub> ) <sub>2</sub> C <sub>6</sub> H <sub>3</sub>	26 (75) <sup>[d]</sup>	12(4) <sup>[d]</sup>
		<b>107b</b> , 4-NO <sub>2</sub> C <sub>6</sub> H <sub>4</sub>	23 (70) <sup>[d]</sup>	5(6) <sup>[d]</sup>
		<b>107c</b> , 4- <sup>t</sup> BuC <sub>6</sub> H <sub>4</sub>	13(89) <sup>[d]</sup>	6(7) <sup>[d]</sup>
		<b>107d</b> , 4-CNC <sub>6</sub> H <sub>4</sub>	35 (80) <sup>[d]</sup>	8(2) <sup>[d]</sup>
		<b>107e</b> , 4-CF <sub>3</sub> C <sub>6</sub> H <sub>4</sub>	28 (85) <sup>[d]</sup>	7(4) <sup>[d]</sup>
		<b>107f</b> , 4(CO <sub>2</sub> Me)C <sub>6</sub> H <sub>4</sub>	13 (85) <sup>[d]</sup>	6(8) <sup>[d]</sup>
		<b>107g</b> , 3,5-Cl <sub>2</sub> C <sub>6</sub> H <sub>3</sub>	38 (90) <sup>[d]</sup>	10(3) <sup>[d]</sup>
		<b>107h</b> , 4-MeOC <sub>6</sub> H <sub>4</sub>	8 (33) <sup>[d]</sup>	7(7) <sup>[d]</sup>
2		<b>108a</b> , 3,5(CF <sub>3</sub> ) <sub>2</sub> C <sub>6</sub> H <sub>3</sub>	<b>A</b> , 28, <b>B</b> , 15	10
		<b>108b</b> , 4-NO <sub>2</sub> C <sub>6</sub> H <sub>4</sub>	<b>A/B</b> , 20	8
		<b>108e</b> , 4-CF <sub>3</sub> C <sub>6</sub> H <sub>4</sub>	<b>A</b> , 17; <b>B</b> , 9	7
3		<b>109a</b> , 3,5(CF <sub>3</sub> ) <sub>2</sub> C <sub>6</sub> H <sub>3</sub>	<b>A</b> , 33, <b>B</b> , 24	1
		<b>109b</b> , 4-NO <sub>2</sub> C <sub>6</sub> H <sub>4</sub>	( <b>A</b> , 51, <b>B</b> , 34) <sup>[d]</sup>	(0.3) <sup>[d]</sup>
			<b>A</b> , 32, <b>B</b> , 22	3
			( <b>A</b> , 45, <b>B</b> , 28) <sup>[d]</sup>	(1) <sup>[d]</sup>
4		<b>110a</b> , 3,5(CF <sub>3</sub> ) <sub>2</sub> C <sub>6</sub> H <sub>3</sub>	42	3
		<b>110b</b> , 4-NO <sub>2</sub> C <sub>6</sub> H <sub>4</sub>	30	3.5
		<b>110e</b> , 4-CF <sub>3</sub> C <sub>6</sub> H <sub>4</sub>	30	5
5		<b>111</b> , 4-NO <sub>2</sub> C <sub>6</sub> H <sub>4</sub>	30	8
6		<b>112</b> , 3,5(CF <sub>3</sub> ) <sub>2</sub> C <sub>6</sub> H <sub>3</sub>	<b>A</b> , 9, <b>B</b> , 11	25

[a] General procedure for catalytic reactions: Ru(TPP)CO (10 mg, 1.34×10<sup>-2</sup> mmol) in refluxing benzene (30 mL); mol ratios cat/ArN<sub>3</sub>/olefin = 1:50:250. [b] Determined by <sup>1</sup>H NMR (2,4-dinitrotoluene as the internal standard). [c] Time required to reach complete conversion of the starting ArN<sub>3</sub>. [d] Reaction run in neat refluxing olefin.

It is likely that complex **113** derives from the reaction of the mono-imido Ru(IV)(TPP)(Ar<sup>a</sup>N)CO complex with another molecule of aryl azide. Unfortunately, the formation of **113** occurred without observable intermediates and every attempt to detect a ruthenium (IV) species failed. It is possible that the intermediate Ru(IV) complex reacts with a second azide molecule at a much faster rate than the starting Ru(TPP)(CO) does. However, Ru(IV)(TPP)(Ar<sup>a</sup>N)CO may also rapidly disproportionate to the bis-imido **113** and Ru(TPP)CO, analogously to what was proposed in the literature for isostructural ruthenium(IV) oxo porphyrins.<sup>123, 395</sup>

Complex **113** was fully characterised (see experimental section) and remained stable for a long period of time at room temperature decomposing only when exposed to a coordinating solvent such as THF. The NMR spectrum in CDCl<sub>3</sub> (figure 2.3) revealed a chemical shift of the aromatic azide hydrogen atoms due to the ring current effect of the porphyrin

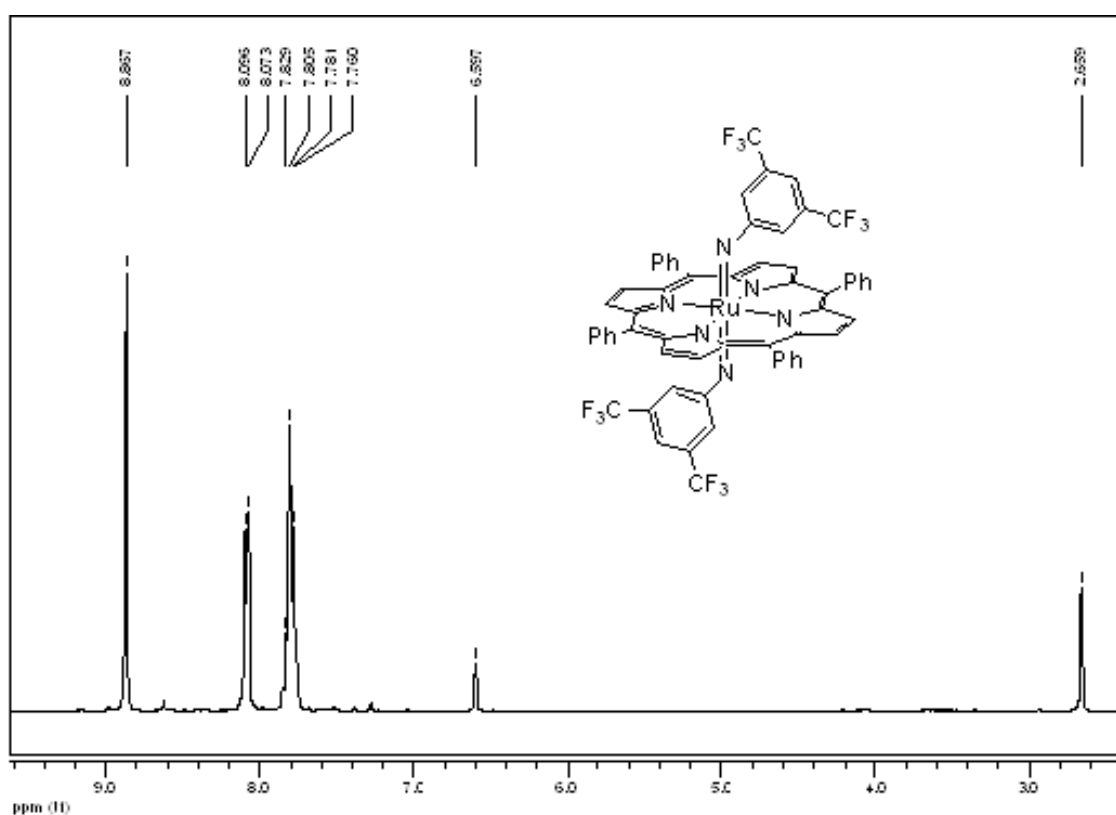


**Figure 2.3.** <sup>1</sup>H NMR spectrum of complex **113** in CDCl<sub>3</sub>.

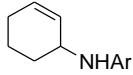
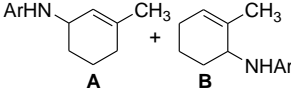
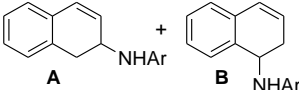
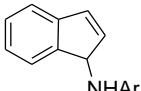
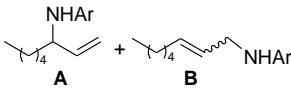
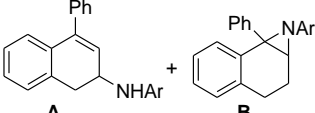
The X-ray diffraction on a single crystal sample confirmed the molecular structure (figure 2.4). The two ArN ligands are syn-periplanar (i.e. almost perfectly eclipsed about the N1---N2 axis). The Ru-N distances, 1.808(4) and 1.806(4) Å for N1 and N2 respectively, are in the range of double bonds, thus confirming the imido nature of the ligand. The nitrogen lone pairs are available as demonstrated by the Ru-N-C angles, which are extremely bent (139.8(3) and 143.7(4)°, respectively).<sup>396</sup> However, no intermolecular contact occurs at these two, crystallographically independent, atoms. This is certainly due to the absence of any H-



dihydronaphthalene (table 2.6, run 6), the formation of the aziridine ring was also observed in accord to what we had already reported on the Ru(porphyrin)CO catalysed aziridination of olefins.<sup>240</sup>

To better investigate the catalytic role of **113**, the reaction of cyclohexene with Ar<sup>a</sup>N<sub>3</sub> was run in 1 mL of C<sub>6</sub>D<sub>6</sub> at 65 °C in the presence of 10 mg of **113** (8.6×10<sup>-3</sup> mmol) using a mol ratio **113**/aryl azide/cyclohexene = 1:10:20. The progress of the reaction was monitored by <sup>1</sup>H NMR. The formation of the corresponding allylic amine was accompanied by the disappearance of the signals relative to **113** and those attributable to a new ruthenium porphyrin species (**115**) became evident. This new complex was visible by <sup>1</sup>H NMR until the complete aryl azide conversion and then the formation of several signals in the porphyrin region indicated a decomposition process.

**Table 2.6.** Complex **113**-mediated allylic amination by Ar<sup>a</sup>N<sub>3</sub><sup>[a]</sup>

run	product <sup>[b]</sup>	yield (%) <sup>[b]</sup>	time (h) <sup>[c]</sup>
1		<b>107a</b> , 74(99) <sup>[d]</sup>	16(1) <sup>[d]</sup>
2		<b>108a</b> , A, 38(49) <sup>[d]</sup> B, 22(39) <sup>[d]</sup>	20(2) <sup>[d]</sup>
3		<b>109a</b> , A, 39 B, 21	1.5
4		<b>110a</b> , 55(70) <sup>[d]</sup>	1.5(0.5) <sup>[d]</sup>
5		<b>112</b> , A, 5(11) <sup>[d]</sup> B, 6(11) <sup>[d]</sup>	40 <sup>[e]</sup> (6) <sup>[d]</sup>
6		<b>114</b> , A, 33 B, 28	1.5

[a] General procedure for catalytic reactions: **113** (15 mg, 1.28×10<sup>-2</sup> mmol) in refluxing benzene (30 mL); mol ratios cat/Ar<sup>a</sup>N<sub>3</sub>/olefin = 1:50:250. [b] Determined by <sup>1</sup>H NMR (2,4-dinitrotoluene as the internal standard). [c] Time required to reach complete conversion of the starting Ar<sup>a</sup>N<sub>3</sub>. [d] Reaction run in neat refluxing olefin. [e] Ar<sup>a</sup>N<sub>3</sub> conversion = 85%.

To isolate the complex observed during the NMR analysis, the reaction was performed on a larger scale (30 mg of **113**, 2.57·10<sup>-2</sup> mmol) and followed by IR spectroscopy, monitoring the intensity of the 2116 cm<sup>-1</sup> absorption of the N<sub>3</sub> group of the azide. The reaction was stopped at 90% of aryl azide conversion to avoid the formation of decomposition products and refrigerated to yield a little amount of purple crystals.

The X-ray structure reported in figure 2.5 shows that **115** is the bis-amido complex Ru(TPP)(Ar<sup>a</sup>NC<sub>6</sub>H<sub>9</sub>)<sub>2</sub>. Here the molecule sits on an inversion centre and the Ru-N1 distance is much larger than in **113** (namely

1.962(3) Å) and in the range of typical amido bonds. Ru1-N3-C31 and Ru1-N3-C41 angles have typical values of 122.2(3) and 124.0(3) ° respectively, with the N3-C31-C41 plane perpendicular to the TPP one. N3-C31 in **115** (1.417(5) Å) is longer than N1-C1 (1.361(6) Å) or N2-C2 (1.392(4) Å) in **113**. The porphyrin-Ru bonds are slightly shorter than in **113** (2.042-2.047 Å). The intermolecular contacts are all quite long in the absence of strong interactions. Nevertheless, no empty volume is left in the crystal.

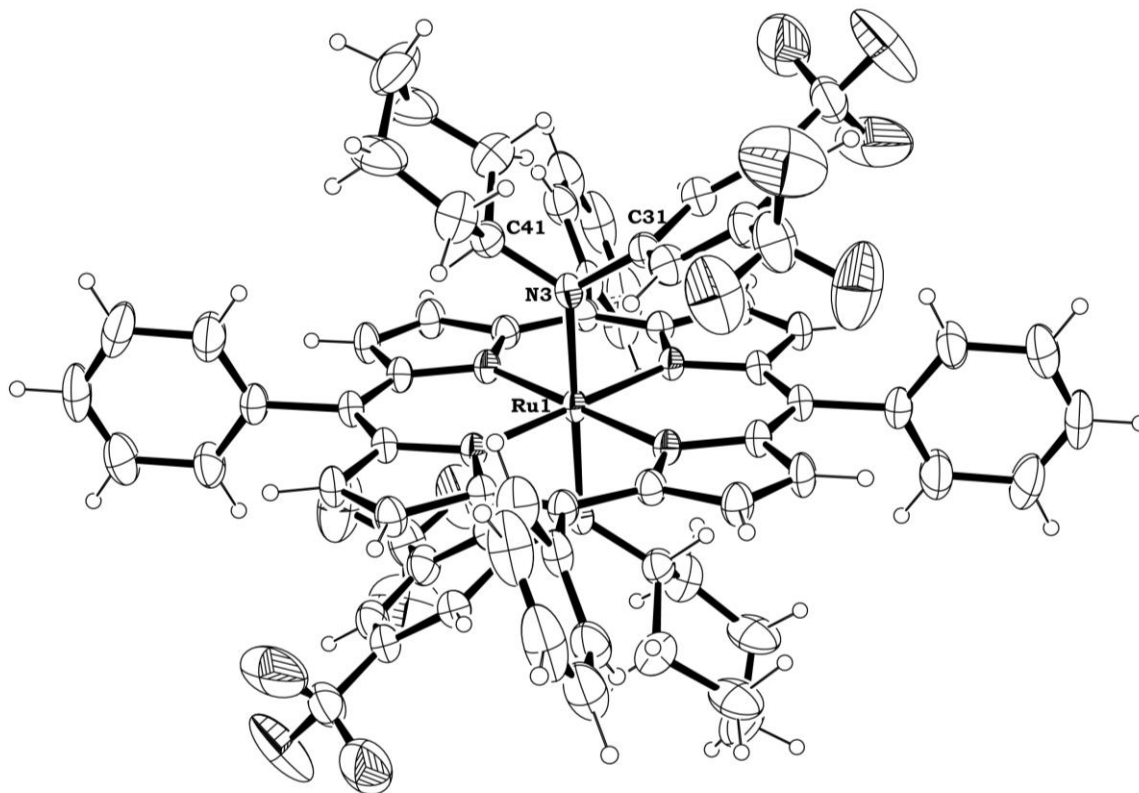
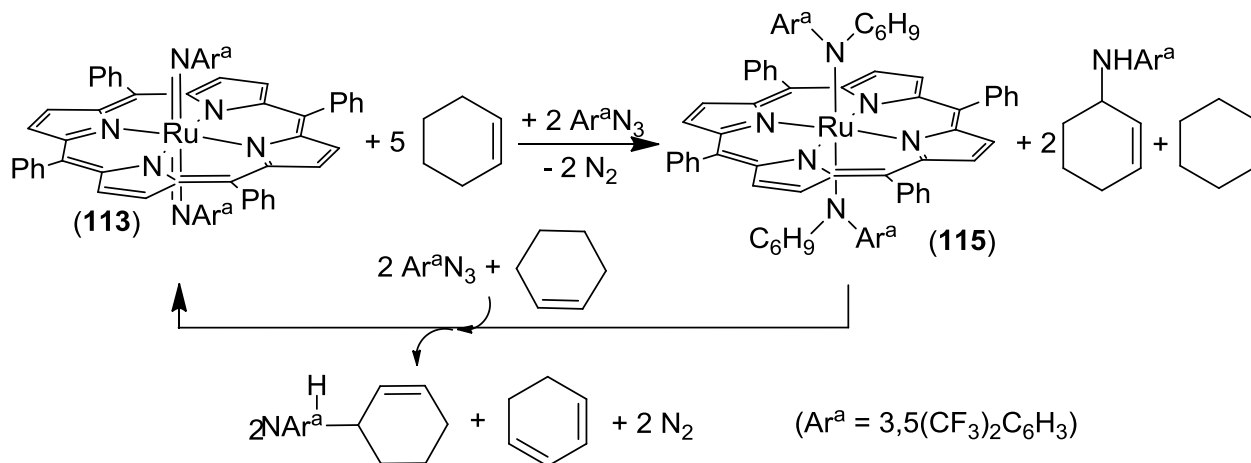


**Figure 2.5.** Molecular structure of **115**, ellipsoids are drawn at 30% probability.

We tried to synthesise **115** in large amounts but, due to its chemical instability, pure **115** was isolated in a low yield (18%), together with the allylic amine and unidentified ruthenium species. Complex **115** is stable for a few days at -15 °C in the solid state, for some hours in a benzene solution and rapidly decomposes in the majority of solvents, especially in coordinating ones. The diamagnetic behaviour of **115** indicates the formation of a ruthenium (IV) compound with  $S = 0$ . A recent DFT study is in accord with our experimental results.<sup>398</sup>

If **115** was left standing in pure cyclohexene or in a mixture benzene/cyclohexene the fast formation of the corresponding allylic amine and of uncharacterised ruthenium products was observed. Complex **115** could be accumulated in solution only under catalytic conditions in which both  $\text{Ar}^{\text{a}}\text{N}_3$  and cyclohexene are present and the olefin concentration is larger than that of the azide. Conversely, in the situation of  $[\text{Ar}^{\text{a}}\text{N}_3] > [\text{cyclohexene}]$ , complex **115** was completely converted into **113**. We have studied this reaction dissolving **115** (6.85 mg,  $5.15 \times 10^{-3}$  mmol) in a  $\text{C}_6\text{D}_6$  (1 mL) solution of  $\text{Ar}^{\text{a}}\text{N}_3$  and cyclohexene in a mol ratio **115**/aryl azide/cyclohexene = 1:50:10. The reaction was monitored by following the  $^1\text{H}$  NMR pyrrolic signals of the porphyrin. After a few minutes at 65 °C the formation of **113** was observed and after 4 hours **115** was no

longer detectable by  $^1\text{H}$  NMR spectroscopy. It should be noted that if at this point more cyclohexene (60 equiv) was added to the mixture, complex **115** was regenerated to indicate a reversible process. The  $^1\text{H}$  NMR spectra also disclosed the catalytic formation of the allylic amine. Data collected up to now suggests a mechanism for the allylic amination of cyclohexene in which both complexes **113** and **115** are implicated (Scheme 2.8).



**Scheme 2.8.** Mechanistic hypothesis for the reaction between cyclohexene and Ar<sup>a</sup>N<sub>3</sub> catalysed by complex **113**

The synthesis of **115** requires the abstraction of two hydrogen atoms that, in our opinion, are associated to the **113**-mediated<sup>399, 400</sup> reduction of a stoichiometric amount of cyclohexene to cyclohexane. A reduction of benzene is to be excluded because the allylic amination of cyclohexene occurred in high yields also in neat olefin (Table 2.6, entry 1). The complete inhibition of the reaction when the **113** catalysed amination of cyclohexene was run in the presence of TEMPO (2,2,6,6-tetramethylpiperidine-*N*-oxide) indicates that the “NAr” insertion into the C-H bond proceeds via radical intermediates, as previously reported for similar catalytic systems.<sup>210, 401</sup> The reversible **115** to **113** process occurs by a hydrogen atom transfer (HAT) reaction in which cyclohexene is oxidized to 1,3-cyclohexadiene which was identified at the end of the catalytic reaction by GC-MS and  $^1\text{H}$  NMR analyses. The latter was not present as an impurity in the starting cyclohexene, as evidenced by the same technique. Unfortunately, the presence of cyclohexane could not be detected by GC-MS spectroscopy because its signal overlaps with that of cyclohexene.

The hypothesis illustrated in Scheme 2.8 is supported by the  $^1\text{H}$  NMR and GC-MS analyses of the amination of 1,2-dihydronaphthalene which reveals, apart from the corresponding allylic amine, also the presence of naphthalene and the benzylic amine of 1,2,3,4-tetrahydronaphthalene. The formation of the latter compound indicates that 1,2-dihydronaphthalene was partly reduced to 1,2,3,4-tetrahydronaphthalene that, being a benzylic substrate for the nitrene transfer reaction, was aminated. The involvement of the hydrocarbon substrate in the HAT process can explain the need for an olefin excess for the catalytic reaction to proceed. In fact, if allylic aminations were run with the olefin as the limiting agent the consumption of Ar<sup>a</sup>N<sub>3</sub> was not complete. It should be emphasised that the active role of **115** was further supported by its catalytic activity in the allylic amination of cyclohexene, that was maintained for two further runs when additional

amounts of the reagents were added before the complete consumption of  $\text{Ar}^a\text{N}_3$  to avoid the catalyst decomposition.

In order to assess if the formation of a bis-imido complex is a general reaction, we have also studied the reactivity of  $\text{Ru}(\text{TPP})\text{CO}$  towards other aryl azides. The reactions between  $\text{Ru}(\text{TPP})\text{CO}$  and  $\text{ArN}_3$  ( $\text{Ar} = 4\text{-CF}_3\text{C}_6\text{H}_4\text{N}_3$ ,  $4\text{-NO}_2\text{C}_6\text{H}_4\text{N}_3$ ,  $4\text{-CNC}_6\text{H}_4\text{N}_3$ ) were monitored by  $^1\text{H}$  NMR ( $\text{C}_6\text{D}_6$ ). After the addition of the selected azide an immediate modification of the  $\text{Ru}(\text{TPP})\text{CO}$  spectrum was observed. The coordination of the nitrene ligand to the metal centre has been suggested on the basis of the change of the typical porphyrin region and for the appearance of signals in the same NMR region (2-7 ppm) where aromatic hydrogen atoms of the azide were detected for **113** (figure 2.3). In every reaction tested the new formed complex was stable for a short period of time and the disappearance of the signals, attributed to the coordinated aryl group, indicated a decomposition process.

The reaction between  $\text{Ru}(\text{TTP})\text{CO}$  and  $\text{Ar}^e\text{N}_3$  ( $\text{Ar}^e = 4\text{-CF}_3\text{C}_6\text{H}_4\text{N}_3$ ) was repeated on a larger scale and stopped after 30 minutes to avoid any decomposition. The purple complex  $\text{Ru}(\text{TPP})(\text{NAr}^e)_2$  (**116**) was isolated in 60% yield and fully characterised. Unreacted  $\text{Ru}(\text{TPP})\text{CO}$  was also present in the reaction mixture. Complex **116** was stable in the solid state under an inert atmosphere for several days but it partially decomposed in solution, making it difficult to determine its molecular structure by X-ray diffraction analysis. Nevertheless, we proposed the formation of the bis imido complex **116** on the basis of the 1D and 2D NMR spectra that showed a perfect similitude with those of complex **113**. The  $^1\text{H}$  NMR spectrum (figure 2.6) showed the presence of AA'BB' pattern for the aromatic azide moiety at 5.94 and 2.61 ppm. All the other analytical data agreed with the proposed structure.

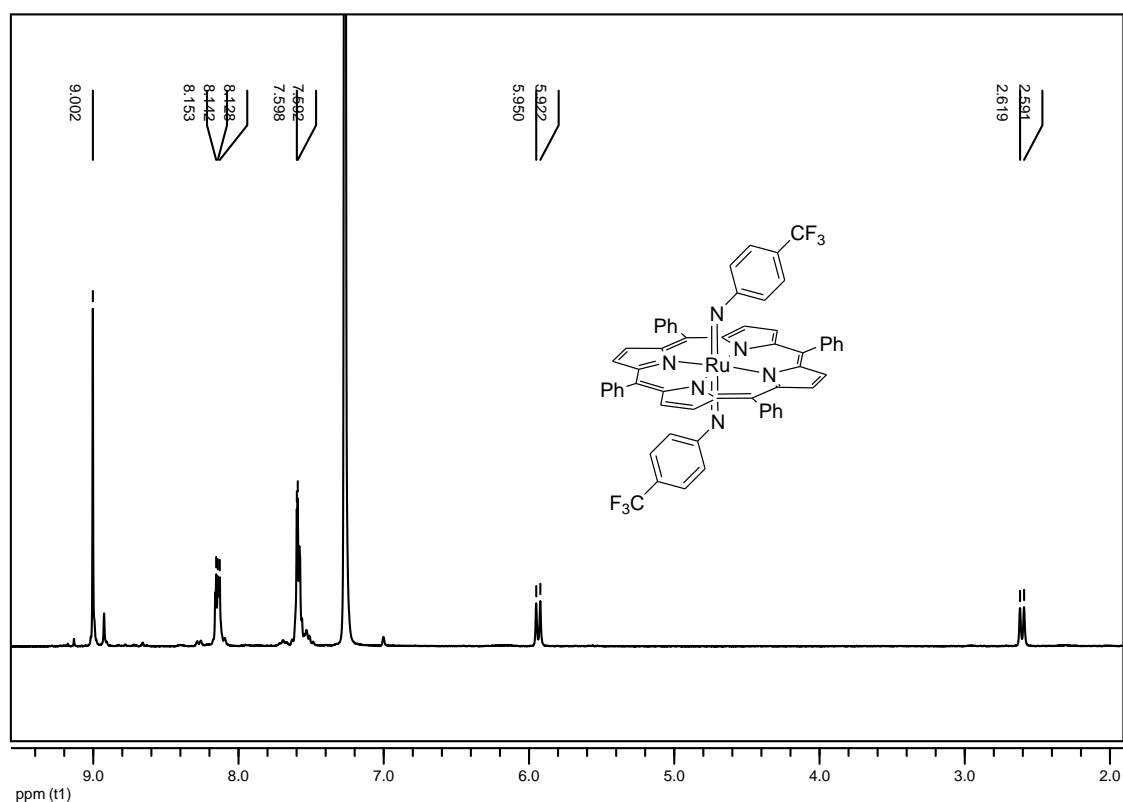


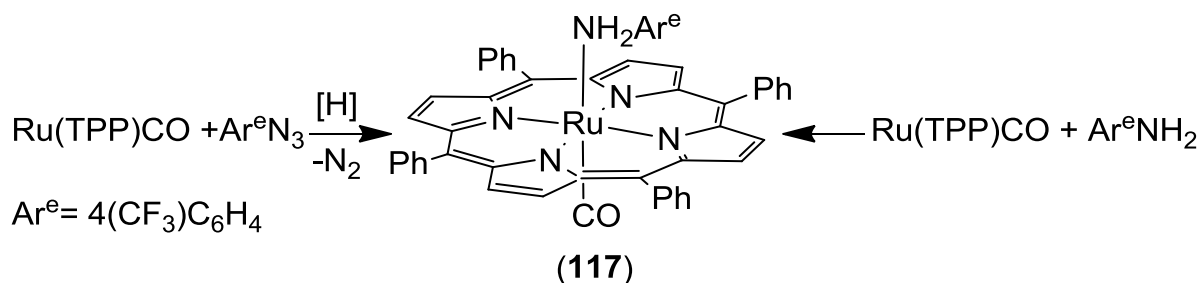
Figure 2.6.  $^1\text{H}$  NMR spectra in  $\text{C}_6\text{D}_6$  of complex **116**.



Complex **116** was refluxed in cyclohexene for 3 hours to give the allylic amine (54%) and it was catalytically active in the reaction between cyclohexene and  $\text{Ar}^e\text{N}_3$  using a catalytic mol ratio **116**/azide = 1:50 in refluxing cyclohexene. After 2.5 hours the allylic amine **107e** was recovered in 55% yield. Complex **116** was also a competent catalyst in the allylic amination of 1-methyl cyclohexene, indene and 1-octene by  $\text{Ar}^e\text{N}_3$ ; the corresponding allylic amines were formed with yields comparable with those obtained using  $\text{Ru}(\text{TPP})\text{CO}$  as the catalyst.

The reaction between  $\text{Ru}(\text{TPP})\text{CO}$  and 4 equivalents of  $\text{Ar}^e\text{N}_3$  was refluxed in  $\text{C}_6\text{H}_6$  for 3 hours to better figure out the observed decomposition pathway. The complex  $\text{Ru}(\text{TPP})(\text{Ar}^e\text{NH}_2)\text{CO}$  (**117**) has been isolated from the reaction mixture in 37% yield. Ruthenium unidentified compounds deriving from the decomposition of **116** accounted for the rest of the reaction mass balance with respect to the starting  $\text{Ru}(\text{TPP})\text{CO}$ .

The structure of **117** was definitely assigned by comparing its analytical data with those of the reaction product between  $\text{Ru}(\text{TPP})\text{CO}$  and 4- $\text{CF}_3\text{C}_6\text{H}_4\text{NH}_2$  (scheme 2.9).



**Scheme 2.9.** Synthesis of complex **117**

Complex **117** exhibited different spectra in  $\text{CDCl}_3$  and in  $\text{C}_6\text{D}_6$  due to the *aromatic solvent-induced shift* (ASIS)<sup>402, 403</sup> effect (figure 2.7); however in both cases a signal at negative ppm values was observed (-3.43 ppm and -4.06 ppm in  $\text{CDCl}_3$  and  $\text{C}_6\text{D}_6$  respectively). The signal disappeared after adding  $\text{D}_2\text{O}$  and the  $^2\text{H}$  NMR spectrum in  $\text{C}_6\text{D}_6$  disclosed the presence of a signal at -13.43 ppm; this data confirms the coordination of an aryl amine to the ruthenium atom.

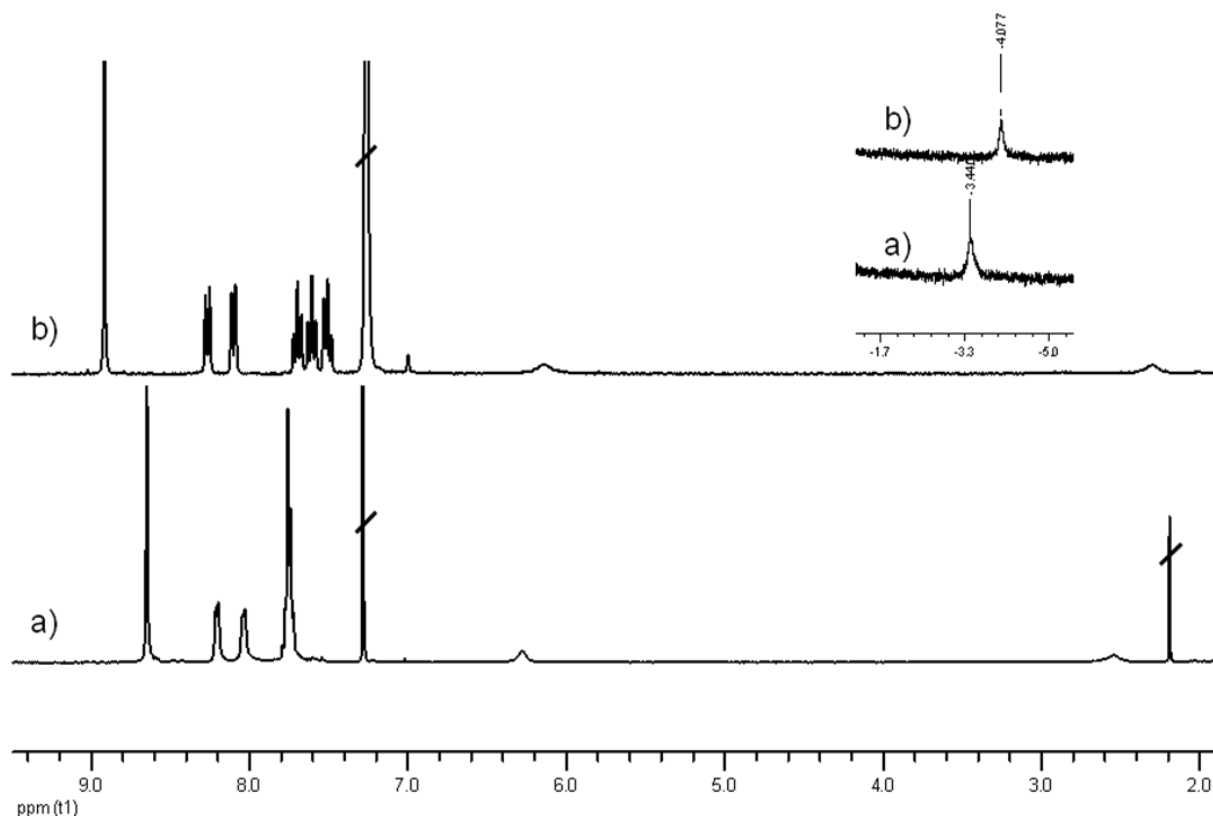


**Figure 2.7.**  $^1\text{H}$  NMR spectra of **117** in  $\text{CDCl}_3$ (a) and  $\text{C}_6\text{D}_6$  (b).

To explain the formation of **117** we propose that, as already suggested for the synthesis of **113**, the first step of the reaction between  $\text{Ru}(\text{TPP})\text{CO}$  and  $\text{Ar}^{\text{e}}\text{N}_3$  yields a mono-imido ruthenium(IV) complex which is too reactive to be detected. This intermediate can react with another molecule of aryl azide yielding **116** or can decompose to regenerate  $\text{Ru}(\text{TPP})\text{CO}$ . The so-formed  $\text{Ru}(\text{TPP})\text{CO}$  can be “trapped” by  $\text{Ar}^{\text{e}}\text{NH}_2$  yielding **117**. The presence of  $\text{Ar}^{\text{e}}\text{NH}_2$  in solution is due to a partial aryl azide decomposition mediated by the ruthenium catalyst, which can promote hydrogen atom abstraction reactions.<sup>401</sup> Clearly, we cannot exclude that the direct reaction of the starting  $\text{Ru}(\text{TPP})\text{CO}$  with  $\text{Ar}^{\text{e}}\text{NH}_2$  can also be in part responsible for the formation of **117**.

Considering that complex **117** can also be formed during the catalytic reaction, we have studied its catalytic activity in the allylic amination of several olefins using the same experimental conditions reported in table 2.5. Obtained data were comparable with those observed in  $\text{Ru}(\text{TPP})\text{CO}$ -mediated reactions indicating that  $\text{Ar}^{\text{e}}\text{NH}_2$ , eventually formed during the catalytic cycle, is not a catalyst inhibitor.

Synthetic results described up to now suggest that, depending on the electronic nature of the employed aryl azide, both bis and mono-imido complexes can be involved in allylic aminations of cyclohexene and an active role is probably also played by mono-imido species.

### 2.3.1. Kinetics Study of the Allylic Amination

To shed some light into the Ru(TPP)CO catalysed allylic amination of cyclohexene, a kinetic study was undertaken employing  $\text{Ar}^e\text{N}_3$  ( $\text{Ar}^e = 4\text{-CF}_3\text{C}_6\text{H}_4\text{N}_3$ ) or  $\text{Ar}^a\text{N}_3$  ( $\text{Ar}^a = 3,5(\text{CF}_3)_2\text{C}_6\text{H}_3\text{N}_3$ ) as nitrogen sources. The reactions were followed by IR spectroscopy, monitoring the intensity of the aryl azide absorption ( $\text{Ar}^e\text{N}_3$  at  $2102\text{ cm}^{-1}$  and  $\text{Ar}^a\text{N}_3$  at  $2116\text{ cm}^{-1}$ ). All kinetic experiments were run at  $75\text{ }^\circ\text{C}$  to avoid boiling of benzene in those reactions in which it was present.

The rate of the reaction between cyclohexene and  $\text{Ar}^e\text{N}_3$  showed a first-order dependence on azide and Ru(TPP)CO concentrations. However, a zero order dependence on cyclohexene concentration (the other solvent being benzene) was observed (figure 2.8). Observed data leads to the kinetic equation  $v = -d[\text{Ar}^e\text{N}_3]/dt = k_{\text{obs}}[\text{Ru(TPP)CO}][\text{Ar}^e\text{N}_3]$

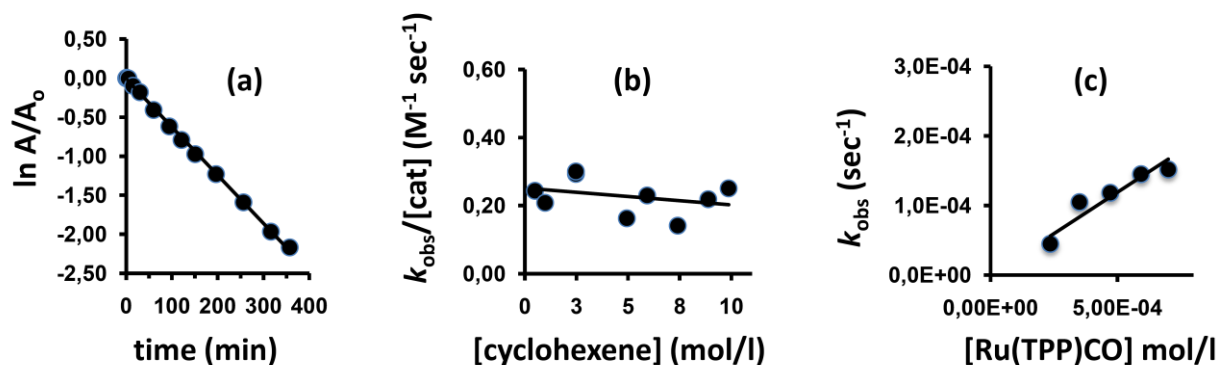
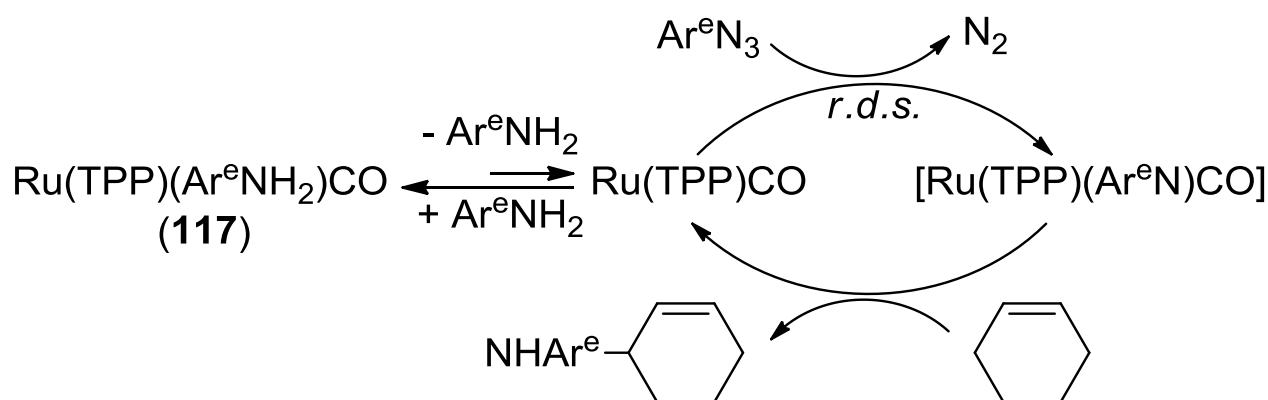


**Figure 2.8.** Kinetic dependence of the reaction rate with respect to  $4\text{-CF}_3\text{C}_6\text{H}_4\text{N}_3$  (a), cyclohexene (b) and Ru(TPP)CO concentrations (c).

Sampling the reaction mixture during a catalytic reaction and examining it by TLC allowed the observation of  $\text{Ru(TPP)(CO)(Ar}^e\text{NH}_2)$  as the only identifiable complex. Together with the observed kinetics, this observation is consistent with a reaction mechanism in which the *rate determining step* is the formation of a mono-imido complex that very quickly reacts with the olefin forming the allylic amine and regenerating Ru(TPP)CO. We suggest that Ru(TPP)CO is in equilibrium with  $\text{Ru(TPP)(Ar}^e\text{NH}_2)\text{CO}$  (**117**) for the presence of aniline as a reaction by-product. This mechanistic hypothesis envisages that **117** should be the only product accumulated in solution in accord with the experimental observation (scheme 2.10).



**Scheme 2.10.** Mechanistic hypothesis for the reaction between cyclohexene and 4-CF<sub>3</sub>C<sub>6</sub>H<sub>4</sub>N<sub>3</sub> catalysed by Ru(TPP)CO

Note that an active role of the bis-imido complex **116** under these conditions is not supported by the kinetic experiments. In particular, it would be difficult to explain the observation of a ruthenium carbonyl complex even at the end of the reaction if the coordinated CO had been lost in the formation of **116**.

The same kinetics has been observed for the reaction of 4-NO<sub>2</sub>C<sub>6</sub>H<sub>4</sub>N<sub>3</sub> with cyclohexene catalysed by Ru(TPP)CO.

The kinetics of the Ru(TPP)CO-catalysed reaction between Ar<sup>a</sup>N<sub>3</sub> and cyclohexene was more complex than previously discussed. A first order dependence on the aryl azide was observed but the rate order dependence on the olefin concentration is not unique. A first-order dependence was observed up to an olefin concentration of 3 M and then the reaction rate was almost independent from the quantity of cyclohexene present in solution (figure 2.9, a). This behaviour indicates the coexistence of at least two mechanisms which occur contemporaneously with the prevalence of one or the other depending on the olefin concentration.

The kinetics of the reaction between Ar<sup>a</sup>N<sub>3</sub> and cyclohexene was also studied in the presence of Ru(TPP)(NAr<sup>a</sup>)<sub>2</sub> (**113**) and a first order with respect to the aryl azide concentration was observed. The rate dependence on olefin concentration showed both similarities and differences with respect to that observed using Ru(TPP)CO as the catalyst. A first-order dependence on cyclohexene concentration was again obtained up to a 3 M concentration, but an inhibiting effect at higher concentrations was evident (figure 2.9, b), rather than the flat dependence visible in figure 2.9, a.

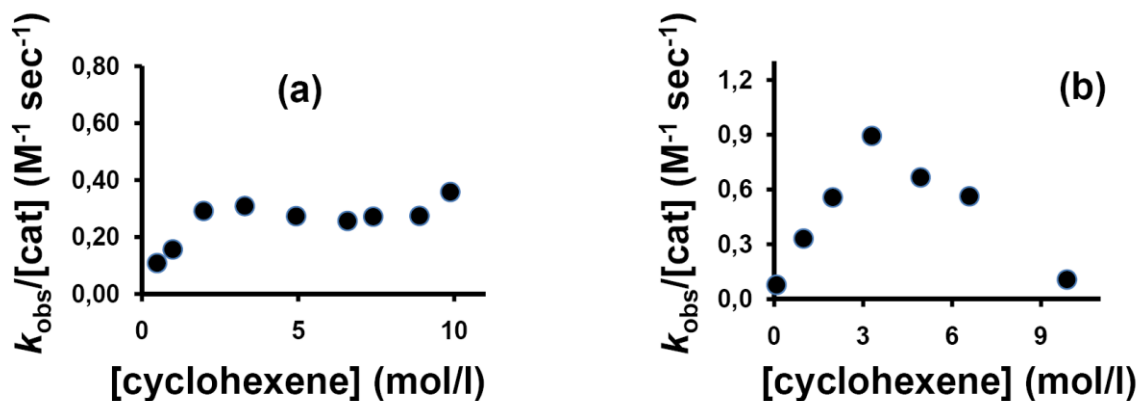
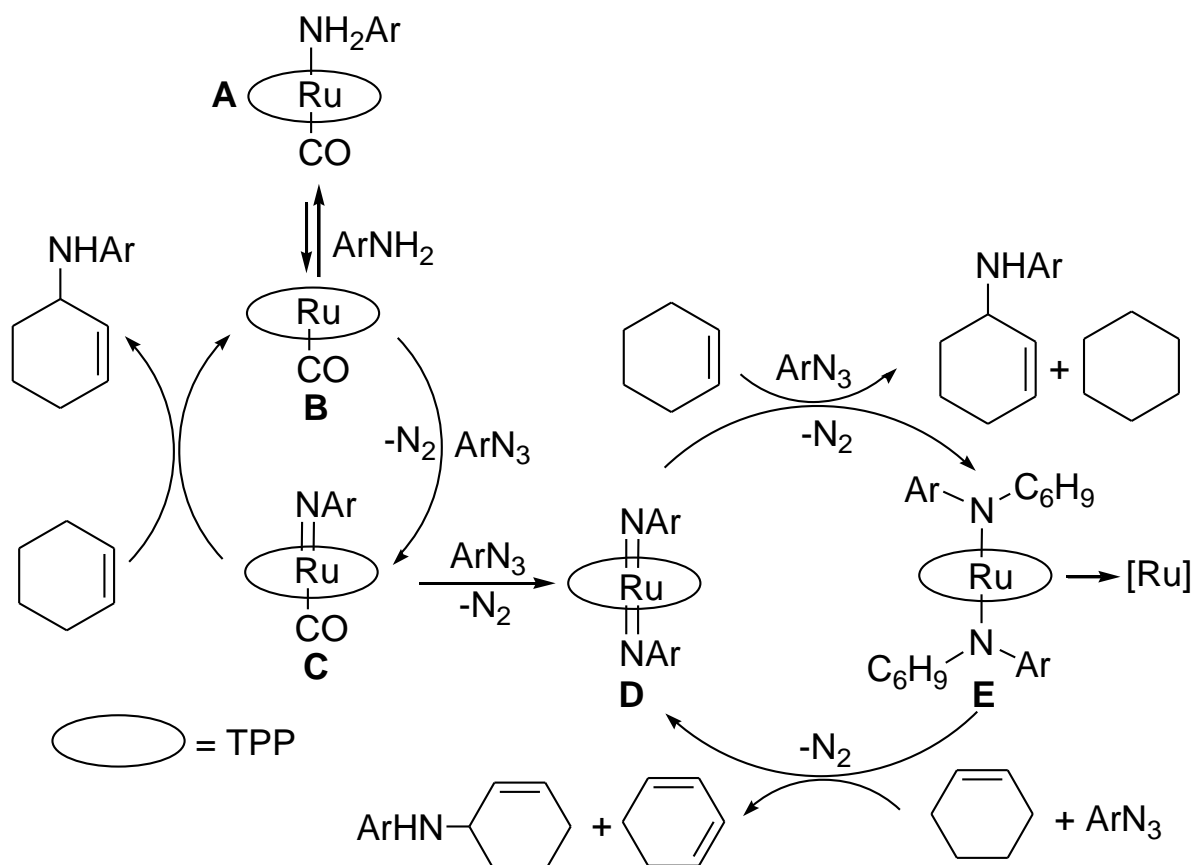


**Figure 2.9.** Kinetic dependence of the reaction rate with respect to olefin concentrations in the reaction between cyclohexene and 3,5(CF<sub>3</sub>)<sub>2</sub>C<sub>6</sub>H<sub>3</sub>N<sub>3</sub> catalysed by Ru(TPP)CO (a) or complex **113** (b).

Keeping in mind the results of the synthetic studies discussed above, all the experimental results can be accounted by the general reaction scheme shown in Scheme 2.11.



**Scheme 2.11.** Mechanistic hypothesis for the allylic amination of cyclohexene by aryl azides catalysed by Ru(TPP)CO

The reaction of Ru(TPP)CO (**B** in the scheme 2.11) with ArN<sub>3</sub> initially forms a mono-imido complex (**C**). In the case of Ar = 4-CF<sub>3</sub>C<sub>6</sub>H<sub>4</sub>, the reaction with cyclohexene, yielding the allylic amine and regenerating **B**, is faster than the reaction with a second azide molecule for all cyclohexene concentrations tested. Thus, the second cycle in the scheme is not operating and the kinetics is a clear first order in azide and ruthenium complex (*r.d.s.* formation of the mono-imido complex **C**) and zero order with respect to cyclohexene (fast reaction). Ru(TPP)CO, in equilibrium with the amine complex **117**, is the resting state of the catalyst, in accord with the experimental observations. Note that in the case of the stoichiometric reaction between Ru(TPP)CO and 4-CF<sub>3</sub>C<sub>6</sub>H<sub>4</sub>N<sub>3</sub> previously described this clearly does not hold. In the latter case there is no olefin available to trap complex **C** and the reaction evolves to the bis-imido complex **D**.

In the case of Ar = 3,5-(CF<sub>3</sub>)<sub>2</sub>C<sub>6</sub>H<sub>3</sub>, the situation is more complex. The higher reactivity of the bis-trifluoromethylated azide renders the formation of the bis-imido complex **D** more competitive than when only a single electron-withdrawing group (CF<sub>3</sub> or NO<sub>2</sub>) is present. The rate dependence of the catalytic reaction on olefin concentration shown in figure 2.9-a can be explained by assuming that at low cyclohexene concentration formation of **D** is relevant during the reaction. The reaction of the latter with cyclohexene becomes rate-determining and the kinetics is first order with respect to the olefin. At a higher cyclohexene concentration, reaction of **C** with the olefin become faster than the reaction with another azide molecule and the same situation observed in the case of Ar = 4-CF<sub>3</sub>C<sub>6</sub>H<sub>4</sub> is obtained (zero order kinetics in cyclohexene).

When the bis-imino complex **113** was employed as the catalyst, the situation at low olefin concentration parallels that observed for Ru(TPP)CO. However, the two kinetics cannot give the same behaviour at high olefin concentration because no CO is present in the former case and a complex of type **C** cannot be formed. Under these conditions, the resting state of the complex gradually shifts towards the bis-amido complex **E**. The rate of the reaction should be independent of olefin concentration, but it must be considered that complex **E** shows a low stability and easily decomposes. Thus a faster catalyst deactivation is observed when this type of complex is accumulated in solution. Such a gradual decomposition can be difficult to separate in any single kinetic experiment by the natural rate decrease due to azide consumption and it easily results in a lower apparent first order kinetic constant.

It may be finally noted that the lower slope of the low cyclohexene concentration branch of figure 2.9-a, with respect to that in figure 2.9-b, is consistent with the contemporary competition of two catalytic cycles in the former case, only one of which is accelerated by an increase in olefin concentration. In theory, it may be possible to calculate the relative weight of the two catalytic cycles by the observed differences, but the number of available data points does not allow this calculation to perform reliably.

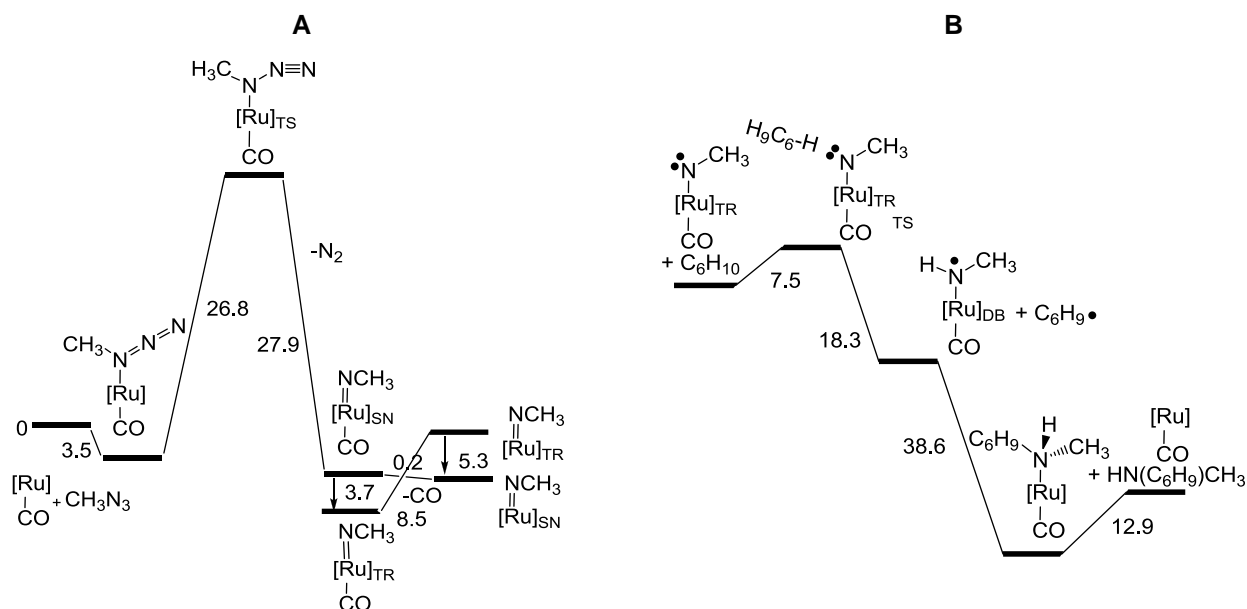
In conclusion the allylic amination of cyclohexene catalysed by ruthenium porphyrin complexes occurs at least with two different mechanisms and that one prevails over the other depending on the nature of the employed aryl azide and the olefin concentration. Experimental and kinetic data indicates that both mono and bis-imido species can be involved in the nitrene transfer reaction but the high reactivity of the mono-imido derivative precluded any characterisation. However, the isolation of its decomposition products and kinetic data suggest that the mono imido complex is mainly responsible for the catalytic reaction when using aryl azides showing low electron withdrawing behaviour. On the other hand, if an aryl azide bearing two strong electron withdrawing substituents such as two CF<sub>3</sub> groups is employed, the mono imido complex

rapidly reacts with the aryl azide to be further oxidised to the bis-imido complex which becomes the reaction catalyst.

To better clarify the role of mono and bis-imido complexes in the nitrene transfer reaction into an allylic C-H bond, a computational study was performed by C. Mealli and G. Manca, from University of Florence.

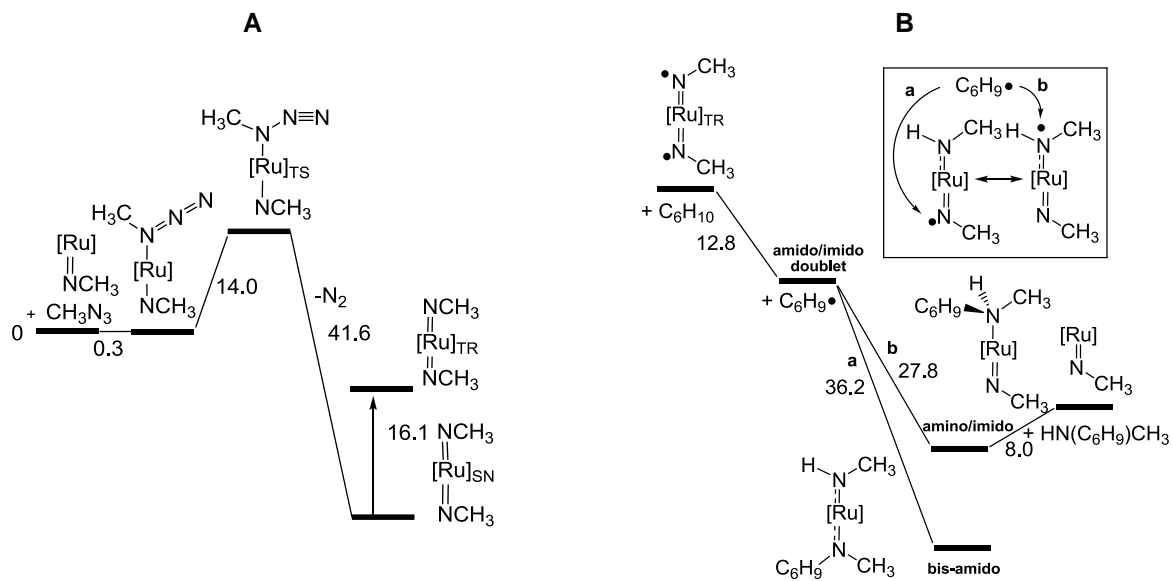
The kinetic and spectroscopic, illustrated in the paragraph 2.3,<sup>390, 404</sup> suggested the existence of the two catalytic mechanisms highlighted in Scheme 2.11. A particular relevance had the very reactive species  $[\text{Ru}](\text{NAr})(\text{CO})$ , **C** obtained upon the activation of one aryl azide molecule over  $[\text{Ru}](\text{CO})$ .

The theoretical study confirms that the first step of the cycle is the formation of a mono-imido complex  $\text{Ru}^{\text{IV}}(\text{TPP})(\text{NAr})(\text{CO})$  (scheme 2.12-A) which can undergo a singlet→triplet interconversion to confer a diradical character to the “ArN” ligand. Hence, the activation of the allylic C-H bond of cyclohexene ( $\text{C}_6\text{H}_{10}$ ) occurs through a C-H••N adduct detected as a Transition State. The formation of the desired allylic amine follows a “rebound” mechanism in which the nitrogen and carbon atoms radicals couple to yield the organic product. The release of the allylic amine restores the initial  $\text{Ru}(\text{TPP})(\text{CO})$  complex and allows the catalytic cycle to resume by the activation of another azide molecule (Scheme 2.12-B).



**Scheme 2.12.**

On the singlet PES, the CO ligand may be however dismissed from the mono-imido complex  $\text{Ru}^{\text{IV}}(\text{TPP})(\text{NAr})(\text{CO})_{\text{SN}}$  opening the way to an alternative catalytic cycle which also leads to allylic amine through comparable key steps. A second azide molecule occupies the freed coordination site of  $\text{Ru}(\text{TPP})(\text{NAr})_{\text{SN}}$  to form the bis-imido complex  $\text{Ru}(\text{TPP})(\text{NAr})_2$  (scheme 2.13-A) which is also prone to the intersystem crossing with the consequent C-H radical activation (scheme 2.13-B)



The process continues till the azide reactant is present. The interconnected cycles have similarly high exergonic balances.

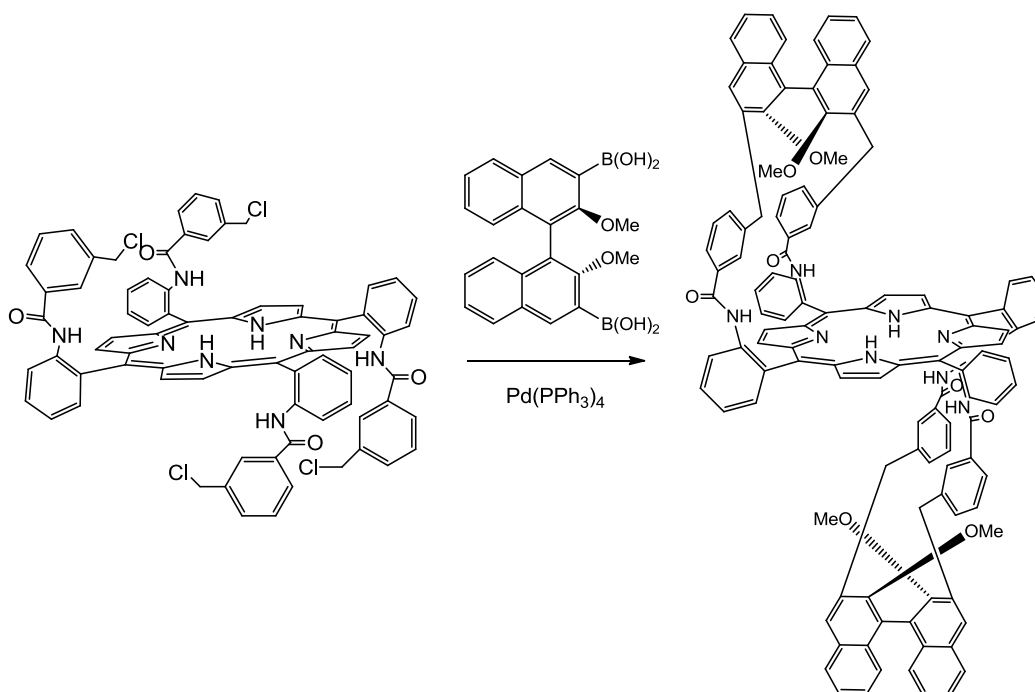


## 2.4. Cyclopropanation Reactions

Compounds containing cyclopropane units play a crucial role in both synthetic and pharmaceutical chemistry due to the high reactivity<sup>405</sup> and biological properties<sup>406,407</sup> of the three-membered ring. Consequently, the interest of the research community in developing new methodologies to synthesise cyclopropanes is strongly increasing<sup>264, 408, 409</sup> and the one-pot reaction of diazo compounds with olefins is a sustainable and atom-efficient strategy<sup>410, 411</sup> due to the formation of N<sub>2</sub> as the only stoichiometric by-product.

Catalytic enantio- and diastereoselective olefin cyclopropanations<sup>172, 265, 412-414</sup> have been extensively explored and metal porphyrin complexes represent a very active and stereoselective class of catalysts.<sup>336, 415</sup> Ruthenium,<sup>266, 416, 417</sup> osmium,<sup>418, 419</sup> rhodium<sup>295, 420</sup> and iridium<sup>360</sup> porphyrins show an excellent efficiency but their cost and toxicity prompted the scientific community to investigate the activity of the more eco-friendly first row transition metal porphyrin complexes, such as cobalt<sup>179, 325, 330, 336</sup> and iron<sup>268, 421, 422</sup> derivatives. Iron porphyrins were employed in for the first time in 1999<sup>423</sup> and since then their use in porphyrin catalysis remains a challenge.

Some years ago our research group reported on the catalytic efficiency of chiral cobalt(II)-binaphthyl porphyrins in asymmetric cyclopropanations,<sup>341</sup> and recorded positive data, encouraging us to synthesise a structurally related chiral porphyrin **119** (Scheme 2.14) which was obtained in one single Suzuki coupling step from previously reported porphyrin **118**<sup>424</sup> (35%) and fully characterised.



Scheme 2.14.

The rationale for starting from porphyrin **118** is that various structures strapped on the latter revealed to be overhung above the coordination site.<sup>425, 426</sup> Owing to its 5,10 and 15,20 bis-strapped conformation,

porphyrin **119** has one  $C_2$  axis within the porphyrin plane and exhibits an open space on each side for the substrate access and at the same time a steric chiral bulk surrounding the N-core. Furthermore, X-ray data of related structures based on the same type of picket indicate pre-organized yet flexible handles.<sup>425, 427</sup> Beside, the  $^1\text{H}$  NMR analysis of **119** in  $\text{CDCl}_3$  solution revealed a well resolved spectrum with sharp signals for most protons indicating this pre-organization. For instance, the eight benzylic protons appear as two AB systems between 3.5 and 4 ppm. The observed pattern for the  $\beta$ -pyrrolic protons composed of two typical doublets (4.7 Hz) and two singlets confirms the proposed symmetry in solution. In **119**, conversely to its diethylmalonate counterpart in which both pickets are bound on one carbon atom,<sup>424</sup> the quite large binap linker (c.a. 7.4 Å) is expected to reject the two pickets outside of the cavity. This outwards orientation of the pickets in **119** is reflected in the chemical shifts of the four protons  $\text{H}_{e/e'}$  which resonate as two singlets at 7.23 and 7.36 ppm, where they appear at 6.19 ppm in **118** and 4.84 ppm in its diethylmalonate analogue. This conformation is also verified by the observed nuclear Overhauser effects between  $\text{H}_f$  and the amide protons and  $\text{H}_f$  and  $\text{H}_\beta$  (scheme 2.14, figure 2.10).

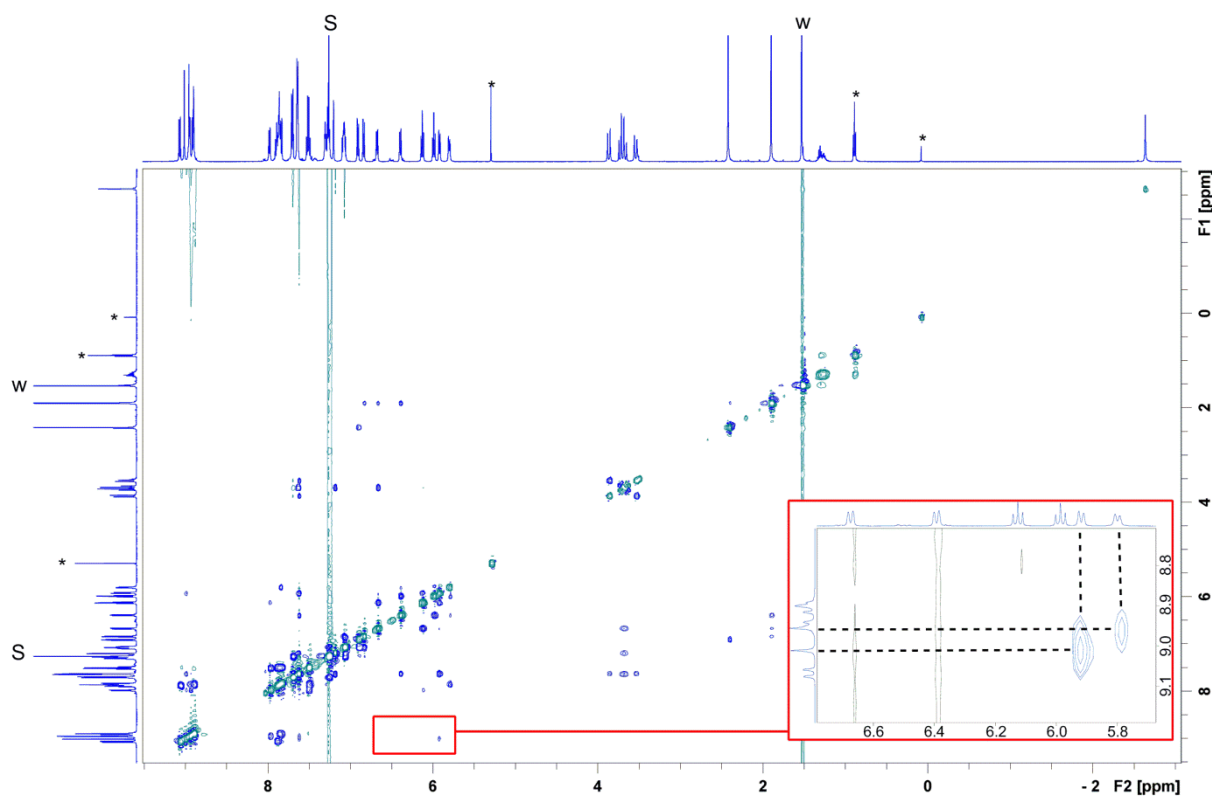
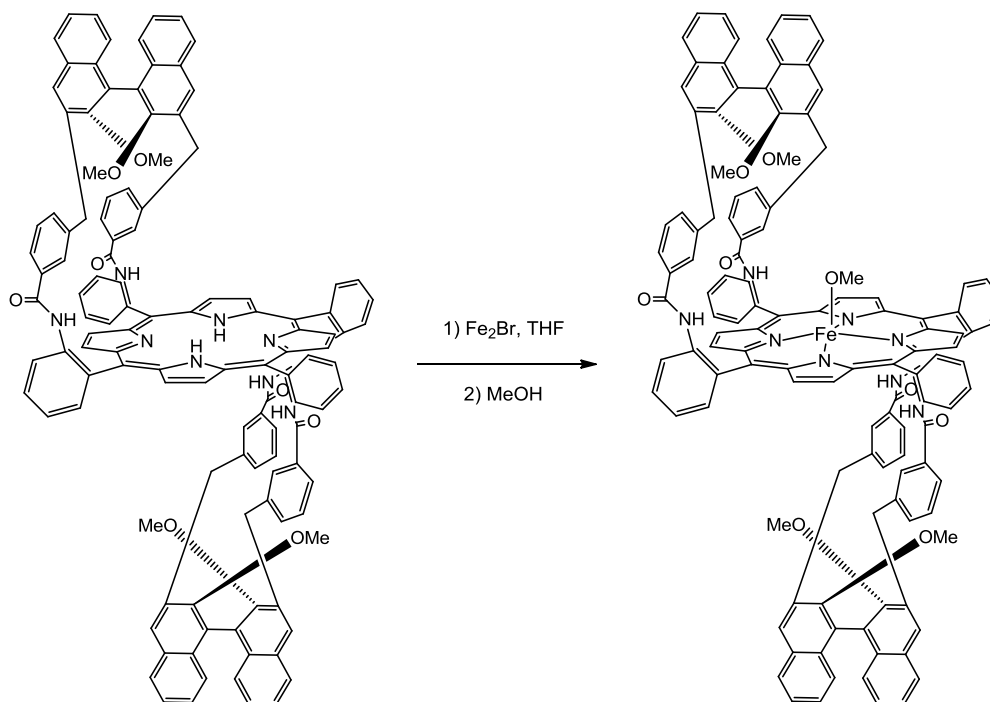


**Figure 2.10.** ROESY 2D NMR spectrum (500 MHz, 298 K) of compound **119** in  $\text{CDCl}_3$  (S =  $\text{CHCl}_3$ , w = water, \* = traces of residual solvents or grease).

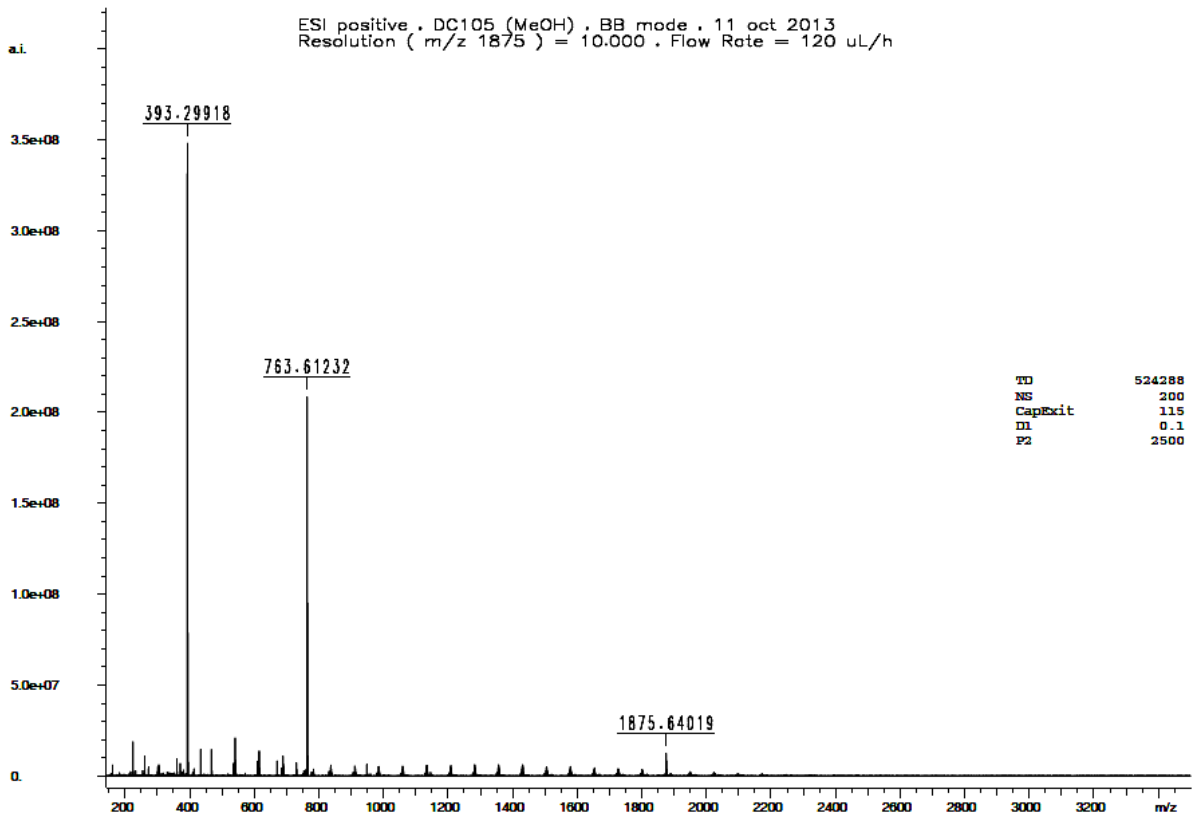
Finally, the two signals from the binap methoxy groups (2.42 and 1.89 ppm) experience a shielding of 1.44 and 0.91 ppm relatively to 2,2'-dimethyl-3,3'-dimethyl-1,1'-binaphthalene as a reference, indicating that they are neither strongly differentiated nor very close to the porphyrin, but yet above the macrocycle as depicted in Scheme 2.14.

The reaction of **119** with  $\text{FeBr}_2$  afforded **119Fe** ( $\text{Fe} = \text{Fe}^{\text{III}}(\text{OMe})$ ) by the initial formation of the iron (II) porphyrin complex which was oxidised by the atmospheric oxygen in the presence of  $\text{CH}_3\text{OH}$  yielding the desired complex (Scheme 2.25) in quantitative yield.<sup>168, 428</sup>

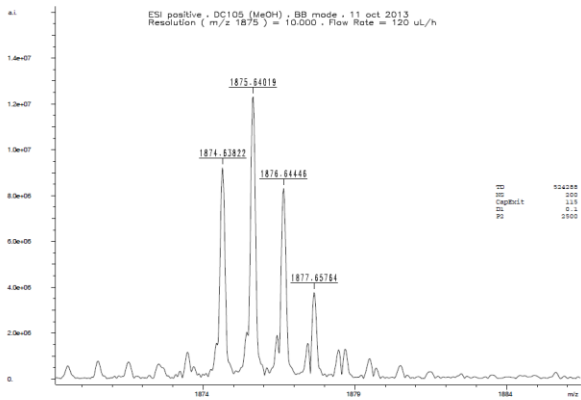


**Scheme 2.15.** Synthesis of **119Fe**

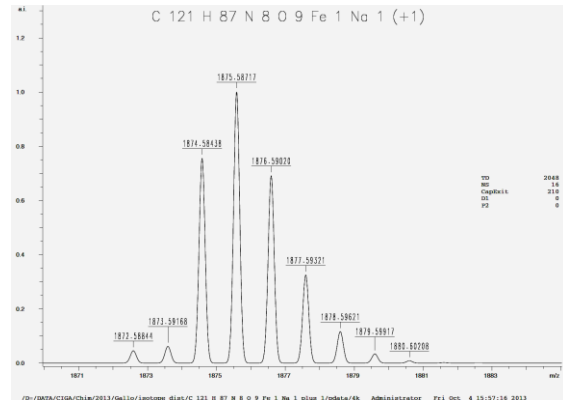
Complex **119Fe** was characterised by elemental analysis,  $[\alpha]_D^{20}$ , IR, UV-Vis spectroscopies. The high resolution MS-ESI analysis (figure 2.11) revealed the presence of the methoxy ligand while the ESR spectroscopy confirmed the oxidation state of the iron (III) centre ( $S = 5/2$ ).



/D:/DATA/CIGA/Chin/2013/Gallo/DC105/9/pdata/1 Administrator Fri Oct 11 17:05:22 2013



/D:/DATA/CIGA/Chin/2013/Gallo/DC105/9/pdata/1 Administrator Fri Oct 11 17:06:29 2013



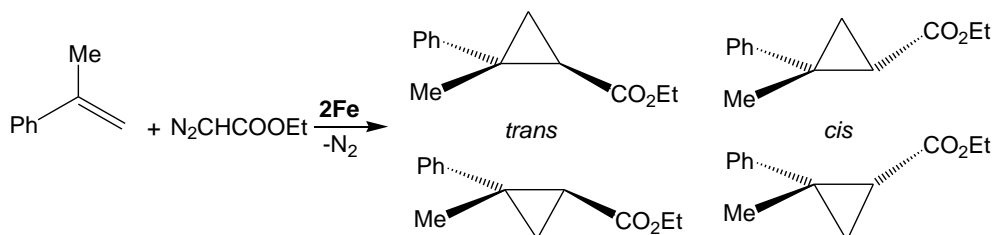
/D:/DATA/CIGA/Chin/2013/Gallo/Isotope\_diat/C\_121\_H\_87\_N\_8\_O\_9\_Fe\_1\_Na\_1\_psim\_3/pdata/4k Administrator Fri Oct 11 15:57:18 2013

a) Experimental MS-ESI spectrum

b) Simulation of MS-ESI spectrum

Figure 2.11 MS-ESI spectrum of complex 119Fe [M+Na<sup>+</sup>]

The catalytic activity of **119Fe** was initially tested in the model reaction of  $\alpha$ -methylstyrene with ethyl diazoacetate (EDA) (Scheme 2.16).



**Scheme 2.16.** Cyclopropanation of  $\alpha$ -methylstyrene by EDA

In order to optimise the experimental conditions we started screening several reaction solvents by using 1% of catalyst. As reported in Table 2.7, we have always obtained excellent *trans*-diastereoselectivities (94-99%) with the exception of DCM (Table 2.7, entry 3) where no reaction was observed.

**Table 2.7.** Reaction solvent screening of the  $\alpha$ -methylstyrene cyclopropanation by EDA<sup>a</sup>

entry	T(°C)	solvent	t(min) <sup>b</sup>	yield(%) <sup>c</sup>	<i>trans/cis</i> <sup>c</sup>	ee (%) <sup>d</sup>
1	25°	benzene	5	87	96:4	72
2	25°	toluene	5	85	99:1	75
3	25°	DCM	-	-	-	-
4	25°	hexane	120	70	94:6	40
5	0°	toluene	5	89	99:1	75

<sup>a</sup>**119Fe**/EDA/ $\alpha$ -methylstyrene = 1:100:250 (5.0 mg,  $2.70 \times 10^{-6}$  mol of the catalyst in 5.0 mL of the desired solvent).

<sup>b</sup>Time required for the complete EDA conversion monitored by IR spectroscopy. <sup>c</sup>Determined by <sup>1</sup>H NMR (2,4-dinitrotoluene as the internal standard). <sup>d</sup>Enantiomeric excess of the *trans*(*R,R*) major diastereomer determined by HPLC analysis using a chiral column (DAI-CEL CHIRALCEL, IB, hexane/<sup>i</sup>PrOH = 99.75:0.25).

A much lower *ee* value was obtained by using hexane as a solvent (Table 2.7, entry 4) whilst for toluene and benzene comparable results (Table 2.7, entries 1 and 2) were obtained. Surprisingly, we did not register any improvements in enantioselectivity by decreasing the temperature from room temperature to 0°C (compare entries 2 and 5, Table 2.7). Collected data suggested toluene as the best reaction solvent, then it was employed to further optimise the catalytic conditions.

Firstly, we performed the reaction without an olefin excess which is usually required to avoid the formation of side-products due to decomposition of the diazo compound (table 2.8, entries 1 and 2). The use of an equimolar EDA/olefine ratio is of particular importance when expensive olefins are the substrates.

**Table 2.8.** Optimization of the catalyst loading and reaction temperature.

entry	% cat.	T(°C)	t (min) <sup>a</sup>	yield (%) <sup>b</sup>	trans/cis <sup>b</sup>	ee (%) <sup>c</sup>
1 <sup>d</sup>	1	25°	5	75	99:1	73
2 <sup>e</sup>	0.1	25°	5	75	97:3	68
3 <sup>e</sup>	0.01	25°	5	72	94:6	58
4 <sup>e</sup>	0.01	0°	5	>99	98:2	78
5 <sup>f</sup>	0.01	0°	36	83	99:1	74
6 <sup>e</sup>	0.01	-15°	420	72	99:1	79
7 <sup>e</sup>	0.01	-20°	540	70	>99:1	79
8 <sup>e</sup>	0.01	-78°	600	70	>99:1	87
9 <sup>e</sup>	0.005	25°	480	55	95:5	57

<sup>a</sup>Time required for the complete EDA conversion monitored by IR spectroscopy. <sup>b</sup>Determined by <sup>1</sup>H-NMR (2,4-dinitrotoluene as the internal standard). <sup>c</sup>Enantiomeric excess of the *trans*(*R,R*) major diastereomer determined by HPLC analysis using a chiral column (DAI-CEL CHIRALCEL, IB, hexane/*i*-PrOH = 99.75:0.25). <sup>d</sup>**119Fe**/EDA (5.0 mg, 2.70x10<sup>-6</sup> mol) was dissolved into 5.0 mL of toluene with an equimolar  $\alpha$ -methylstyrene/EDA ratio. <sup>e</sup>145.0  $\mu$ L of a **119Fe** toluene solution (3.72x10<sup>-3</sup> mol/L) was added to 2.0 mL of an equimolar  $\alpha$ -methylstyrene/EDA toluene solution. <sup>f</sup>EDA was added dropwise by a syringe pump.

Cyclopropanes were obtained in good yields also using a very low catalytic loading of 0.01% (table 2.8, entries 3-8) and the catalytic efficiency was not improved by the slowly addition of EDA to the reaction mixture (table 2.7, entry 5). Fumarate and maleate accounted for the rest of the mass balance according to NMR analyses.

It should be noted that a catalyst loading of 0.005 % (TON of 2x10<sup>4</sup>, Table 2.8, entry 9) is one of the highest observed for cyclopropanations<sup>323, 358</sup> and to the best of our knowledge, it is the highest reported TON for metallo porphyrin-based catalysts. To achieve the best catalyst loading/reaction time relationship, 0.01% of **119Fe** was employed to better investigate the effect of the temperature on the enantioselectivity. The best value of 87% *ee* was obtained at -78°C but unfortunately the reaction time greatly increased (Table 2, entry 8). Conversely, when the reaction was run at 0 °C very good diastereo- and enantioselectivity (*trans/cis* = 98:2, *ee<sub>trans</sub>* = 78%) were observed with a complete EDA conversion in only 5 minutes (Table 2.8, entry 4). To our delight the consequent TOF of 120,000/h was never reported for porphyrin-mediated cyclopropanations and it can be the starting point for an industrial application of this methodology.

In order to test the catalyst robustness, a reaction with 0.1% of **119Fe** (6.0 mg) was run at 0 °C by using 0.340 mL of EDA (3.24 mmol) and 0.421 mL of  $\alpha$ -methylstyrene (3.24 mmol) in 17.0 mL of toluene. After the complete EDA consumption, EDA and  $\alpha$ -methylstyrene were added again to the catalytic mixture for two more consecutive times. The three runs were completed in 5, 10 and then 10 minutes respectively. The NMR analyses of the crude, performed under nitrogen at the end of the third run, revealed 90% of a total yield, 98% of *trans*-diastereoselectivity with 75% of *ee<sub>trans</sub>*.

Considering that EDA is known to be a mild reducing agent<sup>429</sup> and the importance to avoid any oxidative degradations, we performed the cyclopropanation of  $\alpha$ -methylstyrene with a catalyst/olefin/EDA ratio of 1:1000:1100.<sup>430</sup> The improvement of the reaction yield (from 75% to 85%) indicated a positive catalytic effect of the EDA excess.

Data collected up to now indicated that the best catalytic results were obtained in toluene at 0 °C with 0.01% of a catalyst loading and by using a slight EDA excess. We are currently employing the optimised catalytic conditions to study the scope of the reaction.

In conclusion **119Fe** promotes the cyclopropanation of  $\alpha$ -methylstyrene by EDA with excellent *trans* diastereoselectivities (94-99%), and good enantioselectivities ( $ee_{trans}$  up to 87%). To the best of our knowledge, the outstanding values of TON and TOF (20,000 and 120,000/h respectively) were never reported for metallo-porphyrin catalysed cyclopropanations and the robustness of the catalyst under an inert atmosphere allowed three catalytic recycles. Finally, high cyclopropane yields were obtained without using an olefin excess in accord with the industrial request for sustainable processes, especially when expensive olefins are involved.

Further studies are currently devoted to expand the reaction scope by testing the cyclopropanation of several olefins by differently substituted diazo derivatives.

## 2.5. Conclusion.

In conclusion in this Ph.D thesis we have reported the synthesis of new porphyrins and their metal complexes to use as catalysts to promote the formation of C-C and C-N bonds. The reported organic transformations were optimised giving a great attention to the sustainability of the synthetic methodologies. All the amination reactions were performed by using aryl azides as amination agents which are able to transfer the nitrene functionality to an organic framework by forming the eco-friendly molecular nitrogen as the only stoichiometric side-product. The same synthetic strategy was applied to perform olefin cyclopropanations where diazocompounds were used as carbene precursors.

Metal porphyrin complexes demonstrated to be competent catalysts in all the reported reactions. In the case of the intramolecular amination of biaryl azides metal porphyrins were also very active to promote a tandem reaction in which the amination step was followed by an oxidation process to yield phenanthridines, an important class of biological relevant compounds. It is worth noting that the amination of activated  $sp^3$  C-H bonds assumes a particular relevance in view of the potentiality of these reactions: low cost hydrocarbons can be transformed in high added value nitrogen containing compounds in a single step and by using low catalyst loading.

The optimization of the described organic transformations was also carried out by studying the catalytic mechanisms. Kinetic and theoretical studies as well as the isolation of catalytic intermediates were fundamental to shed some lights into catalytic cycles. A particular attention was devoted to this aspect because we strongly believe that the comprehension of catalytic mechanisms can be essential to plan new and more efficient synthetic methodologies in the future.

In order to improve the applicability of metal porphyrins to the synthesis of biological and/or pharmaceutical compounds, a new chiral porphyrin was then synthesised. The iron (III) complex of this new ligand was very active in the cyclopropanation of olefins, outstanding TON and TOF were observed. In addition to that the porphyrin complex was very stable in catalytic conditions to allow the recycle of the catalyst for three consecutive times.

# **3. Experimental Section.**



### 3.1. General

Unless otherwise specified, all the reactions were carried out under a nitrogen atmosphere employing standard Schlenk techniques and magnetic stirring. Toluene, THF, *n*-hexane and benzene were dried by M. Braun SPS-800 solvent purification system. 1,2-Dichlorobenzene,  $\alpha$ -methylstyrene, cyclohexene, 1-octene were distilled over sodium and kept under nitrogen. All the other starting materials were commercial products used as received. The purity of 2-amino biaryls, 2-azido biaryls,  $\alpha$ -methylstyrene employed was checked by GC-MS or  $^1\text{H}$  NMR analysis. NMR spectra were recorded at room temperature on a Bruker AC-300, on a Bruker Avance 300-DRX, operating at 300 MHz for  $^1\text{H}$ , at 75 MHz for  $^{13}\text{C}$  and at 282 MHz for  $^{19}\text{F}$ , or on a Bruker Avance 400-DRX spectrometers, operating at 400 MHz for  $^1\text{H}$  and at 100 MHz for  $^{13}\text{C}$ . Chemical shift (ppm) are reported relative to TMS. The  $^1\text{H}$  NMR signals of the compounds described in the following have been attributed by COSY and NOESY techniques. Assignments of the resonance in  $^{13}\text{C}$  NMR were made using the APT pulse sequence and HSQC and HMBC techniques. GC-MS analyses were performed on Shimadzu QP5050A instrument. Infrared spectra were recorded on a Varian Scimitar FTS 1000 spectrophotometer. UV/Vis spectra were recorded on an Agilent 8453E instrument.  $[\alpha]_{\text{D}}$  values are given in  $10^{-1}\text{deg cm}^2 \text{g}^{-1}$ . Elemental analyses and mass spectra were recorded in the analytical laboratories of Milan University.

#### Computational Details.

The models were firstly optimized at B3LYP-DFT<sup>431</sup> level of theory and later with B97D functional within the Gaussian09 program. All the optimized structures were validated as minima and/or transition states by computed vibrational frequencies, with the exception of  $[\text{Ru}](\text{N}(\text{C}_6\text{H}_9)\text{CH}_3)_2 \text{SN}$  and  $[\text{Ru}]_2$  due to the lack of adequate computing power. Some selected structures have been also investigated with the BP86 functional mainly with the purpose of understanding the factors for the intersystem crossing, which is a fundamental aspect of this study. All the calculations were based on the CPCM model<sup>432, 433</sup> for the benzene solvent used in the experiments. The effective Stuttgart/Dresden core potential (SDD)<sup>434</sup> was adopted for the ruthenium atom, while for all the other atoms the basis set was 6-31G, with the addition of the polarization functions (d, p). Qualitative MO arguments have been developed with the help of the CACAO package,<sup>435</sup> after verifying a relative good the consistency between the DFT and EHMO wave functions.

## 3.2. Synthesis of Ruthenium Source.

### 3.2.1. Synthesis of $\text{Ru}_3(\text{CO})_{12}$

A solution of ruthenium trichloride (1.242 g,  $4.75 \times 10^{-3}$  mol) (considering the ruthenium salt as trihydrated) was dissolved in methanol (50 mL) inside a 100 mL glass liner. The liner was placed inside a Schlenk tube with a wide neck under dinitrogen, which was then cooled to  $-78^\circ\text{C}$ . The dark mixture was frozen, the liner was closed with a screw cap that contained glass wood that allows gaseous reagents to exchange and the Schlenk tube was evacuated and filled with dinitrogen three times. The flask was rapidly transferred into a stainless steel autoclave with a magnetic stirrer. The autoclave was then rapidly evacuated and filled with dinitrogen three times. CO (50 bar) was then charged at room temperature, and the steel autoclave was placed in a preheated oil bath at  $120^\circ\text{C}$  and stirred for about 8 hours. After cooling at room temperature and venting the autoclave, the glass liner was removed, and the resulting orange suspension was collected and dried under reduced pressure. The crude  $\text{Ru}_3(\text{CO})_{12}$  was purified on a short silica gel column (dichloromethane as eluent) or by extraction in continuous with tetrahydrofuran on a celite pad. (736 mg, 72.7 %)

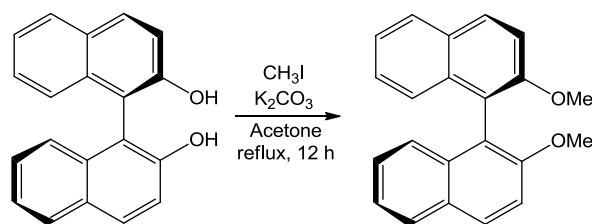
Elemental Analysis calc. for  $\text{C}_{12}\text{O}_{12}\text{Ru}_3$ : C, 22.54; O, 30.03; Ru, 47.43; found: C, 23.01;

$\nu_{\text{max}}$  ( $\text{CH}_2\text{Cl}_2$ )/ $\text{cm}^{-1}$ : 2059.1 (s), 2027.9 (s), 2010.6 (m)

$\nu_{\text{max}}$  (nujol)/ $\text{cm}^{-1}$ : 2059.7 (s), 2015.4 (s), 1996.6 (s)

### 3.3. Synthesis of chiral binaphthyl derivateives.

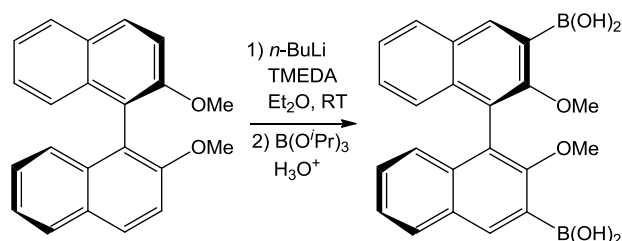
#### 3.3.1. Synthesis of (*R*)-2,2'-dimethoxy-1,1'-binaphthyl



A suspension of (*R*)-(+)-1,1'-bi(2-naphthol) (3.01 g,  $1.05 \times 10^{-2}$  mol) was heated in 45 mL of acetone to give a homogeneous solution. To this solution were added potassium carbonate (4.95 g,  $3.5 \times 10^{-2}$  mol), methyl iodide (3.92 mL,  $6.3 \times 10^{-2}$  mol), and the mixture was heated under reflux conditions for 12 h. The mixture concentrated to 10 mL, which was cooled to room temperature and treated with 50 mL of water. The mixture stirred for 8 h, and the resulting solid was washed with water and dried to afford (*R*)-2,2'-dimethoxy-1,1'-dinaphthyl as a white powder (2.87 g, 87%).

$^1\text{H NMR}$  (300 MHz,  $\text{DMSO-}d_6$ , 300 K):  $\delta$  = 8.06 (d,  $J$  = 9.0 Hz, 2H), 7.94 (d,  $J$  = 8.0 Hz, 2H), 7.60 (d,  $J$  = 9.0 Hz, 2H), 7.31 (t,  $J$  = 7.3 Hz, 2H), 7.21 (t,  $J$  = 7.6 Hz, 2H), 6.89 (d,  $J$  = 8.4 Hz, 2H), 3.70 (s, 6H).

#### 3.3.2. Synthesis of (*R*)-3,3'-bis(dihydroxyborane)-2,2'-dimethoxy-1,1'-binaphthyl

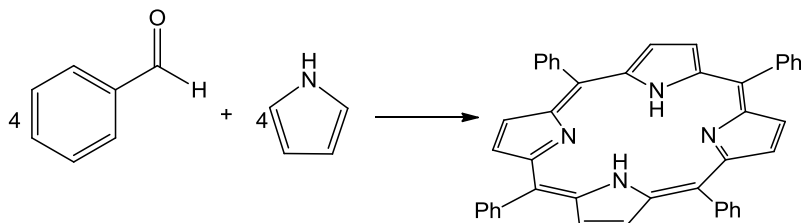


1.6 M *n*-BuLi in hexane (3.04 mL,  $4.87 \times 10^{-3}$  mol) was added at room temperature to a solution of tetramethylethylenediamine (0.973 mL,  $6.49 \times 10^{-3}$  mol) in ether (25 mL). The solution was stirred for 30 min, solid (*R*)-2,2'-dimethoxy-1,1'-dinaphthyl (0.510 g,  $1.62 \times 10^{-3}$  mol) was added in one portion, and the reaction mixture was stirred for 3 h. The resulting light brown suspension was cooled to  $-78^\circ\text{C}$ , and triisopropylborate (2.24 mL,  $9.73 \times 10^{-3}$  mol) was added over a period of 10 min. The solution was allowed to warm to room temperature and stirred for 12 h. The reaction mixture was cooled to  $0^\circ\text{C}$ , and 1 M HCl solution (15 mL) was added, and the resulting solution was stirred at room temperature for 2 h. The organic layer was washed with 1 M HCl solution and brine, dried over  $\text{Na}_2\text{SO}_4$ , and finally dried under reduced pressure (0.652, 99%).

$^1\text{H NMR}$  (300 MHz,  $\text{CDCl}_3$ , 300 K):  $\delta$  = 8.62 (s, 2H), 7.99 (d,  $J$  = 8.1 Hz, 2H), 7.44 (t,  $J$  = 7.2 Hz, 2H), 7.32 (t,  $J$  = 7.4 Hz, 2H), 7.16 (d,  $J$  = 8.7 Hz, 2H), 6.03 (s, 4H), 3.31 (s, 6H).

## 3.4. Synthesis of Porphyrins Ligands

### 3.4.1. Synthesis of *meso*-tetraphenyl-porphyrin TPPH<sub>2</sub>



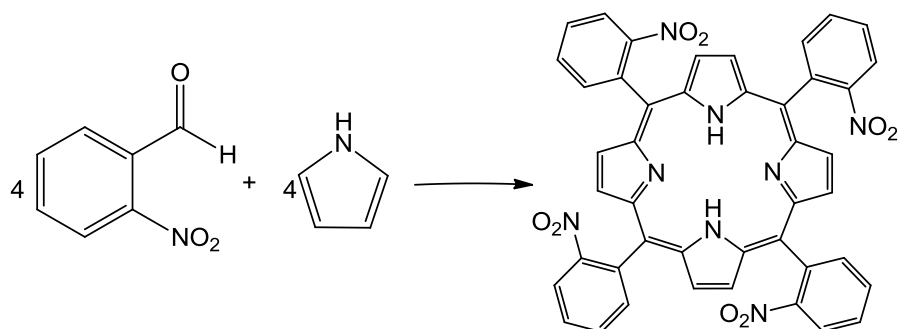
A one liter two necks round-bottom flask equipped with an equilibrating funnel and a condenser was charged with propionic acid (500 mL) and reagent grade benzaldehyde (36.5 mL, 360 mmol). The colorless mixture was stirred at room temperature until all the aldehyde is completely dissolved, and then it was heated at 50°C. A solution of distilled pyrrole (25 mL, 360 mmol) in propionic acid (30 mL) was then added dropwise in about 10 minutes. The resulting mixture was refluxed in air for 30 minutes. During this period the mixture turned first to red and then to violet-black. The resulting dark suspension was then washed with methanol (50 mL), water (50 mL) and finally again with methanol until the filtrate was clear. The crystalline purple solid was finally dried *in vacuo* (10.6 g, 8.2 %).

Elemental Analysis calc. for. C<sub>44</sub>H<sub>30</sub>N<sub>4</sub>: C, 86.25; H, 4.92; N, 9.11; found: C, 85.89; H, 5.14; N, 8.96.

$\lambda_{\max}$  (CH<sub>2</sub>Cl<sub>2</sub>)/nm 417, 514 (log  $\epsilon_M$  5.98 and 4.63).

<sup>1</sup>H NMR (300 MHz, CDCl<sub>3</sub>, 300 K):  $\delta$  = 8.88 (s, 8H, H <sub>$\beta$</sub> ), 8.26 (s, 8H, H <sub>$\alpha$</sub> ), 7.79 (s, 12H, H <sub>$m$</sub> +H <sub>$p$</sub> ), -2.70 (s, NH).

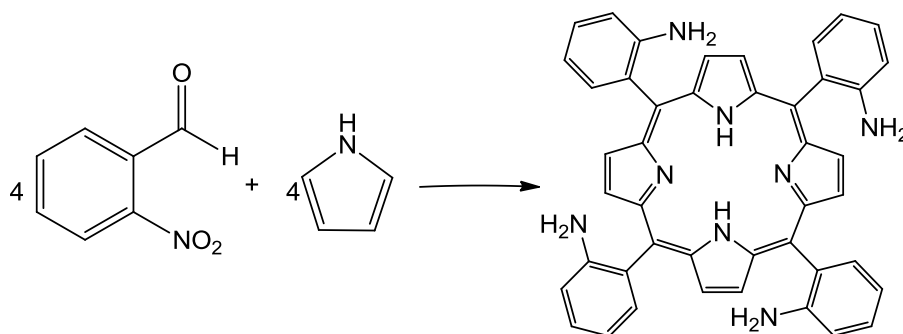
### 3.4.2. Synthesis of *meso*-tetrakis(2-nitrophenyl)porphyrin TNPPH<sub>2</sub>



A three liter three necks round-bottom flask equipped with an equilibrating funnel and refrigerator was charged with acetic acid (2L). 2-Nitrobenzaldehyde (101.5 g, 672 mmol) was added and the mixture was stirred at room temperature until all the aldehyde is dissolved. The solution was slowly brought to reflux and then distilled pyrrole (46 mL, 659 mmol) was added dropwise in about 15 minutes. The mixture was refluxed

for 45 minutes (turned before to red and then to violet-black), then cooled slowly, and when it reached about 60°C chloroform (500 mL) was gradually added. The dark suspension was finally filtered at room temperature, and the collected solid was washed with dichloromethane and dried *in vacuo* (10.7 g, 8.2%).

### 3.4.3. Synthesis of *meso*-tetrakis(2-aminophenyl)porphyrin TAPPH<sub>2</sub>

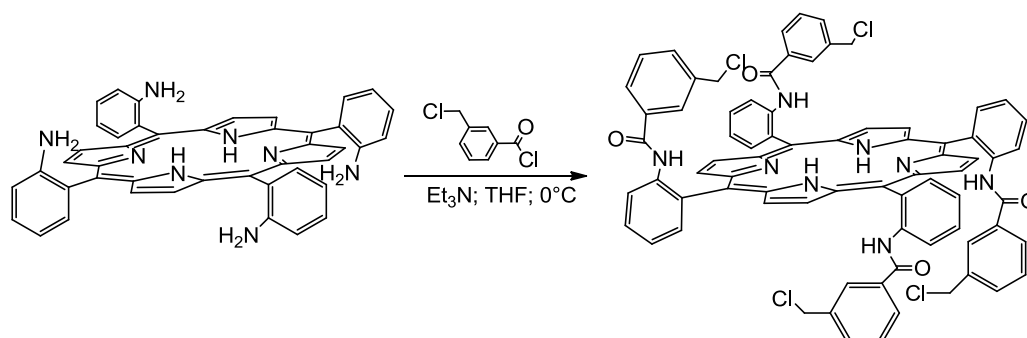


TNPPH<sub>2</sub> (10.5 g, 13.2 mmol) was suspended in air in dichloromethane (1.5 mL). The dark suspension was acidified with chloridric acid 35% (57 mL, 646 mmol) under vigorous magnetic stirring and then SnCl<sub>2</sub>·2H<sub>2</sub>O (76.5 g, 339 mmol) was added at the green suspension. The mixture was then refluxed in air for three hours, cooled at room temperature, neutralized with NH<sub>4</sub>OH 30% and stirred for additional two hours. The red suspension was filtered through a pad of sea sand to separate the inorganic side-product. The phases were separated and the organic layer was washed three times with water and finally dried under reduced pressure giving a purple product.

The so obtained four atropisomers of TAPPH<sub>2</sub> were separated by column chromatography on silica gel, (15 μm, eluent dichloromethane-methanol 99:1 as a purple band. Fractions containing the desired atropisomer were collected, the solvent was evaporated to dryness under vacuum at room temperature and finally recrystallized from chloroform-methanol 1:1 by slow evaporation of solvents at room temperature, giving a violet crystalline solid (1.2 g, 13.5% respect to the starting TNPPH<sub>2</sub>). The fractions containing the three not desired isomer of TAPPH<sub>2</sub> were collected and the solvent was evaporated under reduced pressure. The residual purple solid was taken up in chloroform and refluxed overnight in air to newly obtain the statistical distribution of four isomers.

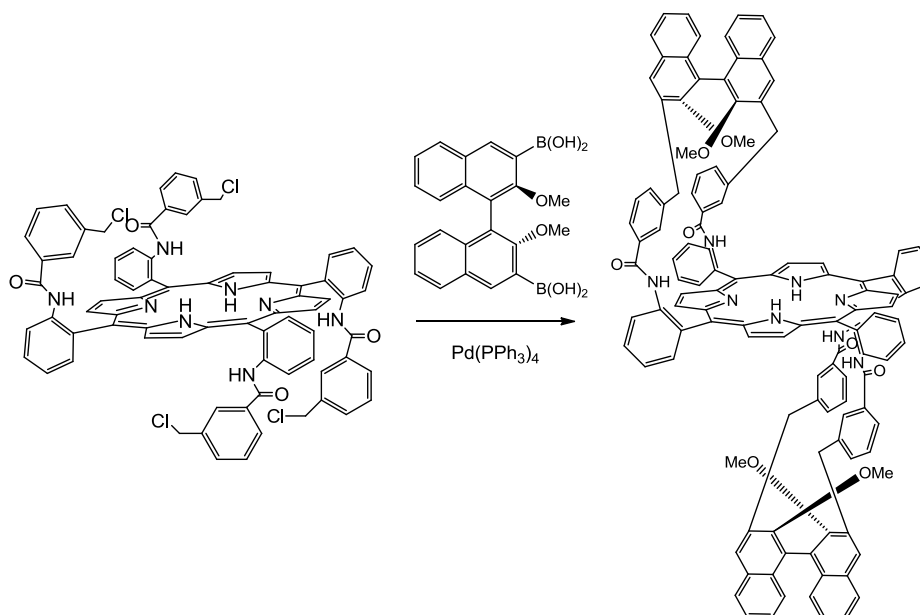
Atropisomer ααββ: <sup>1</sup>H NMR (200 MHz, CDCl<sub>3</sub>, 300K) δ: 8.91 (s, 8H, H<sub>β</sub>), 7.84 (d, *J* = 7.5 Hz, 4H, H<sub>d</sub>), 7.60 (pst, *J* = 7.5 Hz, 4H, H<sub>c</sub>), 7.16 (pst, *J* = 7.5 Hz, 4H, H<sub>b</sub>), 7.12 (d, *J* = 7.5 Hz, 4H, H<sub>a</sub>), 3.54 (broad s, 8H, NH<sub>2</sub>), -2.96 (s, 2H, NH<sub>pirr</sub>).

### 3.4.4. Synthesis of porphyrin 118



TAPP<sub>H<sub>2</sub></sub> (1.06 g, 1.53 mmol) was suspended in air in THF (150 mL). The dark suspension was cooled to 0°C in an ice bath and a solution of 1.8 mL of 3-(chloromethyl)benzoylchloride in 10 mL of THF was added dropwise. The mixture was stirred overnight and then was dried under reduced pressure. Finally the crude was purified by column flash chromatography on silica gel (15 μm, eluent dichloromethane) (**118**, 1.94 g, 96%).

### 3.4.5. Synthesis of porphyrin 119



In a dried 100 mL Schlenk flask, porphyrin **118** (0.300 g,  $2.33 \times 10^{-4}$  mol), (*R*)-2,2'-dimethoxy-1,1'-binaphthyl-3,3'-diboronic acid (0.226 g,  $5.60 \times 10^{-4}$  mol), tetrakis(triphenyl-phosphine)palladium(0) (0.108 g,  $9.34 \times 10^{-5}$  mol) and potassium carbonate (0.516 g,  $3.71 \times 10^{-3}$  mol) were dissolved in 16.0 mL of toluene, 5.0 mL of ethanol and 8.0 mL of water. The biphasic solution was refluxed under nitrogen atmosphere for 4 hours until the complete consumption of **118** that was monitored by TLC. The resulting mixture was allowed to reach room temperature and the biphasic solution was diluted with 50.0 mL of saturated aqueous NH<sub>4</sub>Cl and 50.0 mL of CH<sub>2</sub>Cl<sub>2</sub> and then it was separated. The aqueous phase was extracted with an additional 2×50 mL

of CH<sub>2</sub>Cl<sub>2</sub>, and the combined organic phases were washed with 1×50 mL of water and 1×50 mL of saturated aqueous NaHCO<sub>3</sub>. The organic phase was dried over Na<sub>2</sub>SO<sub>4</sub> and filtered. The filtrate was concentrated *in vacuo* and then purified by chromatography (SiO<sub>2</sub> 15-40 μm, eluent dichloromethane:methanol = 99.5:0.5). (**119**, 0.143 g, 35%).

Elemental Analysis calc. for C<sub>120</sub>H<sub>86</sub>N<sub>8</sub>O<sub>8</sub>: C, 81.52; H, 4.90; N, 6.34; found: C, 81.26; H, 4.97; N, 5.94.

$\nu_{\max}$  (CH<sub>2</sub>Cl<sub>2</sub>)/cm<sup>-1</sup>. 3685 (w), 3412 (w), 1711 (w), 1676 (w), 1519 (w), 1445 (w), 1418 (w), 1359 (w), 1305 (w), 1240 (w), 1101 (w), 1009 (w).  $\nu_{\max}$ (ATR)/cm<sup>-1</sup> 3421 (w), 3417 (w), 3056 (w), 2963 (w), 2938 (w), 1681 (w), 1580 (w), 1511 (w), 1443 (w), 1302 (w), 1260 (w), 1101 (w) 1012 (w).

$\lambda_{\max}$  (CH<sub>2</sub>Cl<sub>2</sub>)/nm 423, 518 (log  $\epsilon_M$  4.87 and 3.66).

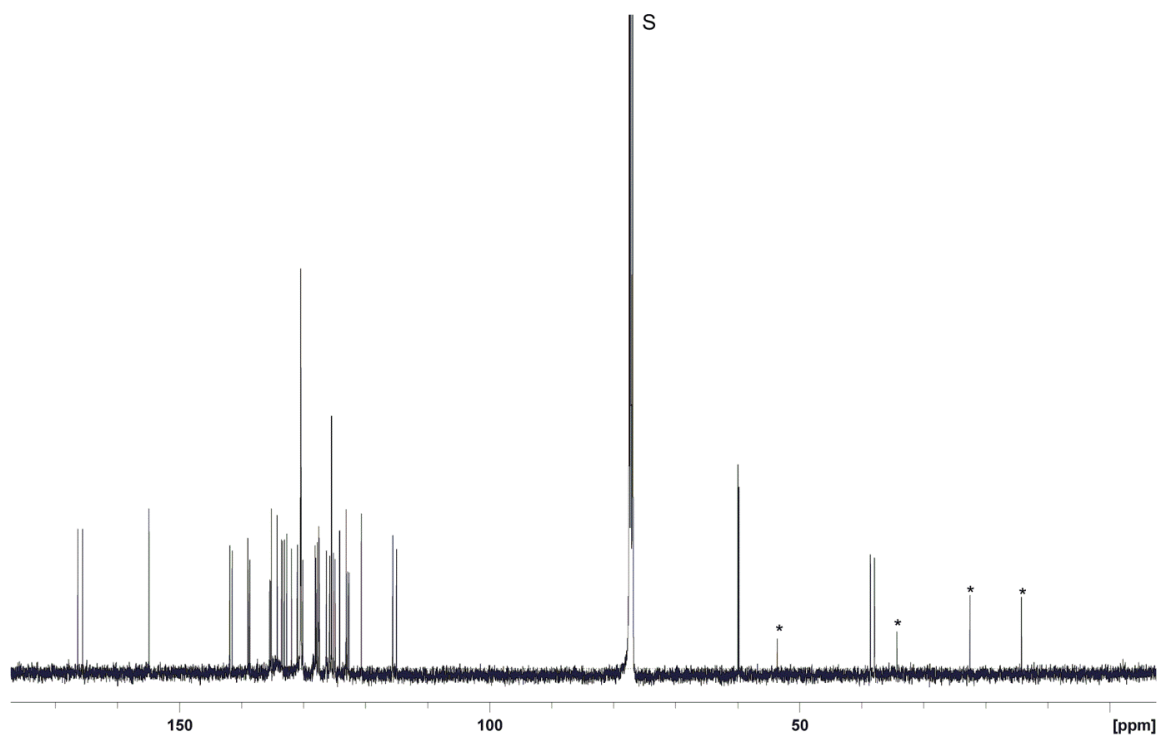
$[\alpha]_D^{20} = -809.524$  (c = 7×10<sup>-4</sup> g/100mL; in CH<sub>2</sub>Cl<sub>2</sub>).

m/z (ESI) 1767 [M]

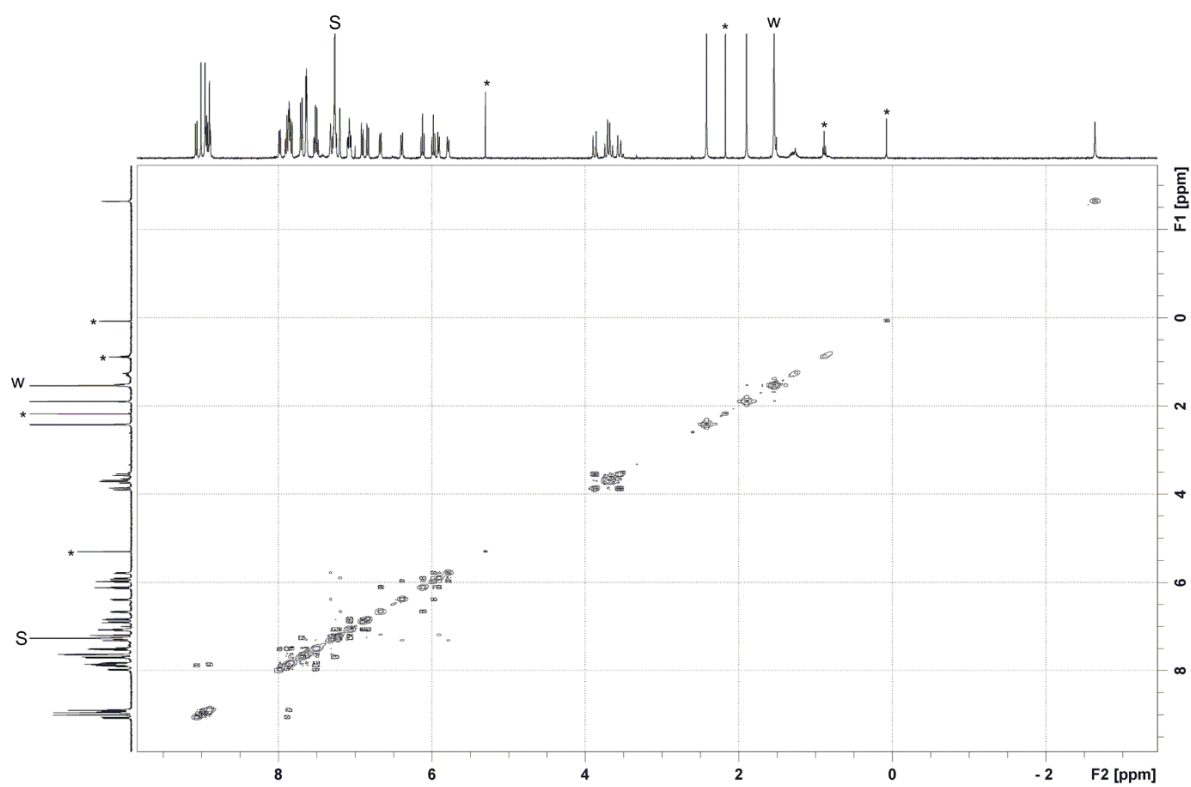
<sup>1</sup>H NMR (500 MHz, CDCl<sub>3</sub>, 298 K)  $\delta$  9.07 (t, 2H, *J* = 8 Hz, HAr<sub>meso</sub>), 9.00 (s, 2H, H<sub>βpyr</sub>), 8.95 (s, 2H, H<sub>βpyr</sub>), 8.94 (d, 2H, *J* = 4 Hz, H<sub>βpyr</sub>), 8.90 (t, 2H, *J* = 8 Hz, HAr<sub>meso</sub>), 8.88 (d, 2H, *J* = 4 Hz, H<sub>βpyr</sub>), 7.98 (dd, 2H, *J*<sub>1</sub> = 1 Hz, *J*<sub>2</sub> = 8 Hz, HAr<sub>meso</sub>), 7.89 (dt, 2H, *J*<sub>1</sub> = 1 Hz, *J*<sub>2</sub> = 8 Hz, HAr<sub>meso</sub>), 7.86 (dt, 2H, *J*<sub>1</sub> = 1 Hz, *J*<sub>2</sub> = 8 Hz, HAr<sub>meso</sub>), 7.85 (s, 2H, NHCO), 7.83 (dd, 2H, *J*<sub>1</sub> = 1 Hz, *J*<sub>2</sub> = 8 Hz, HAr<sub>meso</sub>), 7.70 (d, 4H, *J* = 8 Hz, HAr<sub>binap</sub>), 7.64 (s, 2H, HAr<sub>binap</sub>), 7.63 (s, 2H, HAr<sub>binap</sub>), 7.62 (s, 2H, NHCO), 7.51 (dt, 2H, *J*<sub>1</sub> = 1 Hz, *J*<sub>2</sub> = 8 Hz, HAr<sub>meso</sub>), 7.49 (dt, 2H, *J*<sub>1</sub> = 1 Hz, *J*<sub>2</sub> = 8 Hz, HAr<sub>meso</sub>), 7.32 (s, 2H, HAr<sub>strap</sub>), 7.27 (m, 2H, HAr<sub>binap</sub>), 7.19 (s, 2H, HAr<sub>strap</sub>), 7.07 (m, 2H, HAr<sub>binap</sub>), 6.90 (d, 2H, *J* = 8 Hz, HAr<sub>binap</sub>), 6.83 (d, 2H, *J* = 8 Hz, HAr<sub>binap</sub>), 6.67 (d, 2H, *J* = 8 Hz, HAr<sub>strap</sub>), 6.39 (d, 2H, *J* = 8 Hz, HAr<sub>strap</sub>), 6.12 (t, 2H, *J* = 8 Hz, HAr<sub>strap</sub>), 5.98 (t, 2H, *J* = 8 Hz, HAr<sub>strap</sub>), 5.91 (d, 2H, *J* = 8 Hz, HAr<sub>strap</sub>), 5.78 (d, 2H, *J* = 8 Hz, HAr<sub>strap</sub>), 3.87 (d, 2H, *J* = 8 Hz, CH<sub>2</sub>), 3.72 (d, 2H, *J* = 8 Hz, CH<sub>2</sub>), 3.66 (d, 2H, *J* = 8 Hz, CH<sub>2</sub>), 3.55 (d, 2H, *J* = 8 Hz, CH<sub>2</sub>), 2.42 (s, 6H, OMe), 1.89 (s, 6H, OMe), -2.64 (s, 2H, NH<sub>int</sub>)

<sup>13</sup>C NMR (75 MHz, CDCl<sub>3</sub>, 298 K)  $\delta$  166.3, 165.6, 154.9(0), 154.8(7), 141.8, 141.5, 138.9, 138.6, 135.4, 135.2, 135.1, 134.2, 133.5, 133.4, 133.0, 132.6, 131.9, 130.9, 130.4(5), 130.4(2), 130.3(9) (2C), 130.3(5) (2C), 130.1, 128.1, 128.0, 127.7, 127.5(3), 127.4(9), 127.4(3), 126.3, 125.7(5), 125.4(4), 125.4(2), 125.1, 124.9, 124.1, 123.1, 122.8, 122.6, 120.6, 115.6, 115.0, 59.9, 59.8, 38.5, 37.9.

$^{13}\text{C}$  NMR spectrum (125 MHz, 298 K) of compound **119** in  $\text{CDCl}_3$  (S =  $\text{CDCl}_3$ , \* = traces of residual solvents).

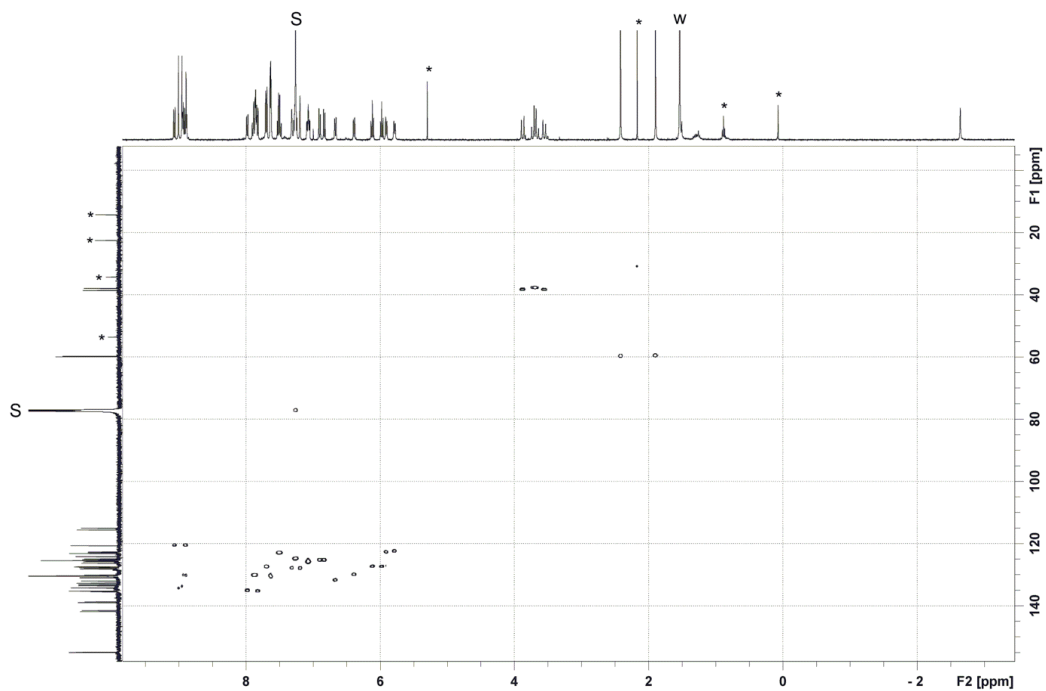


COSY 2D NMR spectrum (500 MHz, 298 K) of compound **119** in  $\text{CDCl}_3$  (S =  $\text{CHCl}_3$ , w = water, \* = traces of residual solvents or grease).

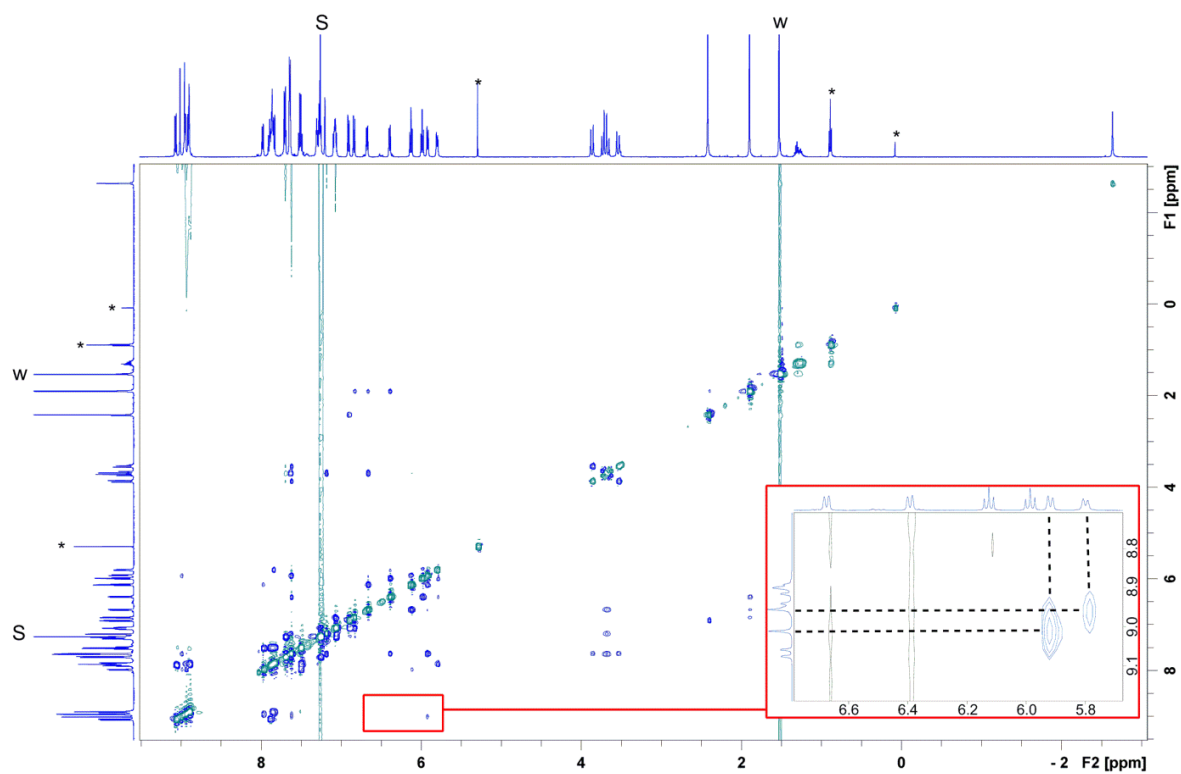




HMQC 2D NMR spectrum (500 MHz, 298 K) of compound **119** in CDCl<sub>3</sub> (S = CHCl<sub>3</sub>, w = water, \* = traces of residual solvents or grease).

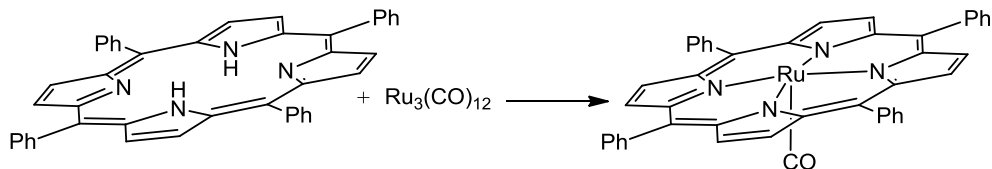


ROESY 2D NMR spectrum (500 MHz, 298 K) of compound **119** in CDCl<sub>3</sub> (S = CHCl<sub>3</sub>, w = water, \* = traces of residual solvents or grease).



## 3.5. Synthesis of Metal-Porphyrin Complexes

### 3.5.2. Synthesis of Ru(TPP)CO



$\text{Ru}_3(\text{CO})_{12}$  (0.575 g, 0.899 mmol) and  $\text{TPPH}_2$  (1.24 g, 2.03 mmol) were suspended in dry decalin (50 mL) under nitrogen atmosphere. The reaction mixture was refluxed for 4 hours and the resulting solid was collected and washed with *n*-hexane (3x10 mL) to remove residual decalin. The violet solid was then purified by flash-chromatography on silica. Toluene was used to elute unreacted  $\text{Ru}_3(\text{CO})_{12}$ ,  $\text{CH}_2\text{Cl}_2/n$ -hexane = 7:3 to elute  $\text{TPPH}_2$  and finally  $\text{CHCl}_3$  to yield  $\text{Ru}(\text{TPP})\text{CO}$  (1.03 g, 69%).

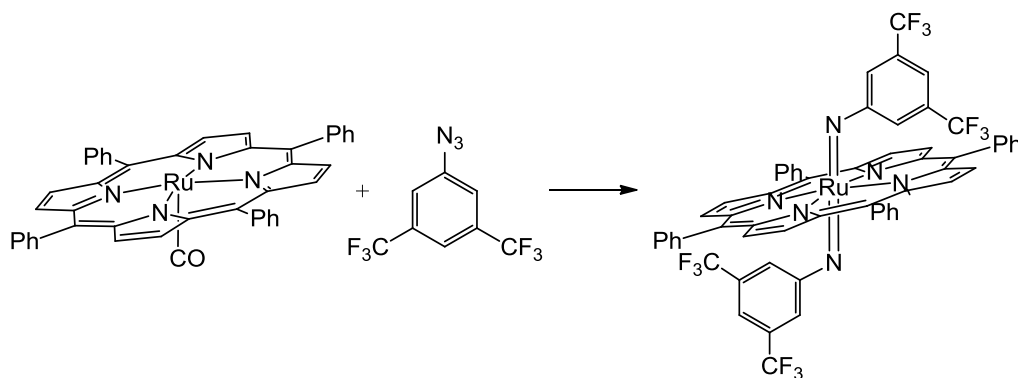
Elemental Analysis calc. for  $\text{C}_{45}\text{H}_{28}\text{N}_4\text{ORu}$ : C, 72.86; H, 3.80; N, 7.55. Found: C, 72.38; H, 4.05; N, 7.22.

$\nu_{\text{max}}$  (ATR)/ $\text{cm}^{-1}$ : 1948.4n(CO)

$\lambda_{\text{max}}$  ( $\text{CH}_2\text{Cl}_2$ )/nm: 412, 528, 588 (log  $\epsilon_{\text{M}}$  5.38, 4.29 and 3.51).

$^1\text{H}$  NMR (500 MHz,  $\text{CDCl}_3$ , 298 K)  $\delta$ : = 8.71 (s, 8H,  $\text{H}_\beta$ ), 8.23-8.20 (m, 4H,  $\text{H}_\alpha$  or  $\text{H}_\gamma$ ), 8.15-8.12 (m, 4H,  $\text{H}_\alpha$  or  $\text{H}_\gamma$ ), 7.74-7.69 (m, 12H,  $\text{H}_{\text{m+p}}$ ).

### 3.5.3. Synthesis of complex 113



3,5-Bis(trifluoromethyl)phenyl azide (223 mg, 0.87 mmol) was added to a benzene (60 mL) suspension of  $\text{Ru}(\text{TPP})(\text{CO})$  (210 mg, 0.28 mmol). The resulting dark solution was refluxed under nitrogen for 4 hours until the complete consumption of  $\text{Ru}(\text{TPP})(\text{CO})$  (TLC,  $\text{SiO}_2$ , petroleum ether/ $\text{CH}_2\text{Cl}_2$ =7:3). The mixture was evaporated to dryness and the residue purified by chromatography (alumina, petroleum ether/dichloromethane = 8:2) (**113**, 230 mg, 70%).

Elemental Analysis calc. for C<sub>60</sub>H<sub>34</sub>N<sub>6</sub>F<sub>12</sub>Ru: C, 61.70; H, 2.93; N, 7.20; found: C, 61.34; H, 2.99; N, 7.55.

$\nu_{\max}$ (ATR)/cm<sup>-1</sup> 1014 (oxidation marker), 877 (imido band);

$\nu_{\max}$  (CH<sub>2</sub>Cl<sub>2</sub>)/cm<sup>-1</sup>: 1016 (oxidation marker);

$\nu_{\max}$  (nujol)/cm<sup>-1</sup>: 1016 (oxidation marker), 878 (imido band);

$\lambda_{\max}$  (CH<sub>2</sub>Cl<sub>2</sub>)/nm: 419, 526 (log  $\epsilon_M$  5.03 and 4.00)

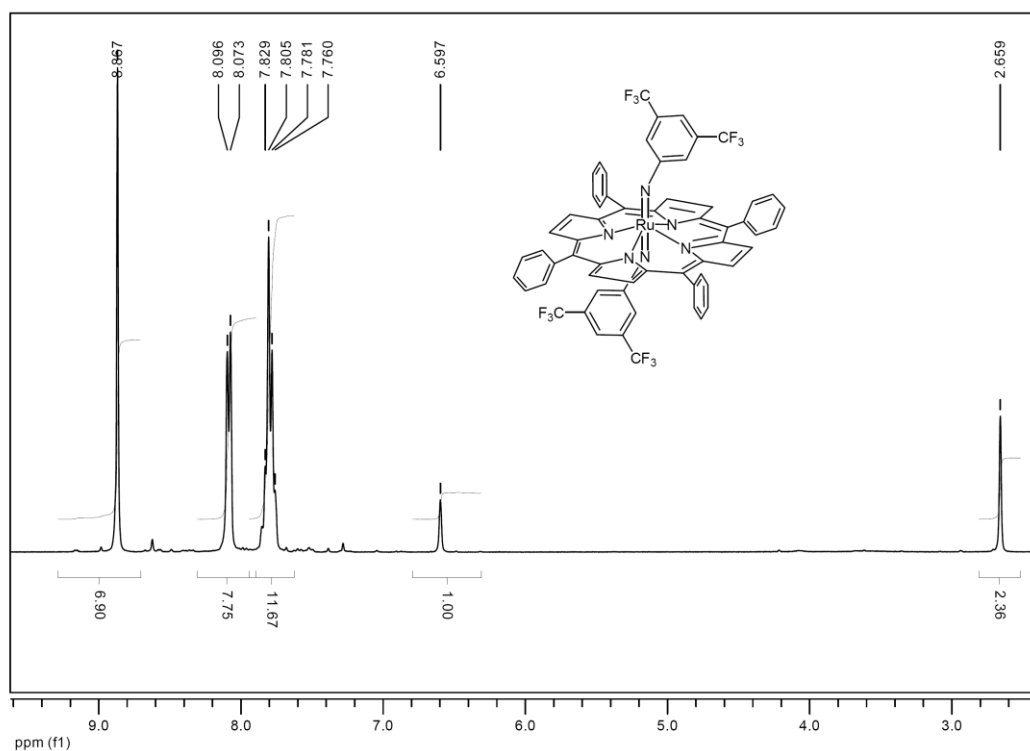
m/z (ESI) 1169 [M+1]

<sup>1</sup>H NMR (300 MHz, CDCl<sub>3</sub>, 298 K)  $\delta$ : 8.87 (8 H, s, H <sub>$\beta$</sub> ), 8.08 (8 H, d,  $J$  = 6.9 Hz, H<sub>o</sub>), 7.83-7.76 (12 H, m, H<sub>m-p</sub>), 6.60 (2 H, s, H<sub>Ar</sub>), 2.66 (4H, s, H<sub>Ar</sub>);

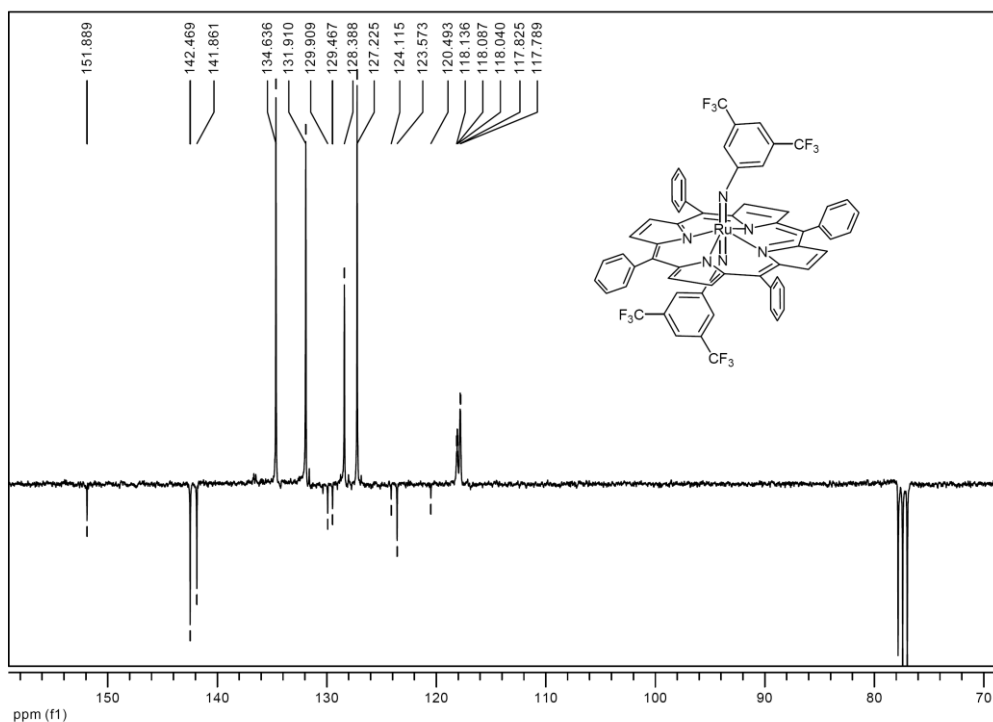
<sup>13</sup>C NMR (75 MHz, CDCl<sub>3</sub>, 298 K)  $\delta$ : 151.9 (C), 142.5 (C), 141.9 (C), 134.6 (CH), 131.9 (CH), 129.7 (q,  $J$  = 33.2 Hz, C-CF<sub>3</sub>), 128.4 (CH), 127.2 (CH), 123.6 (C), 122.3 (q,  $J$  271.7 Hz, CF<sub>3</sub>), 118.1 (CH), 117.8 (CH);

<sup>19</sup>F NMR (282 MHz, CDCl<sub>3</sub>, 298 K)  $\delta$ : -64.06

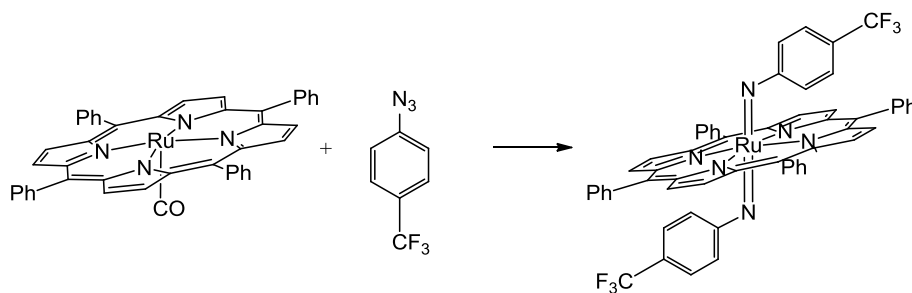
<sup>1</sup>H NMR of complex **113** (CDCl<sub>3</sub>).



NMR of complex **113** (CDCl<sub>3</sub>).



### 3.5.4. Synthesis of complex **116**



4-(Trifluoromethyl)phenyl azide (74.0 mg, 0.393 mmol) was added to a benzene (50 mL) suspension of Ru(TPP)CO (145 mg, 0.197 mmol) to give a dark solution which was refluxed under nitrogen for 30 minutes. The mixture was concentrated to 30 ml and filtered to eliminate unreacted Ru(TPP)CO. The resulting solution was evaporated to dryness and *n*-hexane (20 mL) was added. The purple solid was collected in a filter and dried *in vacuo* (**116**, 88 mg, 60%).

Elemental Analysis calc. for C<sub>58</sub>H<sub>37</sub>F<sub>6</sub>N<sub>6</sub>Ru C, 67.44; H, 3.61; N, 8.14; found: : C, 67.87; H, 3.98; N, 8.05.

$\nu_{\max}$ (ATR)/cm<sup>-1</sup>: 1011 (oxidation marker), 838 (imido band);

$\nu_{\max}$  (CH<sub>2</sub>Cl<sub>2</sub>)/cm<sup>-1</sup>: 1015 (oxidation marker);

$\nu_{\max}$  (nujol)/ $\text{cm}^{-1}$ : 1012 (oxidation marker), 842 (imido band);

$\lambda_{\max}$  ( $\text{CH}_2\text{Cl}_2$ )/nm: 417 and 530 ( $\log \epsilon_M$  5.42 and 4.27);

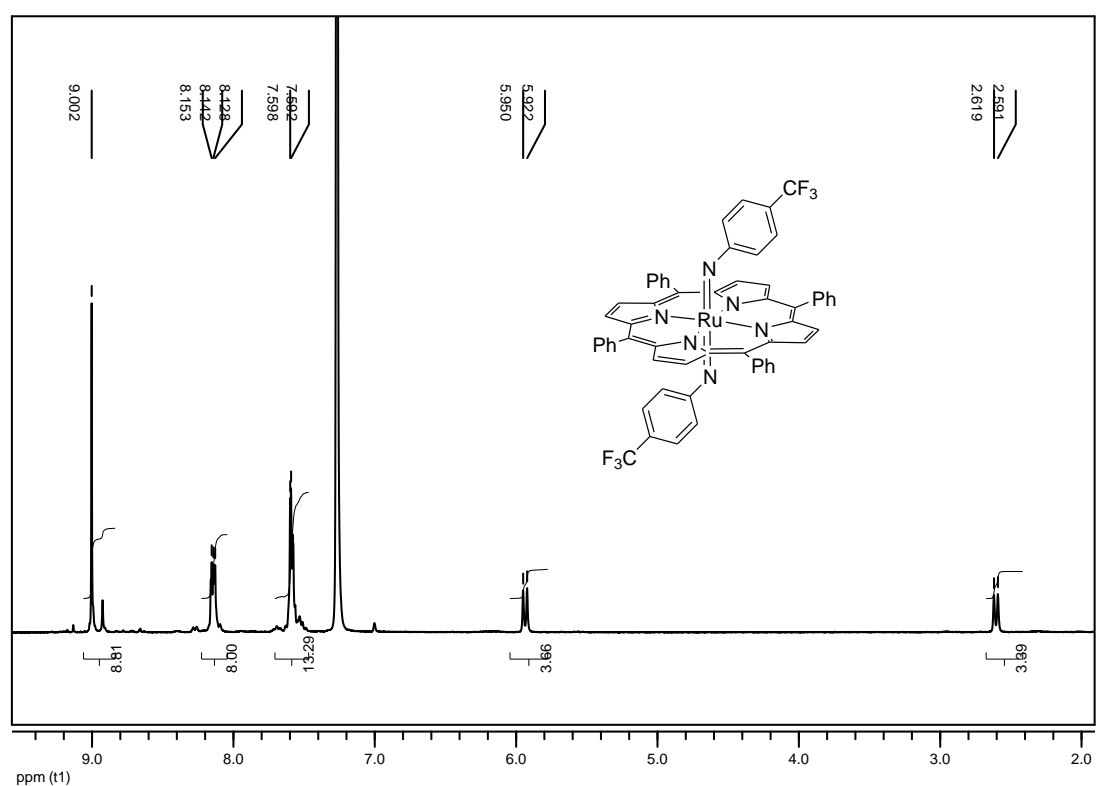
$m/z$  (ESI) 1033 [ $M+1$ ];

$^1\text{H}$  NMR (300 MHz,  $\text{C}_6\text{D}_6$ , 298 K)  $\delta$ : 9.00 (8H, s,  $\text{H}_\beta$ ), 8.15 (8H, d,  $J = 9.1$  Hz,  $\text{H}_\alpha$ ), 7.59-7.58 (12H, m,  $\text{H}_m$ ), 5.94 (4H, d,  $J = 8.4$  Hz,  $\text{H}_{Ar}$ ), 2.61 (4H, d,  $J = 8.4$  Hz,  $\text{H}_{Ar}$ );

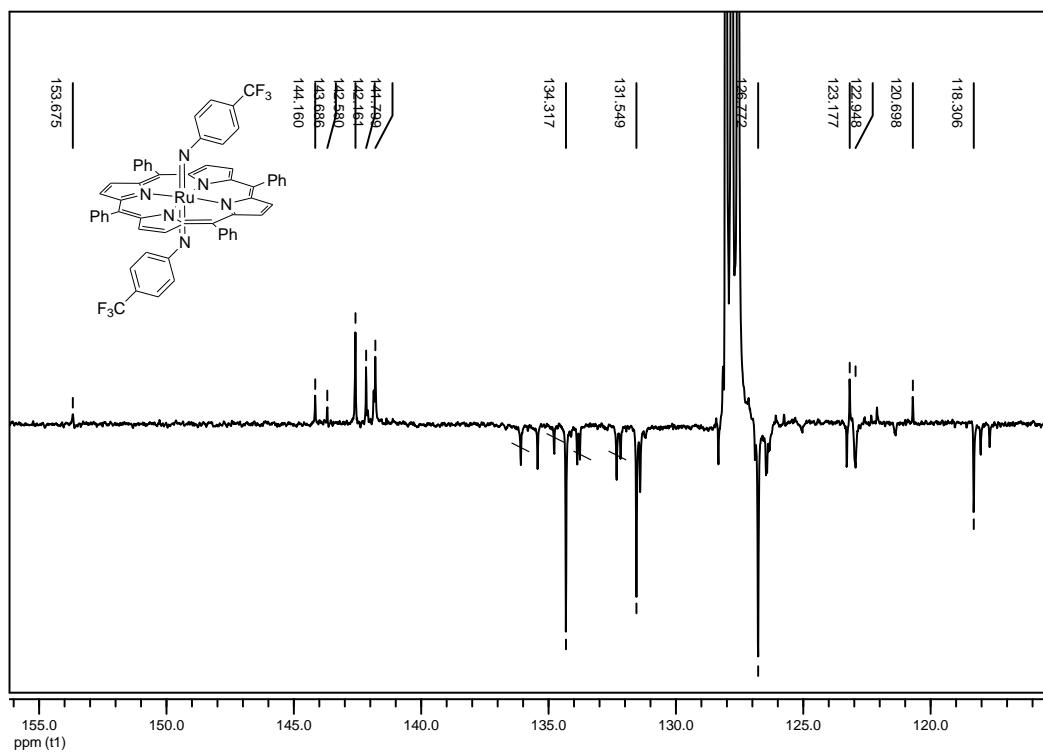
$^{13}\text{C}$  NMR (75 MHz,  $\text{C}_6\text{D}_6$ , 298 K)  $\delta$ : 154.0 (C), 144.5 (C), 142.9 (C), 142.6 (C), 142.0 ( $\text{CCF}_3$ , q,  $J$  27.2 Hz), 134.7 (CH), 131.5 (CH), 126.8 (CH), 122.9 (CH), 121.9 ( $\text{CF}_3$ , q, 185.9 Hz), 118.3 (CH); the complex partly decomposes during the analysis;

$^{19}\text{F}$  NMR (282 MHz,  $\text{CDCl}_3$ , 298 K)  $\delta$ : -62.6.

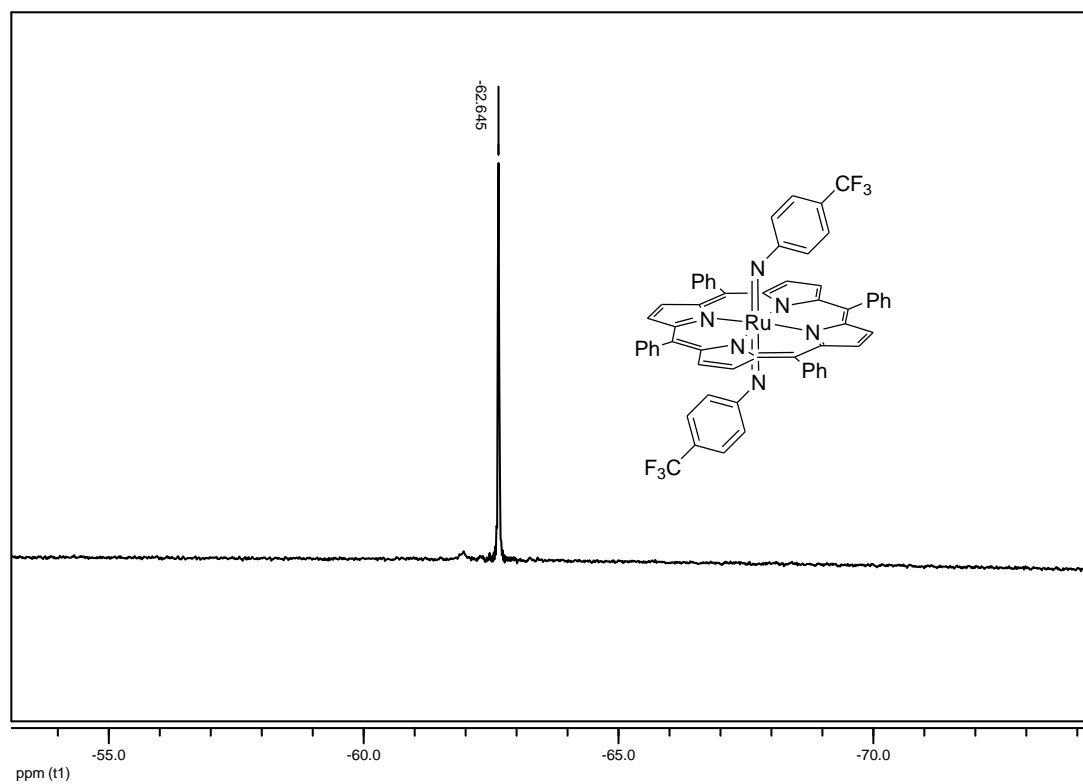
$^1\text{H}$  NMR of complex **116** ( $\text{C}_6\text{D}_6$ )



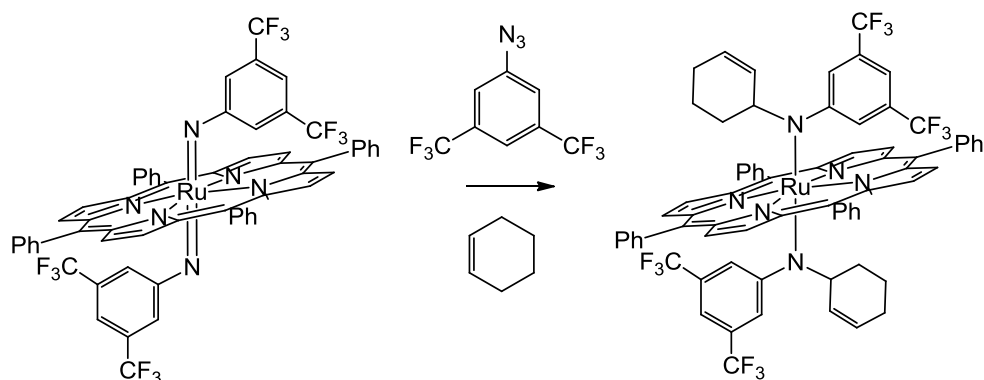
$^{13}\text{C}$  NMR of complex **116** ( $\text{C}_6\text{D}_6$ )



$^{19}\text{F}$  NMR of complex **116** ( $\text{C}_6\text{D}_6$ )



### 3.5.5. Synthesis of 115



Complex **113** (99 mg,  $8.5 \times 10^{-2}$  mmol) was added to a benzene (15 mL) solution of 3,5-bis(trifluoromethyl)phenyl azide (217 mg,  $8.4 \times 10^{-1}$  mmol) and cyclohexene (0.42 mL, 4.25 mmol). The resulting solution was stirred at 75 °C and the arylazide conversion was monitored by IR spectroscopy measuring the  $N_3$  characteristic absorbance at  $2116 \text{ cm}^{-1}$ . After 4 hours (60% of  $ArN_3$  conversion) the TLC analysis (alumina, petroleum ether/dichloromethane = 8:2) showed the complete consumption of **113**. The reaction mixture was concentrated to 2 mL and petroleum ether (20 mL) was added. The resulting suspension was filtered to eliminate a dark insoluble residue and concentrated to 10 mL. The resulting purple solid was collected by filtration and dried *in vacuo* (**115**, 20 mg, 18%). The GC-MS analysis of the solution revealed the presence of the allylic amine *N*-(cyclohex-2-enyl)-3,5-bis(trifluoromethyl)benzenamine.

Elemental Analysis calc. for  $C_{72}H_{52}F_{12}N_6Ru$ : C, 65.01; H, 3.94; N, 6.32; found: C, 65.20; H, 4.03; N, 6.20;

$\nu_{\text{max}}$  (ATR)/ $\text{cm}^{-1}$ : 1008 (oxidation marker);

$\nu_{\text{max}}$  (nujol)/ $\text{cm}^{-1}$ : 1013 (oxidation marker);

$\lambda_{\text{max}}$  ( $\text{CH}_2\text{Cl}_2$ )/nm: 414 and 526 ( $\log \epsilon_M$  4.80 and 3.92);

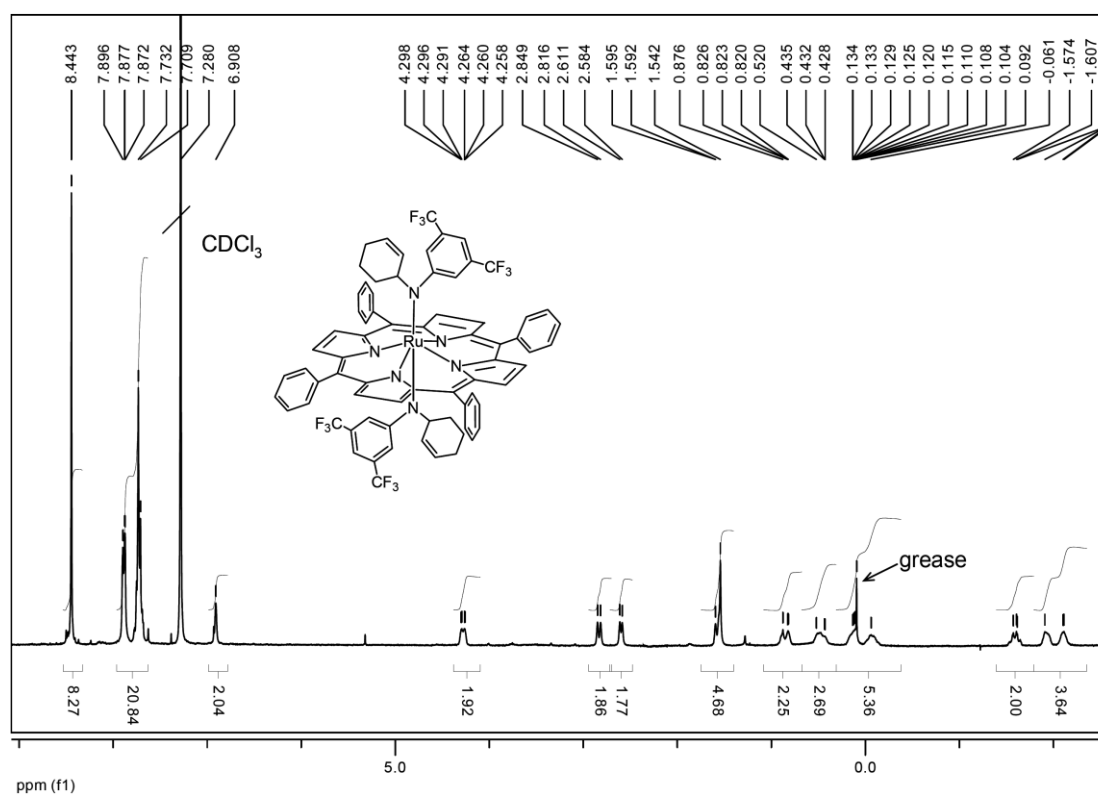
$m/z$  (ESI) 1331 [ $M+1$ ];

$^1\text{H}$  NMR (300 MHz,  $\text{CDCl}_3$ , 298 K)  $\delta$ : 8.44 (8 H, s,  $H_\beta$ ), 7.90-7.87 (8 H, m,  $H_o$ ), 7.75-7.71 (12 H, m,  $H_{m-p}$ ), 6.91 (2 H, s,  $H_{Ar}$ ), 4.30-4.26 (2 H, m,  $\text{CH}-\text{CH}=\text{CH}$ ), 2.85-2.82 (2 H, m,  $H_{Ar}$ ), 2.61-2.59 (2 H, m,  $H_{Ar}$ ), 1.60-1.54 (2 H, m,  $\text{CH}=\text{CH}-\text{CH}_2$  overlapping with  $\text{H}_2\text{O}$ ), 0.88-0.82 (2 H, m,  $\text{CH}=\text{CH}-\text{CHH}$ ), 0.52-0.43 (2 H, m,  $\text{CH}=\text{CH}-\text{CHH}$ ), 0.13-0.09 (2 H, m,  $\text{CH}_2-\text{CHH}-\text{CH}_2$  overlapping with grease), -0.04-(-0.10) (2 H, m,  $\text{CH}_2-\text{CHH}-\text{CH}_2$ ), -1.57-(-1.62) (2 H, m,  $\text{N}-\text{CH}-\text{CHH}$ ), -1.91-(-1.95) (2 H, m,  $\text{N}-\text{CH}-\text{CHH}$ ), -2.10-(-2.13) (2 H, m,  $\text{N}-\text{CH}$ ); (5)

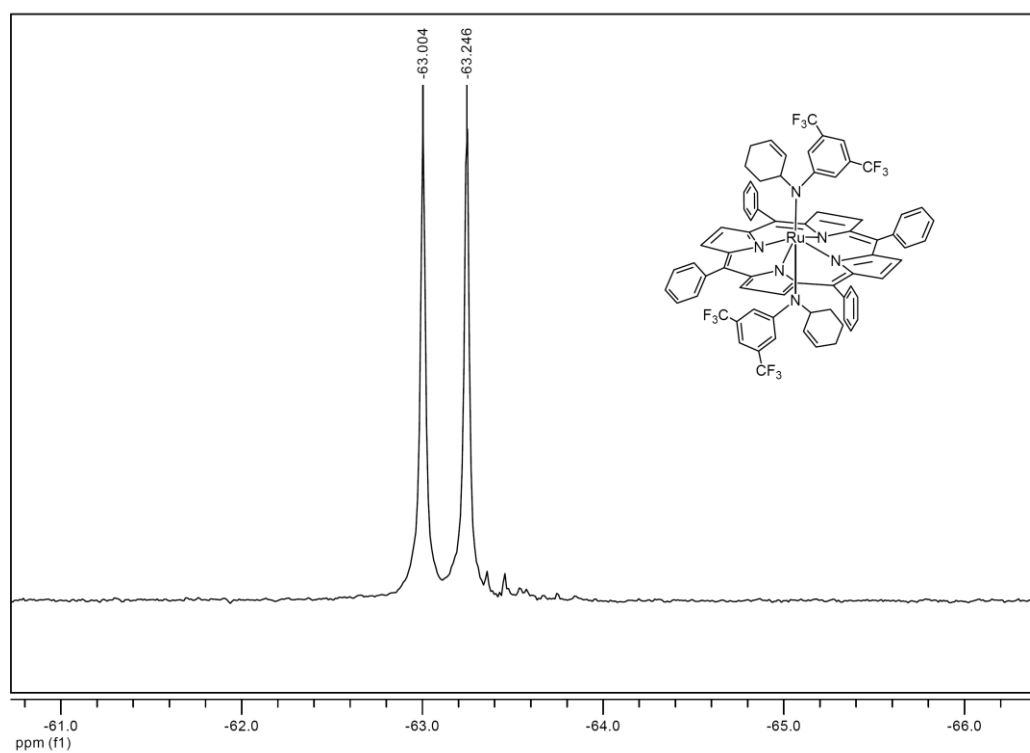
The  $^{13}\text{C}$  NMR spectrum is not reported because **115** partly decomposes during the experiment.

$^{19}\text{F}$  NMR (282 MHz,  $\text{CDCl}_3$ , 298 K)  $\delta$ : -63.25, -63.00.

$^1\text{H}$  NMR of complex **115** ( $\text{CDCl}_3$ ).

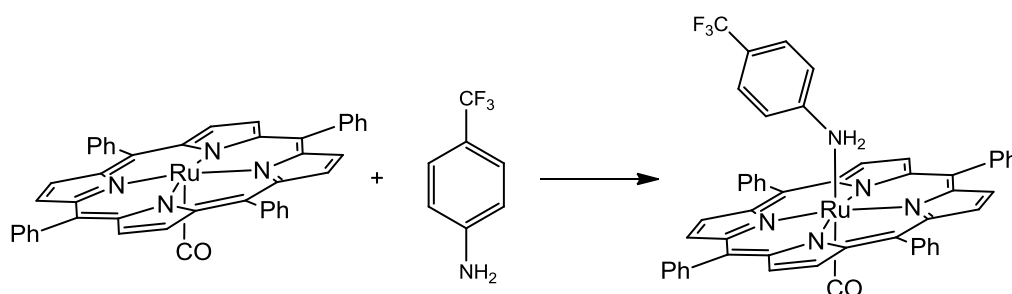


$^{19}\text{F}$  NMR of complex **115** ( $\text{CDCl}_3$ ).





### 3.5.6. Synthesis of 117



**Method a:** 4(Trifluoromethyl)aniline (45.9 mg,  $2.85 \times 10^{-1}$  mmol) was added to a benzene (50 mL) suspension of Ru(TPP)CO (105.6 mg,  $1.4 \times 10^{-1}$  mmol). The resulting red solution was stirred at room temperature for 30 minutes, concentrate to 2 mL and then *n*-hexane (15 mL) was added. The resulting red solid was collect in a filter and dried *in vacum* (**117**, 95 mg, 75%). **Method b:** 4(Trifluoromethyl)phenyl azide (151.2 mg,  $8.08 \times 10^{-1}$  mmol) was added to a benzene (50 mL) suspension of Ru(TPP)CO (149.9 mg,  $2.02 \times 10^{-1}$  mmol). The resulting dark solution was refluxed under nitrogen for 3 hours and then filtered to remove insoluble products deriving from **116** decomposition. The solution was evaporated to dryness and *n*-hexane (15 mL) was added. The resulting solid was collected in a filter and dried *in vacuo* (**117**, 67.5 mg, 37%).

Elemental Analysis calc. for  $C_{52}H_{34}F_3N_5ORu$ : C, 69.17; H, 3.80; N, 7.77; found: : C, 68.87; H, 4.11; N, 7.49;

$\nu_{\max}$  (ATR)/ $cm^{-1}$ : 1964 (stretching CO) 1008 (oxidation marker);

$\nu_{\max}$  (nujol)/ $cm^{-1}$ : 1965 (stretching CO), 1009 (oxidation marker);

$\nu_{\max}$  ( $CH_2Cl_2$ )/ $cm^{-1}$ : 1942 (stretching CO), 1009 (oxidation marker)

$\lambda_{\max}$  ( $CH_2Cl_2$ )/nm: 411 and 530 ( $\log \epsilon_M$  5.42 and 4.39);

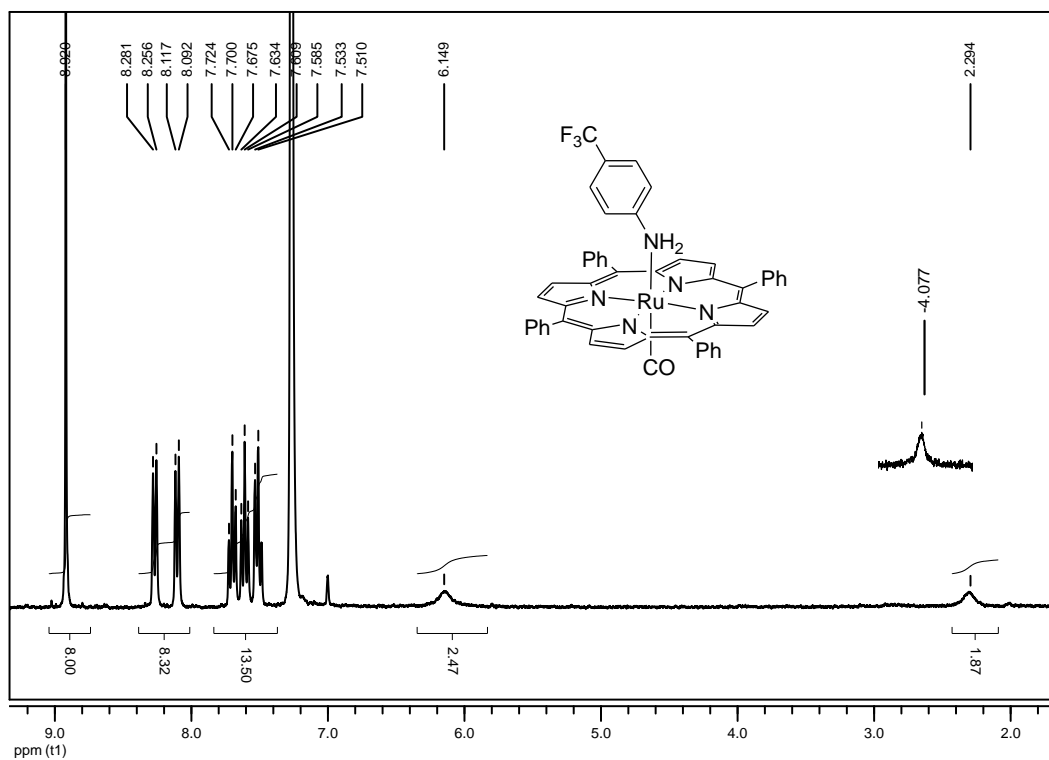
$m/z$  (FAB) 902.

$^1H$  NMR (300 MHz,  $C_6D_6$ , 298 K)  $\delta$ : 8.93 (8H, s,  $H_\beta$ ), 8.27 (4H, d,  $J$  7.5 Hz,  $H_o$ ), 8.10 (4H, d,  $J$  7.5 Hz,  $H_o'$ ), 7.70 (4H, pst,  $J$  7.5 Hz,  $H_m$ ), 7.61 (4H, pst,  $J$  7.5 Hz,  $H_p$ ), 7.51 (4H, pst,  $J$  7.5 Hz,  $H_m'$ ), 6.15 (2H, m,  $H_{Ar}$ ), 2.29 (2H, m,  $H_{Ar}$ ), -4.08 (2H, br s,  $NH_2$ ).

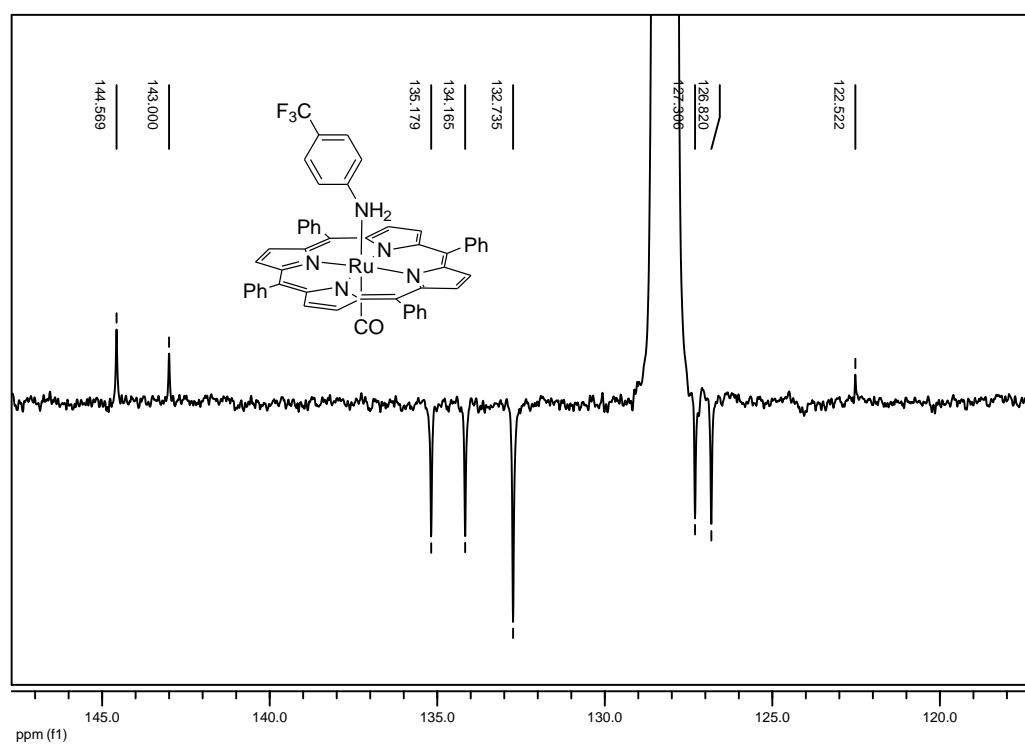
$^{13}C$  NMR (75 MHz,  $C_6D_6$ , 298 K)  $\delta$ : 144.6 (C), 143.0 (C), 135.2 (CH), 134.2 (CH), 132.7 (CH), 127.3 (CH), 126.8 (CH), 122.5 (C);

$^{19}F$  NMR (282 MHz,  $CDCl_3$ , 298 K)  $\delta$ : -61.9.

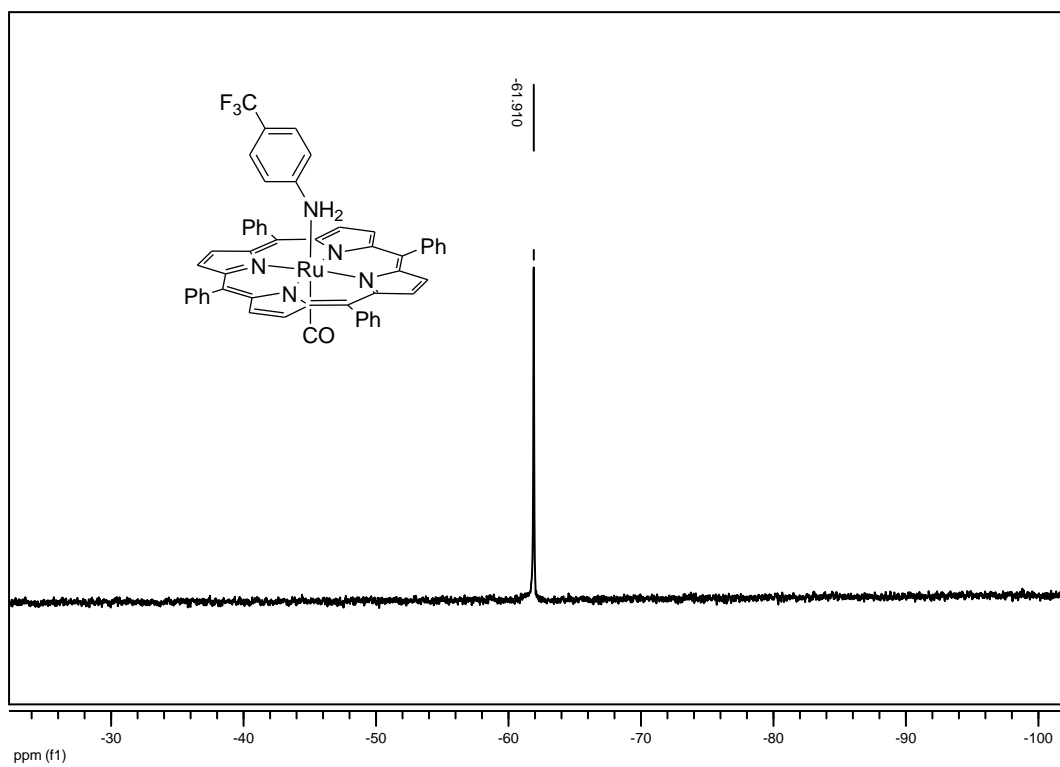
$^1\text{H}$  NMR of complex 117 ( $\text{C}_6\text{D}_6$ )



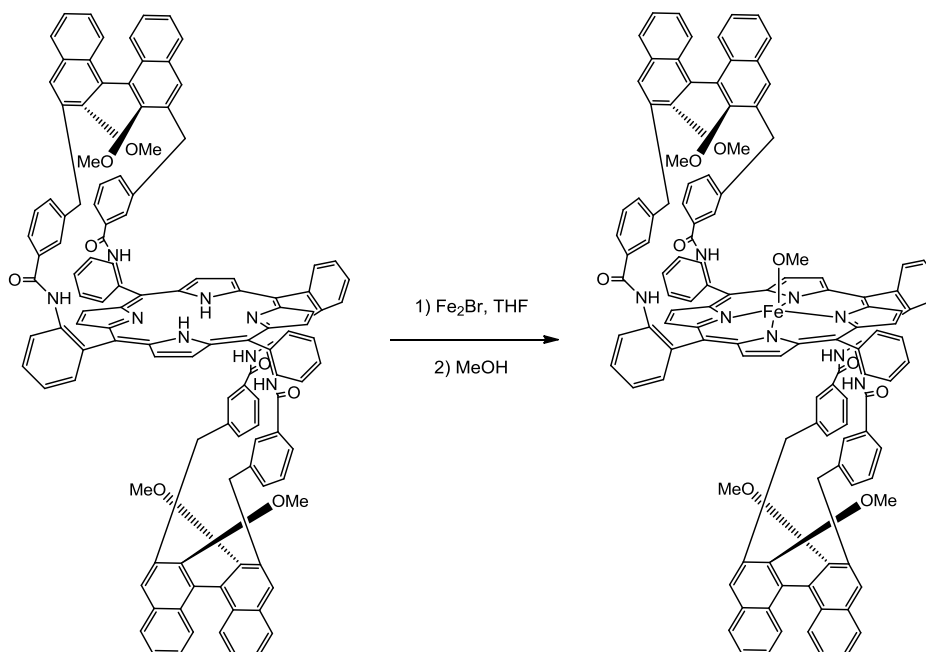
$^{13}\text{C}$  NMR of complex 117 ( $\text{C}_6\text{D}_6$ )



$^{19}\text{F}$  NMR of complex **117** ( $\text{C}_6\text{D}_6$ )



### 3.5.7. Synthesis of Fe(119)(OCH<sub>3</sub>)



In a dried 50 mL Schlenk flask, **119** (0.078 g,  $4.40 \times 10^{-5}$  mol) and FeBr<sub>2</sub> (0.047 g,  $2.20 \times 10^{-4}$  mol) were dissolved in 25.0 mL of THF. The dark solution was refluxed under nitrogen atmosphere for 24 hours until the complete consumption of **119** that was monitored by TLC. The mixture was evaporated to dryness and the residue purified by chromatography (alumina 0.063-0.200 mm, eluent dichloromethane/methanol = 99.5:0.5). **119Fe** 0.081 g, 99 %).

Elemental Analysis calc. for C<sub>120</sub>H<sub>84</sub>FeN<sub>8</sub>O<sub>8</sub>: C, 79.11; H, 4.65; N, 6.15; found: C, 78.83; H, 4.73; N, 6.05.

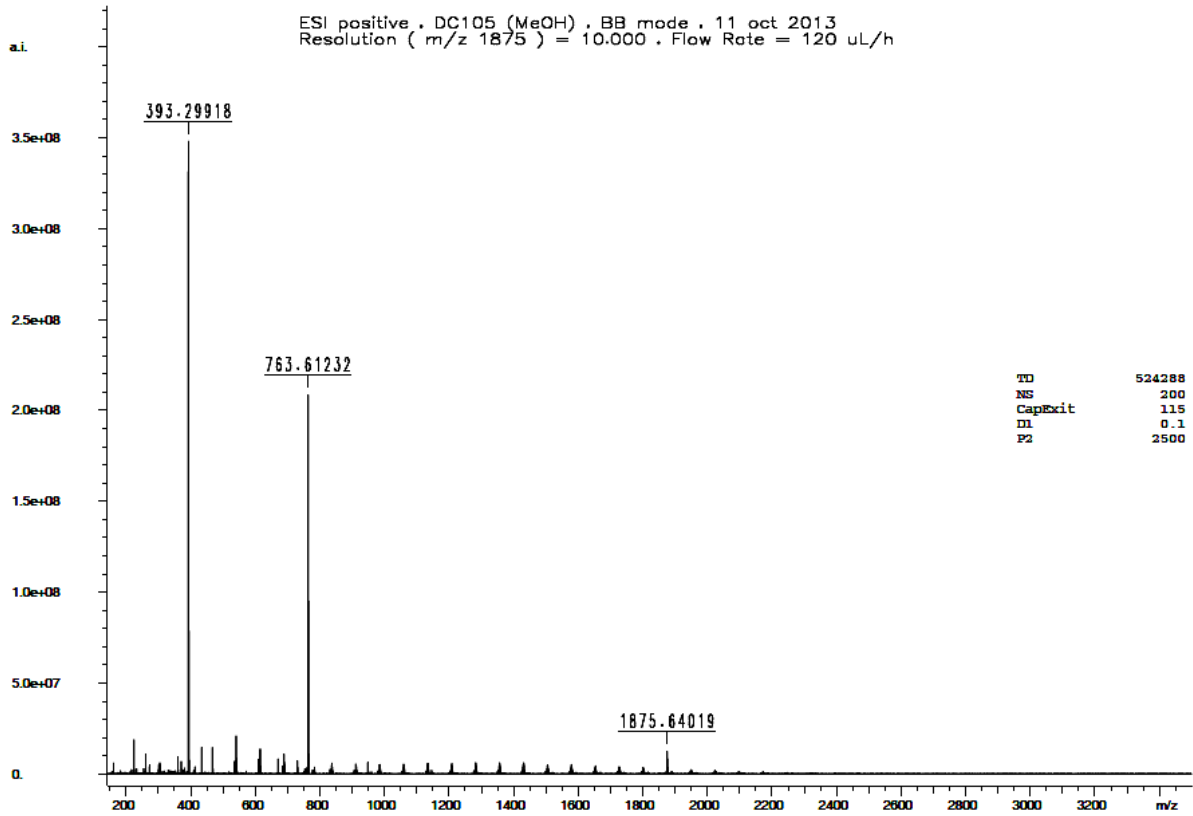
$\nu_{\max}$  (CH<sub>2</sub>Cl<sub>2</sub>)/cm<sup>-1</sup>: 3685 (w), 3418 (w), 1723 (w), 1676 (w), 1605 (w), 1516 (w), 1278 (w), 1098 (w), 1009 (w).

$\lambda_{\max}$  (CH<sub>2</sub>Cl<sub>2</sub>)/nm 420, 576 (log  $\epsilon_M$  4.58 and 3.35).

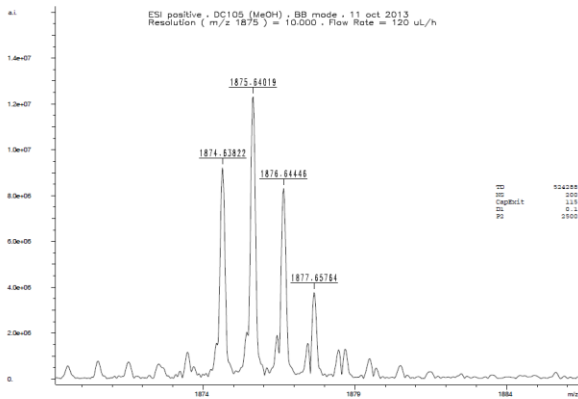
$[\alpha]_D^{20} = -625.000$  (c =  $8 \times 10^{-4}$  g/100mL; in CH<sub>2</sub>Cl<sub>2</sub>).

m/z (ESI) 1852 [M+Na]

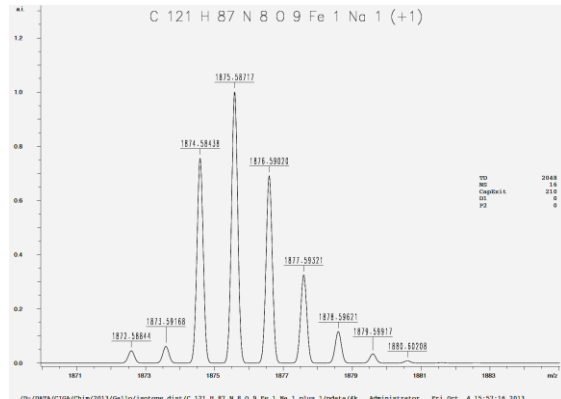
MS-ESI spectrum of complex **119Fe** [M+Na<sup>+</sup>]



/D:/DATA/CIGA/Chin/2013/Gallo/DC105/9/pdata/1 Administrator Fri Oct 11 17:05:22 2013



/D:/DATA/CIGA/Chin/2013/Gallo/DC105/9/pdata/1 Administrator Fri Oct 11 17:06:23 2013



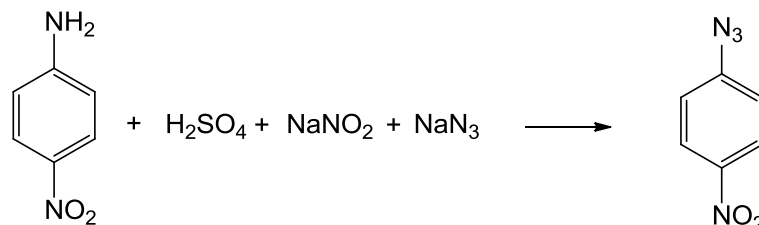
/D:/DATA/CIGA/Chin/2013/Gallo/Isotope dilu/C 121 H 87 N 8 O 9 Fe 1 Na 1 plus 1/pdata/6k Administrator Fri Oct 4 15:57:18 2013

c) Experimental MS-ESI spectrum

d) Simulation of MS-ESI spectrum

## 3.6. Synthesis of Aryl Azides

### 3.6.1. Synthesis of 4-NO<sub>2</sub>phenylazide.

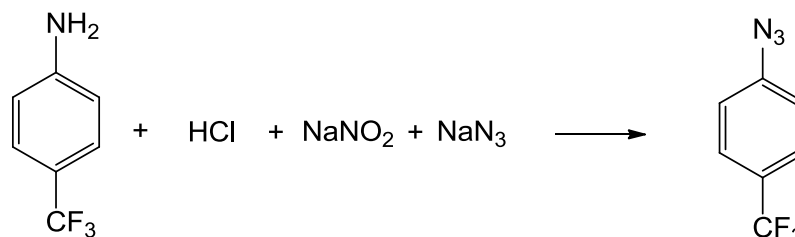


4-Nitroaniline (5.2 g, 38 mmol) was dissolved in 30% H<sub>2</sub>SO<sub>4</sub> (75 mL). The yellow mixture was gently heated to promote the dissolution of the aniline and then was placed in an ice-water bath. To the cold yellow solution was added a solution of NaNO<sub>2</sub> (2.75 g, 40 mmol) in 25 mL of water. When the solution turned to pale yellow urea (1.3 g, 22 mmol) was added in one portion. Under vigorous magnetic stirring a solution of sodium azide (3.5 g, 54 mmol) in water (20 mL) was added to the cold mixture in about 15 minutes. The resulting yellow forming mixture was then allowed to reach room temperature and further stirred for 30 minutes. Dichloromethane (100 mL) was then added under vigorous stirring. The organic layer was collected, dried over Na<sub>2</sub>SO<sub>4</sub>, concentrated under reduced pressure to about 10 mL and *n*-hexane (150 mL) was slowly added under vigorous magnetic stirring. The so formed yellow solid was collected and dried under reduced pressure (4.3 g, 70%).

$\nu_{\max}$  (nujol)/cm<sup>-1</sup>: 2125 (N<sub>3</sub> stretching)

<sup>1</sup>H NMR (300 MHz, C<sub>6</sub>D<sub>6</sub>, 300 K)  $\delta$ : 7.62 (d, 2H, *J* = 9.1 Hz), 6.15 (d, 2H, *J* = 9.1 Hz).

### 3.6.2. Synthesis of 4-CF<sub>3</sub>-phenylazide



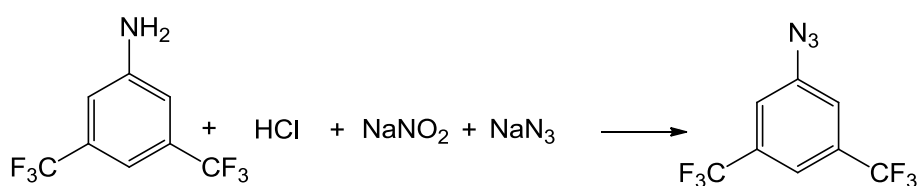
4-CF<sub>3</sub>aniline (3.0 mL, 2.52×10<sup>-2</sup> mol) was dissolved in a solution of 30 mL of HCl 37% and 42 mL of H<sub>2</sub>O. The mixture was placed in an ice-water bath. To the cold yellow solution was added a solution of NaNO<sub>2</sub> (2.28 g, 33 mmol) in 30 mL of water. When the solution turned to pale yellow urea (66 mg, 11 mmol) was added in one portion. Under vigorous magnetic stirring a solution of sodium azide (3.2 g, 49 mmol) in water (45 mL) was added to the cold mixture in about 15 minutes. The resulting yellow forming mixture was then allowed to reach room temperature and further stirred for 30 minutes. Diisopropyl ether (50 mL) was

then added and the inorganic layer was washed three times with 50 mL of diisopropyl ether. The organic phase was collected and dried over  $\text{Na}_2\text{SO}_4$ . Finally, the anhydrous solution was filtered and the solution was dried under reduced pressure (3.18 g, 68%).

$\nu_{\text{max}}$  (nujol)/ $\text{cm}^{-1}$ : 2129 ( $\text{N}_3$  stretching)

$^1\text{H NMR}$  (300 MHz,  $\text{CDCl}_3$ , 300 K)  $\delta$ : 7.63 (d, 2H,  $J = 8.4$  Hz), 7.14 (d, 2H,  $J = 8.4$  Hz).

### 3.6.3. Synthesis of 3,5-( $\text{CF}_3$ )<sub>2</sub>-phenylazide

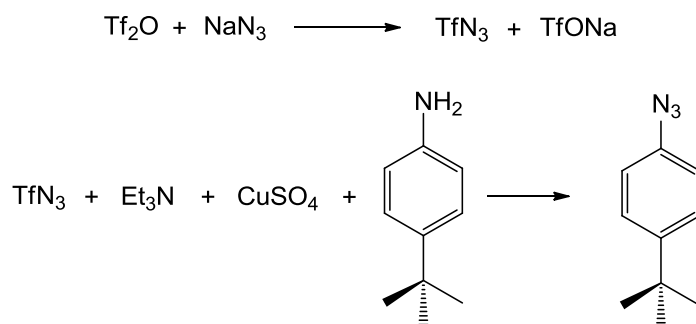


3,5-( $\text{CF}_3$ )-aniline (3.75 mL,  $2.41 \times 10^{-2}$  mol) was dissolved in a solution of 30 mL of HCl 37% and 42 mL of  $\text{H}_2\text{O}$ . The mixture was placed in an ice-water bath. To the cold yellow solution was added a solution of  $\text{NaNO}_2$  (2.23 g,  $3.32 \times 10^{-2}$  mol) in 30 mL of water. When the solution turned to pale yellow urea (63 mg,  $1.1 \times 10^{-2}$  mol) was added in one portion. Under vigorous magnetic stirring a solution of sodium azide (3.2 g,  $4.9 \times 10^{-2}$  mol) in water (45 mL) was added to the cold mixture in about 15 minutes. The resulting yellow forming mixture was then allowed to reach room temperature and further stirred for 30 minutes. Diisopropyl ether (50 mL) was then added and the inorganic layer was washed three times with 50 mL of diisopropyl ether. The organic phase was collected and dried over  $\text{Na}_2\text{SO}_4$ . Finally, the anhydrous solution was filtered and the solution was dried under reduced pressure (3.86 g, 70%).

$\nu_{\text{max}}$  ( $\text{CH}_2\text{Cl}_2$ )/ $\text{cm}^{-1}$ : 2125 ( $\text{N}_3$  stretching)

$^1\text{H NMR}$  (300 MHz,  $\text{CDCl}_3$ , 300 K)  $\delta$ : 7.66 (s, 1H,  $\text{H}_{\text{Ar}}$ ), 7.46 (s, 2H,  $\text{H}_{\text{Ar}}$ ).

### 3.6.4. Synthesis of 4-<sup>t</sup>Bu-phenylazide



A solution of NaN<sub>3</sub> (15g, 0.22 mol), water (32 mL) and CH<sub>2</sub>Cl<sub>2</sub> was cooled at 0°C. Under vigorous magnetic stirring trifluoromethanesulfonic anhydride (Tf<sub>2</sub>O) (10g; 3.5×10<sup>-2</sup>mol) was added and the mixture was further stirred for 2 hours at 0°C. Then the organic layer was washed with CH<sub>2</sub>Cl<sub>2</sub> and dried over Na<sub>2</sub>SO<sub>4</sub>.

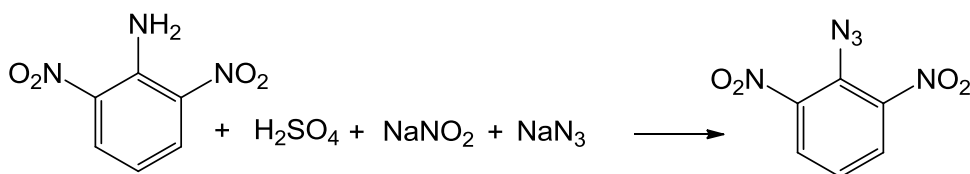
Subsequently, to a solution of 4-tert-butylaniline (1.9 mL, 1.2×10<sup>-2</sup>mol) in CH<sub>2</sub>Cl<sub>2</sub> were added 5 mL of Et<sub>3</sub>N and a solution of CuSO<sub>4</sub> (95.6 mg, 3.81×10<sup>-4</sup>mol) in 2 mL of water. Then the solution of TfN<sub>3</sub> in CH<sub>2</sub>Cl<sub>2</sub>, previously prepared, and 8 mL of MeOH were added to the reaction mixture to make the solution monophasic.

The resulting mixture was stirred at room temperature for other 2 hours, 30 mL of a saturated solution of NaHCO<sub>3</sub> were added to the mixture and the organic layer was extracted with CH<sub>2</sub>Cl<sub>2</sub> (3×30 mL). The organic phase was washed with brine and dried over MgSO<sub>4</sub>. The crude was purified by flash chromatography (silica, petroleum ether) (1.35 g, 65%).

$\nu_{\max}$  (CH<sub>2</sub>Cl<sub>2</sub>)/cm<sup>-1</sup>: 2123 (N<sub>3</sub> stretching)

<sup>1</sup>H NMR (300 MHz, CDCl<sub>3</sub>, 300 K)  $\delta$ : 7.39 (d, 2H, *J* = 8.7 Hz), 6.99 (d, 2H, *J* = 8.7 Hz), 1.34 (s, 9H, CH<sub>3</sub>).

### 3.6.5. Synthesis of 2,6-(NO<sub>2</sub>)<sub>2</sub>-phenylazide



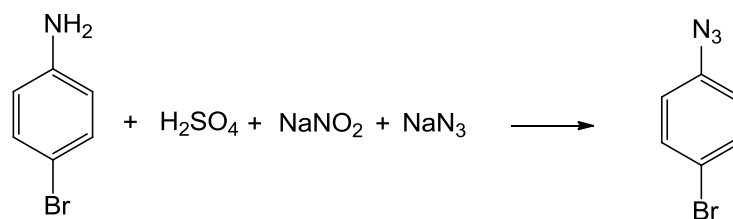
2,6(NO<sub>2</sub>)<sub>2</sub>-aniline (4.8 g, 26 mmol) was dissolved in a solution of H<sub>2</sub>SO<sub>4</sub> 30% (50 mL). The solution was gently heated to promote the dissolution of the aniline then it was placed in an ice-water bath. To the cold pale violet solution, a solution of NaNO<sub>2</sub> (1.97 g, 28.2 mmol) in 25 mL of water was then added dropwise. Then urea (462 mg, 7.65 mmol) was added in one portion and under vigorous magnetic stirring a solution of sodium azide (2.13 g, 320 mmol) in water (20 mL) was added. The resulting mixture was allowed to reach room temperature and further stirred for 1 hour. Diethyl ether (50 mL) was added, the organic layer was separated, and the aqueous layer washed with diethyl ether (2 × 50 mL). The organic layer was collected, dried over Na<sub>2</sub>SO<sub>4</sub> filtered and finally evaporated to dryness under reduced pressure affording the desired product (4.06 g, 74%).

$\nu_{\max}$  (CH<sub>2</sub>Cl<sub>2</sub>)/cm<sup>-1</sup>: 2305 (N<sub>3</sub> stretching)

<sup>1</sup>H NMR (300 MHz, C<sub>6</sub>D<sub>6</sub>, 300 K)  $\delta$ : 9.18 (s, 1H, H<sub>Ar</sub>), 8.60 (s, 2H, H<sub>Ar</sub>).



### 3.6.6. Synthesis of 4-Br-phenylazide



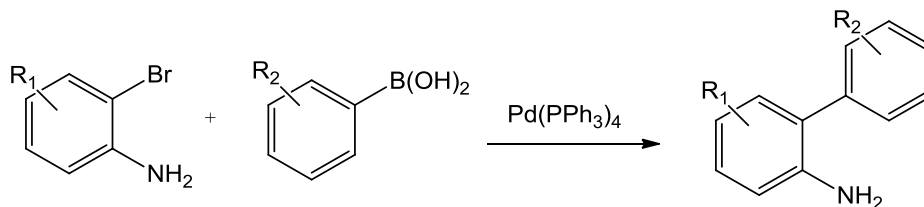
4-Br-aniline (3.64 g, 21.2 mmol) were dissolved in a solution of  $\text{H}_2\text{SO}_4$  30% (50 mL). The mixture was gently heated to promote the dissolution of the aniline then was placed in an ice-water bath. To the cold pale violet solution was added dropwise a solution of  $\text{NaNO}_2$  (1.83 g, 26.5 mmol) in 30 mL of water in 15 minutes. The pale yellow solution was allowed to stir at  $0^\circ\text{C}$  for 30 minutes, and then urea (217 mg, 3.62 mmol) was added in one portion and the solution was stirred at  $0^\circ\text{C}$  for another 15 minutes. Under vigorous magnetic stirring a solution of sodium azide (1.77 g, 27.2 mmol) in water (30 mL) was then added to the cold mixture in about 20 minutes. The resulting brown foaming mixture was then allowed to reach room temperature and further stirred for 1 hour. Diethyl ether (50 mL) was then added, the organic layer was separated, and the aqueous layer washed with diethyl ether ( $2 \times 50$  mL). The organic layer was collected, dried over  $\text{Na}_2\text{SO}_4$  filtered and finally dried under reduced pressure, affording the desired product as yellow-orange oil (3.44 g, 82%).

$\nu_{\text{max}}$  (nujol)/ $\text{cm}^{-1}$ : 2128 ( $\text{N}_3$  stretching)

$^1\text{H}$  NMR (300 MHz,  $\text{C}_6\text{D}_6$ , 300 K):  $\delta = 7.70$  (d, 2H,  $J = 8.4$  Hz), 6.40 (d, 2H,  $J = 8.4$  Hz).

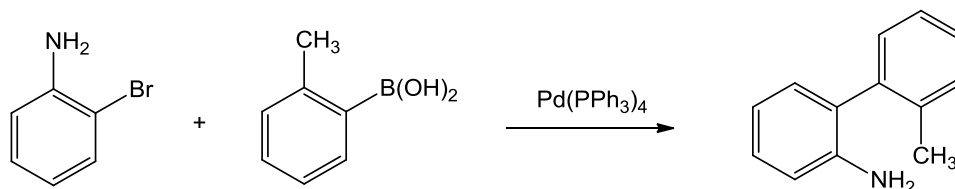
## 3.7. Synthesis of 2-Amino Biaryls

### 3.7.1. General Procedure for the Preparation of 2-Aminobiaryls



In a dry 100 mL round bottom flask, phenylboronic acid (1.00 g, 8.20 mmol, 1.3 equiv), K<sub>2</sub>CO<sub>3</sub> (3.48 g, 25.2 mmol, 4.0 equiv), and Pd(PPh<sub>3</sub>)<sub>4</sub> (0.730 g, 0.631 mmol, 0.1 equiv) were then dissolved in 30 mL of toluene, 20 mL of H<sub>2</sub>O, and 10 mL of EtOH. 2-Bromoaniline (1.08 g, 0.715 mL, 6.31 mmol, 1.0 equiv) was added, and the resulting mixture was heated to 95 °C for 16 hours. After cooling, the biphasic solution was diluted with 100 mL of saturated aqueous NH<sub>4</sub>Cl and 100 mL of CH<sub>2</sub>Cl<sub>2</sub> and separated. The aqueous phase was extracted with an additional 2 × 100 mL of CH<sub>2</sub>Cl<sub>2</sub>, and the combined organic phases were washed 1 × 100 mL of water and 1 × 100 mL of saturated aqueous NaHCO<sub>3</sub>. The organic phase was dried over Na<sub>2</sub>SO<sub>4</sub> and filtered. The filtrate was concentrated *in vacuo* to afford a brown oil. Purification by flash chromatography (EtOAc:hexanes) afforded the product.

### 3.7.2. 2'-Methylbiphenyl-2-amine (102a)



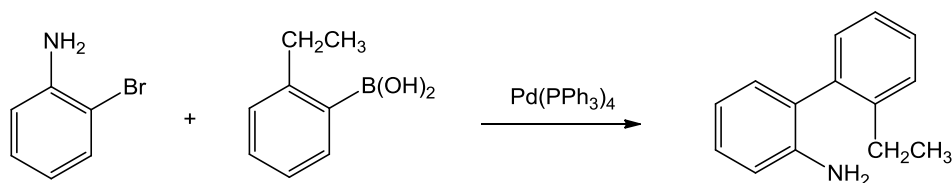
The general procedure was followed with 0.200 g of 2-bromoaniline ( $1.16 \times 10^{-3}$  mol), 0.192 g of 2-methylphenylboronic acid ( $1.41 \times 10^{-3}$  mol), 0.138 g of Pd(PPh<sub>3</sub>)<sub>4</sub> ( $1.19 \times 10^{-4}$  mol), and 0.645 g of K<sub>2</sub>CO<sub>3</sub> ( $4.66 \times 10^{-3}$  mol) in 20 mL of toluene, 7.0 mL of ethanol and 8.0 mL of H<sub>2</sub>O. Purification by flash chromatography (EtOAc:hexanes) afforded 2'-methylbiphenyl-2-amine as tan oil (0.204 g, 96 %).

<sup>1</sup>H NMR (300 MHz, CDCl<sub>3</sub>, 298 K)  $\delta$ : 7.29-7.23 (m, 3H), 7.21-7.19 (m, 1H), 7.16 (td,  $J^1 = 8.0$  Hz,  $J^2 = 1.5$  Hz, 1H), 7.00 (dd,  $J^1 = 7.5$  Hz,  $J^2 = 1.5$  Hz, 1H), 6.81-6.78 (m, 1H), 6.75 (d,  $J = 8.0$  Hz, 1H), 3.46 (s, 2H), 2.16 (s, 3H);

<sup>13</sup>C NMR (75 MHz, CDCl<sub>3</sub>, 298 K)  $\delta$ : 143.6 (C), 138.6 (C), 137.0 (C), 130.2 (CH), 130.0 (CH), 128.3 (CH), 127.7 (CH), 127.4 (C), 126.1 (CH), 118.2 (CH), 115.0 (CH), 19.6 (CH<sub>3</sub>).

*m/z* (ESI) 183 [M<sup>+</sup>];

### 3.7.3. 2'-Ethylbiphenyl-2-amine (102b)



The general procedure was followed with 0.200 g of 2-bromoaniline ( $1.16 \times 10^{-3}$  mol), 0.209 g of 2-ethylphenylboronic acid ( $1.40 \times 10^{-3}$  mol), 0.135 g of  $\text{Pd}(\text{PPh}_3)_4$  ( $1.17 \times 10^{-4}$  mol), and 0.643 g of  $\text{K}_2\text{CO}_3$  ( $4.66 \times 10^{-3}$  mol) in 20 mL of toluene, 7.0 mL of ethanol and 8.0 mL of  $\text{H}_2\text{O}$ . Purification by flash chromatography (EtOAc:hexanes) afforded 2'-ethylbiphenyl-2-amine as tan oil (0.224 g, 98 %).

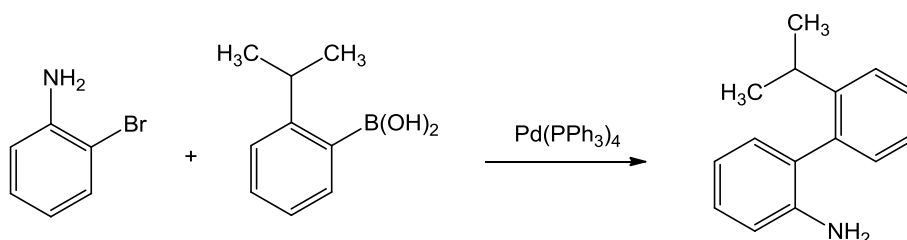
Elemental Analysis calc. for  $\text{C}_{14}\text{H}_{15}\text{N}$ : C, 85.24; H, 7.66; N, 7.10; found: C, 85.40; H, 7.71; N, 6.93.

$^1\text{H}$  NMR (300 MHz,  $\text{CDCl}_3$ , 300 K)  $\delta$ : 7.34 (2H, dd,  $J_3 = 6.1$  Hz,  $J_4 = 1.6$  Hz,  $\text{H}_{\text{Ar}}$ ), 7.26-7.19 (3H, m,  $\text{H}_{\text{Ar}}$ ), 7.08 (1H, dd,  $J_3 = 7.6$  Hz,  $J_4 = 1.6$  Hz,  $\text{H}_{\text{Ar}}$ ), 6.91 (2H, pst,  $J = 7.0$  Hz,  $\text{H}_{\text{Ar}}$ ), 4.50 (2H, br,  $\text{NH}_2$ ), 2.53 (1H, dq,  $J_2 = 14.5$ ,  $J_3 = 7.4$ ,  $\text{CHH}$ ), 2.48 (1H, dq,  $J_2 = 14.5$ ,  $J_3 = 7.4$ ,  $\text{CHH}$ ), 1.10 (3H, t,  $J = 7.4$  Hz,  $\text{CH}_3$ );

$^{13}\text{C}$  NMR (75 MHz,  $\text{CDCl}_3$ , 298 K)  $\delta$ : 143.5 (C), 137.9 (C), 130.8 (CH), 130.6 (CH), 129.1 (CH), 128.7 (CH), 128.5 (CH), 126.5 (CH), 119.8 (CH), 116.6 (CH), 26.5 ( $\text{CH}_2$ ), 15.6 ( $\text{CH}_3$ ). Two quaternary carbon atoms were not detected.

$m/z$  (ESI) 197 [ $\text{M}^+$ ];

### 3.7.4. 2'-Isopropylbiphenyl-2-amine (102c)



The general procedure was followed with 0.200 g of 2-bromoaniline ( $1.16 \times 10^{-3}$  mol), 0.238 g of 2-isopropylphenylboronic acid ( $1.45 \times 10^{-3}$  mol), 0.137 g of  $\text{Pd}(\text{PPh}_3)_4$  ( $1.19 \times 10^{-4}$  mol), and 0.651 g of  $\text{K}_2\text{CO}_3$  ( $4.70 \times 10^{-3}$  mol) in 20 mL of toluene, 7.0 mL of ethanol and 8.0 mL of  $\text{H}_2\text{O}$ . Purification by flash chromatography (EtOAc:hexanes) afforded 2'-isopropylphenyl-2-amine as tan oil (0.235 g, 96 %).

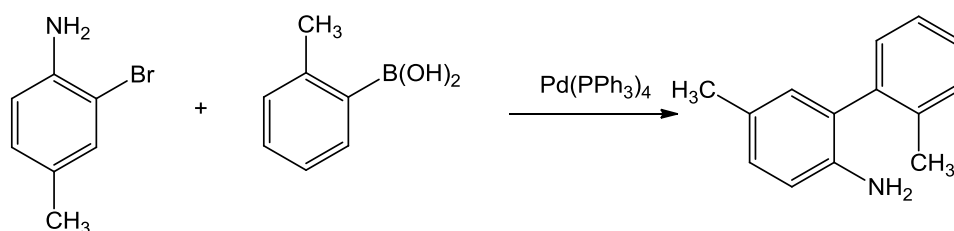
Elemental Analysis calc. for  $\text{C}_{15}\text{H}_{17}\text{N}$ : C, 85.26; H, 8.11; N, 6.63; found: C, 85.43; H, 8.22; N, 6.54.

$^1\text{H}$  NMR (300 MHz,  $\text{CDCl}_3$ , 300 K)  $\delta$ : 7.45-7.35 (2H, m,  $\text{H}_{\text{Ar}}$ ), 7.25-7.18 (3H, m,  $\text{H}_{\text{Ar}}$ ), 7.05 (1H, d, 2,  $J = 7.4$  Hz,  $\text{H}_{\text{Ar}}$ ), 6.89-6.81 (2H, m,  $\text{H}_{\text{Ar}}$ ), 3.50 (2H, br,  $\text{NH}_2$ ), 2.87 (1H, qq, Hz,  $J^3 = 6.9$  Hz,  $J^3 = 6.9$  Hz, CH) 1.21 (3H, d,  $J = 6.9$  Hz,  $\text{CH}_3$ ), 1.12 (3H, d,  $J = 6.9$  Hz,  $\text{CH}_3$ );

$^{13}\text{C}$  NMR (75 MHz,  $\text{CDCl}_3$ , 298 K)  $\delta$ : 162.7 (C), 148.2 (C), 137.5 (C), 130.8 (CH), 130.7 (CH), 128.7 (CH), 128.6 (CH), 126.4 (CH), 126.2 (CH), 119.0 (CH), 115.8 (CH), 30.2 (CH), 25.0 ( $\text{CH}_3$ ), 23.9 ( $\text{CH}_3$ ). One quaternary carbon atom was not detected;

$m/z$  (ESI) 211 [ $\text{M}^+$ ];

### 3.7.5. 2',5-Dimethylbiphenyl-2-amine (102d)



The general procedure was followed with 0.200 g of 2-bromo-4-methylaniline ( $1.07 \times 10^{-3}$  mol), 0.183 g of 2-methylphenylboronic acid ( $1.34 \times 10^{-3}$  mol), 0.130 g of  $\text{Pd}(\text{PPh}_3)_4$  ( $1.12 \times 10^{-4}$  mol), and 0.603 g of  $\text{K}_2\text{CO}_3$  ( $4.36 \times 10^{-3}$  mol) in 20 mL of toluene, 7.0 mL of ethanol and 8.0 mL of  $\text{H}_2\text{O}$ . Purification by flash chromatography (EtOAc:hexanes) afforded 2',5-dimethylbiphenyl-2-amine as tan oil (0.199 g, 94 %).

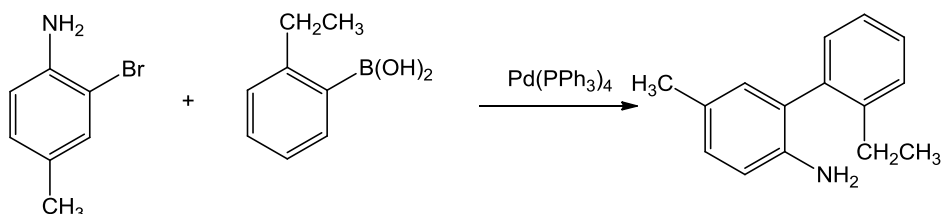
Elemental Analysis calc. for  $\text{C}_{14}\text{H}_{15}\text{N}$ : C, 85.24; H, 7.66; N, 7.10; found: C, 85.31; H, 7.70; N, 7.03.

$^1\text{H}$  NMR (300 MHz,  $\text{CDCl}_3$ , 300 K)  $\delta$ : 7.45-7.34 (4H, m,  $\text{H}_{\text{Ar}}$ ), 7.13 (1H, dd,  $J^3 = 8.0$  Hz,  $J^4 = 1.5$  Hz,  $\text{H}_{\text{Ar}}$ ), 7.0 (1H, d,  $J^4 = 1.5$  Hz,  $\text{H}_{\text{Ar}}$ ), 6.80 (1H, d,  $J = 8.0$  Hz,  $\text{H}_{\text{Ar}}$ ), 3.46 (2H, s,  $\text{NH}_2$ ) 2.44 (3H, s,  $\text{CH}_3$ ), 2.35 (3H, s,  $\text{CH}_3$ ).

$^{13}\text{C}$  NMR (75 MHz,  $\text{CDCl}_3$ , 298 K)  $\delta$ : 162.7 (C), 148.2 (C), 137.5 (C), 130.8 (CH), 130.7 (CH), 128.7 (CH), 128.6 (CH), 126.4 (CH), 126.2 (CH), 119.0 (CH), 115.8 (CH), 30.2 (CH), 25.0 ( $\text{CH}_3$ ), 23.9 ( $\text{CH}_3$ ). One quaternary carbon atom was not detected;

$m/z$  (ESI) 197 [ $\text{M}^+$ ];

### 3.7.6. 2'-Ethyl-5-methylbiphenyl-2-amine (102e)



The general procedure was followed with 0.200 g of 2-bromo-4-methylaniline ( $1.07 \times 10^{-3}$  mol), 0.194 g of 2-ethylphenylboronic acid ( $1.29 \times 10^{-3}$  mol), 0.125 g of  $\text{Pd}(\text{PPh}_3)_4$  ( $1.08 \times 10^{-4}$  mol), and 0.596 g of  $\text{K}_2\text{CO}_3$  ( $4.31 \times 10^{-3}$  mol) in 20 mL of toluene, 7.0 mL of ethanol and 8.0 mL of  $\text{H}_2\text{O}$ . Purification by flash chromatography (EtOAc:hexanes) afforded 2'-ethyl-5-methylbiphenyl-2-amine as tan oil (0.222 g, 97%).

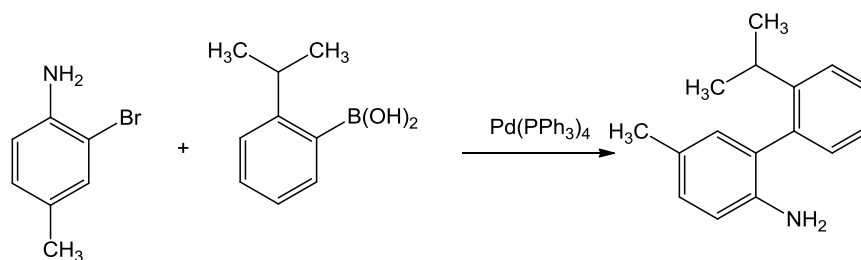
Elemental Analysis calc. for  $\text{C}_{15}\text{H}_{17}\text{N}$ : C, 85.26; H, 8.11; N, 6.63; found: C, 85.32; H, 8.20; N, 6.56;

$^1\text{H}$  NMR (300 MHz,  $\text{CDCl}_3$ , 300 K)  $\delta$ : 7.36-7.34 (2H, m,  $\text{H}_{\text{Ar}}$ ), 7.31-7.24 (1H, m,  $\text{H}_{\text{Ar}}$ ), 7.20 (1H, d,  $J = 7.0$  Hz,  $\text{H}_{\text{Ar}}$ ), 7.01 (1H, dd,  $J^3 = 8.0$  Hz,  $J^4 = 1.8$  Hz,  $\text{H}_{\text{Ar}}$ ), 6.87 (1H, d,  $J^4 = 1.6$  Hz,  $\text{H}_{\text{Ar}}$ ), 6.71 (1H, d,  $J^3 = 8.0$  Hz,  $\text{H}_{\text{Ar}}$ ), 3.30 (2H, br,  $\text{NH}_2$ ), 2.57 (1H, dq,  $J^2 = 14.9$  Hz,  $J^3 = 7.6$  Hz,  $\text{CHH}$ ), 2.52 (1H, dq,  $J^2 = 14.9$  Hz,  $J^3 = 7.6$  Hz,  $\text{CHH}$ ), 2.29 (3H, s,  $\text{CH}_3$ ), 1.11 (3H, t,  $J = 7.6$  Hz,  $\text{CH}_3$ ).

$^{13}\text{C}$  NMR (75 MHz,  $\text{CDCl}_3$ , 298 K)  $\delta$ : 143.4 (C), 141.6 (C), 138.6 (C), 131.2 (CH), 130.6 (CH), 129.2 (CH), 129.0 (CH), 128.2 (CH), 127.8 (C), 127.6 (C), 126.4 (CH), 115.6 (CH), 26.5 ( $\text{CH}_2$ ), 20.8 ( $\text{CH}_3$ ), 15.6 ( $\text{CH}_3$ ).

$m/z$  (ESI) 211 [ $\text{M}^+$ ];

### 3.7.7. 2'-Isopropyl-5-methylbiphenyl-2-amine (102f)



The general procedure was followed with 0.200 g of 2-bromo-4-methylaniline ( $1.07 \times 10^{-3}$  mol), 0.213 g of 2-isopropylphenylboronic acid ( $1.30 \times 10^{-3}$  mol), 0.125 g of  $\text{Pd}(\text{PPh}_3)_4$  ( $1.08 \times 10^{-4}$  mol), and 0.598 g of  $\text{K}_2\text{CO}_3$  ( $4.32 \times 10^{-3}$  mol) in 20 mL of toluene, 7.0 mL of ethanol and 8.0 mL of  $\text{H}_2\text{O}$ . Purification by flash chromatography (EtOAc:hexanes) afforded 2'-isopropyl-5-methylbiphenyl-2-amine as tan oil (0.205 g, 85%).

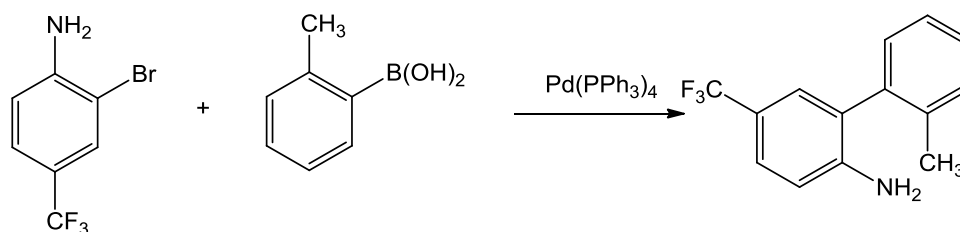
Elemental Analysis calc. for  $\text{C}_{16}\text{H}_{19}\text{N}$ : C, 85.28; H, 8.50; N, 6.22; found: C, 85.37; H, 8.63; N, 6.14;

$^1\text{H}$  NMR (300 MHz,  $\text{CDCl}_3$ , 300 K)  $\delta$ : 7.45-7.35 (2H, m,  $\text{H}_{\text{Ar}}$ ), 7.28-7.17 (2H, m,  $\text{H}_{\text{Ar}}$ ), 7.02 (1H, dd,  $J^3 = 8.0$  Hz,  $J^4 = 1.5$  Hz,  $\text{H}_{\text{Ar}}$ ), 6.87 (1H, bs,  $\text{H}_{\text{Ar}}$ ), 6.73 (1H, d,  $J = 8.0$  Hz,  $\text{H}_{\text{Ar}}$ ), 3.35 (2H, br,  $\text{NH}_2$ ), 2.90 (1H, qq,  $J^3 = 6.9$  Hz,  $J^3' = 6.9$  Hz, CH), 2.31 (3H, s,  $\text{CH}_3$ ), 1.22 (3H, d,  $J = 6.9$  Hz,  $\text{CH}_3$ ), 1.13 (3H, d,  $J = 6.9$  Hz,  $\text{CH}_3$ ).

$^{13}\text{C}$  NMR (75 MHz,  $\text{CDCl}_3$ , 298 K)  $\delta$ : 148.2 (C), 141.4 (C), 137.8 (C), 131.2 (CH), 130.6 (CH), 129.2 (CH), 128.5 (CH), 128.1 (C), 127.9 (C), 126.3 (CH), 126.1 (CH), 115.7 (CH), 30.2 (CH), 25.1 ( $\text{CH}_3$ ), 23.9 ( $\text{CH}_3$ ), 20.9 ( $\text{CH}_3$ ).

$m/z$  (ESI) 225 [ $\text{M}^+$ ];

### 3.7.8. 2'-Methyl-5-(trifluoromethyl)biphenyl-2-amine (102g)



The general procedure was followed with 0.200 g of 2-bromo-4-trifluoromethylaniline ( $8.3 \times 10^{-4}$  mol), 0.136 g of 2-methylphenylboronic acid ( $1.02 \times 10^{-3}$  mol), 0.098 g of Pd(PPh<sub>3</sub>)<sub>4</sub> ( $8.50 \times 10^{-5}$  mol), and 0.462 g of K<sub>2</sub>CO<sub>3</sub> ( $3.3 \times 10^{-3}$  mol) in 20 mL of toluene, 7.0 mL of ethanol and 8.0 mL of H<sub>2</sub>O. Purification by flash chromatography (EtOAc:hexanes) afforded 2'-methyl-5-(trifluoromethyl)biphenyl-2-amine as tan oil (0.186 g, 89%).

Elemental Analysis calc. for C<sub>14</sub>H<sub>12</sub>F<sub>3</sub>N: C, 66.93; H, 4.81; N, 5.57; found: C, 67.08; H, 4.95; N, 5.43.

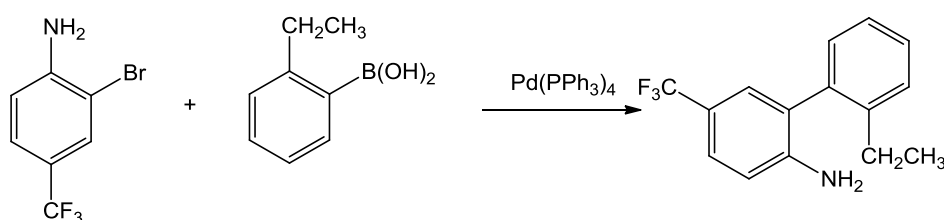
<sup>1</sup>H NMR (300 MHz, CDCl<sub>3</sub>, 300 K)  $\delta$ : 7.44 (1H, dd,  $J^3 = 8.4$  Hz,  $J^4 = 2.1$  Hz, H<sub>Ar</sub>), 7.35-7.28 (4H, m, H<sub>Ar</sub>), 7.22 (1H, d,  $J = 6.2$  Hz, H<sub>Ar</sub>), 6.82 (1H, d,  $J = 8.4$  Hz, H<sub>Ar</sub>), 3.81 (2H, br, NH<sub>2</sub>) 2.19 (3H, s, CH<sub>3</sub>).

<sup>13</sup>C NMR (75 MHz, CDCl<sub>3</sub>, 298 K)  $\delta$ : 146.8 (C), 137.4 (C), 137.3 (C), 130.9 (CH), 130.4 (CH), 128.7 (CH), 127.7 (CH, q,  $J = 3.7$  Hz), 127.0 (C), 126.8 (CH), 126.0 (CH, q,  $J = 3.7$  Hz), 125.2 (CF<sub>3</sub>, q,  $J = 125.2$  Hz), 120.5 (CCF<sub>3</sub> q,  $J = 32.5$  Hz), 114.8 (CH), 19.9 (CH<sub>3</sub>);

<sup>19</sup>F NMR (282 MHz; CDCl<sub>3</sub>, 300K)  $\delta$ : -61.3;

m/z (ESI) 251 [M<sup>+</sup>];

### 3.7.9. 2'-Ethyl-5-(trifluoromethyl)biphenyl-2-amine (102h)



The general procedure was followed with 0.200 g of 2-bromo-4-trifluoromethylaniline ( $8.3 \times 10^{-4}$  mol), 0.151 g of 2-ethylphenylboronic acid ( $1.02 \times 10^{-3}$  mol), 0.098 g of Pd(PPh<sub>3</sub>)<sub>4</sub> ( $8.50 \times 10^{-5}$  mol), and 0.468 g of K<sub>2</sub>CO<sub>3</sub> ( $3.4 \times 10^{-3}$  mol) in 20 mL of toluene, 7.0 mL of ethanol and 8.0 mL of H<sub>2</sub>O. Purification by flash chromatography (EtOAc:hexanes) afforded 2'-ethyl-5-(trifluoromethyl)biphenyl-2-amine as tan oil (0.174 g, 79%).

Elemental Analysis calc. for C<sub>15</sub>H<sub>14</sub>F<sub>3</sub>N: C, 67.91; H, 5.32; N, 5.28; found: C, 68.09; H, 5.45; N, 5.18.

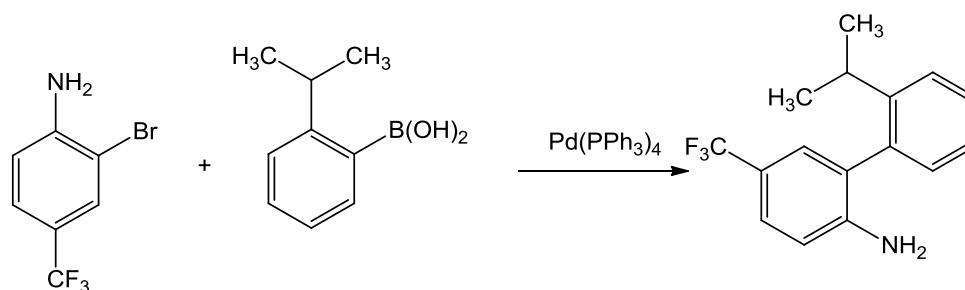
$^1\text{H}$  NMR (300 MHz,  $\text{CDCl}_3$ , 300 K)  $\delta$ : 7.46 (1H, dd,  $J^3 = 8.4$  Hz,  $J^4 = 1.4$  Hz,  $\text{H}_{\text{Ar}}$ ), 7.42-7.40 (2H, m,  $\text{H}_{\text{Ar}}$ ), 7.34-7.28 (2H, m,  $\text{H}_{\text{Ar}}$ ), 7.21 (1H, d,  $J = 7.4$  Hz,  $\text{H}_{\text{Ar}}$ ), 6.81 (1H, d,  $J = 8.4$  Hz,  $\text{H}_{\text{Ar}}$ ), 3.82 (2H, br,  $\text{NH}_2$ ) 2.54 (1H, dq,  $J^2 = 14.9$  Hz,  $J^3 = 7.6$  Hz,  $\text{CHH}$ ), 2.51 (1H, dq,  $J^2 = 14.9$  Hz,  $J^3 = 7.6$  Hz,  $\text{CHH}$ ), 1.13 (3H, t,  $J = 7.6$  Hz,  $\text{CH}_3$ ).

$^{13}\text{C}$  NMR (75 MHz,  $\text{CDCl}_3$ , 298 K)  $\delta$ : 147.3 (C), 143.5 (C), 136.9 (C), 130.5 (CH), 129.4 (CH), 129.0 (CH), 127.9 (CH, q,  $J = 3.7$  Hz), 126.9 (C), 126.80 (CH), 126.00 (CH, q,  $J = 3.7$  Hz), 125.3 ( $\text{CF}_3$ , q,  $J = 268.8$  Hz), 120.1 ( $\text{CCF}_3$ , q,  $J = 32.2$  Hz), 114.6 (CH), 26.5 ( $\text{CH}_2$ ), 15.6 ( $\text{CH}_3$ ).

$^{19}\text{F}$  NMR (282 MHz;  $\text{CDCl}_3$ , 300K)  $\delta$ : -61.3.

$m/z$  (ESI) 265 [ $\text{M}^+$ ];

### 3.7.10. 2'-Isopropyl-5-(trifluoromethyl)biphenyl-2-amine (102i)



The general procedure was followed with 0.200 g of 2-bromo-4-trifluoromethylaniline ( $8.3 \times 10^{-4}$  mol), 0.166 g of 2-isopropylphenylboronic acid ( $1.02 \times 10^{-3}$  mol), 0.098 g of  $\text{Pd}(\text{PPh}_3)_4$  ( $8.50 \times 10^{-5}$  mol), and 0.462 g of  $\text{K}_2\text{CO}_3$  ( $3.3 \times 10^{-3}$  mol) in 20 mL of toluene, 7.0 mL of ethanol and 8.0 mL of  $\text{H}_2\text{O}$ . Purification by flash chromatography (EtOAc:hexanes) afforded 2'-isopropyl-5-(trifluoromethyl)biphenyl-2-amine as tan oil (0.111 g, 48%).

Elemental Analysis calc. for  $\text{C}_{16}\text{H}_{16}\text{F}_3\text{N}$ : C, 68.80; H, 5.77; N, 5.01; found: C, 68.97; H, 5.91; N, 4.93;

$^1\text{H}$  NMR (300 MHz,  $\text{CDCl}_3$ , 300 K)  $\delta$ : 7.49-7.40 (3H, m,  $\text{H}_{\text{Ar}}$ ), 7.32-7.27 (2H, m,  $\text{H}_{\text{Ar}}$ ), 7.17 (1H, d,  $J = 7.5$  Hz,  $\text{H}_{\text{Ar}}$ ), 6.80 (1H, d,  $J = 8.4$  Hz,  $\text{H}_{\text{Ar}}$ ), 3.81 (2H, br,  $\text{NH}_2$ ) 2.81 (1H, qq,  $J^3 = 6.9$  Hz,  $J^3 = 6.9$  Hz, CH), 1.23 (3H, d,  $J = 6.9$  Hz,  $\text{CH}_3$ ), 1.13 (3H, d,  $J = 6.9$  Hz,  $\text{CH}_3$ );

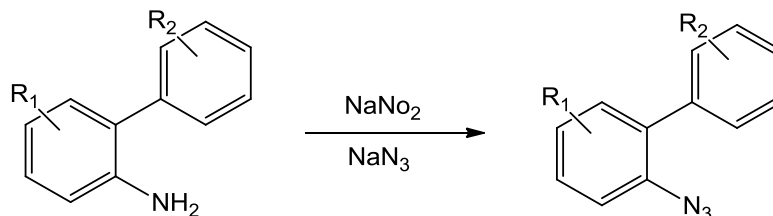
$^{13}\text{C}$  NMR (75 MHz,  $\text{CDCl}_3$ , 298 K)  $\delta$ : 148.2 (C), 147.4 (C), 136.2 (C), 130.5 (CH), 129.1 (CH), 127.9 (CH, q,  $J = 3.7$  Hz), 127.0 (C), 126.7 (CH), 126.4 (CH), 126.0 (CH, q,  $J = 3.7$  Hz), 125.3 ( $\text{CF}_3$ , q, 269.0 Hz), 120.1 ( $\text{CCF}_3$  q,  $J = 32.4$  Hz), 114.5 (CH), 30.4 (CH), 25.0 ( $\text{CH}_3$ ), 23.8 ( $\text{CH}_3$ ).

$^{19}\text{F}$  NMR (282 MHz;  $\text{CDCl}_3$ , 300K)  $\delta$ : -61.3;

$m/z$  (ESI) 279 [ $\text{M}^+$ ];

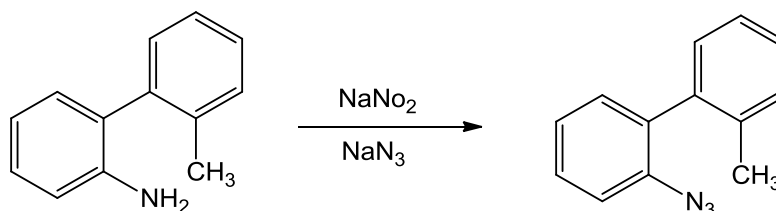
## 3.8. Synthesis of 2-Azido Biaryls

### 3.8.1. General Procedure for the Preparation of 2-Azido Biaryls



In a 50 mL flask, 2-aminobiphenyl (0.250 g, 1.48 mmol, 1.0 equiv) was dissolved in 10 mL of HOAc and 5 mL of H<sub>2</sub>O and placed in an ice bath. NaNO<sub>2</sub> (0.142 g, 2.07 mmol, 1.4 equiv) was added slowly, and the resulting mixture was stirred at 0 °C for one hour. NaN<sub>3</sub> (0.144 g, 2.22 mmol, 1.5 equiv) was then added slowly, and the resulting mixture was warmed to ambient temperature, and stirred for 30 minutes. The solution was diluted with 20 mL of water and 20 mL of CH<sub>2</sub>Cl<sub>2</sub> and basified by the slow addition of K<sub>2</sub>CO<sub>3</sub> until bubbling ceased. The phases were separated and the aqueous phase was extracted with an additional 2 × 20 mL of CH<sub>2</sub>Cl<sub>2</sub>. The combined organic phases were washed 1 × 20 mL of water and 1 × 20 mL of brine. The resulting organic phase and dried over Na<sub>2</sub>SO<sub>4</sub> and filtered. The filtrate was concentrated *in vacuo* to afford an oil. Purification by flash chromatography (EtOAc:hexanes) afforded the product, which was stored in the freezer.

### 3.8.2. 2-Azido-2'-methylbiphenyl (103a)



The general procedure was followed with 0.486 g of 2'-methylbiphenyl-2-amine ( $2.65 \times 10^{-3}$  mol), 0.278 g of NaNO<sub>2</sub> ( $4.04 \times 10^{-3}$  mol), and 0.276 g of NaN<sub>3</sub> ( $4.25 \times 10^{-3}$  mol) in 17 mL of acetic acid and 9 mL of H<sub>2</sub>O. Purification by flash chromatography (EtOAc:hexanes) afforded 2-azido-2'-methylbiphenyl as tan oil (0.462 g, 83%).

$\nu_{\max}$  (CH<sub>2</sub>Cl<sub>2</sub>)/cm<sup>-1</sup>: 2125 (N<sub>3</sub> stretching)

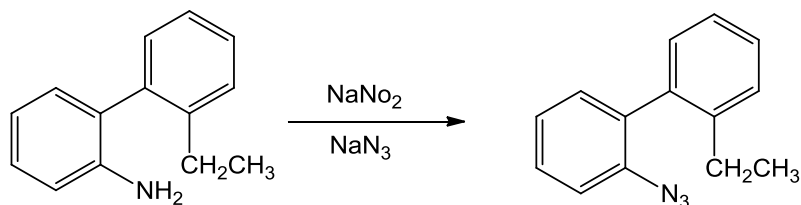
<sup>1</sup>H NMR (300 MHz, CDCl<sub>3</sub>, 300 K)  $\delta$ : 7.43-7.39 (m, 1H), 7.32-7.22 (m, 4H), 7.20-7.19 (m, 2H), 7.14-7.13 (m, 1H), 2.14 (s, 3H);

<sup>13</sup>C NMR (75 MHz, CDCl<sub>3</sub>, 298 K)  $\delta$ : 138.0 (C), 137.9 (C), 136.4 (C), 133.7 (C), 131.3 (CH), 129.8 (2 CH), 128.7 (CH), 128.0 (CH), 125.6 (CH), 124.7 (CH), 118.4 (CH), 20.0 (CH<sub>3</sub>);



m/z (ESI) 209 [ $M^+ - 28$ ].

### 3.8.3. 2-Azido-2'-ethylbiphenyl (103b)



The general procedure was followed with 1.119 g of 2'-ethylbiphenyl-2-amine ( $5.67 \times 10^{-3}$  mol), 0.598 g of NaNO<sub>2</sub> ( $8.68 \times 10^{-3}$  mol), and 0.606 g of NaN<sub>3</sub> ( $9.33 \times 10^{-3}$  mol) in 37 mL of acetic acid and 20 mL of H<sub>2</sub>O. Purification by flash chromatography (EtOAc:hexanes) afforded 2-azido-2'-ethylbiphenyl as tan oil (1.022 g, 80%).

$\nu_{\max}$  (CH<sub>2</sub>Cl<sub>2</sub>)/cm<sup>-1</sup>: 2126 (N<sub>3</sub> stretching)

$\lambda_{\max}$  (1,2-dichlorobenzene)/nm: 296 and 355

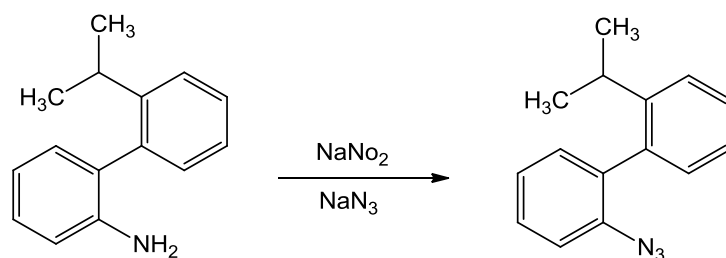
Elemental Analysis calc. for C<sub>14</sub>H<sub>13</sub>N<sub>3</sub>: C, 75.31; H, 5.87; N, 18.82; found: C, 75.47; H, 5.91; N, 18.63;

<sup>1</sup>H NMR (300 MHz, CDCl<sub>3</sub>, 300 K)  $\delta$ : 7.46-7.41 (1H, m, H<sub>Ar</sub>), 7.38-7.33 (2H, m, H<sub>Ar</sub>), 7.29-7.20 (4H, m, H<sub>Ar</sub>), 7.13 (1H, d,  $J = 7.4$  Hz, H<sub>Ar</sub>), 2.50 (1H, dq,  $J^2 = 15.5$  Hz,  $J^3 = 7.9$  Hz, CHH), 2.45 (1H, dq,  $J^2 = 15.5$  Hz,  $J^3 = 7.9$  Hz, CHH), 1.09 (3H, t,  $J = 7.9$  Hz, CH<sub>3</sub>);

<sup>13</sup>C NMR (75 MHz, CDCl<sub>3</sub>, 298 K)  $\delta$ : 142.7 (C), 138.4 (C), 137.8 (C), 134.0 (C), 131.8 (CH), 130.4 (CH), 129.0 (CH), 128.6 (CH), 128.5 (CH), 125.8 (CH), 124.9 (CH), 118.7 (CH), 26.6 (CH<sub>2</sub>), 15.4 (CH<sub>3</sub>);

m/z (ESI) 195 [ $M^+ - 28$ ].

### 3.8.4. 2-Azido-2'-isopropylbiphenyl (103c)



The general procedure was followed with 0.339 g of 2'-isopropylbiphenyl-2-amine ( $1.60 \times 10^{-3}$  mol), 0.167 g of NaNO<sub>2</sub> ( $2.42 \times 10^{-3}$  mol), and 0.169 g of NaN<sub>3</sub> ( $2.60 \times 10^{-3}$  mol) in 11 mL of acetic acid and 4 mL of H<sub>2</sub>O. Purification by flash chromatography (EtOAc:hexanes) afforded 2-azido-2'-isopropylbiphenyl as tan oil (0.199 g, 53%).

$\nu_{\max}$  (CH<sub>2</sub>Cl<sub>2</sub>)/cm<sup>-1</sup>: 2127 (N<sub>3</sub> stretching)

$\lambda_{\max}$  (1,2-dichlorobenzene)/nm: 296 and 358;

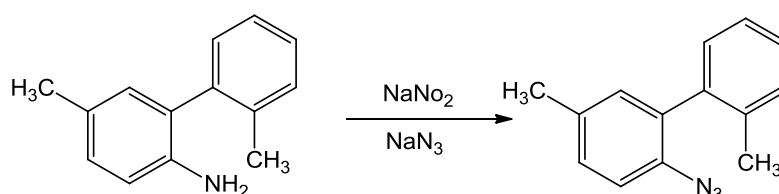
Elemental Analysis calc. for C<sub>15</sub>H<sub>15</sub>N<sub>3</sub>: C, 75.92; H, 6.37; N, 17.71; found: C, 76.11; H, 6.61; N, 17.43;

<sup>1</sup>H NMR (300 MHz, CDCl<sub>3</sub>, 300 K)  $\delta$ : 7.46-7.40 (3H, m, H<sub>Ar</sub>), 7.28-7.21 (4H, m, H<sub>Ar</sub>), 7.10 (1H, d,  $J$  = 6.9 Hz, H<sub>Ar</sub>), 2.75 (1H, qq,  $J^3$  = 6.9 Hz,  $J^{3'}$  = 6.9 Hz, CH), 1.24 (3H, d,  $J$  = 6.9 Hz, CH<sub>3</sub>) 1.10 (3H, d,  $J$  = 6.9 Hz, CH<sub>3</sub>);

<sup>13</sup>C NMR (75 MHz, CDCl<sub>3</sub>, 298 K)  $\delta$ : 147.5 (C), 138.5 (C), 137.2 (C), 134.1 (C), 131.9 (CH), 130.3 (CH), 129.0 (CH), 128.8 (CH), 125.7 (CH, two signals overlapping), 124.9 (CH), 118.7 (CH), 30.5 (CH), 24.9 (CH<sub>3</sub>), 23.7 (CH<sub>3</sub>);

$m/z$  (ESI) 209 [M<sup>+</sup>-28].

### 3.8.5. 2-Azido-2',5-dimethylbipheny (103d)



The general procedure was followed with 0.326 g of 2',5-Dimethylbiphenyl-2-amine ( $1.66 \times 10^{-3}$  mol), 0.178 g of NaNO<sub>2</sub> ( $2.58 \times 10^{-3}$  mol), and 0.174 g of NaN<sub>3</sub> ( $2.68 \times 10^{-3}$  mol) in 11 mL of acetic acid and 6 mL of H<sub>2</sub>O. Purification by flash chromatography (EtOAc:hexanes) afforded 2-azido-2',5-dimethylbipheny as tan oil (0.299 g, 81%).

$\nu_{\max}$  (CH<sub>2</sub>Cl<sub>2</sub>)/cm<sup>-1</sup>: 2123 (N<sub>3</sub> stretching)

$\lambda_{\max}$  (1,2-dichlorobenzene)/nm: 297;

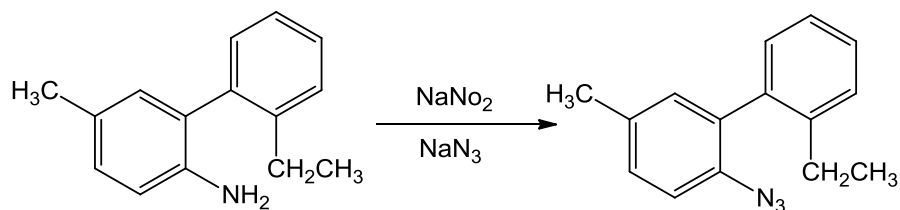
Elemental Analysis calc. for C<sub>14</sub>H<sub>13</sub>N<sub>3</sub>: C, C, 75.31; H, 5.87; N, 18.82; found: : C, 75.48; H, 5.96; N, 18.58;

<sup>1</sup>H NMR (300 MHz, CDCl<sub>3</sub>, 300 K)  $\delta$ : 7.31-7.21 (3H, m, H<sub>Ar</sub>), 7.15-7.12 (2H, m, H<sub>Ar</sub>), 7.02 (1H, bs, H<sub>Ar</sub>), 2.38 (3H, s, CH<sub>3</sub>), 2.17 (3H, s, CH<sub>3</sub>);

<sup>13</sup>C NMR (75 MHz, CDCl<sub>3</sub>, 298 K)  $\delta$ : 138.6 (C), 136.8 (C), 135.5 (C), 134.8 (C), 133.9 (C), 132.2 (CH), 130.1 (CH, two signals overlapping), 129.7 (CH), 128.3 (CH), 125.9 (CH), 118.6 (CH), 21.2 (CH<sub>3</sub>), 20.3 (CH<sub>3</sub>);

$m/z$  (ESI) 195 [M<sup>+</sup>-28].

### 3.8.6. 2-Azido-2'-ethyl-5-methylbiphenyl (103e)



The general procedure was followed with 0.554 g of 2'-Ethyl-5-methylbiphenyl-2-amine ( $1.62 \times 10^{-3}$  mol), 0.282 g of NaNO<sub>2</sub> ( $4.08 \times 10^{-3}$  mol), and 0.283 g of NaN<sub>3</sub> ( $4.31 \times 10^{-3}$  mol) in 18 mL of acetic acid and 9 mL of H<sub>2</sub>O. Purification by flash chromatography (EtOAc:hexanes) afforded 2-azido-2'-ethyl-5-methylbiphenyl as tan oil (0.504 g, 81%).

$\nu_{\max}$  (CH<sub>2</sub>Cl<sub>2</sub>)/cm<sup>-1</sup>: 2123 (N<sub>3</sub> stretching)

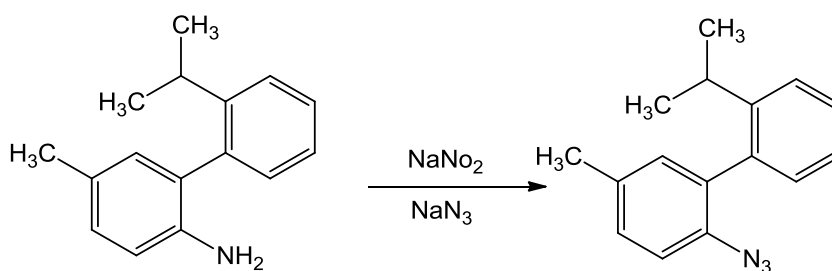
$\lambda_{\max}$  (1,2-dichlorobenzene)/nm: 297;

Elemental Analysis calc. for C<sub>15</sub>H<sub>15</sub>N<sub>3</sub>: C, 75.92; H, 6.37; N, 17.71; found: C, 76.12; H, 6.50; N, 17.51;

<sup>1</sup>H NMR (300 MHz, CDCl<sub>3</sub>, 300 K)  $\delta$ : 7.40-7.33 (2H, m, H<sub>Ar</sub>), 7.29-7.22 (2H, m, H<sub>Ar</sub>), 7.16-7.12 (2H, m, H<sub>Ar</sub>), 7.05 (1H, bs, H<sub>Ar</sub>), 2.52 (1H, dq,  $J^2 = 15.4$  Hz,  $J^3 = 7.6$  Hz CHH), 2.47 (1H, dq,  $J^2 = 15.4$  Hz,  $J^3 = 7.6$  Hz CHH), 2.39 (3H, s, CH<sub>3</sub>), 1.12 (3H, t,  $J = 7.6$  Hz, CH<sub>3</sub>);

<sup>13</sup>C NMR (75 MHz, CDCl<sub>3</sub>, 298 K)  $\delta$ : 142.7 (C), 138.0 (C), 135.6 (C), 134.6 (C), 133.8 (C), 132.4 (CH), 130.3 (CH), 129.6 (CH), 128.5 (CH), 128.4 (CH), 125.8 (CH), 118.6 (CH), 26.6 (CH<sub>2</sub>), 21.2 (CH<sub>3</sub>), 15.4 (CH<sub>3</sub>);  
m/z (ESI) 209 [M<sup>+</sup>-28].

### 3.8.7. 2-Azido-2'-isopropyl-5-methylbiphenyl (103f)



The general procedure was followed with 0.300 g of 2'-isopropyl-5-methylbiphenyl-2-amine ( $1.33 \times 10^{-3}$  mol), 0.138 g of NaNO<sub>2</sub> ( $2.01 \times 10^{-3}$  mol), and 0.139 g of NaN<sub>3</sub> ( $2.14 \times 10^{-3}$  mol) in 9 mL of acetic acid and 5 mL of H<sub>2</sub>O. Purification by flash chromatography (EtOAc:hexanes) afforded 2-azido-2'-isopropyl-5-methylbiphenyl as tan oil (0.285 g, 85%).

$\nu_{\max}$  (CH<sub>2</sub>Cl<sub>2</sub>)/cm<sup>-1</sup>: 2122 (N<sub>3</sub> stretching)

$\lambda_{\max}$  (1,2-dichlorobenzene)/nm: 298 and 379;

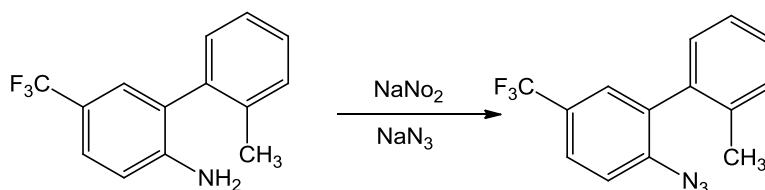
Elemental Analysis calc. for C<sub>16</sub>H<sub>17</sub>N<sub>3</sub>: C, 76.46; H, 6.82; N, 16.72; found: C, 76.61; H, 6.99; N, 16.95;

<sup>1</sup>H NMR (300 MHz, CDCl<sub>3</sub>, 300 K) δ: 7.41-7.40 (2H, m, H<sub>Ar</sub>), 7.27-7.22 (2H, m, H<sub>Ar</sub>), 7.15-7.08 (2H, m, H<sub>Ar</sub>), 7.03 (1H, bs, H<sub>Ar</sub>), 2.77 (1H, qq, *J*<sup>3</sup> = 6.9 Hz, *J*<sup>3'</sup> = 6.9 Hz, CH), 2.39 (3H, s, CH<sub>3</sub>), 1.25 (3H, d, *J* = 6.9 Hz, CH<sub>3</sub>), 1.11 (3H, d, *J* = 6.9 Hz, CH<sub>3</sub>);

<sup>13</sup>C NMR (75 MHz, CDCl<sub>3</sub>, 298 K) δ: 147.4 (C), 137.3 (C), 135.7 (C), 134.6 (C), 134.0 (C), 132.4 (CH), 130.3 (CH), 129.6 (CH), 128.7 (CH), 125.6 (CH, two signals overlapping), 118.6 (CH), 30.4 (CH), 24.9 (CH<sub>3</sub>), 23.7 (CH<sub>3</sub>), 21.2 (CH<sub>3</sub>);

*m/z* (ESI) 223 [M<sup>+</sup>-28].

### 3.8.8. 2-Azido-2'-methyl-5-(trifluoromethyl)biphenyl (103g)



The general procedure was followed with 0.310 g of 2'-methyl-5-trifluoromethylbiphenyl-2-amine (1.24×10<sup>-3</sup> mol), 0.132 g of NaNO<sub>2</sub> (1.91×10<sup>-3</sup> mol), and 0.132 g of NaN<sub>3</sub> (2.08×10<sup>-3</sup> mol) in 8 mL of acetic acid and 5 mL of H<sub>2</sub>O. Purification by flash chromatography (EtOAc:hexanes) afforded 2-azido-2'-methyl-5-(trifluoromethyl)biphenyl as tan oil (0.302 g, 88%).

*v*<sub>max</sub> (CH<sub>2</sub>Cl<sub>2</sub>)/cm<sup>-1</sup>: 2124 (N<sub>3</sub> stretching)

*λ*<sub>max</sub> (1,2-dichlorobenzene)/nm: 296 and 347;

Elemental Analysis calc. for C<sub>14</sub>H<sub>10</sub>F<sub>3</sub>N<sub>3</sub>: C, 60.65; H, 3.64; N, 15.16; found: C, 60.72; H, 3.81; N, 15.33;

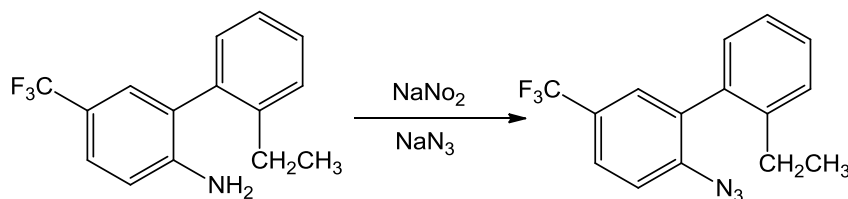
<sup>1</sup>H NMR (300 MHz, CDCl<sub>3</sub>, 300 K) δ: 7.68 (1H, dd, *J*<sup>3</sup> = 8.4 Hz, *J*<sup>4</sup> = 1.7 Hz, H<sub>Ar</sub>), 7.49 (1H, d, *J* = 1.7 Hz, H<sub>Ar</sub>), 7.38-7.26 (4H, m, H<sub>Ar</sub>), 7.14 (1H, d, *J* = 7.4 Hz, H<sub>Ar</sub>), 2.16 (3H, s, CH<sub>3</sub>);

<sup>13</sup>C NMR (75 MHz, CDCl<sub>3</sub>, 298 K) δ: 142.0 (C), 137.0 (C), 136.7 (C), 134.6 (C), 130.4 (CH), 130.1 (CH), 129.0 (CH), 128.8 (CH, *q*, *J* = 3.7 Hz), 127.3 (CCF<sub>3</sub>, *q*, *J* = 32.9 Hz), 126.1 (CH, 2 signals overlapping), 124.3 (CF<sub>3</sub>, *q*, *J* = 270 Hz), 119.1 (CH), 20.2 (CH<sub>3</sub>);

<sup>19</sup>F NMR (282 MHz; CDCl<sub>3</sub>, 298 K) δ: -62.4;

*m/z* (ESI) 199 [M<sup>+</sup>-28].

### 3.8.9. 2-Azido-2'-ethyl-5-(trifluoromethyl)biphenyl (103h)



The general procedure was followed with 0.413 g of 2'-ethyl-5-trifluoromethylbiphenyl-2-amine ( $1.56 \times 10^{-3}$  mol), 0.162 g of  $\text{NaNO}_2$  ( $2.35 \times 10^{-3}$  mol), and 0.163 g of  $\text{NaN}_3$  ( $2.51 \times 10^{-3}$  mol) in 10 mL of acetic acid and 4 mL of  $\text{H}_2\text{O}$ . Purification by flash chromatography (EtOAc:hexanes) afforded 2-azido-2'-ethyl-5-(trifluoromethyl)biphenyl as tan oil (0.285 g, 63%).

$\nu_{\text{max}}$  ( $\text{CH}_2\text{Cl}_2$ )/ $\text{cm}^{-1}$ : 2122 ( $\text{N}_3$  stretching)

$\lambda_{\text{max}}$  (1,2-dichlorobenzene)/nm: 296 and 353;

Elemental Analysis calc. for  $\text{C}_{15}\text{H}_{12}\text{F}_3\text{N}_3$ : C, 61.85; H, 4.15; N, 14.43; found: C, 61.97; H, 4.21; N, 14.33;

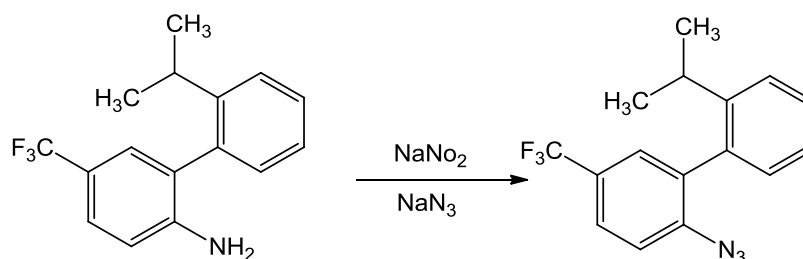
$^1\text{H}$  NMR (300 MHz,  $\text{CDCl}_3$ , 300 K)  $\delta$ : 7.69 (1H, dd,  $J^3 = 8.4$  Hz,  $J^4 = 1.5$  Hz,  $\text{H}_{\text{Ar}}$ ), 7.51 (1H, d,  $J = 1.5$  Hz,  $\text{H}_{\text{Ar}}$ ), 7.45-7.27 (4H, m,  $\text{H}_{\text{Ar}}$ ), 7.13 (1H, d,  $J = 7.5$  Hz,  $\text{H}_{\text{Ar}}$ ), 2.50 (1H, dq,  $J^2 = 15.1$  Hz,  $J^3 = 7.5$  Hz,  $\text{CHH}$ ), 2.43 (1H, dq,  $J^2 = 15.1$  Hz,  $J^3 = 7.5$  Hz,  $\text{CHH}$ ), 1.11 (3H, t,  $J = 7.5$  Hz,  $\text{CH}_3$ );

$^{13}\text{C}$  NMR (75 MHz,  $\text{CDCl}_3$ , 298 K)  $\delta$ : 142.7 (C), 142.1 (C), 136.4 (C), 134.4 (C), 130.2 (CH), 129.2 (CH), 128.9 (CH, q,  $J = 3.7$  Hz), 128.7 (CH), 127.1 ( $\text{CCF}_3$ , q,  $J = 32.9$  Hz), 126.2 (CH), 126.0 (CH), 124.3 ( $\text{CF}_3$ , q,  $J = 270.0$  Hz), 119.0 (CH), 26.6 ( $\text{CH}_2$ ), 15.4 ( $\text{CH}_3$ );

$^{19}\text{F}$  NMR (282 MHz;  $\text{CDCl}_3$ , 298 K)  $\delta$ : -62.4;

$m/z$  (ESI) 263 [ $\text{M}^+ - 28$ ].

### 3.8.10. 2-Azido-2'-isopropyl-5-(trifluoromethyl)bipheny (103i)



The general procedure was followed with 0.438 g of 2'-isopropyl-5-trifluoromethylbiphenyl-2-amine ( $1.57 \times 10^{-3}$  mol), 0.168 g of NaNO<sub>2</sub> ( $2.43 \times 10^{-3}$  mol), and 0.165 g of NaN<sub>3</sub> ( $2.54 \times 10^{-3}$  mol) in 11 mL of acetic acid and 6 mL of H<sub>2</sub>O. Purification by flash chromatography (EtOAc:hexanes) afforded 2-azido-2'-isopropyl-5-(trifluoromethyl)biphenyl as tan oil (0.398 g, 83%).

$\nu_{\max}$  (CH<sub>2</sub>Cl<sub>2</sub>)/cm<sup>-1</sup>: 2120 (N<sub>3</sub> stretching)

$\lambda_{\max}$  (1,2-dichlorobenzene)/nm: 296 and 358;

Elemental Analysis calc. for C<sub>16</sub>H<sub>14</sub>F<sub>3</sub>N<sub>3</sub>: C, 62.95; H, 4.62; N, 13.76; found: C, 63.13; H, 4.85; N, 13.61;

<sup>1</sup>H NMR (300 MHz, CDCl<sub>3</sub>, 300 K)  $\delta$ : 7.71 (1H, dd,  $J^b = 8.4$  Hz,  $J^d = 1.5$  Hz, H<sub>Ar</sub>), 7.53 (1H, d,  $J = 1.5$  Hz, H<sub>Ar</sub>), 7.47-7.46 (2H, m, H<sub>Ar</sub>), 7.37-7.27 (2H, m, H<sub>Ar</sub>), 7.12 (1H, d,  $J = 7.6$  Hz, H<sub>Ar</sub>), 2.71 (1H, qq,  $J^b = 6.9$  Hz,  $J^c = 6.9$  Hz, CH), 1.28 (3H, d,  $J = 6.9$  Hz, CH<sub>3</sub>), 1.14 (3H, d,  $J = 6.9$  Hz, CH<sub>3</sub>);

<sup>13</sup>C NMR (75 MHz, CDCl<sub>3</sub>, 298 K)  $\delta$ : 147.5 (C), 142.3 (C), 135.8 (C), 134.6 (C), 130.2 (CH), 129.4 (CH), 128.9 (CH, q,  $J = 3.6$  Hz), 126.5 (CCF<sub>3</sub>, q,  $J = 32.9$  Hz), 126.1 (CH, q,  $J = 3.6$  Hz), 125.9 (CH, two signals overlaid), 124.3 (CF<sub>3</sub>, q,  $J = 270.0$  Hz), 119.0 (CH), 30.7 (CH), 24.9 (CH<sub>3</sub>), 23.7 (CH<sub>3</sub>);

<sup>19</sup>F NMR (282 MHz; CDCl<sub>3</sub>, 298 K)  $\delta$ : -62.4;

m/z (ESI) 277 [M<sup>+</sup>-28].

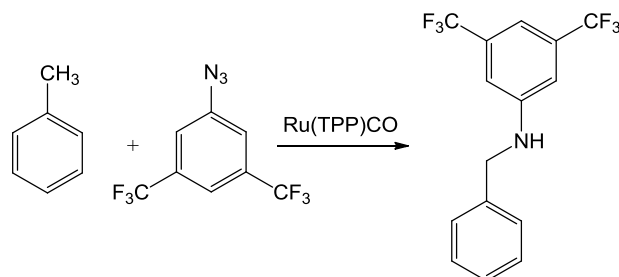
## 3.9. Intermolecular Benzilic Amination

### 3.9.1. General procedure for catalytic reactions

**Method A:** In a typical run, Ru(TPP)CO (36.0 mg,  $4.85 \times 10^{-2}$  mmol) and the azide (0.606 mmol) were dissolved into the hydrocarbon (30 mL). The reaction solution was then heated at 100 °C by using a preheated oil bath. The consumption of the azide was monitored by TLC up to the point that its spot was no longer observable, and then by IR spectroscopy measuring the characteristic azide absorbance in the region 2095–2130  $\text{cm}^{-1}$ . The reaction was considered to be finished when the absorbance of the latter peak was below 0.03 (using a 0.5 mm thick cell). The solution was then concentrated to dryness and the residue was purified by flash chromatography using *n*-hexane/ethyl acetate = 9:1 as eluent mixture or analysed by  $^1\text{H}$  NMR with 2,4-dinitrotoluene as internal standard.

**Method B:** The amination reaction was repeated refluxing Ru(TPP)CO (10.0 mg,  $1.35 \times 10^{-2}$  mmol) and the azide (0.674 mmol) in the hydrocarbon (30 mL). The consumption of the azide was monitored by TLC up to the point that its spot was no longer observable, and then by IR spectroscopy measuring the characteristic azide absorbance in the region 2095–2130  $\text{cm}^{-1}$ . The reaction was considered to be finished when the absorbance of the azide measured was below 0.03 (using a 0.5 mm thick cell). The solution was then concentrated to dryness and the residue was analyzed by  $^1\text{H}$  NMR with 2,4-dinitrotoluene as internal standard.

### 3.9.2. N-benzyl-3,5-bis(trifluoromethyl)benzenamine (95a)



The general procedure A was followed with 16 mg of Ru(TPP)CO ( $2.17 \times 10^{-5}$  mol), 80 mg of 3,5-(CF<sub>3</sub>)<sub>2</sub>-arylazide ( $3.15 \times 10^{-4}$  mol), and 15 mL of toluene. (yield 14%, determined by  $^1\text{H}$  NMR with 2,4-dinitrotoluene as internal standard).

The general procedure B was followed with 4.8 mg of Ru(TPP)CO ( $6.74 \times 10^{-6}$  mol), 81 mg of 3,5-(CF<sub>3</sub>)<sub>2</sub>-arylazide ( $3.15 \times 10^{-4}$  mol), and 15 mL of toluene. (yield 66%, determined by  $^1\text{H}$  NMR with 2,4-dinitrotoluene as internal standard).

Elemental Analysis calc. for C<sub>15</sub>H<sub>11</sub>F<sub>6</sub>N : C, 56.43; H, 3.47; N, 4.39.; found: C, 56.70; H, 3.50; N, 4.27;

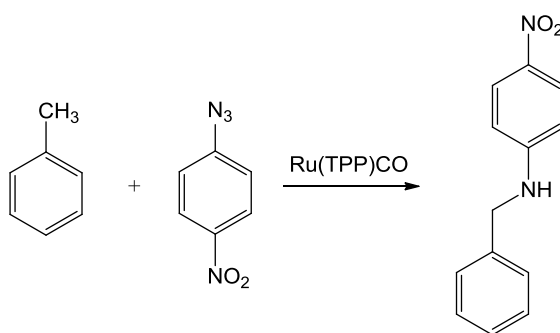
$^1\text{H}$  NMR (300 MHz,  $\text{CDCl}_3$ , 300 K)  $\delta$ : 7.43-7.31 (m, 5H,  $\text{H}_{\text{Ar}}$ ), 7.19 (s, 1H,  $\text{H}_{\text{Ar}}$ ), 6.99 (s, 2H,  $\text{H}_{\text{Ar}}$ ), 4.56 (broad, 1H, NH), 4.39 (s, 1H,  $\text{CH}_2$ );

$^{13}\text{C}$  NMR (75 MHz,  $\text{CDCl}_3$ , 298 K)  $\delta$ : 149.0 (C), 138.0 (C), 132.9 (q,  $J = 33.0$  Hz, C- $\text{CF}_3$ , 2C overlapping), 129.3 (CH), 128.3 (CH), 127.9 (CH), 123.9 (q,  $J = 271.5$  Hz,  $\text{CF}_3$ , 2C overlapping), 112.3 (CH), 110.8 (broad, CH), 48.4 ( $\text{CH}_2$ );

$^{19}\text{F}$  NMR (282 MHz;  $\text{CDCl}_3$ , 298 K)  $\delta$ : -63.53;

$m/z$  (ESI) 319 [ $\text{M}^+$ ].

### 3.9.3. *N*-benzyl-4-nitrobenzenamine (95b)

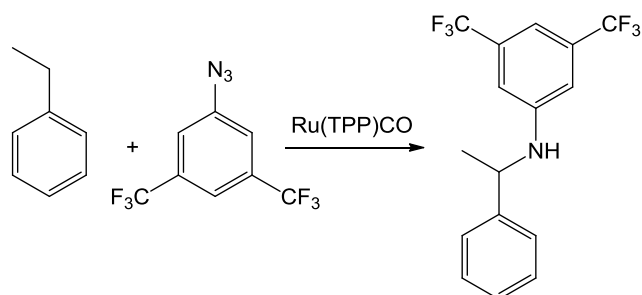


The general procedure A was followed with 18 mg of  $\text{Ru}(\text{TPP})\text{CO}$  ( $2.44 \times 10^{-5}$  mol), 52 mg of 4- $\text{NO}_2$ -arylazide ( $3.14 \times 10^{-4}$  mol), and 15 mL of toluene. (yield 25%, determined by  $^1\text{H}$  NMR with 2,4-dinitrotoluene as internal standard).

The general procedure B was followed with 5.0 mg of  $\text{Ru}(\text{TPP})\text{CO}$  ( $6.74 \times 10^{-6}$  mol), 52 mg of 4- $\text{NO}_2$ -arylazide ( $3.15 \times 10^{-4}$  mol), and 15 mL of toluene. (yield 25%, determined by  $^1\text{H}$  NMR with 2,4-dinitrotoluene as internal standard).

The collected analytical data for *N*-benzyl-4-nitrobenzenamine are in agreement with those reported in the literature.<sup>257</sup>

### 3.9.4. 3,5-bis(trifluoromethyl)-*N*-(1-phenylethyl)benzenamine (96a)



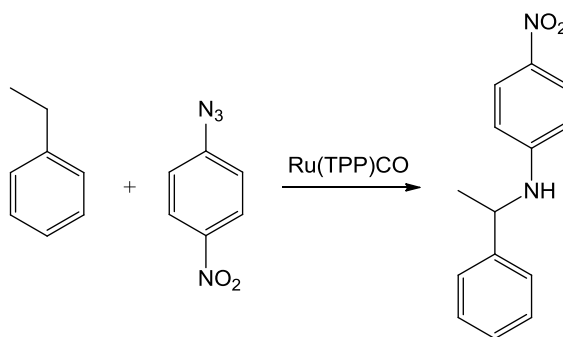


The general procedure A was followed with 19 mg of Ru(TPP)CO ( $2.63 \times 10^{-5}$  mol), 84 mg of 3,5-(CF<sub>3</sub>)<sub>2</sub>-arylazide ( $3.29 \times 10^{-4}$  mol), and 15 mL of ethylbenzene. (yield 31%, determined by <sup>1</sup>H NMR with 2,4-dinitrotoluene as internal standard).

The general procedure B was followed with 4.8 mg of Ru(TPP)CO ( $6.74 \times 10^{-6}$  mol), 81 mg of 3,5-(CF<sub>3</sub>)<sub>2</sub>-arylazide ( $3.15 \times 10^{-4}$  mol), and 15 mL of ethylbenzene. (yield 85%, determined by <sup>1</sup>H NMR with 2,4-dinitrotoluene as internal standard).

The collected analytical data for 3,5-bis(trifluoromethyl)-*N*-(1-phenylethyl)benzenamine are in agreement with those reported in the literature.<sup>257</sup>

### 3.9.5. 4-nitro-*N*-(1-phenylethyl)benzenamine (96b)

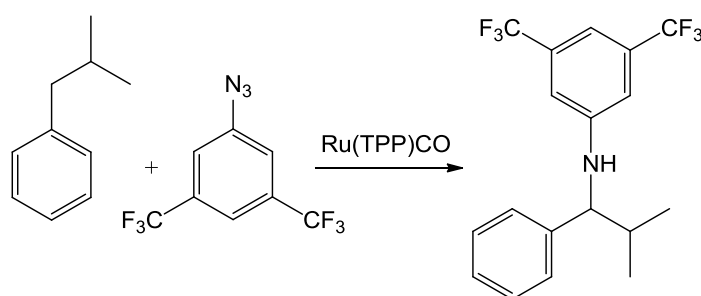


The general procedure A was followed with 17 mg of Ru(TPP)CO ( $2.32 \times 10^{-5}$  mol), 48 mg of 4-NO<sub>2</sub>-arylazide ( $2.94 \times 10^{-4}$  mol), and 15 mL of ethylbenzene. (yield 80%, determined by <sup>1</sup>H NMR with 2,4-dinitrotoluene as internal standard).

The general procedure B was followed with 4.9 mg of Ru(TPP)CO ( $6.61 \times 10^{-6}$  mol), 52 mg 4-NO<sub>2</sub>-arylazide ( $3.17 \times 10^{-4}$  mol), and 15 mL of ethylbenzene. (yield 20%, determined by <sup>1</sup>H NMR with 2,4-dinitrotoluene as internal standard).

The collected analytical data for 4-nitro-*N*-(1-phenylethyl)benzenamine are in agreement with those reported in the literature.<sup>436</sup>

### 3.9.6. 3,5-bis(trifluoromethyl)-*N*-(2-methyl-1-phenylpropyl)benzenamine (97a)

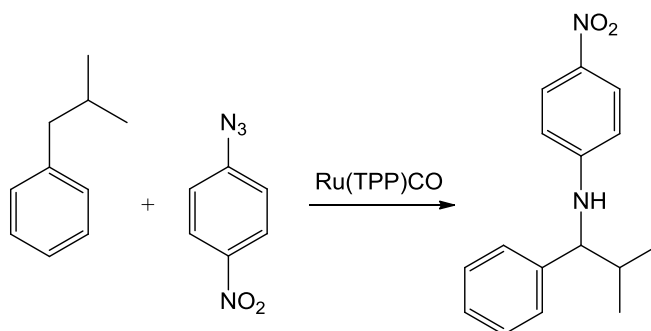


The general procedure A was followed with 15 mg of Ru(TPP)CO ( $2.02 \times 10^{-5}$  mol), 64 mg of 3,5-(CF<sub>3</sub>)<sub>2</sub>-arylazide ( $2.51 \times 10^{-4}$  mol), and 15 mL of isobutylbenzene. (yield 67%, determined by <sup>1</sup>H NMR with 2,4-dinitrotoluene as internal standard).

The general procedure B was followed with 4.9 mg of Ru(TPP)CO ( $6.61 \times 10^{-6}$  mol), 82 mg 3,5-(CF<sub>3</sub>)<sub>2</sub>-arylazide ( $3.21 \times 10^{-4}$  mol), and 15 mL of isobutylbenzene. (yield 75%, determined by <sup>1</sup>H NMR with 2,4-dinitrotoluene as internal standard).

The collected analytical data for 3,5-bis(trifluoromethyl)-*N*-(2-methyl-1-phenylpropyl)benzenamine are in agreement with those reported in the literature.<sup>390</sup>

### 3.9.7. 2,6-bis(nitro)-*N*-(2-methyl-1-phenylpropyl)benzenamine (97b)



The general procedure A was followed with 17 mg of Ru(TPP)CO ( $2.29 \times 10^{-5}$  mol), 52 mg of 4-NO<sub>2</sub>-arylazide ( $3.18 \times 10^{-4}$  mol), and 15 mL of isobutylbenzene. (yield 57%, determined by <sup>1</sup>H NMR with 2,4-dinitrotoluene as internal standard).

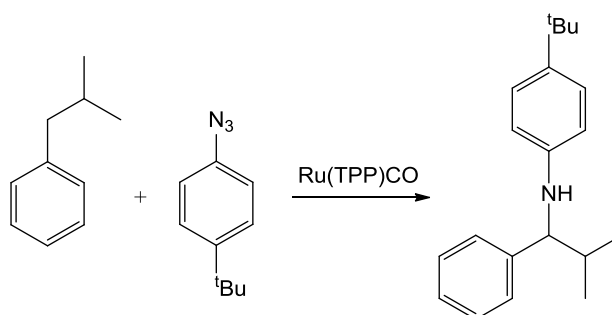
The general procedure B was followed with 5.0 mg of Ru(TPP)CO ( $6.74 \times 10^{-6}$  mol), 57 mg of 4-NO<sub>2</sub>-arylazide ( $3.37 \times 10^{-4}$  mol), and 15 mL of isobutylbenzene. (yield 40%, determined by <sup>1</sup>H NMR with 2,4-dinitrotoluene as internal standard).

Elemental Analysis calc. for  $C_{16}H_{18}N_2O_2$ : C, 71.09; H, 6.71; N, 10.36; found: C, 71.32; H, 6.95; N, 10.54;

$^1H$  NMR (300 MHz,  $CDCl_3$ , 300 K)  $\delta$ : 8.00 (d, 2H,  $J = 9.20$  Hz,  $H_{Ar}$ ), 7.37-7.25 (m, 5H,  $H_{Ar}$ ), 6.48 (d, 2H,  $J = 9.20$  Hz,  $H_{Ar}$ ), 4.89 (broad, 1H, NH), 4.23 (d, 1H,  $J = 6.24$  Hz,  $CHNH$ ), 2.19-2.05 (m, 1H,  $CH(CH_3)_2$ ), 1.04 (d, 3H,  $J = 6.78$  Hz,  $CH_3$ ), 0.95 (d, 3H,  $J = 6.78$  Hz,  $CH_3$ );

$^{13}C$  NMR (75 MHz,  $CDCl_3$ , 298 K)  $\delta$ : 153.1 (C), 141.0 (C), 138.5 (C), 129.0 (CH, 2C overlapping), 128.0 (CH), 127.3 (CH, 2C overlapping), 126.6 (CH), 112.2 (CH), 64.0 (CH), 35.0 (CH), 20.0 ( $CH_3$ ), 19.1 ( $CH_3$ );  
 $m/z$  (ESI) 270 [ $M^+$ ].

### 3.9.8. N-(2-methyl-1-phenylpropyl)-4-tert-butylbenzenamine (97c)



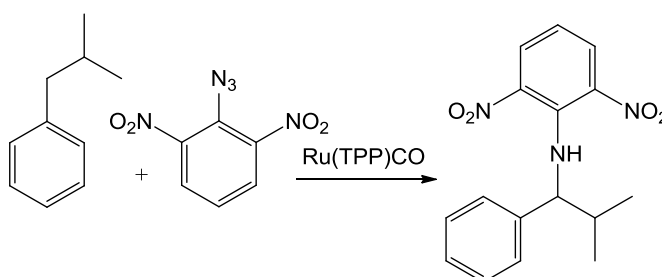
The general procedure A was followed with 14 mg of Ru(TPP)CO ( $1.86 \times 10^{-5}$  mol), 48 mg of 4- $t$ Bu-arylazide ( $2.40 \times 10^{-4}$  mol), and 15 mL of isobutylbenzene. (yield 10%, determined by  $^1H$  NMR with 2,4-dinitrotoluene as internal standard).

Elemental Analysis calc. for  $C_{20}H_{27}N$ : C, 85.35; H, 9.67; N, 4.98.; found: C, 85.21; H, 9.74; N, 5.23;

$^1H$  NMR (300 MHz,  $CDCl_3$ , 300 K)  $\delta$ : 7.33-7.28 (m, 5H,  $H_{Ar}$ ), 7.11 (d, 2H,  $J = 7.12$  Hz,  $H_{Ar}$ ), 6.51 (d, 2H,  $J = 7.12$  Hz,  $H_{Ar}$ ), 4.09 (broad, 1H,  $CHNH$ ), 4.07 (broad, 1H, NH), 2.01 (m, 1H,  $CH(CH_3)_2$ ), 1.24 (s, 9H,  $t$ Bu), 1.00 (d, 3H,  $J = 6.78$  Hz,  $CH_3$ ), 0.92 (d, 3H,  $J = 6.78$  Hz,  $CH_3$ );

$^{13}C$  NMR (75 MHz,  $CDCl_3$ , 298 K)  $\delta$ : 128.1 (CH, 2C overlapping), 127.3 (CH, 2C overlapping), 126.8 (CH), 126.0 (CH, 2C overlapping), 110.0 (CH, 2C overlapping), 31.5 ( $CH_3$ , 3C overlapping,  $t$ Bu), 19.7 ( $CH_3$ ), 18.7 ( $CH_3$ ), quaternary carbons and two CH were not detected;

### 3.9.9. 2,6-bis(nitro)-N-(2-methyl-1-phenylpropyl)benzenamine (97d)



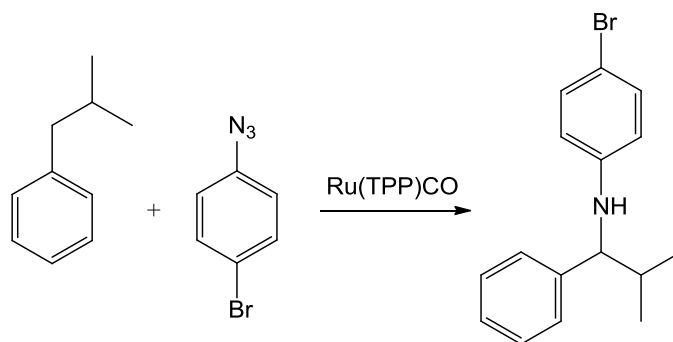
The general procedure A was followed with 13 mg of Ru(TPP)CO ( $1.74 \times 10^{-5}$  mol), 47 mg of 2,6-(NO<sub>2</sub>)<sub>2</sub>-arylazide ( $2.23 \times 10^{-4}$  mol), and 15 mL of isobutylbenzene. (yield 31%, determined by <sup>1</sup>H NMR with 2,4-dinitrotoluene as internal standard).

Elemental Analysis calc. for C<sub>16</sub>H<sub>17</sub>N<sub>3</sub>O<sub>4</sub>: C, 60.94; H, 5.43; N, 13.33; found: C, 61.26; H, 5.69; N, 13.55;

<sup>1</sup>H NMR (300 MHz, CDCl<sub>3</sub>, 300 K)  $\delta$ : 8.56 (d, 2H, *J* = 8.3 Hz, H<sub>Ar</sub>), 7.74-7.71 (m, 2H, H<sub>Ar</sub>), 7.57-7.53 (m, 3H, H<sub>Ar</sub>), 6.80 (t, 1H, *J* = 8.3 Hz, H<sub>Ar</sub>), 4.24 (m, 2H, NH e CHNH), 1.69 (m, 1H, CH(CH<sub>3</sub>)<sub>2</sub>), 0.93 (m, 6H, (CH<sub>3</sub>)<sub>2</sub>);

<sup>13</sup>C NMR (75 MHz, CDCl<sub>3</sub>, 298 K)  $\delta$ : 168.1 (C), 134.5 (CH, 2C overlapping), 131.2 (CH, 3C overlapping), 129.2 (CH, 2C overlapping), 114.3 (CH), 68.5 (CH), 39.1 (CH), 14.4 (CH<sub>3</sub>), 11.3 (CH<sub>3</sub>). Two quaternary carbons were not detected;

### 3.9.10. N-(2-methyl-1-phenylpropyl)-4-bromobenzenamine (97e)



The general procedure A was followed with 14 mg of Ru(TPP)CO ( $1.86 \times 10^{-5}$  mol), 48 mg of 4-Br-arylazide ( $2.40 \times 10^{-4}$  mol), and 15 mL of isobutylbenzene. (yield 48%, determined by <sup>1</sup>H NMR with 2,4-dinitrotoluene as internal standard).

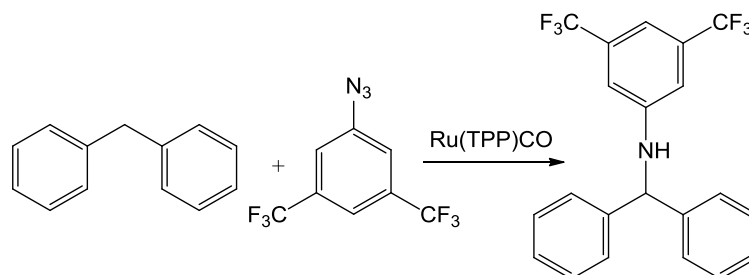
Elemental Analysis calc. for C<sub>16</sub>H<sub>18</sub>BrN: C, 63.17; H, 5.96; N, 4.60; found: C, 63.51; H, 6.06; N, 4.82;

<sup>1</sup>H NMR (300 MHz, CDCl<sub>3</sub>, 300 K)  $\delta$ : 7.33-7.26 (m, 5H, H<sub>Ar</sub>), 7.14 (d, 2H, *J* = 8.8 Hz, H<sub>Ar</sub>), 6.40 (d, 2H, *J* = 8.8 Hz, H<sub>Ar</sub>), 4.10 (broad, 1H, NH), 4.08 (m, 1H, CHNH), 2.06 (m, 1H, CH(CH<sub>3</sub>)<sub>2</sub>), 1.00 (d, 3H, *J* = 6.8 Hz, CH<sub>3</sub>), 0.93 (d, 3H, *J* = 6.8 Hz, CH<sub>3</sub>);

<sup>13</sup>C NMR (75 MHz, CDCl<sub>3</sub>, 298 K)  $\delta$ : 131.7 (CH, 2C overlapping), 128.3 (CH, 3C overlapping), 127.5 (CH, 2C overlapping), 115.0 (CH, 2C overlapping), 55.3 (CH), 34.7 (CH), 19.6 (CH<sub>3</sub>), 18.7 (CH<sub>3</sub>). Three quaternary carbons were not detected;

m/z (ESI) 304 [M<sup>+</sup>].

### 3.9.11. *N*-benzhydryl-3,5-bis(trifluoromethyl)benzenamine (98a)



The general procedure A was followed with 14 mg of Ru(TPP)CO ( $1.87 \times 10^{-5}$  mol), 60 mg of 3,5-(CF<sub>3</sub>)<sub>2</sub>-arylazide ( $2.34 \times 10^{-4}$  mol), and 15 mL of diphenylmethane. (yield 65%, determined by <sup>1</sup>H NMR with 2,4-dinitrotoluene as internal standard).

Elemental Analysis calc. for C<sub>21</sub>H<sub>15</sub>F<sub>6</sub>: C, 63.80; H, 3.82; N, 3.54.; found: C, 64.02; H, 3.90; N, 3.40;

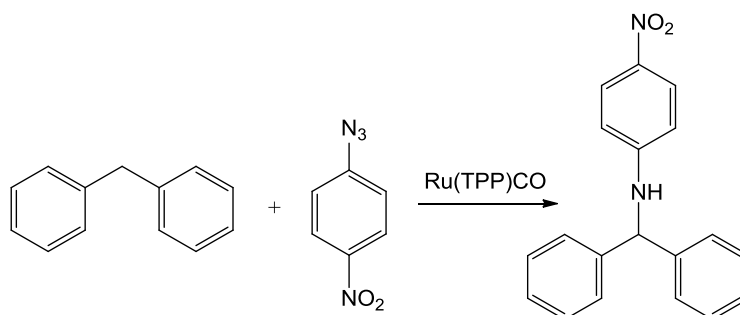
<sup>1</sup>H NMR (300 MHz, CDCl<sub>3</sub>, 300 K) δ: 7.37-7.31 (m, 6H, H<sub>Ar</sub>), 7.26-7.22 (m, 4H, H<sub>Ar</sub>), 7.19 (s, 1H, H<sub>Ar</sub>), 6.93 (s, 2H, H<sub>Ar</sub>), 5.60 (m, 1H, CHNH), 4.72 (broad, 1H, NH);

<sup>13</sup>C NMR (75 MHz, CDCl<sub>3</sub>, 298 K) δ: 147.7 (C), 141.3 (C), 132.1 (q, *J* = 32.7 Hz, C-CF<sub>3</sub>, 2C overlapping), 129.1 (CH), 128.0 (CH), 127.3 (CH), 123.5 (q, *J* = 271.1 Hz, CF<sub>3</sub>, 2C overlapping), 112.7 (CH), 110.5 (CH), 62.8 (CH);

<sup>19</sup>F NMR (282 MHz; CDCl<sub>3</sub>, 298 K) δ: -63.53;

*m/z* (ESI) 395 [M<sup>+</sup>].

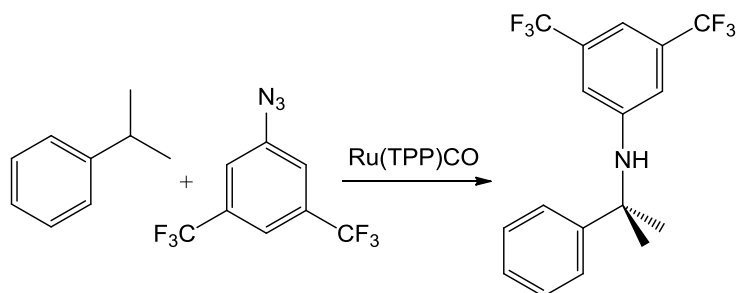
### 3.9.12. *N*-benzhydryl-4-nitrobenzenamine (98b)



The general procedure A was followed with 17 mg of Ru(TPP)CO ( $2.29 \times 10^{-5}$  mol), 52 mg of 4-NO<sub>2</sub>-arylazide ( $3.18 \times 10^{-4}$  mol), and 15 mL of diphenylmethane. (yield 55%, determined by <sup>1</sup>H NMR with 2,4-dinitrotoluene as internal standard).

The collected analytical data for 3,5-bis(trifluoromethyl)-*N*-(1-phenylethyl)benzenamine are in agreement with those reported in the literature.<sup>257</sup>

### 3.9.13. 3,5-bis(trifluoromethyl)-*N*-(2-phenylpropan-2-yl)benzenamine (99a)

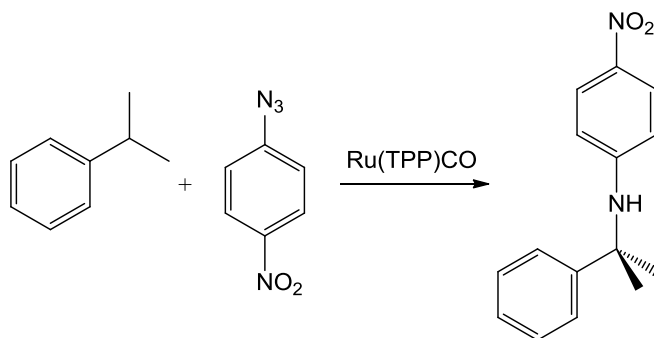


The general procedure A was followed with 17 mg of Ru(TPP)CO ( $2.29 \times 10^{-5}$  mol), 72 mg of 3,5-(CF<sub>3</sub>)<sub>2</sub>-arylazide ( $2.82 \times 10^{-4}$  mol), and 15 mL of isopropylbenzene. (yield 31%, determined by <sup>1</sup>H NMR with 2,4-dinitrotoluene as internal standard).

The general procedure B was followed with 4.9 mg of Ru(TPP)CO ( $6.61 \times 10^{-6}$  mol), 82 mg 3,5-(CF<sub>3</sub>)<sub>2</sub>-arylazide ( $3.21 \times 10^{-4}$  mol), and 15 mL of isopropylbenzene. (yield 90%, determined by <sup>1</sup>H NMR with 2,4-dinitrotoluene as internal standard).

The collected analytical data for 3,5-bis(trifluoromethyl)-*N*-(2-methyl-1-phenylpropyl)benzenamine are in agreement with those reported in the literature.<sup>390</sup>

### 3.9.14. 4-nitro-*N*-(2-phenylpropan-2-yl)benzenamine (99b)

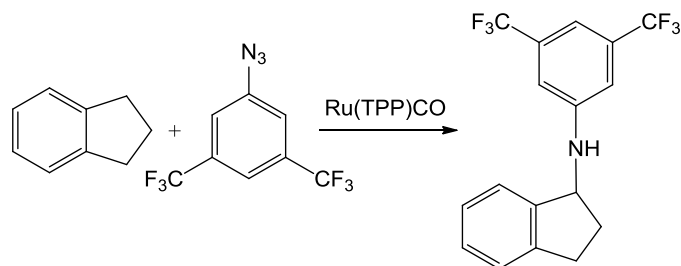


The general procedure A was followed with 18 mg of Ru(TPP)CO ( $2.44 \times 10^{-5}$  mol), 54 mg of 4-NO<sub>2</sub>-arylazide ( $3.27 \times 10^{-4}$  mol), and 15 mL of isopropylbenzene. (yield 41%, determined by <sup>1</sup>H NMR with 2,4-dinitrotoluene as internal standard).

The general procedure B was followed with 4.9 mg of Ru(TPP)CO ( $6.61 \times 10^{-6}$  mol), 56 mg 4-NO<sub>2</sub>-arylazide ( $3.42 \times 10^{-4}$  mol), and 15 mL of isopropylbenzene. (yield 30%, determined by <sup>1</sup>H NMR with 2,4-dinitrotoluene as internal standard).

The collected analytical data for 4-nitro-*N*-(2-phenylpropan-2-yl)benzenamine are in agreement with those reported in the literature.<sup>257</sup>

### 3.9.15. N-(3,5-bis(trifluoromethyl)phenyl)-2,3-dihydro-1H-inden-1-amine (100a)



The general procedure A was followed with 23 mg of Ru(TPP)CO ( $3.11 \times 10^{-5}$  mol), 99 mg of 3,5-(CF<sub>3</sub>)<sub>2</sub>-arylazide ( $3.89 \times 10^{-4}$  mol), and 15 mL of indane. (yield 53%, determined by <sup>1</sup>H NMR with 2,4-dinitrotoluene as internal standard).

The general procedure B was followed with 4.9 mg of Ru(TPP)CO ( $6.61 \times 10^{-6}$  mol), 79 mg 3,5-(CF<sub>3</sub>)<sub>2</sub>-arylazide ( $3.11 \times 10^{-4}$  mol), and 15 mL of isopropylbenzene. (yield 80%, determined by <sup>1</sup>H NMR with 2,4-dinitrotoluene as internal standard).

Elemental Analysis calc. for C<sub>17</sub>H<sub>13</sub>F<sub>6</sub>N: C, 59.13; H, 3.79; N, 4.06.; found: C, 59.02; H, 3.90; N 4.17;

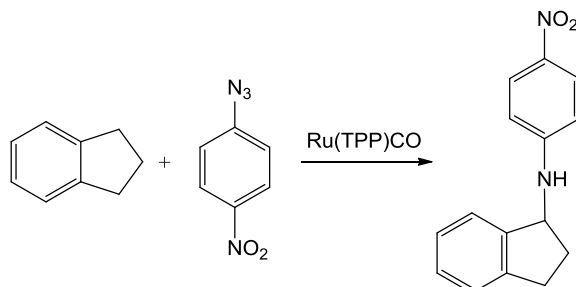
<sup>1</sup>H NMR (300 MHz, CDCl<sub>3</sub>, 300 K)  $\delta$ : 7.38-7.28 (m, 4H, H<sub>Ar</sub>), 7.21 (s, 1H, H<sub>Ar</sub>), 7.07 (s, 2H, H<sub>Ar</sub>), 5.08 (m, 1H, CHNH), 4.39 (broad, 1H, NH), 3.09-2.95 (m, 2H, CH<sub>2</sub>), 2.70-2.62 (m, 1H, NHCHH), 2.00-1.92 (m, 1H, NHCCH);

<sup>13</sup>C NMR (75 MHz, CDCl<sub>3</sub>, 298 K)  $\delta$ : 144.0 (C), 133.0 (q,  $J = 32.4$  Hz, C-CF<sub>3</sub>, 2C overlapping), 128.9 (CH), 127.4 (CH), 125.5 (CH), 124.5 (CH), 123.9 (q,  $J = 271.1$  Hz, CF<sub>3</sub>), 112.6 (CH), 110.6 (CH), 58.9 (CH), 33.8 (CH<sub>2</sub>), 30.7 (CH<sub>2</sub>);

<sup>19</sup>F NMR (282 MHz; CDCl<sub>3</sub>, 298 K)  $\delta$ : -63.50;

$m/z$  (ESI) 345 [M<sup>+</sup>].

### 3.9.16. 2,3-dihydro-N-(4-nitrophenyl)-1H-inden-1-amine (100b)



The general procedure A was followed with 18 mg of Ru(TPP)CO ( $2.47 \times 10^{-5}$  mol), 55 mg of 4-NO<sub>2</sub>-arylazide ( $3.34 \times 10^{-4}$  mol), and 15 mL of indane. (yield 54%, determined by <sup>1</sup>H NMR with 2,4-dinitrotoluene as internal standard).

The general procedure B was followed with 4.9 mg of Ru(TPP)CO ( $6.61 \times 10^{-6}$  mol), 56 mg 4-NO<sub>2</sub>-arylazide ( $3.42 \times 10^{-4}$  mol), and 15 mL of indane. (yield 30%, determined by <sup>1</sup>H NMR with 2,4-dinitrotoluene as internal standard).

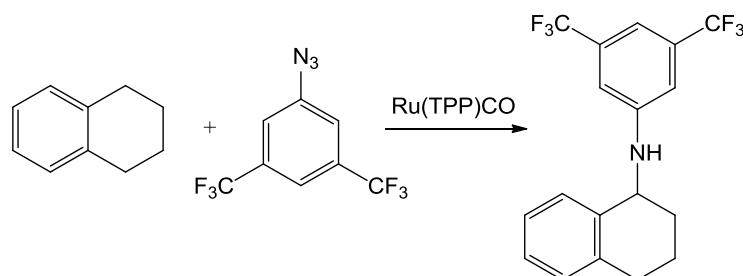
Elemental Analysis calc. for C<sub>15</sub>H<sub>14</sub>N<sub>2</sub>O<sub>2</sub>: C, 70.85; H, 5.55; N, 11.02; found: C, 70.52; H, 5.89; N, 11.45;

<sup>1</sup>H NMR (300 MHz, CDCl<sub>3</sub>, 300 K)  $\delta$ : 8.15 (d, 2H, *J* = 9.16 Hz, H<sub>Ar</sub>), 7.38-7.27 (m, 4H, H<sub>Ar</sub>), 6.67 (d, 2H, *J* = 9.16 Hz, H<sub>Ar</sub>), 5.15-5.10 (m, 1H, CHNH), 4.74 (m, 1H, NH), 3.11-3.06 (m, 1H, CHH), 3.02-2.96 (m, 1H, CHH), 2.68-2.63 (m, 1H, NHCHH), 2.02-1.96 (m, 1H, NHCHH);

<sup>13</sup>C NMR (75 MHz, CDCl<sub>3</sub>, 298 K)  $\delta$ : 152.7 (C), 143.6 (C), 142.7 (C), 138.2 (C), 128.6 (CH), 127.0 (CH), 126.5 (CH, 2C overlapping), 125.2 (CH), 124.1 (CH), 111.5 (CH, 2C overlapping), 58.3 (CH), 33.5 (CH<sub>2</sub>), 30.2 (CH<sub>2</sub>);

*m/z* (ESI) 254 [M<sup>+</sup>].

### 3.9.17. N-(3,5-bis(trifluoromethyl)phenyl)-1,2,3,4-tetrahydronaphthalen-1-amine (101a)



The general procedure A was followed with 11 mg of Ru(TPP)CO ( $1.46 \times 10^{-5}$  mol), 46 mg of 3,5-(CF<sub>3</sub>)<sub>2</sub>-arylazide ( $1.82 \times 10^{-4}$  mol), and 15 mL of 1,2,3,4-Tetrahydronaphthalene (yield 60%, determined by <sup>1</sup>H NMR with 2,4-dinitrotoluene as internal standard).

Elemental Analysis calc. for C<sub>18</sub>H<sub>15</sub>F<sub>6</sub>N: C, 60.17; H, 4.21; N, 3.90.; found: C, 59.92; H, 3.90; N, 4.17;

<sup>1</sup>H NMR (300 MHz, CDCl<sub>3</sub>, 300 K)  $\delta$ : 7.36-7.32 (m, 1H, H<sub>Ar</sub>), 7.26-7.21 (m, 2H, H<sub>Ar</sub>), 7.20-7.16 (m, 1H, H<sub>Ar</sub>), 7.02 (s, 2H, H<sub>Ar</sub>), 4.72-4.68 (m, 1H, CHNH), 4.35 (broad, 1H, NH), 2.90-2.80 (m, 2H, CHNHCH<sub>2</sub>CH<sub>2</sub>CH<sub>2</sub>), 2.06-1.98 (m, 1H, CHNHCH<sub>2</sub>CH<sub>2</sub>CH<sub>2</sub>), 1.95-1.86 (m, 1H, CHNHCH<sub>2</sub>CH<sub>2</sub>CH<sub>2</sub>);

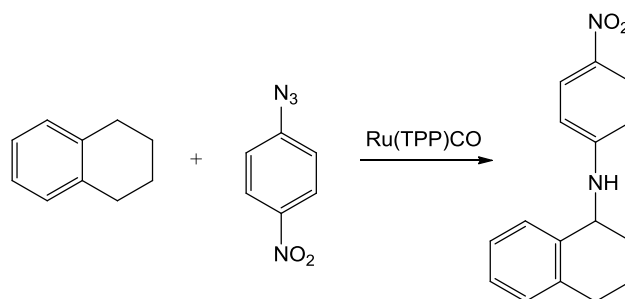
<sup>13</sup>C NMR (75 MHz, CDCl<sub>3</sub>, 298 K)  $\delta$ : 148.2 (C), 138.1 (C), 137.0 (C), 132.0 (q, *J* = 32.4 Hz, C-CF<sub>3</sub>, 2C overlapping), 129.8 (CH), 129.4 (CH), 128.1 (CH), 126.8 (CH), 124.0 (q, *J* = 271.0 Hz, CF<sub>3</sub>, 2C overlapping), 112.2 (CH, 2C overlapping), 110.4 (CH), 51.5 (CH), 29.5 (CH<sub>2</sub>), 28.8 (CH<sub>2</sub>), 19.7 (CH<sub>2</sub>);

<sup>19</sup>F NMR (282 MHz; CDCl<sub>3</sub>, 298 K)  $\delta$ : -63.50;

*m/z* (ESI) 359 [M<sup>+</sup>].



### 3.9.18. 1,2,3,4-tetrahydro-N-(4-nitrophenyl)naphthalen-1-amine (101b)



The general procedure A was followed with 17 mg of Ru(TPP)CO ( $2.29 \times 10^{-5}$  mol), 51 mg of 4-NO<sub>2</sub>-arylazide ( $3.09 \times 10^{-4}$  mol), and 15 mL of 1,2,3,4-Tetrahydronaphthalene (yield 50%, determined by <sup>1</sup>H NMR with 2,4-dinitrotoluene as internal standard).

Elemental Analysis calc. for C<sub>16</sub>H<sub>16</sub>N<sub>2</sub>O<sub>2</sub>: C, 71.62; H, 6.01; N, 10.44.; found: C, 71.44; H, 5.89; N, 10.65;

<sup>1</sup>H NMR (300 MHz, CDCl<sub>3</sub>, 300 K)  $\delta$ : 8.13 (d, 2H,  $J = 9.00$  Hz, H<sub>Ar</sub>), 7.18-7.00 (m, 4H, H<sub>Ar</sub>), 5.91 (d, 2H,  $J = 9.00$  Hz, H<sub>Ar</sub>), 4.18 (broad, 1H, CHNH), 3.77 (d, 1H,  $J = 7.90$  Hz, NH), 2.63-2.48 (m, 2H, CH<sub>2</sub>), 1.49-1.42 (m, 4H, CH<sub>2</sub>);

<sup>13</sup>C NMR (75 MHz, CDCl<sub>3</sub>, 298 K)  $\delta$ : 162.7 (C), 152.7 (C), 138.1 (C), 136.5 (C), 129.8 (CH), 129.3 (CH), 128.2 (CH), 127.0 (CH), 126.8 (CH, 2C overlapping), 111.5 (CH, 2C overlapping), 51.4 (CH), 29.5 (CH<sub>2</sub>), 29.1 (CH<sub>2</sub>), 19.8 (CH<sub>2</sub>);

$m/z$  (ESI) 268 [M<sup>+</sup>].

### 3.9.19. General procedure for kinetic measurements

To a Schlenk flask under a dinitrogen atmosphere were added the catalyst, 4(NO<sub>2</sub>)C<sub>6</sub>H<sub>4</sub>N<sub>3</sub> and toluene in this order. When required, benzene was added at this point. The flask was capped with a rubber septum and immediately placed in an oil bath preheated at 75 °C. The solution was stirred for one minute to dissolve all reagents and 0.2 mL solution was withdrawn for IR analysis. The consumption of the azide was followed by IR spectroscopy ( $\nu_{\text{N}_3} = 2120 \text{ cm}^{-1}$ ) by withdrawing samples of the solution at regular times. Since all reactions are run in the presence of a large excess of toluene, the apparent first order constants were fitted to the equation  $-d[\text{ArN}_3]/dt = k_{\text{app}}[\text{Ru(TPP)CO}][\text{ArN}_3]$ . The concentration of Ru(TPP)CO was calculated on the exact amount of catalyst weighed in each run and was considered to remain constant during the reaction.

### 3.8.17. Determination of kinetics order with respect to 4-NO<sub>2</sub>-arylazide by using Ru(TPP)CO as catalyst.

Catalytic reactions were carried out as described in general procedure for kinetic measurement by using Ru(TPP)CO (36.3 mg,  $4.89 \times 10^{-5}$  mol), 4-NO<sub>2</sub>-arylazide (99.5 mg,  $6.07 \times 10^{-4}$  mol) were dissolved in 30 mL of

toluene in a Schlenk flask under N<sub>2</sub>. Rate constant with respect to 4-NO<sub>2</sub>-arylazide was determined using the equation  $\ln A = \ln A_0 - kt$  (A = IR absorbance value at time t and A<sub>0</sub> = IR absorbance value at zero time).

### 3.8.18. Determination of kinetics order with respect to Ru(TPP)CO.

Catalytic reactions were carried out as described in general procedure for kinetic measurement by using 100 mg of 4-NO<sub>2</sub>-arylazid and 30 mL of toluene. Four different amounts of Ru(TPP)CO were employed:

a) 9.1 mg,  $1.23 \times 10^{-5}$  mol, b) 19.0 mg,  $2.56 \times 10^{-5}$  mol, c) 29.3 mg,  $3.95 \times 10^{-5}$  mol, d) 36.3 mg,  $4.89 \times 10^{-5}$  mol.

For each reaction, rate constant with respect to Ru(TPP)CO was determined using the equation  $\ln A = \ln A_0 - kt$  (A = IR absorbance value at time t and A<sub>0</sub> = IR absorbance value at zero time).

### 3.8.19. Determination of kinetics order with respect to toluene.

Catalytic reactions were carried out as described in general procedure for kinetic measurement by using Ru(TPP)CO (36.3 mg,  $4.89 \times 10^{-5}$  mol) and 100 mg of 4-NO<sub>2</sub>-arylazid. Four different mixtures of toluene and benzene were employed:

a) Toluene / Benzene = 7.5 mL / 22.5 mL, b) Toluene / Benzene = 15 mL / 15 mL, c) Toluene / Benzene = 22.5 mL / 7.5 mL, d) Toluene / Benzene = 30 mL / 0 mL.

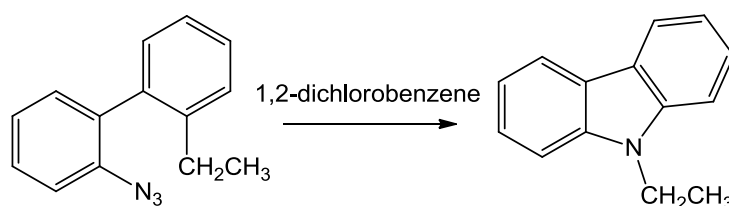
For each reaction, rate constant with respect to toluene was determined using the equation  $\ln A = \ln A_0 - kt$  (A = IR absorbance value at time t and A<sub>0</sub> = IR absorbance value at zero time).

## 3.10. Intramolecular Benzylic Amination

### Synthesis of dihydrophenanthridines and phenanthridines

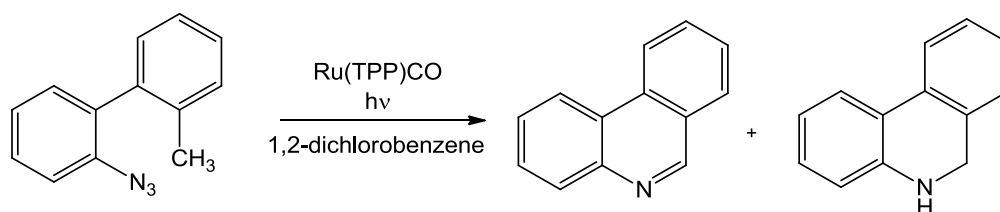
**General procedure for catalytic reactions.** In a typical run, the catalyst (2.0 mg,  $2.70 \times 10^{-6}$  mol) and 2-azido biaryl ( $2.70 \times 10^{-4}$  mol) were dissolved in 1,2-dichlorobenzene (20 mL) under a  $N_2$  atmosphere. The resulting solution was heated at 120 °C using a preheated oil bath, and irradiated by an halogen lamp (400 W). The consumption of 2-azido biaryl was monitored by IR spectroscopy measuring the  $N_3$  characteristic absorbance in the range 2120-2127  $cm^{-1}$ . The reaction was considered finished when the azide absorbance was below 0.03 (by using a 0.5 mm-thickness cell). The solution was then evaporated to dryness and analysed by  $^1H$  NMR with 2,4-dinitrotoluene as an internal standard. To isolate phenanthridines, the reaction was left stirred while exposed to air at 120 °C for an additional two hours after the complete consumption of the azide. The reaction mixture was evaporated to dryness and the residue purified by flash chromatography.

#### 4-Ethyl-9H-carbazole (104a)



2-Azido-2'-ethylbiphenyl (60.0 mg,  $2.70 \times 10^{-4}$  mol) was dissolved in 1,2-dichlorobenzene (20 mL). The resulting solution was refluxed in a preheated oil bath. The consumption of 2-Azido-2'-ethylbiphenyl was monitored by IR spectroscopy measuring the  $N_3$  characteristic absorbance (2123  $cm^{-1}$ ). The reaction was considered finished when the absorbance of the 2-azido biaryls was below 0.03 (by using a 0.5 mm-thickness cell). The solution was then evaporated to dryness and analyzed by  $^1H$  NMR with 2,4-dinitrotoluene as an internal standard (92% yield). **Method b:** The synthetic procedure reported above was repeated at 120 °C by irradiating the reaction mixture with an halogen lamp (400 W) (97% yield). Analytic data are in accord with those reported in the literature.

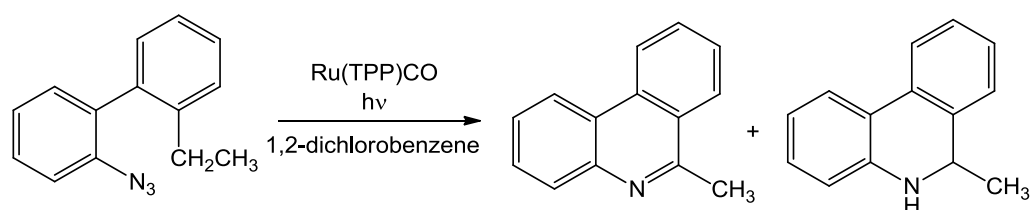
#### 3.10. Phenanthridine (106a)



The general procedure was followed with 2.00 mg of Ru(TPP)CO ( $2.70 \times 10^{-6}$  mol), 59.1 mg 2-azido-2'methylbiphenyl ( $2.83 \times 10^{-4}$  mol), 1,2-dichlorobenzene (20 mL) under a  $N_2$  atmosphere. (yield 35 %, determined by  $^1H$  NMR with 2,4-dinitrotoluene as internal standard).

The  $^1H$  NMR spectrum, run under nitrogen after the complete consumption of the azide, showed the presence of **102a** (31%), **104a** (20%) and **106a** (47%). The flash-chromatographic purification (*n*-hexane/ethyl acetate = 6:4 as eluent) yielded **106a** as a pure compound (35%). Analytic data are in accord with those reported in the literature.<sup>384</sup>

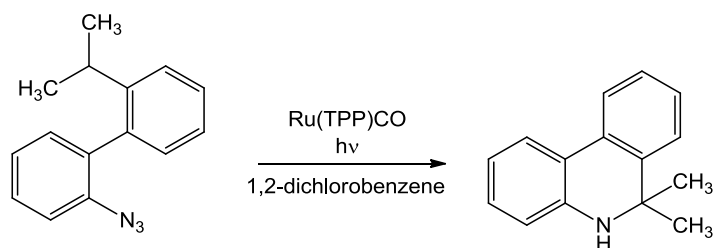
### 3.10. 6-Methylphenanthridine (106b).



The general procedure was followed with 2.00 mg of Ru(TPP)CO ( $2.70 \times 10^{-6}$  mol), 6.33 mg of 2-azido-2'ethylbiphenyl ( $2.84 \times 10^{-4}$  mol), 1,2-dichlorobenzene (20 mL) under a  $N_2$  atmosphere.

The  $^1H$  NMR spectrum, run under nitrogen after the complete consumption of the azide, showed the presence of **1b** (11%), **4b** (46%) and **5b** (32%). The further oxidation process yielded **5b** (78%). The flash-chromatographic purification (*n*-hexane/ethyl acetate = 9:1 as eluent) yielded **5b** as a pure compound. Analytic data are in accord with the those reported in the literature.<sup>383</sup>

### 3.10. 6,6-Dimethyl-5,6-dihydrophenanthridine (105c)



The general procedure was followed with 1.00 mg of Ru(TPP)CO ( $1.35 \times 10^{-6}$  mol), 31.3 g of 2-azido-2'isopropylbiphenyl ( $1.33 \times 10^{-4}$  mol), 1,2-dichlorobenzene (10 mL) under a  $N_2$  atmosphere. The flash-chromatographic purification (*n*-hexane/ethyl acetate = 6:4 as eluent) yielded **105c** as a pure compound (77%).

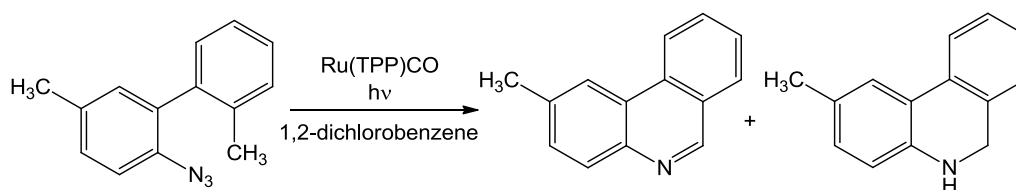
Elemental Analysis calc. for C<sub>15</sub>H<sub>15</sub>N: C, 86.08; H, 7.22; N, 6.69; found: C, 86.52; H, 7.40; N, 6.45;

<sup>1</sup>H NMR (300 MHz, CDCl<sub>3</sub>, 300 K) δ: 7.75 (2H, pst, *J* = 8.4 Hz, H<sub>Ar</sub>), 7.37-7.28 (3H, m, H<sub>Ar</sub>), 7.15 (1H, pst, *J* = 7.5 Hz, H<sub>Ar</sub>), 6.91 (1H, pst, *J* = 7.5 Hz, H<sub>Ar</sub>), 6.80 (1H, d, *J* = 7.9 Hz, H<sub>Ar</sub>), 1.58 (6H, s, CH<sub>3</sub>), NH was not detected;

<sup>13</sup>C NMR (75 MHz, CDCl<sub>3</sub>, 298 K) δ: 142.5 (C), 140.9 (C), 130.8 (C), 129.2 (CH), 128.0 (CH), 127.6 (CH), 123.8 (CH), 123.7 (CH), 123.1 (CH), 122.4 (C), 120.1 (CH), 116.4 (CH), 54.2 (C), 29.6 (CH<sub>3</sub>);

*m/z* (ESI) 209 [M<sup>+</sup>].

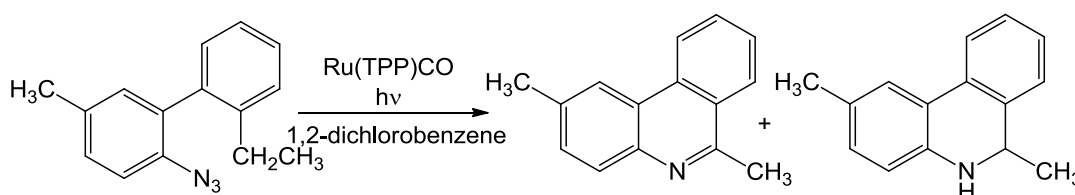
### 3.10. 2-Methylphenanthridine (106d).



The general procedure was followed with 2.00 mg of Ru(TPP)CO ( $2.70 \times 10^{-6}$  mol), 61.4 mg of 2-azido-2',5-dimethylbiphenyl ( $2.75 \times 10^{-4}$  mol), 1,2-dichlorobenzene (20 mL) under a N<sub>2</sub> atmosphere.

The <sup>1</sup>H NMR spectrum, run under nitrogen after the complete consumption of the azide, showed the presence of **102d** (35%), **104d** (14%) and **106d** (48%). The flash-chromatographic purification (*n*-hexane/ethyl acetate = 9:1 as eluent) yielded **106d** as a pure compound (30%). Analytic data are in accord with those reported in the literature.<sup>385</sup>

### 3.10. 2,6-Dimethylphenanthridine (106e).



The general procedure was followed with 2.00 mg of Ru(TPP)CO ( $2.70 \times 10^{-6}$  mol), 66.9 mg of 2-azido-2'-ethyl-5-methylbiphenyl ( $2.82 \times 10^{-4}$  mol), 1,2-dichlorobenzene (20 mL) under a N<sub>2</sub> atmosphere.

The <sup>1</sup>H NMR spectrum, run under nitrogen after the complete consumption of the azide, showed the presence of **102e** (8%), **105e** (38% based on <sup>1</sup>H NMR spectrum: δ<sub>H</sub> (300, MHz, CDCl<sub>3</sub>) 4.51 (1H, q, *J* = 6.4 Hz, CH), 2.34 (3H, s, CH<sub>3</sub>), 1.43 (3H, d, *J* = 6.4 Hz, CH<sub>3</sub>)) and **106e** (52%). The further oxidation process yielded **106e** (90%). The flash-chromatographic purification (*n*-hexane/ethyl acetate = 6:4 as eluent) yielding **106e** as a pure compound

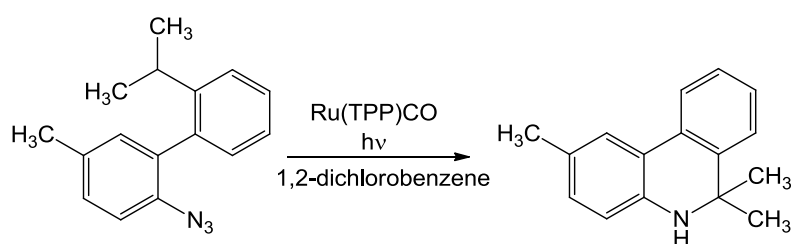
Elemental Analysis calc. for C<sub>15</sub>H<sub>13</sub>N: C, 86.92; H, 6.32; N, 6.76; found: C, 87.05; H, 6.55; N, 6.32;

<sup>1</sup>H NMR (300 MHz, CDCl<sub>3</sub>, 300 K) δ: . 8.65 (1H, d, *J* = 8.1 Hz, H<sub>Ar</sub>), 8.35 (1H, s, H<sub>Ar</sub>), 8.25 (1H, d, *J* = 8.1 Hz, H<sub>Ar</sub>), 8.12 (1H, d, *J* = 7.5 Hz, H<sub>Ar</sub>), 7.88 (1H, pst, *J* = 8.1 Hz, H<sub>Ar</sub>), 7.73 (1H, pst, *J* = 8.1 Hz, H<sub>Ar</sub>), 7.58 (1H, d, *J* = 7.5 Hz, H<sub>Ar</sub>), 3.11 (3H, s, CH<sub>3</sub>), 2.64 (3H, s, CH<sub>3</sub>);

<sup>13</sup>C NMR (75 MHz, CDCl<sub>3</sub>, 298 K) δ: 162.7 (C), 158.3 (C), 133.1 (C), 131.7 (CH), 131.2 (CH), 128.3 (CH), 128.0 (CH), 127.3 (CH), 126.0 (C), 124.1 (C), 122.8 (CH), 122.1 (CH), 31.3 (CH<sub>3</sub>), 22.3 (CH<sub>3</sub>). One quaternary carbon atom was not detected;

*m/z* (ESI) 207 [M<sup>+</sup>].

### 3.10. 2,6,6-Trimethyl-5,6-dihydrophenanthridine (105f)



The general procedure was followed with 2.00 mg of Ru(TPP)CO (2.70×10<sup>-6</sup> mol), 67.78 mg of 2-azido-2'-isopropyl-5-methylbiphenyl (2.70×10<sup>-4</sup> mol), 1,2-dichlorobenzene (20 mL) under a N<sub>2</sub> atmosphere.

The <sup>1</sup>H NMR spectrum, run under nitrogen after the complete consumption of the azide, showed the presence of **105f** (85%). The flash-chromatographic purification (*n*-hexane/ethyl acetate = 6:4 as eluent) yielded **105f** as a pure compound (80%).

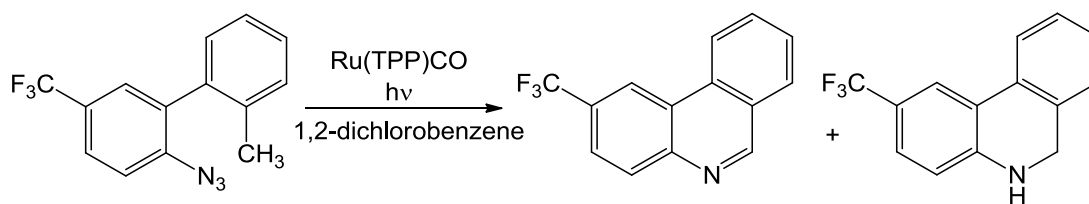
Elemental Analysis calc. for C<sub>16</sub>H<sub>17</sub>N: C, 86.05; H, 7.67; N, 6.27; found: C, 86.34; H, 7.74; N, 6.24;

<sup>1</sup>H NMR (300 MHz, CDCl<sub>3</sub>, 300 K) δ: 7.77 (1H, d, *J* = 7.6 Hz, H<sub>Ar</sub>), 7.56 (1H, bs, H<sub>Ar</sub>), 7.35-7.30 (3H, m, H<sub>Ar</sub>), 6.98 (1H, dd, *J*<sup>3</sup> = 8.0 Hz, *J*<sup>4</sup> = 1.1 Hz, H<sub>Ar</sub>), 6.73 (1H, d, *J* = 8.0 Hz, H<sub>Ar</sub>), 2.36 (3H, s, CH<sub>3</sub>), 1.57 (6H, s, CH<sub>3</sub>), NH was not detected;

<sup>13</sup>C NMR (75 MHz, CDCl<sub>3</sub>, 298 K) δ: 140.6 (C), 139.6 (C), 130.4 (C), 129.5 (CH), 129.0 (C), 127.5 (CH), 127.2 (CH), 123.9 (CH), 123.3 (CH), 122.7 (CH), 122.1 (C), 116.2 (CH), 54.1 (C), 29.0 (CH<sub>3</sub>), 20.9 (CH<sub>3</sub>);

*m/z* (ESI) 223 [M<sup>+</sup>].

### 3.10. 2-(Trifluoromethyl)phenanthridine (106g)



The general procedure was followed with 2.00 mg of Ru(TPP)CO ( $2.70 \times 10^{-6}$  mol), 75.6 mg of 2-azido-2'-methyl-5-(trifluoromethyl)biphenyl ( $2.73 \times 10^{-4}$  mol), 1,2-dichlorobenzene (20 mL) under a  $N_2$  atmosphere.

The  $^1H$  NMR spectrum, run under nitrogen after the complete consumption of the azide, showed the presence of **102g** (17%), **104g** (9%), **105g** (24% based on  $^1H$  NMR spectrum:  $\delta_H$  (300, MHz,  $CDCl_3$ ) 4.49 (2H, bs,  $CH_2$ ) and **106g** (48%). The further oxidation process yielded **106g** (72%). The flash-chromatographic purification (*n*-hexane/ethyl acetate = 5:5 as eluent) yielded **106g** as a pure compound (65%).

Elemental Analysis calc. for  $C_{14}H_8F_3N$ : C, 68.02; H, 3.26; N, 5.67; found: C, 68.37; H, 3.45; N, 5.22;

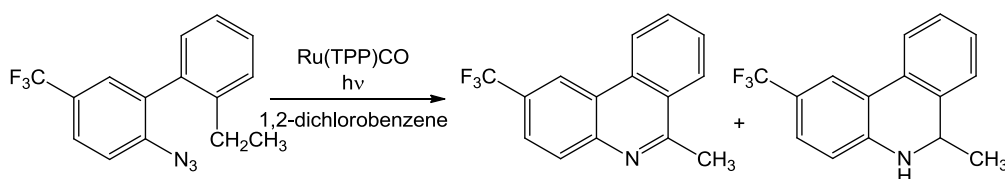
$^1H$  NMR (300 MHz,  $CDCl_3$ , 300 K)  $\delta$ : 9.40 (1H, s,  $H_{Ar}$ ), 8.88 (1H, s,  $H_{Ar}$ ), 8.67 (1H, d,  $J = 8.2$  Hz,  $H_{Ar}$ ), 8.33 (1H, d,  $J = 8.0$  Hz,  $H_{Ar}$ ), 8.13 (1H, d,  $J = 8.0$  Hz,  $H_{Ar}$ ), 8.00-7.95 (2H, m,  $H_{Ar}$ ), 7.82 (1H, pst,  $J = 8.0$  Hz,  $H_{Ar}$ );

$^{13}C$  NMR (75 MHz,  $CDCl_3$ , 298 K)  $\delta$ : 156.0 (CH), 146.3 (C), 132.6 (C), 132.1 (CH), 131.5 (CH), 129.4 (CH), 128.8 (CH), 127.0 (C), 126.5 (C), 125.1 (CH, q,  $J = 3.7$  Hz), 124.7 ( $CF_3$ , q,  $J = 270.0$  Hz), 122.3 (CH), 120.5 (CH, q,  $J = 4.0$  Hz),  $CCF_3$  was not detected;

$^{19}F$  NMR (282 MHz;  $CDCl_3$ , 298 K)  $\delta$ : -62.1

$m/z$  (ESI) 247 [ $M^+$ ].

### 3.10. 6-Methyl-2-(trifluoromethyl)phenanthridine (106h)



The general procedure was followed with 2.00 mg of Ru(TPP)CO ( $2.70 \times 10^{-6}$  mol), 78.9 mg of 2-azido-2'-ethyl-5-(trifluoromethyl)biphenyl ( $2.71 \times 10^{-4}$  mol), 1,2-dichlorobenzene (20 mL) under a  $N_2$  atmosphere.

The  $^1H$  NMR spectrum, run under nitrogen after the complete consumption of the azide, showed the presence of **102h** (5%), **105h** (85% based on  $^1H$  NMR spectrum:  $\delta_H$  (300, MHz,  $CDCl_3$ ) 7.91 (1H, s,  $H_{Ar}$ ), 7.73 (1H, d,  $J = 7.5$  Hz,  $H_{Ar}$ ), 7.34-7.31 (3H, m,  $H_{Ar}$ ), 7.16 (1H, d,  $J = 7.5$  Hz,  $H_{Ar}$ ), 6.68 (1H, d,  $J = 8.4$  Hz,  $H_{Ar}$ ), 4.63 (1H, q,  $J = 6.4$  Hz, CH), 4.28 (1H, br, NH), 1.45 (3H, d,  $J = 6.4$  Hz,  $CH_3$ ) and **106h** (10%). The

further oxidation process yielded **106h** (95%). The flash-chromatographic purification (*n*-hexane/ethyl acetate = 6:4 as eluent) yielded **106h** as a pure compound (80%).

Elemental Analysis calc. for C<sub>15</sub>H<sub>10</sub>F<sub>3</sub>N: C, 68.96; H, 3.86; N, 5.36; found: C, 69.03; H, 3.95; N, 5.20;

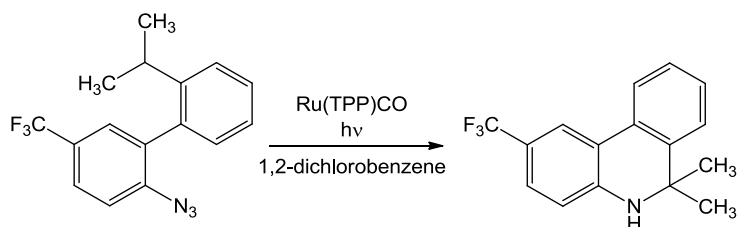
<sup>1</sup>H NMR (300 MHz, CDCl<sub>3</sub>, 300 K) δ: 8.84 (1H, s, H<sub>Ar</sub>), 8.69 (1H, d, *J* = 8.1 Hz, H<sub>Ar</sub>), 8.30 (1H, d, *J* = 8.4 Hz, H<sub>Ar</sub>), 8.22 (1H, d, *J* = 8.4 Hz, H<sub>Ar</sub>), 7.97-7.92 (2H, m, H<sub>Ar</sub>), 7.80 (1H, pst, *J* = 8.1 Hz, H<sub>Ar</sub>), 3.11 (3H, s, CH<sub>3</sub>);

<sup>13</sup>C NMR (75 MHz, CDCl<sub>3</sub>, 298 K) δ: 144.3 (C), 142.8 (C), 131.6 (CH), 130.6 (CH), 128.6 (CH), 127.0 (CH), 125.0 (CH, *q*, *J* = 3.7 Hz), 122.8 (CH), 122.3 (C), 120.2 (CH, *q*, *J* = 3.7 Hz), 22.8 (CH<sub>3</sub>). CF<sub>3</sub> and three quaternary carbon atoms were not detected;

<sup>19</sup>F NMR (282 MHz; CDCl<sub>3</sub>, 298 K) δ: -62.1

*m/z* (ESI) 261 [M<sup>+</sup>].

### 3.10. 6,6-Dimethyl-2-(trifluoromethyl)-5,6-dihydrophenanthridine (**105i**).



The general procedure was followed with 1.00 mg of Ru(TPP)CO (1.35×10<sup>-6</sup> mol), 42.3 mg of 2-azido-2-isopropyl-5-(trifluoromethyl)biphenyl (1.39×10<sup>-4</sup> mol), 1,2-dichlorobenzene (20 mL) under a N<sub>2</sub> atmosphere.

The <sup>1</sup>H NMR spectrum, run under nitrogen after the complete consumption of the azide, showed the presence of **105i** (98%). The flash-chromatographic purification (*n*-hexane/ethyl acetate = 6:4 as eluent) yielded **105i** as a pure compound (70%).

Elemental Analysis calc. for C<sub>16</sub>H<sub>14</sub>F<sub>3</sub>N: C, 69.30; H, 5.09; N, 5.05; found: C, 69.45; H, 5.15; N, 4.98;

<sup>1</sup>H NMR (300 MHz, CDCl<sub>3</sub>, 300 K) δ: 7.95 (1H, bs, H<sub>Ar</sub>), 7.78 (1H, dd, *J*<sup>3</sup> = 7.5 Hz, *J*<sup>4</sup> = 2.2 Hz, H<sub>Ar</sub>), 7.39-7.30 (4H, m, H<sub>Ar</sub>), 6.68 (1H, d, *J* = 8.4 Hz, H<sub>Ar</sub>), 4.08 (1H, bs, NH), 1.56 (6H, s, CH<sub>3</sub>);

<sup>13</sup>C NMR (75 MHz, CDCl<sub>3</sub>, 298 K) δ: 146.1 (C), 140.8 (C), 129.6 (C), 128.6 (CH), 127.8 (CH), 126.1 (CH, *q*, *J* = 3.7 Hz), 123.8 (CH), 123.0 (CH), 121.2 (C), 120.9 (CH, *q*, *J* = 3.7 Hz), 115.3 (CH), 54.3 (C), 30.4 (CH<sub>3</sub>). CF<sub>3</sub> and one quaternary carbon atom were not detected;

<sup>19</sup>F NMR (282 MHz; CDCl<sub>3</sub>, 298 K) δ: -61.5;

*m/z* (ESI) 277 [M<sup>+</sup>].

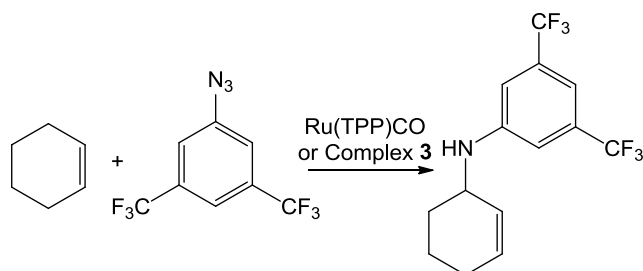


## 3.11. Allylic Amination

### 3.11.1. General procedure for catalytic reactions

**Method A:** In a typical run, the catalyst ( $1.3 \times 10^{-5}$  mol) and the aryl azide ( $6.3 \times 10^{-4}$  mol) were added to a benzene (30 mL) solution of the olefin ( $3.4 \times 10^{-4}$  mol). The resulting solution was refluxed using a preheated oil bath. The consumption of the arylazide was monitored by TLC up to the point that its spot was no longer observable, and then by IR spectroscopy measuring the  $N_3$  characteristic absorbance in the range 2095–2130  $\text{cm}^{-1}$ . The reaction was considered to be finished when the absorbance of the azide measured was below 0.03 (by using a 0.5 mm-thickness cell). The solution was then evaporated to dryness and analyzed by  $^1\text{H}$  NMR with 2,4-dinitrotoluene as an internal standard. The residue was then purified by flash chromatography on deactivated silica adding 10%  $\text{Et}_3\text{N}$  to the eluent (*n*-hexane/ethyl acetate) during the packing of the column. **Method b:** The synthetic procedure reported above was repeated using the olefin as reaction solvent.

#### 3.9.1. *N*-(cyclohex-2-enyl)-3,5-bis(trifluoromethyl)benzenamine (107a)



The general procedure A was followed with 11 mg of Ru(TPP)CO ( $1.5 \times 10^{-5}$  mol), 0.18 g of 3,5-( $\text{CF}_3$ )<sub>2</sub>-arylazide ( $7.4 \times 10^{-4}$  mol), 0.37 mL of cyclohexene ( $3.7 \times 10^{-3}$  mol) in 30 mL of benzene. (yield 26%, determined by  $^1\text{H}$  NMR with 2,4-dinitrotoluene as internal standard).

The general procedure B was followed with 11 mg of Ru(TPP)CO ( $1.5 \times 10^{-6}$  mol), 0.18 mg 3,5-( $\text{CF}_3$ )<sub>2</sub>-arylazide ( $7.4 \times 10^{-4}$  mol), in 30 mL of cyclohexene. (yield 75%, determined by  $^1\text{H}$  NMR with 2,4-dinitrotoluene as internal standard).

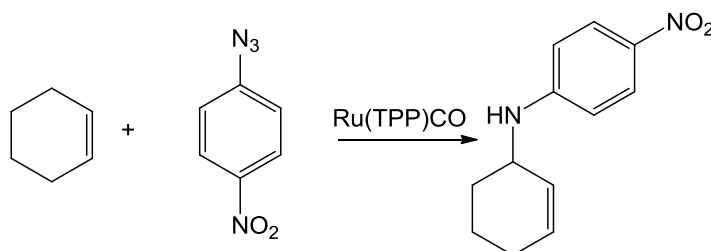
The general procedure A was followed with 15 mg of complex **113** ( $1.28 \times 10^{-5}$  mol), 0.16 g of 3,5-( $\text{CF}_3$ )<sub>2</sub>-arylazide ( $6.4 \times 10^{-4}$  mol), 0.32 mL of cyclohexene ( $3.2 \times 10^{-3}$  mol) in 30 mL of benzene. (yield 74%, determined by  $^1\text{H}$  NMR with 2,4-dinitrotoluene as internal standard).

The general procedure B was followed with 15 mg of complex **113** ( $1.28 \times 10^{-6}$  mol), 0.16 g 3,5-(CF<sub>3</sub>)<sub>2</sub>-arylazide ( $6.4 \times 10^{-4}$  mol), in 30 mL of cyclohexene. (yield 99%, determined by <sup>1</sup>H NMR with 2,4-dinitrotoluene as internal standard).

**Method C:** Complex **115** (17 mg,  $1.28 \times 10^{-5}$  mol) and 0.16 g 3,5-(CF<sub>3</sub>)<sub>2</sub>-arylazide ( $6.4 \times 10^{-4}$  mol) were added to a benzene (30 mL) solution of cyclohexene (0.325 mL,  $3.21 \times 10^{-3}$  mol). The solution was refluxed for 18 hours and evaporated to dryness. (70%, determined by <sup>1</sup>H NMR with 2,4-dinitrotoluene as internal standard).

The collected analytical data for *N*-(cyclohex-2-enyl)-3,5-bis(trifluoromethyl)benzenamine are in agreement with those reported in the literature.<sup>437</sup>

### 3.9.2. *N*-(cyclohex-2-enyl)-4-nitrobenzenamine (107b)



The general procedure A was followed with 12 mg of Ru(TPP)CO ( $1.6 \times 10^{-5}$  mol), 0.13 g of 4-NO<sub>2</sub>-arylazide ( $8.1 \times 10^{-4}$  mol), 0.41 mL of cyclohexene ( $4.0 \times 10^{-3}$  mol) in 30 mL of benzene. (yield 23%, determined by <sup>1</sup>H NMR with 2,4-dinitrotoluene as internal standard).

The general procedure B was followed with 11 mg of Ru(TPP)CO ( $1.5 \times 10^{-6}$  mol), 0.13 g of 4-NO<sub>2</sub>-arylazide ( $8.1 \times 10^{-4}$  mol), in 30 mL of cyclohexene. (yield 70%, determined by <sup>1</sup>H NMR with 2,4-dinitrotoluene as internal standard).

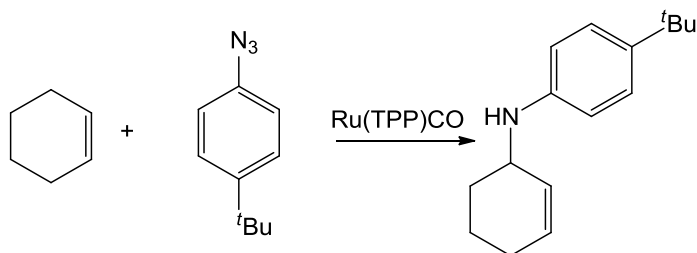
Elemental Analysis calc. for C<sub>12</sub>H<sub>14</sub>N<sub>2</sub>O<sub>2</sub>: C, 77.38; H, 7.58; N, 15.04; found: C, 77.89; H, 7.61; N, 15.01;

<sup>1</sup>H NMR (300 MHz, CDCl<sub>3</sub>, 300 K)  $\delta$ : 8.10 (2H, d,  $J = 9.1$  Hz, H<sub>Ar</sub>), 6.55 (2H, d,  $J = 9.1$  Hz, H<sub>Ar</sub>), 5.97 (1H, m, CH=CH-CH<sub>2</sub>), 5.73 (1H, m, CH=CH-CH<sub>2</sub>), 4.51 (1H, br s, NH), 4.10 (1H, br s, CHNH), 2.09-2.01 (2H, m, CH<sub>2</sub>), 1.98-1.92 (1H, m, CH<sub>2</sub>), 1.80-1.67 (2H, m, CH<sub>2</sub>), 1.63-1.57 (1H, m, CH<sub>2</sub>);

<sup>13</sup>C NMR (75 MHz, CDCl<sub>3</sub>, 298 K)  $\delta$ : 152.7 (C), 132.2 (CH), 127.1 (CH), 126.9 (CH), 111.7 (CH), 48.1 (CH), 28.9 (CH<sub>2</sub>), 25.3 (CH<sub>2</sub>), 19.7 (CH<sub>2</sub>). One quaternary carbon was not detected;

$m/z$  (ESI) 218 [M<sup>+</sup>].

### 3.9.3. 4-*tert*-butyl-*N*-(cyclohex-2-enyl)aniline (107c)



The general procedure A was followed with 12 mg of Ru(TPP)CO ( $1.6 \times 10^{-5}$  mol), 0.14 g of 4-<sup>t</sup>Bu-arylazide ( $8.1 \times 10^{-4}$  mol), 0.41 mL of cyclohexene ( $4.0 \times 10^{-3}$  mol) in 30 mL of benzene. (yield 13%, determined by <sup>1</sup>H NMR with 2,4-dinitrotoluene as internal standard).

The general procedure B was followed with 12 mg of Ru(TPP)CO ( $1.6 \times 10^{-6}$  mol), 0.14 g of 4-<sup>t</sup>Bu-arylazide ( $8.1 \times 10^{-4}$  mol), in 30 mL of cyclohexene. (yield 89%, determined by <sup>1</sup>H NMR with 2,4-dinitrotoluene as internal standard).

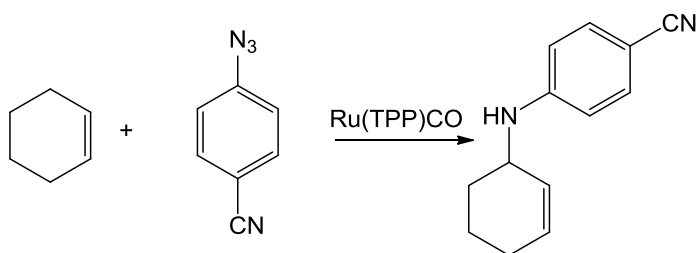
Elemental Analysis calc. for C<sub>16</sub>H<sub>23</sub>N: C, 83.79; H, 10.11; N, 6.11; found: C, 84.01; H, 10.02; N, 6.01;

<sup>1</sup>H NMR (300 MHz, CDCl<sub>3</sub>, 300 K) δ: 7.21 (2H, d, *J* = 8.8 Hz, HAR), 6.59 (2H, d, *J* = 8.8 Hz, HAR), 5.85 (1H, m, CH=CH-CH<sub>2</sub>), 5.80 (1H, m, CH=CH-CH<sub>2</sub>), 3.97 (1H, br s, CHNH), 3.55 (1H, br s, NH), 2.06-2.03 (2H, m, CH<sub>2</sub>), 1.95-1.90 (2H, m, CH<sub>2</sub>), 1.70-1.62 (2H, m, CH<sub>2</sub>), 1.29 (9H, s, C(CH<sub>3</sub>)<sub>3</sub>);

<sup>13</sup>C NMR (75 MHz, CDCl<sub>3</sub>, 298 K) δ: 145.2 (C), 140.3 (C), 130.3 (CH), 129.3 (CH), 126.5 (CH), 113.3 (CH), 48.5 (CH), 34.2 (C), 32.0 (CH<sub>3</sub>), 29.4 (CH<sub>2</sub>), 25.6 (CH<sub>2</sub>), 20.1 (CH<sub>2</sub>);

*m/z* (ESI) 229 [M<sup>+</sup>].

### 3.9.4. 4-(Cyclohex-2-enylamino)benzonitrile (107d)

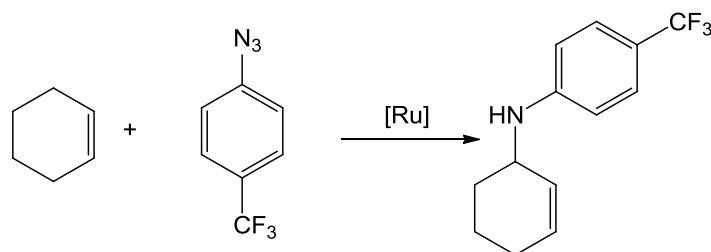


The general procedure A was followed with 13 mg of Ru(TPP)CO ( $1.7 \times 10^{-5}$  mol), 0.13 g of 4-CN-arylazide ( $8.7 \times 10^{-4}$  mol), 0.41 mL of cyclohexene ( $4.0 \times 10^{-3}$  mol) in 30 mL of benzene. (yield 35%, determined by <sup>1</sup>H NMR with 2,4-dinitrotoluene as internal standard).

The general procedure B was followed with 12 mg of Ru(TPP)CO ( $1.6 \times 10^{-6}$  mol), 0.13 g of 4-CN-arylazide ( $8.7 \times 10^{-4}$  mol), in 30 mL of cyclohexene. (yield 80%, determined by <sup>1</sup>H NMR with 2,4-dinitrotoluene as internal standard).

The collected analytical data for 4-(Cyclohex-2-enylamino)benzonitrile are in agreement with those reported in the literature.<sup>438</sup>

### 3.9.5. *N*-(cyclohex-2-enyl)-4-(trifluoromethyl)benzenamine (107e)



The general procedure A was followed with 11 mg of Ru(TPP)CO ( $1.5 \times 10^{-5}$  mol), 0.14 g of 4-CF<sub>3</sub>-arylazide ( $7.4 \times 10^{-4}$  mol), 0.37 mL of cyclohexene ( $3.7 \times 10^{-3}$  mol) in 30 mL of benzene. (yield 28%, determined by <sup>1</sup>H NMR with 2,4-dinitrotoluene as internal standard).

The general procedure B was followed with 12 mg of Ru(TPP)CO ( $1.6 \times 10^{-6}$  mol), 0.15 g of 4-CF<sub>3</sub>-arylazide ( $8.1 \times 10^{-4}$  mol), in 30 mL of cyclohexene. (yield 85%, determined by <sup>1</sup>H NMR with 2,4-dinitrotoluene as internal standard).

The general procedure A was followed with 14 mg of complex **116** ( $1.28 \times 10^{-5}$  mol), 0.12 g of 4-CF<sub>3</sub>-arylazide ( $6.4 \times 10^{-4}$  mol), 0.32 mL of cyclohexene ( $3.2 \times 10^{-3}$  mol) in 30 mL of benzene. (yield 30%, determined by <sup>1</sup>H NMR with 2,4-dinitrotoluene as internal standard).

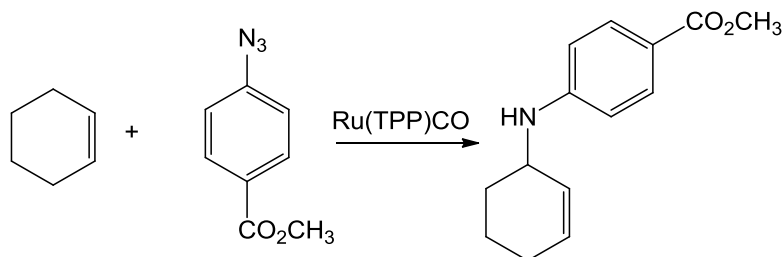
The general procedure B was followed with 14 mg of complex **116** ( $1.28 \times 10^{-6}$  mol), 0.12 g 4-CF<sub>3</sub>-arylazide ( $6.4 \times 10^{-4}$  mol), in 30 mL of cyclohexene. (55 yield %, determined by <sup>1</sup>H NMR with 2,4-dinitrotoluene as internal standard).

The general procedure A was followed with 15 mg of complex **117** ( $1.66 \times 10^{-5}$  mol), 0.15 g of 4-CF<sub>3</sub>-arylazide ( $8.3 \times 10^{-4}$  mol), 0.42 mL of cyclohexene ( $4.1 \times 10^{-3}$  mol) in 30 mL of benzene. (yield 25%, determined by <sup>1</sup>H NMR with 2,4-dinitrotoluene as internal standard).

The general procedure B was followed with 14 mg of complex **117** ( $1.66 \times 10^{-6}$  mol), 0.15 g of 4-CF<sub>3</sub>-arylazide ( $8.3 \times 10^{-4}$  mol), in 30 mL of cyclohexene. (99 yield %, determined by <sup>1</sup>H NMR with 2,4-dinitrotoluene as internal standard).

The collected analytical data for *N*-(cyclohex-2-enyl)-4-(trifluoromethyl)benzenamine are in agreement with those reported in the literature.<sup>439</sup>

### 3.9.6. Methyl 4-(cyclohex-2-enylamino)benzoate (107f)

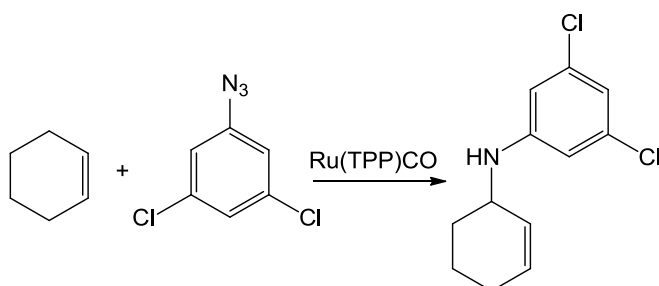


The general procedure A was followed with 11 mg of Ru(TPP)CO ( $1.5 \times 10^{-5}$  mol), 0.13 g of 4-CO<sub>2</sub>CH<sub>3</sub>-arylazide ( $7.4 \times 10^{-4}$  mol), 0.37 mL of cyclohexene ( $3.7 \times 10^{-3}$  mol) in 30 mL of benzene. (yield 13%, determined by <sup>1</sup>H NMR with 2,4-dinitrotoluene as internal standard).

The general procedure B was followed with 12 mg of Ru(TPP)CO ( $1.6 \times 10^{-6}$  mol), 0.14 g of 4-CO<sub>2</sub>CH<sub>3</sub>-arylazide ( $8.1 \times 10^{-4}$  mol), in 30 mL of cyclohexene. (yield 85%, determined by <sup>1</sup>H NMR with 2,4-dinitrotoluene as internal standard).

The collected analytical data for Methyl 4-(cyclohex-2-enylamino)benzoate are in agreement with those reported in the literature.<sup>437</sup>

### 3.9.7. 3,5-Dichloro-N-(cyclohex-2-enyl)benzenamine (107g)

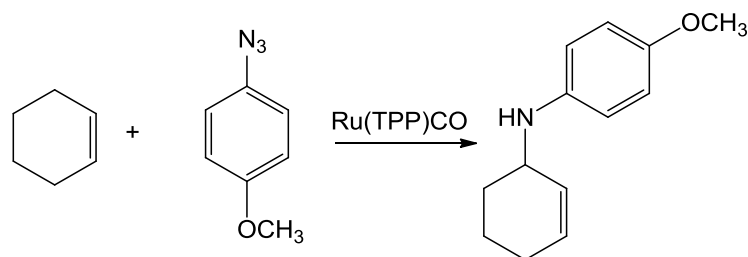


The general procedure A was followed with 11 mg of Ru(TPP)CO ( $1.5 \times 10^{-5}$  mol), 0.14 g of 3,5-Cl<sub>2</sub>-arylazide ( $7.4 \times 10^{-4}$  mol), 0.37 mL of cyclohexene ( $3.7 \times 10^{-3}$  mol) in 30 mL of benzene. (yield 38%, determined by <sup>1</sup>H NMR with 2,4-dinitrotoluene as internal standard).

The general procedure B was followed with 12 mg of Ru(TPP)CO ( $1.6 \times 10^{-6}$  mol), 0.15 g of 3,5-Cl<sub>2</sub>-arylazide ( $8.1 \times 10^{-4}$  mol), in 30 mL of cyclohexene. (yield 90%, determined by <sup>1</sup>H NMR with 2,4-dinitrotoluene as internal standard).

The collected analytical data for 3,5-Dichloro-N-(cyclohex-2-enyl)benzenamine are in agreement with those reported in the literature.<sup>437</sup>

### 3.9.8. *N*-(cyclohex-2-enyl)-4-methoxybenzenamine (107h)

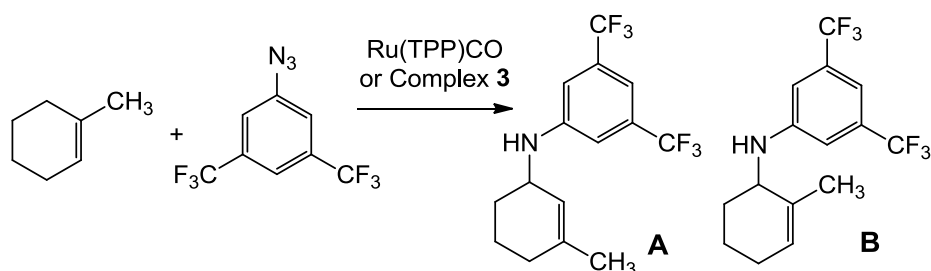


The general procedure A was followed with 11 mg of Ru(TPP)CO ( $1.5 \times 10^{-5}$  mol), 0.11 g of 4-OCH<sub>3</sub>-arylazide ( $7.4 \times 10^{-4}$  mol), 0.37 mL of cyclohexene ( $3.7 \times 10^{-3}$  mol) in 30 mL of benzene. (yield 8%, determined by <sup>1</sup>H NMR with 2,4-dinitrotoluene as internal standard).

The general procedure B was followed with 12 mg of Ru(TPP)CO ( $1.6 \times 10^{-6}$  mol), 0.12 g of 4-OCH<sub>3</sub>-arylazide ( $8.1 \times 10^{-4}$  mol), in 30 mL of cyclohexene. (yield 33%, determined by <sup>1</sup>H NMR with 2,4-dinitrotoluene as internal standard).

The collected analytical data for *N*-(cyclohex-2-enyl)-4-methoxybenzenamine are in agreement with those reported in the literature.<sup>439</sup>

### 3.9.9. 3,5-Bis(trifluoromethyl)-*N*-(3-methylcyclohex-2-enyl)benzenamine (108aA) + 3,5-bis(trifluoromethyl)-*N*-(2-methylcyclohex-2-enyl)benzenamine (108aB)



The general procedure A was followed with 11 mg of Ru(TPP)CO ( $1.5 \times 10^{-5}$  mol), 0.19 g of 3,5-(CF<sub>3</sub>)<sub>2</sub>-arylazide ( $7.4 \times 10^{-4}$  mol), 0.44 mL of 1-methyl-1-cyclohexene ( $3.7 \times 10^{-3}$  mol) in 30 mL of benzene. (yield **A + B** 43 %, **A/B** = 65:36, determined by <sup>1</sup>H NMR with 2,4-dinitrotoluene as internal standard).

The general procedure A was followed with 15 mg of complex **113** ( $1.28 \times 10^{-5}$  mol), 0.16 g of 3,5-(CF<sub>3</sub>)<sub>2</sub>-arylazide ( $6.4 \times 10^{-4}$  mol), 0.38 mL of 1-methyl-1-cyclohexene ( $3.2 \times 10^{-3}$  mol) in 30 mL of benzene. (yield **A + B** 60 %, **A/B** = 63:34, determined by <sup>1</sup>H NMR with 2,4-dinitrotoluene as internal standard).

The general procedure B was followed with 15 mg of complex **113** ( $1.28 \times 10^{-6}$  mol), 0.16 g 3,5-(CF<sub>3</sub>)<sub>2</sub>-arylazide ( $6.4 \times 10^{-4}$  mol), in 30 mL of cyclohexene. (yield **A** + **B** yield 88%, **A/B** = 56:44, determined by <sup>1</sup>H NMR with 2,4-dinitrotoluene as internal standard).

Elemental Analysis calc. for for C<sub>15</sub>H<sub>15</sub>F<sub>6</sub>N C, 55.73; H, 4.68; N, 4.33; found: C, 56.09; H, 4.90; N, 4.67;

Compound **A** <sup>1</sup>H NMR (300 MHz, CDCl<sub>3</sub>, 300 K) δ: 7.11 (1H, s, H<sub>Ar</sub>), 6.93 (2H, s, H<sub>Ar</sub>), 5.44-5.43 (1H, m, CH=C-CH<sub>3</sub>), 4.13 (1H, br s, NH), 4.01 (1H, br s, CHNH), 1.98-1.95 (2H, m, CH<sub>2</sub>), 1.88-1.83 (2H, m, CH<sub>2</sub>), 1.72 (3H, s, CH<sub>3</sub>), 1.71-1.64 (2H, m, CH<sub>2</sub>);

Compound **B** <sup>1</sup>H NMR (300 MHz, CDCl<sub>3</sub>, 300 K) δ: 7.11 (1H, s, H<sub>Ar</sub>), 6.93 (2H, s, H<sub>Ar</sub>), 5.68-5.66 (1H, m, CH=C-CH<sub>3</sub>), 4.13 (1H, br s, NH), 3.84 (1H, br s, CHNH), 2.04-2.02 (2H, m, CH<sub>2</sub>), 1.75 (3H, m, CH<sub>3</sub>), 1.70-1.56 (4H, m, CH<sub>2</sub>)

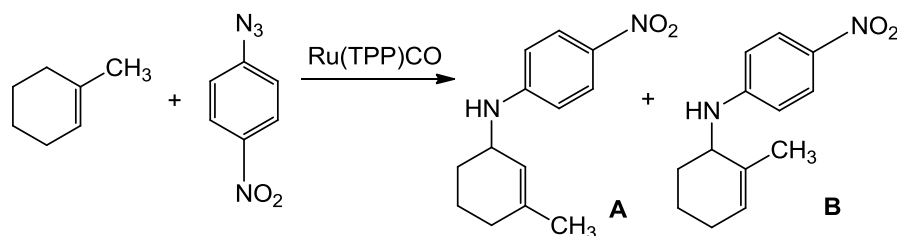
Compound **A** <sup>13</sup>C NMR (75 MHz, CDCl<sub>3</sub>, 298 K) δ: 148.7 (C), 139.7 (C), 132.9 (q, *J* 30.9 Hz, C-CF<sub>3</sub>), 124.0 (q, *J* 270.9 Hz, CF<sub>3</sub>), 121.6 (CH), 112.5 (CH), 110.0 (CH), 48.7 (CH), 30.4 (CH<sub>2</sub>), 28.5 (CH<sub>2</sub>), 24.1 (CH<sub>3</sub>), 20.0 (CH<sub>2</sub>);

Compound **B** <sup>13</sup>C NMR (75 MHz, CDCl<sub>3</sub>, 298 K) δ: 148.2 (C), 133.3 (C), 132.9 (q, *J* 30.9 Hz, C-CF<sub>3</sub>), 127.2 (CH), 124.0 (q, *J* 270.9 Hz, CF<sub>3</sub>), 112.2 (CH), 110.0 (CH), 51.4 (CH), 28.1 (CH<sub>2</sub>), 25.5 (CH<sub>2</sub>), 21.9 (CH<sub>3</sub>), 18.2 (CH<sub>2</sub>);

<sup>19</sup>F NMR (282 MHz; CDCl<sub>3</sub>, 298 K) δ: -63.56

*m/z* (ESI) 323 [M<sup>+</sup>].

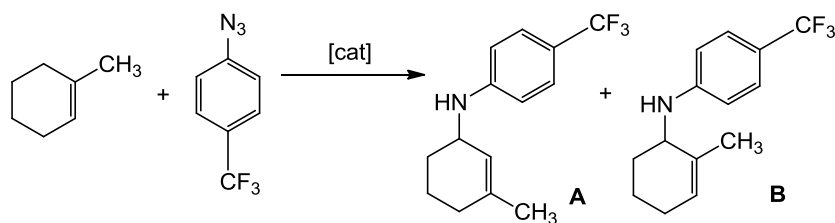
### 3.9.10. *N*-(3-methylcyclohex-2-enyl)-4-nitroaniline (108bA) + *N*-(2-methylcyclohex-2-enyl)-4-nitroaniline (108bB)



The general procedure A was followed with 11 mg of Ru(TPP)CO ( $1.5 \times 10^{-5}$  mol), 0.12 g of 4-NO<sub>2</sub>-arylazide ( $7.4 \times 10^{-4}$  mol), 0.44 mL of 1-methyl-1-cyclohexene ( $3.7 \times 10^{-3}$  mol) in 30 mL of benzene. (yield **A** + **B** 20 %, determined by <sup>1</sup>H NMR with 2,4-dinitrotoluene as internal standard).

The collected analytical data for *N*-(3-methylcyclohex-2-enyl)-4-nitroaniline (**A**) + *N*-(2-methylcyclohex-2-enyl)-4-nitroaniline (**B**) are in agreement with those reported in the literature.<sup>260</sup>

### 3.9.11. *N*-(3-methylcyclohex-2-enyl)-4-trifluoromethylaniline (108eA) + *N*-(2-methylcyclohex-2-enyl)-4-trifluoromethylaniline (108eB)



The general procedure A was followed with 11 mg of Ru(TPP)CO ( $1.5 \times 10^{-5}$  mol), 0.12 g of 4-CF<sub>3</sub>-arylazide ( $7.4 \times 10^{-4}$  mol), 0.44 mL of 1-methyl-1-cyclohexene ( $3.7 \times 10^{-3}$  mol) in 30 mL of benzene. (yield **A + B** 26 %, **A/B** = 65:35, determined by <sup>1</sup>H NMR with 2,4-dinitrotoluene as internal standard).

The general procedure A was followed with 14 mg of complex **116** ( $1.35 \times 10^{-5}$  mol), 0.13 g of 4-CF<sub>3</sub>-arylazide ( $6.7 \times 10^{-4}$  mol), 0.44 mL of 1-methyl-1-cyclohexene ( $3.7 \times 10^{-3}$  mol). (yield **A + B** 30 %, **A/B** = 65:35, determined by <sup>1</sup>H NMR with 2,4-dinitrotoluene as internal standard).

The general procedure A was followed with 15 mg of complex **117** ( $1.66 \times 10^{-5}$  mol), 0.15 g of 4-CF<sub>3</sub>-arylazide ( $8.3 \times 10^{-4}$  mol), 0.44 mL of 1-methyl-1-cyclohexene ( $3.7 \times 10^{-3}$  mol). (yield **A + B** 42 %, **A/B** = 66:33, determined by <sup>1</sup>H NMR with 2,4-dinitrotoluene as internal standard).

The general procedure B was followed with 14 mg of complex **117** ( $1.66 \times 10^{-6}$  mol), 0.15 g of 4-CF<sub>3</sub>-arylazide ( $8.3 \times 10^{-4}$  mol), in 30 mL of 1-methyl-1-cyclohexene. (yield **A + B** 99 %, determined by <sup>1</sup>H NMR with 2,4-dinitrotoluene as internal standard).

Compound **A** <sup>1</sup>H NMR (300 MHz, CDCl<sub>3</sub>, 300 K)  $\delta$ : 7.41 (2H, d, *J* 8.4), 6.63 (2H, d, *J* 8.4), 5.66 (1H, br s, CH=C(CH<sub>3</sub>)), 4.01 (1H, br s, NH), 3.86 (1H, br s, CHNH), 2.05-1.88 (3H, m, CH<sub>2</sub>), 1.77 (3H, s, CH<sub>3</sub>), 1.63-1.56 (3H, m, CH<sub>2</sub>);

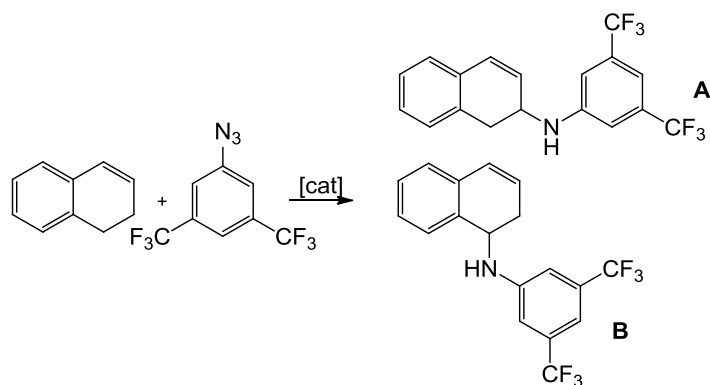
Compound **B** <sup>1</sup>H NMR (300 MHz, CDCl<sub>3</sub>, 300 K)  $\delta$ : 7.40 (2H, d, *J* 8.7), 6.62 (2H, d, *J* 8.7), 5.48 (1H, br s, CH=C(CH<sub>3</sub>)), 4.00 (2H, m, CHNH), 1.98 (2H, m, CH<sub>2</sub>), 1.86-1.84 (1H, m, CH<sub>2</sub>), 1.72 (3H, s, CH<sub>3</sub>), 1.71-1.61 (3H, m, CH<sub>2</sub>);

Compound **A** <sup>13</sup>C NMR (75 MHz, CDCl<sub>3</sub>, 298 K)  $\delta$ : 150.2 (C), 133.5 (C), 126.7 (CH), 126.4 (CH), 118.1 (CCF<sub>3</sub>, q, *J* 32.1 Hz), 111.8 (CH), 50.8 (CH), 28.0 (CH<sub>2</sub>), 25.2 (CH<sub>2</sub>), 21.6 (CH<sub>3</sub>), 17.7 (CH<sub>2</sub>); CF<sub>3</sub> signal was not detected;

Compound **B** <sup>13</sup>C NMR (75 MHz, CDCl<sub>3</sub>, 298 K)  $\delta$ : 150.2 (C), 139.1 (C), 127.0 (CH), 122.4 (CH), 118.7 (q, *J* 32.6 Hz, CCF<sub>3</sub>), 112.5 (CH), 48.4 (CH), 30.4 (CH<sub>2</sub>), 28.7 (CH<sub>2</sub>), 24.2 (CH<sub>3</sub>), 20.1 (CH<sub>3</sub>); CF<sub>3</sub> signal was not detected.

### 3.9.12. *N*-(3,5-bis(trifluoromethyl)phenyl)-1,2-dihydronaphthalen-2-amine (109aA) and *N*-(3,5-bis(trifluoromethyl)phenyl)-1,2-dihydronaphthalen-1-amine (109aB).





The general procedure A was followed with 11 mg of Ru(TPP)CO ( $1.5 \times 10^{-5}$  mol), 0.19 g of 3,5-(CF<sub>3</sub>)<sub>2</sub>-arylazide ( $7.4 \times 10^{-4}$  mol), 0.48 mL of 1,2-dihydronaphthalene ( $3.7 \times 10^{-3}$  mol) in 30 mL of benzene. (yield **A + B** 57 %, **A/B** = 58:42, determined by <sup>1</sup>H NMR with 2,4-dinitrotoluene as internal standard).

The general procedure B was followed with 11 mg of Ru(TPP)CO ( $1.5 \times 10^{-6}$  mol), 0.19 mg 3,5-(CF<sub>3</sub>)<sub>2</sub>-arylazide ( $7.4 \times 10^{-4}$  mol), in 30 mL of 1,2-dihydronaphthalene (yield **A + B** 85 %, **A/B** = 60:40, determined by <sup>1</sup>H NMR with 2,4-dinitrotoluene as internal standard).

The general procedure A was followed with 15 mg of complex **113** ( $1.28 \times 10^{-5}$  mol), 0.16 g of 3,5-(CF<sub>3</sub>)<sub>2</sub>-arylazide ( $6.4 \times 10^{-4}$  mol), 0.48 mL of 1,2-dihydronaphthalene ( $3.7 \times 10^{-3}$  mol) in 30 mL of benzene. (yield **A + B** 60 %, **A/B** = 65:35, determined by <sup>1</sup>H NMR with 2,4-dinitrotoluene as internal standard).

Elemental Analysis calc. for C<sub>18</sub>H<sub>13</sub>F<sub>6</sub>N: C, 60.51; H, 3.67; N, 3.92; found: C, 60.80; H, 3.82; N, 4.00;

Compound **A** <sup>1</sup>H NMR (300 MHz, CDCl<sub>3</sub>, 300 K)  $\delta$ : 7.26-7.13 (5H, m, H<sub>Ar</sub>), 6.95 (2H, s, H<sub>Ar</sub>), 6.65 (1H, d, *J* 9.3 Hz, CH=CH-CH(NH)), 6.08 (1H, dd, *J* 9.3 and 4.5 Hz, CH=CH-CH(NH)), 4.38 (1H, dddd, *J* 8.4, 6.3, 6.3 and 4.5 Hz, CH(NH)), 4.16 (1H, d, *J* 8.4 Hz, NH), 3.12 (1H, dd, *J* 15.9 and 6.3 Hz, CH<sub>2</sub>), 3.02 (1H, dd, *J* 15.9 and 6.3 Hz, CH<sub>2</sub>);

Compound **B** <sup>1</sup>H NMR (300 MHz, CDCl<sub>3</sub>, 300 K)  $\delta$ : 7.34-7.24 (3H, m, H<sub>Ar</sub>), 7.19-7.17 (2H, m, H<sub>Ar</sub>), 7.01 (2H, s, H<sub>Ar</sub>), 6.62 (1H, dt, *J* 9.6 and 1.6 Hz, CH=CH-CH<sub>2</sub>), 6.02 (1H, dt, *J* 9.6 and 4.3 Hz, CH=CH-CH<sub>2</sub>), 4.76 (1H, dt, *J* 8.6 and 6.3 Hz, CH=NH), 4.37 (1H, d, *J* 8.6 Hz, NH), 2.64 (2H, ddd, *J* 6.3, 4.3 and 1.6 Hz, CH<sub>2</sub>);

Compound **A** <sup>13</sup>C NMR (75 MHz, CDCl<sub>3</sub>, 298 K)  $\delta$ : 147.2 (C), 132.4 (q, *J* 32.8 Hz, C-CF<sub>3</sub> overlapping with another quaternary carbon), 129.9 (CH), 128.6 (CH), 127.8 (CH), 127.1 (CH, two signals overlaid), 126.6 (CH), 123.4 (q, *J* 270.8 Hz, CF<sub>3</sub>), 112.1 (CH), 110.2 (CH), 46.4 (CH), 33.3 (CH<sub>2</sub>);

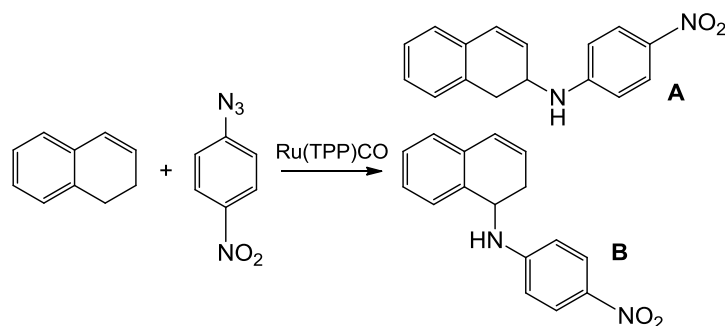
Compound **B** <sup>13</sup>C NMR (75 MHz, CDCl<sub>3</sub>, 298 K)  $\delta$ : 147.7 (C), 134.5 (C), 133.3 (C), 132.6 (q, *J* 32.8 Hz, C-CF<sub>3</sub>), 128.5 (CH), 128.0 (CH), 127.8 (CH), 126.9 (CH, two signals overlaid), 125.7 (CH), 123.5 (q, *J* 270.9 Hz, CF<sub>3</sub>), 112.3 (CH), 110.3 (CH), 50.4 (CH), 29.4 (CH<sub>2</sub>);

Compound **A** <sup>19</sup>F NMR (282 MHz; CDCl<sub>3</sub>, 298 K)  $\delta$ : -63.17;

Compound **B** <sup>19</sup>F NMR (282 MHz; CDCl<sub>3</sub>, 298 K)  $\delta$ : -63.50;

*m/z* (ESI) 357 [M<sup>+</sup>].

### 3.9.13. *N*-(4-nitrophenyl)-1,2-dihydronaphthalen-2-amine (109bA) + *N*-(4-nitrophenyl)-1,2-dihydronaphthalen-1-amine (109bB)



The general procedure A was followed with 12 mg of Ru(TPP)CO ( $1.6 \times 10^{-5}$  mol), 0.13 g of 4-NO<sub>2</sub>-arylazide ( $8.1 \times 10^{-4}$  mol), 0.48 mL of 1,2-dihydronaphthalene ( $3.7 \times 10^{-3}$  mol) in 30 mL of benzene. (yield **A + B** 54 %, **A/B** = 59:41, determined by <sup>1</sup>H NMR with 2,4-dinitrotoluene as internal standard).

The general procedure B was followed with 12 mg of Ru(TPP)CO ( $1.6 \times 10^{-5}$  mol), 0.13 g of 4-NO<sub>2</sub>-arylazide ( $8.1 \times 10^{-4}$  mol), in 30 mL of 1,2-dihydronaphthalene ( $3.7 \times 10^{-3}$  mol) in 30 mL of benzene. (yield **A + B** 73 %, **A/B** = 61:39, determined by <sup>1</sup>H NMR with 2,4-dinitrotoluene as internal standard).

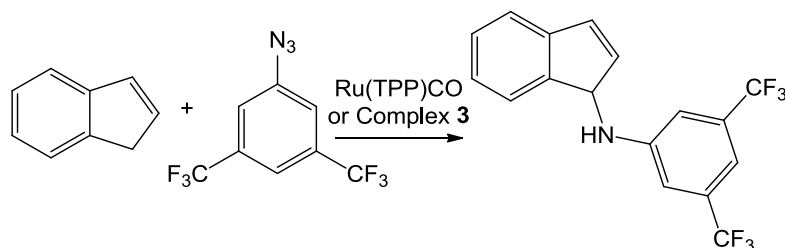
Elemental Analysis calc. for C<sub>16</sub>H<sub>14</sub>N<sub>2</sub>O<sub>2</sub>: C, 82.02; H, 6.02; N, 11.96; found: C, 82.12; H, 6.13; N, 12.00;

Compound **A** <sup>1</sup>H NMR (300 MHz, CDCl<sub>3</sub>, 300 K)  $\delta$ : 8.11 (2H, d, *J* 9.0 Hz, H<sub>Ar</sub>), 7.27-7.16 (4H, m, H<sub>Ar</sub>), 6.69 (1H, d, *J* 9.6 Hz, CH=CH-CH), 6.58 (1H, d, *J* 9.0 Hz, H<sub>Ar</sub>), 6.10 (1H, dd, *J* 9.6 Hz, *J* 4.5 Hz, CH=CH-CH), 4.51 (1H, m, CHNH), 4.46 (1H, m, NH), 3.11 (2H, m, CH<sub>2</sub>);

Compound **A** <sup>13</sup>C NMR (75 MHz, CDCl<sub>3</sub>, 298 K)  $\delta$ : 154.2 (C), 152.3 (C), 130.8 (CH), 129.2 (CH), 128.4 (CH), 127.7 (CH), 127.3 (CH), 126.9 (CH), 112.0 (CH), 47.1 (CH), 34.0 (CH<sub>2</sub>). Two quaternary carbon atoms were not detected;

*m/z* (ESI) 266 [M<sup>+</sup>].

### 3.9.14. *N*-(3,5-bis(trifluoromethyl)phenyl)-1*H*-inden-1-amine (110a)



The general procedure A was followed with 11 mg of Ru(TPP)CO ( $1.5 \times 10^{-5}$  mol), 0.18 g of 3,5-(CF<sub>3</sub>)<sub>2</sub>-arylazide ( $7.4 \times 10^{-4}$  mol), 0.43 mL of indene ( $3.7 \times 10^{-3}$  mol) in 30 mL of benzene. (yield 42 %, determined by <sup>1</sup>H NMR with 2,4-dinitrotoluene as internal standard).

The general procedure A was followed with 15 mg of complex **113** ( $1.28 \times 10^{-5}$  mol), 0.16 g of 3,5-(CF<sub>3</sub>)<sub>2</sub>-arylazide ( $6.4 \times 10^{-4}$  mol), 0.37 mL of indene ( $3.2 \times 10^{-3}$  mol) in 30 mL of benzene. (yield 55%, determined by <sup>1</sup>H NMR with 2,4-dinitrotoluene as internal standard).

The general procedure B was followed with 15 mg of complex **113** ( $1.28 \times 10^{-6}$  mol), 0.16 g 3,5-(CF<sub>3</sub>)<sub>2</sub>-arylazide ( $6.4 \times 10^{-4}$  mol), in 30 mL of indene. (yield 70%, determined by <sup>1</sup>H NMR with 2,4-dinitrotoluene as internal standard).

Elemental Analysis calc. for C<sub>17</sub>H<sub>11</sub>F<sub>6</sub>N: C, 59.48; H, 3.23; N, 4.08; found: C, 59.68; H, 3.38; N, 4.05;

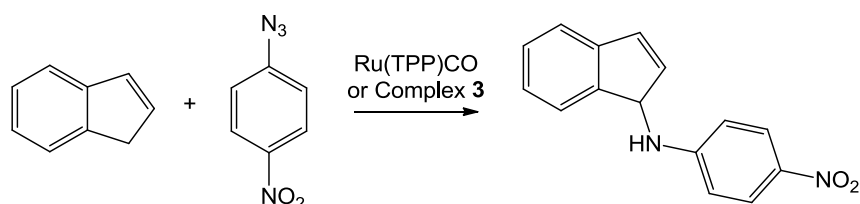
<sup>1</sup>H NMR (300 MHz, CDCl<sub>3</sub>, 300 K)  $\delta$ : 7.46 (1H, d, *J* 7.5 Hz, H<sub>Ar</sub>), 7.38-7.35 (2H, m, H<sub>Ar</sub>), 7.27-7.24 (1H, m, H<sub>Ar</sub>), 7.22 (1H, s, H<sub>Ar</sub>), 7.04 (2H, s, H<sub>Ar</sub>), 6.92 (1H, dd, *J* 5.7 and 1.8 Hz, CH=CH-CH), 6.53 (1H, d, *J* 5.7 and 1.8 Hz, CH=CH-CH), 5.16 (1H, d, *J* 8.7 Hz, CHNH), 4.34 (1H, d, *J* 8.7 Hz, NH);

<sup>13</sup>C NMR (75 MHz, CDCl<sub>3</sub>, 298 K)  $\delta$ : 148.5 (C), 144.0 (C), 143.2 (C), 135.3 (CH), 133.7 (CH), 132.8 (q, *J* 33.4 Hz, C-CF<sub>3</sub>), 128.8 (CH), 126.4 (CH), 123.7 (q, *J* 273.0 Hz, CF<sub>3</sub>), 123.4 (CH), 122.0 (CH), 112.8 (CH), 111.0 (CH), 61.2 (CH);

<sup>19</sup>F NMR (282 MHz; CDCl<sub>3</sub>, 298 K)  $\delta$ : -63.57

*m/z* (ESI) 343 [M<sup>+</sup>].

### 3.9.15. *N*-(4-nitrophenyl)-1*H*-inden-1-amine (110b)



The general procedure A was followed with 11 mg of Ru(TPP)CO ( $1.5 \times 10^{-5}$  mol), 0.12 mg of 4-NO<sub>2</sub>-arylazide ( $7.4 \times 10^{-4}$  mol), 0.43 mL of indene ( $3.7 \times 10^{-3}$  mol) in 30 mL of benzene. (yield 42 %, determined by <sup>1</sup>H NMR with 2,4-dinitrotoluene as internal standard).

The general procedure A was followed with 15 mg of complex **113** ( $1.28 \times 10^{-5}$  mol), 0.11 g of 4-NO<sub>2</sub>-arylazide ( $6.4 \times 10^{-4}$  mol), 0.37 mL of indene ( $3.2 \times 10^{-3}$  mol) in 30 mL of benzene. (yield 55%, determined by <sup>1</sup>H NMR with 2,4-dinitrotoluene as internal standard).

The general procedure B was followed with 15 mg of complex **113** ( $1.28 \times 10^{-6}$  mol), 0.11 g of 4-NO<sub>2</sub>-arylazide ( $6.4 \times 10^{-4}$  mol), in 30 mL of indene. (yield 70%, determined by <sup>1</sup>H NMR with 2,4-dinitrotoluene as internal standard).

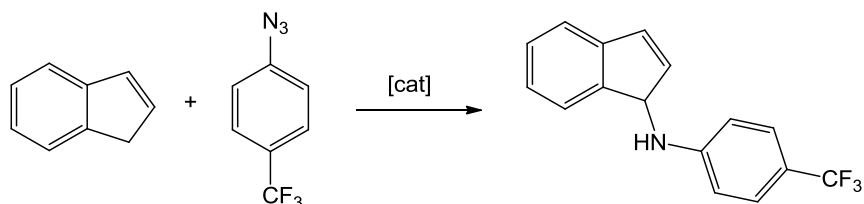
Elemental Analysis calc. for C<sub>15</sub>H<sub>12</sub>N<sub>2</sub>O<sub>2</sub>: C, 81.79; H, 5.49; N, 12.72; found: C, 81.89; H, 5.60; N, 12.77;

<sup>1</sup>H NMR (300 MHz, CDCl<sub>3</sub>, 300 K)  $\delta$ : 8.12 (2H, d,  $J = 9.3$  Hz, H<sub>Ar</sub>), 7.45-7.50 (1H, d,  $J = 7.2$  Hz, H<sub>Ar</sub>), 7.36-7.39 (2H, m, H<sub>Ar</sub>), 7.27-7.24 (1H, m, H<sub>Ar</sub>), 6.94 (1H, dd,  $J = 5.6$  Hz,  $J = 1.2$  Hz, CH=CH-CH) 6.66 (2H, d,  $J = 9.3$  Hz, H<sub>Ar</sub>), 6.53 (1H, dd,  $J = 5.6$  Hz,  $J = 1.8$  Hz, CH=CH-CH), 5.21 (1H, dd,  $J = 8.4$  Hz,  $J = 1.2$  Hz, CHNH), 4.71 (1H, d,  $J = 8.4$  Hz, NH);

<sup>13</sup>C NMR (75 MHz, CDCl<sub>3</sub>, 298 K)  $\delta$ : 153.3 (C), 144.0 (C), 143.4 (C), 139.6 (C), 135.4 (CH), 134.1 (CH), 129.1 (CH), 126.8 (CH), 126.7 (CH), 123.6 (CH), 122.4 (CH), 112.3 (CH), 61.2 (CH);

$m/z$  (ESI) 252 [M<sup>+</sup>].

### 3.9.16. *N*-(4-(trifluoromethyl)phenyl)-1*H*-inden-1-amine (**110e**)



The general procedure A was followed with 11 mg of Ru(TPP)CO ( $1.5 \times 10^{-5}$  mol), 0.14 g of 4-CF<sub>3</sub>-arylazide ( $7.4 \times 10^{-4}$  mol), 0.43 mL of indene ( $3.7 \times 10^{-3}$  mol) in 30 mL of benzene. (yield 30 %, determined by <sup>1</sup>H NMR with 2,4-dinitrotoluene as internal standard).

The general procedure A was followed with 14 mg of complex **116** ( $1.35 \times 10^{-5}$  mol), 0.13 g of 4-CF<sub>3</sub>-arylazide ( $6.7 \times 10^{-4}$  mol), 0.39 mL of indene ( $3.4 \times 10^{-3}$  mol). (yield 14 %, determined by <sup>1</sup>H NMR with 2,4-dinitrotoluene as internal standard).

The general procedure A was followed with 15 mg of complex **117** ( $1.66 \times 10^{-5}$  mol), 0.15 g of 4-CF<sub>3</sub>-arylazide ( $8.3 \times 10^{-4}$  mol), 0.48 mL of indene ( $4.20 \times 10^{-3}$  mol). (yield 17 %, determined by <sup>1</sup>H NMR with 2,4-dinitrotoluene as internal standard).

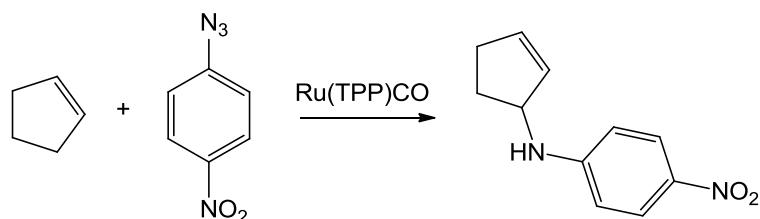
Elemental Analysis calc. for C<sub>16</sub>H<sub>12</sub>NF<sub>3</sub>: C, 69.81; H, 4.39; N, 5.09; found: C, 69.94; H, 4.73; N, 5.56;

<sup>1</sup>H NMR (300 MHz, CDCl<sub>3</sub>, 300 K)  $\delta$ : 7.50 (1H, d,  $J 7.5$  Hz, H<sub>Ar</sub>), 7.45 (2H, d,  $J 8.4$  Hz, H<sub>Ar</sub>), 7.37 (2H, m, H<sub>Ar</sub>), 7.24 (1H, m, H<sub>Ar</sub>), 6.90 (1H, dd,  $J 5.70$  Hz,  $J 1.2$  Hz, CH=CH), 6.74 (2H, d,  $J 8.4$  Hz, H<sub>Ar</sub>), 6.57 (1H, dd,  $J 5.7$  Hz,  $J 1.8$  Hz, CH=CH), 5.18 (1H, d,  $J 8.7$  Hz, CHNH), 4.23 (1H, d,  $J 8.7$  Hz, NH);

<sup>13</sup>C NMR (75 MHz, CDCl<sub>3</sub>, 298 K)  $\delta$ : 150.2 (C), 144.4 (C), 143.0 (C), 135.9 (CH), 132.9 (CH), 126.9 (CH), 126.7 (C), 126.5 (CH), 112.7 (CH), 110.1 (C), 61.1 (CH);

<sup>19</sup>F NMR (282 MHz; CDCl<sub>3</sub>, 298 K)  $\delta$ : -61.40

### 3.9.17. *N*-(cyclopent-2-enyl)-4-nitroaniline (111)



The general procedure A was followed with 11 mg of Ru(TPP)CO ( $1.5 \times 10^{-5}$  mol), 0.12 g of 4-NO<sub>2</sub>-arylazide ( $7.5 \times 10^{-4}$  mol), 0.25 mL of cyclopentene ( $3.7 \times 10^{-3}$  mol) in 30 mL of benzene. (yield 30 %, determined by <sup>1</sup>H NMR with 2,4-dinitrotoluene as internal standard).

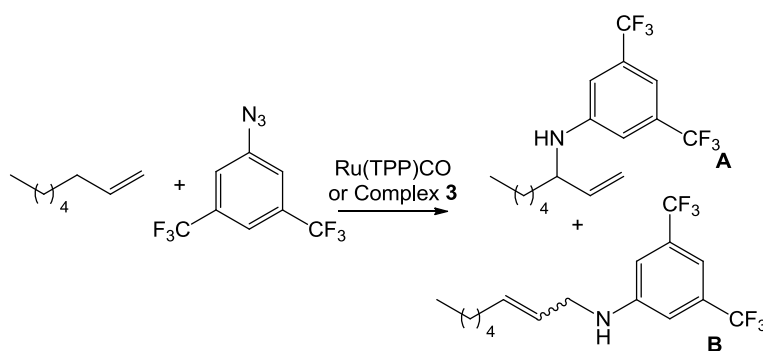
Elemental Analysis calc. for C<sub>11</sub>H<sub>12</sub>N<sub>2</sub>O<sub>2</sub>: C, 64.69; H, 5.92; N, 13.72; found: C, 64.54; H, 5.83; N, 13.98;

<sup>1</sup>H NMR (300 MHz, C<sub>6</sub>D<sub>6</sub>, 300 K)  $\delta$ : 8.12 (2H, d,  $J = 9.0$  Hz, H<sub>Ar</sub>), 5.97 (2H, d,  $J = 9.0$  Hz, H<sub>Ar</sub>), 5.75 (1H, m, CH=CH), 5.47 (1H, m, CH=CH), 4.01 (1H, m, CHNH), 3.73 (1H, br s, NH), 2.20-2.12 (2H, m, CH<sub>2</sub>), 1.93-1.91 (1H, m, CH<sub>2</sub>), 1.30-1.24 (1H, m, CH<sub>2</sub>);

<sup>13</sup>C NMR (75 MHz, CDCl<sub>3</sub>, 298 K)  $\delta$ : 152.5 (C), 138.8 (C), 135.2 (CH), 130.7 (CH), 126.5 (CH), 111.6 (CH), 59.1 (CH), 31.4 (CH<sub>2</sub>), 31.1 (CH<sub>2</sub>);

$m/z$  (ESI) 204 [M<sup>+</sup>].

### 3.9.18. 3,5-Bis(trifluoromethyl)-*N*-(oct-1-en-3-yl)benzenamine (112A) and (*E/Z*)-3,5-bis(trifluoromethyl)-*N*-(oct-2-enyl)benzenamine (112B)



The general procedure A was followed with 11 mg of Ru(TPP)CO ( $1.5 \times 10^{-5}$  mol), 0.18 g of 3,5-(CF<sub>3</sub>)<sub>2</sub>-arylazide ( $7.4 \times 10^{-4}$  mol), 0.59 mL of 1-octene ( $3.7 \times 10^{-3}$  mol) in 30 mL of benzene. (yield **A** + **B** 20 %, **A/B** =45:55, determined by <sup>1</sup>H NMR with 2,4-dinitrotoluene as internal standard).

The general procedure A was followed with 15 mg of complex **113** ( $1.28 \times 10^{-5}$  mol), 0.16 g of 3,5-(CF<sub>3</sub>)<sub>2</sub>-arylazide ( $6.4 \times 10^{-4}$  mol), 0.50 mL of 2-octene ( $3.2 \times 10^{-3}$  mol) in 30 mL of benzene. (yield **A** + **B** 11 %, **A/B** =45:55, determined by <sup>1</sup>H NMR with 2,4-dinitrotoluene as internal standard).

The general procedure B was followed with 15 mg of complex **113** ( $1.28 \times 10^{-6}$  mol), 0.16 g 3,5-(CF<sub>3</sub>)<sub>2</sub>-arylazide ( $6.4 \times 10^{-4}$  mol), in 30 mL of 1-octene. (yield **A** + **B** 22 %, **A/B** =50:50, determined by <sup>1</sup>H NMR with 2,4-dinitrotoluene as internal standard).

Elemental Analysis calc. for C<sub>16</sub>H<sub>19</sub>F<sub>6</sub>N: C, 56.63; H, 5.64; N, 4.13; found: C, 57.02; H, 6.00; N, 4.06;

Compound **A** <sup>1</sup>H NMR (300 MHz, CDCl<sub>3</sub>, 300 K) δ: 7.13 (1 H, s, H<sub>Ar</sub>), 6.94 (2 H, s, H<sub>Ar</sub>), 5.72 (1 H, ddd, *J* 17.2, 10.3 and 6.1 Hz, CH=CH<sub>2</sub>), 5.23 (1 H, d, *J* 17.2 Hz, CH=CH<sub>2</sub>), 5.20 (1H, d, *J* 10.3 Hz, CH=CH<sub>2</sub>), 4.09 (1 H, d, *J* 6.9 Hz, NH), 3.87-3.83 (1 H, m, CH(NH)), 1.65-1.61 (2 H, m, CH<sub>2</sub>), 1.36-1.30 (6 H, m, CH<sub>2</sub>), 0.92 (3 H, pst, *J* 6.9 Hz, CH<sub>3</sub>);

Compound **B** (E/Z = 63:37) (E isomer) <sup>1</sup>H NMR (300 MHz, CDCl<sub>3</sub>, 300 K) δ: 7.16 (1 H, s, H<sub>Ar</sub>), 6.96 (2 H, s, H<sub>Ar</sub>), 5.77-5.64 (1 H, m, CH=CH), 5.54-5.51 (1 H, m, CH=CH), 4.20 (1 H, br s, NH), 3.79-3.76 (2 H, m, CH<sub>2</sub>), 2.09-2.05 (2 H, m, CH<sub>2</sub>CH=CH), 1.40-1.20 (6 H, m, CH<sub>2</sub>), 0.93-0.89 (3 H, m, CH<sub>3</sub>);

(Z isomer) <sup>1</sup>H NMR (300 MHz, CDCl<sub>3</sub>, 300 K) δ: 7.17 (1 H, s, H<sub>Ar</sub>), 6.96 (2 H, s, H<sub>Ar</sub>), 5.77-5.64 (1 H, m, CH=CH), 5.54-5.51 (1 H, m, CH=CH), 4.12 (1H, br s, NH), 3.84-3.81 (2 H, m, CH<sub>2</sub>), 2.17-2.14 (2 H, m, CH<sub>2</sub>CH=CH), 1.40-1.20 (6 H, m, CH<sub>2</sub>), 0.93-0.89 (3 H, m, CH<sub>3</sub>);

Compound **A** <sup>13</sup>C NMR (75 MHz, CDCl<sub>3</sub>, 298 K) δ: 148.5 (C), 138.9 (CH), 132.6 (q, *J* 32.4 Hz, C-CF<sub>3</sub>), 124.0 (q, *J* 270.8 Hz, CF<sub>3</sub>), 116.4 (CH<sub>2</sub>), 112.8 (CH), 110.4 (br, CH), 56.4 (CH), 36.1 (CH<sub>2</sub>), 32.0 (CH<sub>2</sub>), 25.9 (CH<sub>2</sub>), 22.9 (CH<sub>2</sub>), 14.4 (CH<sub>3</sub>);

Compound **B** <sup>13</sup>C NMR (75 MHz, CDCl<sub>3</sub>, 298 K) δ: 148.7 (C), 134.8 (CH), 134.7 (CH), 132.3 (m, C-CF<sub>3</sub>), 125.0 (CH), 124.9 (CH), 112.0 (CH), 111.9 (CH), 110.1 (CH), 45.7 (CH<sub>2</sub>), 40.8 (CH<sub>2</sub>), 32.3 (CH<sub>2</sub>), 31.5 (CH<sub>2</sub>), 31.3 (CH<sub>2</sub>), 29.1 (CH<sub>2</sub>), 28.8 (CH<sub>2</sub>), 27.6 (CH<sub>2</sub>), 22.4 (CH<sub>2</sub>), 14.0 (CH<sub>3</sub>)

<sup>19</sup>F NMR (282 MHz; CDCl<sub>3</sub>, 298 K) δ: -63.55

*m/z* (ESI) 339 [M<sup>+</sup>].

### 3.9.19. ***N*-(3,5-bis(trifluoromethyl)phenyl)-1,2-dihydro-4-phenyl-naphthalen-2-amine (114A) and 1-(3,5-bis(trifluoromethyl)phenyl)-1a,2,3,7b-tetrahydro-7b-phenyl-1*H*-naphtho[2,1-*b*]azirine (114B)**

The general procedure A was followed with 15 mg of complex **113** ( $1.28 \times 10^{-5}$  mol), 0.16 g of 3,5-(CF<sub>3</sub>)<sub>2</sub>-arylazide ( $6.4 \times 10^{-4}$  mol), 0.60 mL of 1-phenyl-3,4-dihydronaphthalene ( $3.2 \times 10^{-3}$  mol) in 30 mL of benzene. (yield **A** + **B** 61 %, **A/B** =54:46, determined by <sup>1</sup>H NMR with 2,4-dinitrotoluene as internal standard).

Elemental Analysis calc. for C<sub>24</sub>H<sub>17</sub>F<sub>6</sub>N C, 66.51; H, 3.95; N, 3.23; found: C, 66.65; H, 4.01; N, 3.18;

Compound **A**  $^1\text{H}$  NMR (300 MHz,  $\text{CDCl}_3$ , 300 K)  $\delta$ : 7.42-7.37 (5H, m,  $\text{H}_{\text{Ar}}$ ), 7.28-7.25 (3H, m,  $\text{H}_{\text{Ar}}$ ), 7.19 (1H, s,  $\text{H}_{\text{Ar}}$ ), 7.14-7.12 (1H, m,  $\text{H}_{\text{Ar}}$ ), 7.01 (2H, s,  $\text{H}_{\text{Ar}}$ ), 6.10 (1H, d,  $J$  4.6 Hz,  $\text{C}(\text{Ph})=\text{CH}-\text{CH}(\text{NH})$ ), 4.51 (1H, m,  $\text{CH}(\text{NH})$ ), 4.26 (1H, d,  $J$  8.9 Hz, NH), 3.22 (1H, dd,  $J$  15.4 and 5.7 Hz,  $\text{CH}_2$ ), 3.05 (1H, dd,  $J$  15.4 and 7.2 Hz,  $\text{CH}_2$ );

Compound **A**  $^{13}\text{C}$  NMR (75 MHz,  $\text{CDCl}_3$ , 298 K)  $\delta$ : 147.8 (C), 142.5 (C), 139.8 (C), 134.2 (C), 134.1 (C), 133.0 (q,  $J$  32.8 Hz,  $\text{C}-\text{CF}_3$ ), 129.3 (CH), 128.8 (CH), 128.4 (CH), 128.3 (CH), 127.4 (CH), 126.8 (CH), 126.6 (CH), 123.9 (q,  $J$  271.0 Hz,  $\text{CF}_3$ ), 112.8 (CH), 110.8 (CH), 47.7 (CH), 34.7 ( $\text{CH}_2$ );

Compound **A**  $^{19}\text{F}$  NMR (282 MHz;  $\text{CDCl}_3$ , 298 K)  $\delta$ : -63.51  
m/z (ESI) 433 [ $\text{M}^+$ ];

Compound **B** was isolated by chromatography in mixture with 1-phenylnaphthalene due to the very similar  $R_f$  values of these compounds in several solvents on both alumina and silica. The presence of 1-phenylnaphthalene was confirmed by GC-MS analysis. The  $^1\text{H}$ ,  $^{13}\text{C}$ ,  $^{19}\text{F}$  spectra of this mixture is reported. The  $^1\text{H}$  and  $^{13}\text{C}$  NMR signals of **B** have been attributed by COSY, NOESY, HSQC and HMBC techniques.

### 3.11.2. General procedure for kinetic measurements

To a Schlenk flask under a nitrogen atmosphere were added the catalyst, aryl azide and cyclohexene in this order. When required, benzene was added at this point. The flask was capped with a rubber septum and immediately placed in an oil bath preheated at 75 °C. The solution was stirred for one minute to dissolve all reagents and 0.2 mL solution was withdrawn for IR analysis. The consumptions of the aryl azide was followed by IR spectroscopy ( $2095\text{-}2130\text{ cm}^{-1}$ ) by withdrawing samples of the solution at regular time. Since all reactions are run in the presence of a large excess of olefin, the apparent first order constants were fitted to the equation  $-\text{d}[\text{ArN}_3]/\text{d}t = k_{\text{app}}[\text{Ru}(\text{TTP})\text{CO}][\text{ArN}_3]$ . The concentrations of catalyst was calculated on the exact amount of catalyst weighed in each run and considered to remain constant during the reaction.

### 3.9.20. Determination of kinetics order with respect to 4- $\text{CF}_3$ -arylazide by using Ru(TPP)CO as catalyst.

Catalytic reactions were carried out as described in general procedure for kinetic measurement by using Ru(TPP)CO (36.3 mg,  $4.89 \times 10^{-5}$  mol), 4- $\text{CF}_3$ -arylazide (99.5 mg,  $6.07 \times 10^{-4}$  mol) were dissolved in 30 mL of cyclohexene in a Schlenk flask under  $\text{N}_2$ . Rate constant with respect to 4- $\text{CF}_3$ -arylazide was determined using the equation  $\ln A = \ln A_0 - kt$  ( $A$  = IR absorbance value at time  $t$  and  $A_0$  = IR absorbance value at zero time).

### 3.9.21. Determination of kinetics order with respect to Ru(TPP)CO.

Catalytic reactions were carried out as described in general procedure for kinetic measurement by using 100 mg of 4-(CF<sub>3</sub>)<sub>2</sub>-arylazide and 30 mL of cyclohexene. Four different amounts of Ru(TPP)CO were employed:

a) 9.1 mg, 1.23×10<sup>-5</sup>mol, b) 19.0 mg, 2.56×10<sup>-5</sup>mol, c) 29.3 mg, 3.95×10<sup>-5</sup>mol, d) 36.3 mg, 4.89×10<sup>-5</sup>mol.

For each reaction, rate constant with respect to Ru(TPP)CO was determined using the equation  $\ln A = \ln A_0 - kt$  (A = IR absorbance value at time t and A<sub>0</sub> = IR absorbance value at zero time).

### 3.9.22. Determination of kinetics order with respect to cyclohexene.

Catalytic reactions were carried out as described in general procedure for kinetic measurement by using Ru(TPP)CO (36.3 mg, 4.89×10<sup>-5</sup>mol) and 100 mg of 4-(CF<sub>3</sub>)<sub>2</sub>-arylazide. Four different mixtures of cyclohexene and benzene were employed:

a) cyclohexene / Benzene = 7.5 mL / 22.5 mL, b) cyclohexene / Benzene = 15 mL / 15 mL, c) cyclohexene / Benzene = 22.5 mL / 7.5 mL, d) cyclohexene / Benzene = 30 mL / 0 mL.

For each reaction, rate constant with respect to cyclohexene was determined using the equation  $\ln A = \ln A_0 - kt$  (A = IR absorbance value at time t and A<sub>0</sub> = IR absorbance value at zero time).

### 3.9.23. Determination of kinetics order with respect to 3,5-(CF<sub>3</sub>)<sub>2</sub>-arylazide by using Ru(TPP)CO as catalyst.

Catalytic reactions were carried out as described in general procedure for kinetic measurement by using Ru(TPP)CO (36.3 mg, 4.89×10<sup>-5</sup>mol), 3,5-(CF<sub>3</sub>)<sub>2</sub>-arylazide (99.5 mg, 6.07×10<sup>-4</sup>mol) were dissolved in 30 mL of cyclohexene in a Schlenk flask under N<sub>2</sub>. Rate constant with respect to 3,5-(CF<sub>3</sub>)<sub>2</sub>-arylazide was determined using the equation  $\ln A = \ln A_0 - kt$  (A = IR absorbance value at time t and A<sub>0</sub> = IR absorbance value at zero time).

### 3.9.24. Determination of kinetics order with respect to Ru(TPP)CO.

Catalytic reactions were carried out as described in general procedure for kinetic measurement by using 100 mg of 3,5-(CF<sub>3</sub>)<sub>2</sub>-arylazide and 30 mL of cyclohexene. Four different amounts of Ru(TPP)CO were employed:

a) 9.1 mg, 1.23×10<sup>-5</sup>mol, b) 19.0 mg, 2.56×10<sup>-5</sup>mol, c) 29.3 mg, 3.95×10<sup>-5</sup>mol, d) 36.3 mg, 4.89×10<sup>-5</sup>mol.

For each reaction, rate constant with respect to Ru(TPP)CO was determined using the equation  $\ln A = \ln A_0 - kt$  (A = IR absorbance value at time t and A<sub>0</sub> = IR absorbance value at zero time).

### 3.9.25. Determination of kinetics order with respect to cyclohexene.



Catalytic reactions were carried out as described in general procedure for kinetic measurement by using Ru(TPP)CO (36.3 mg,  $4.89 \times 10^{-5}$  mol) and 100 mg of 3,5-(CF<sub>3</sub>)<sub>2</sub>-arylazide. Four different mixtures of cyclohexene and benzene were employed:

a) Toluene / Benzene = 7.5 mL / 22.5 mL, b) Toluene / Benzene = 15 mL / 15 mL, c) Toluene / Benzene = 22.5 mL / 7.5 mL, d) Toluene / Benzene = 30 mL / 0 mL.

For each reaction, rate constant with respect to toluene was determined using the equation  $\ln A = \ln A_0 - kt$  ( $A$  = IR absorbance value at time  $t$  and  $A_0$  = IR absorbance value at zero time).

## 3.12. Cyclopropanation Reactions

### 3.12.1. Catalytic procedures

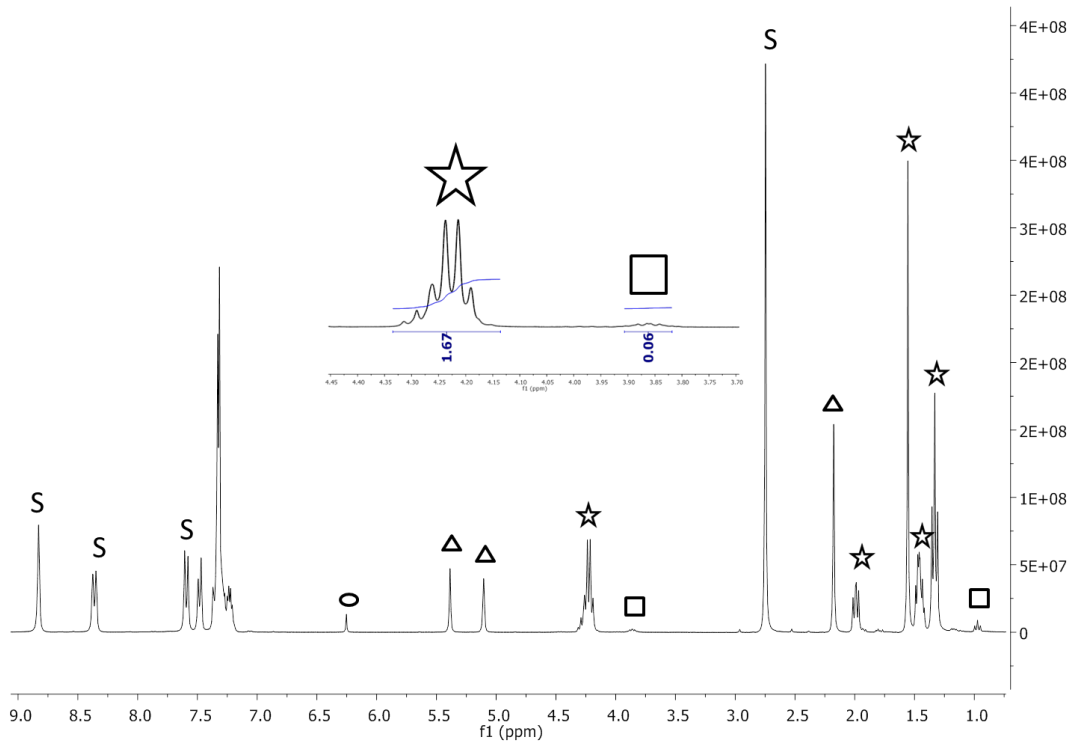
**Method a (runs 1-5, Table 2.7):** In a typical run, **119Fe** (5.0 mg,  $2.70 \times 10^{-6}$  mol) was dissolved in the desired solvent (5.0 mL) and then  $\alpha$ -methylstyrene (0.88 mL,  $6.75 \times 10^{-4}$  mol) and ethyl diazoacetate (EDA) (0.028 mL,  $2.70 \times 10^{-4}$  mol) were added. The consumption of EDA was monitored by IR spectroscopy by measuring the decrease of the characteristic  $N_2$  absorbance at  $2114 \text{ cm}^{-1}$ . The reaction was considered to be finished when the measured EDA absorbance was below 0.03 (by using a 0.5 mm-thickness cell). The solution was then evaporated to dryness and analysed by  $^1\text{H}$  NMR with 2,4-dinitrotoluene as an internal standard, and by HPLC by using a chiral column (DAI-CEL CHRALCEL, IB, *n*-hexane/*i*-PrOH 99.5:0.5). **Method b (run 1, Table 2.8):** The procedure illustrated for *method a* was repeated by using an equimolar  $\alpha$ -methylstyrene/EDA ratio (0.035 mL,  $2.70 \times 10^{-4}$  mol/ 0.028 mL,  $2.70 \times 10^{-4}$  mol). **Method c (runs 2-4 and 6-9, Table 2.8):** 145.0  $\mu\text{L}$  of a **119Fe** toluene solution ( $3.72 \times 10^{-3}$  mol/L) was dissolved in 2.0 mL of toluene before adding equimolar amounts of  $\alpha$ -methylstyrene and EDA. **Method d (run 5, Table 2.8):** The procedure *e* was repeated by adding EDA dropwise by a syringe pump to the reaction mixture.

### 3.12.2. Recycle of Catalyst 119Fe.

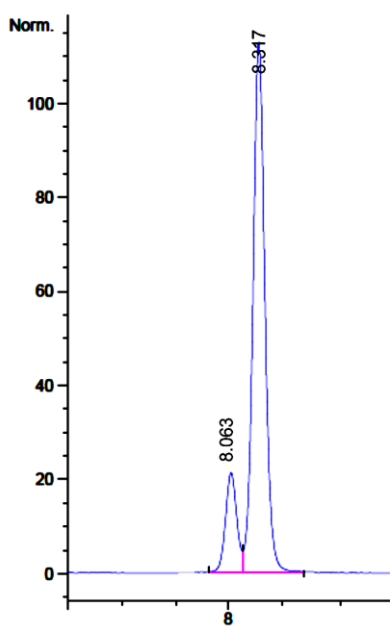
$\alpha$ -Methylstyrene (0.421 mL,  $3.24 \times 10^{-3}$  mol) and ethyl diazoacetate (EDA) (0.340 mL,  $3.24 \times 10^{-3}$  mol) were added to a toluene solution (17.0 mL) of **119Fe** (6.0 mg,  $3.24 \times 10^{-6}$  mol) at  $0^\circ\text{C}$  under nitrogen atmosphere. The consumption of EDA was monitored by IR spectroscopy by measuring the characteristic  $N_2$  absorbance at  $2114 \text{ cm}^{-1}$ . After the complete EDA consumption, EDA and  $\alpha$ -methylstyrene were added again to the catalytic mixture for two more consecutive times. The NMR analyses of the crude revealed 90% of global yield, 98% of *trans*-diastereoselectivity with 75% of  $ee_{trans}$ .

## NMR and HPLC spectra of catalytic cyclopropanation reactions

<b>Legend</b>	<p><b>S</b> Internal standard 2,4-dinitrotoluene</p> <p>○ Maleate</p> <p>○ Fumarate</p> <p>△ <math>\alpha</math>-methylstyrene</p> <p>☆ Cyclopropane <i>trans</i></p> <p>□ Cyclopropane <i>cis</i></p>
---------------	--



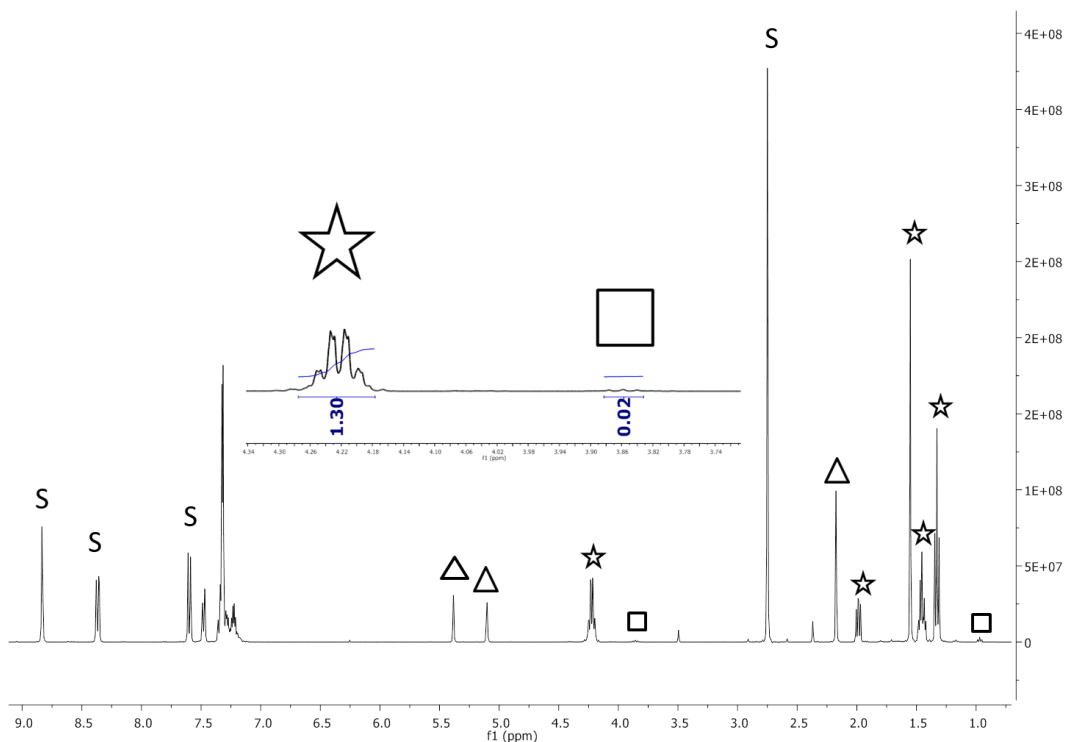
<sup>1</sup>H NMR (CDCl<sub>3</sub>) spectrum of entry 1, Table 2.7.



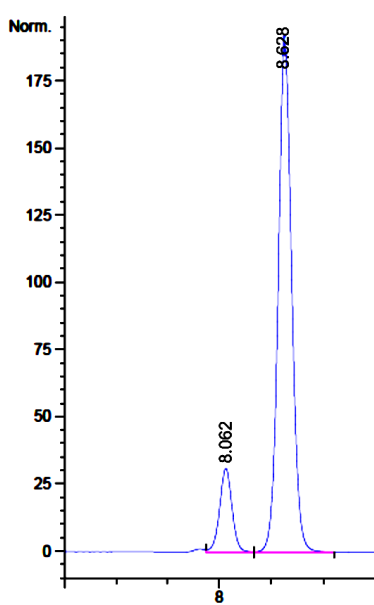
HPLC spectrum of entry 1, Table 2.7.

DAI-CEL CHRALCEL, IB, n-hexane/i-PrOH 99.5:0.5

peak	time (min)	area	percent
1	8.063	14,066	
2	8.317	85,936	
			100,000



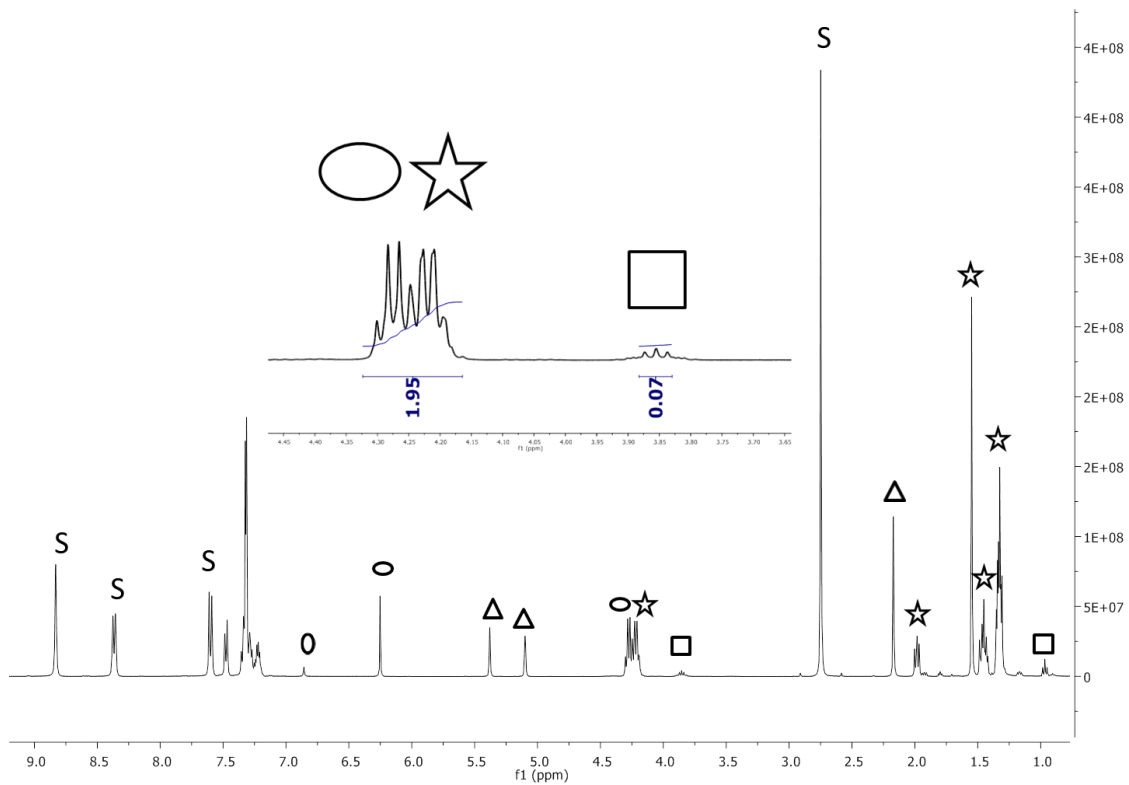
<sup>1</sup>H NMR (CDCl<sub>3</sub>) spectrum of entry 2, Table 2.7



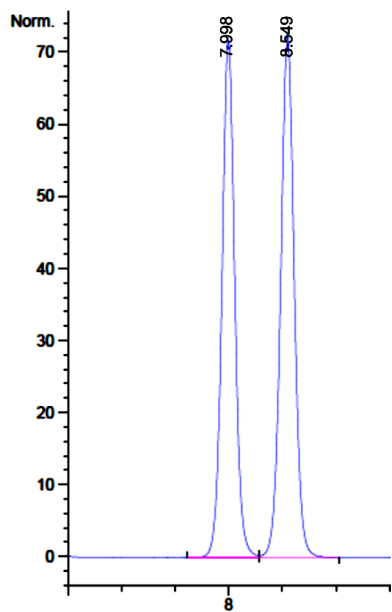
HPLC spectrum of entry 2, Table 2.7.

DAI-CEL CHRALCEL, IB, n-hexane/i-PrOH 99.5:0.5

peak	time (min)	area percent
1	8.062	12,656
2	8.628	87,344
		100,000



<sup>1</sup>H NMR (CDCl<sub>3</sub>) spectrum of entry 4, Table 2.7.

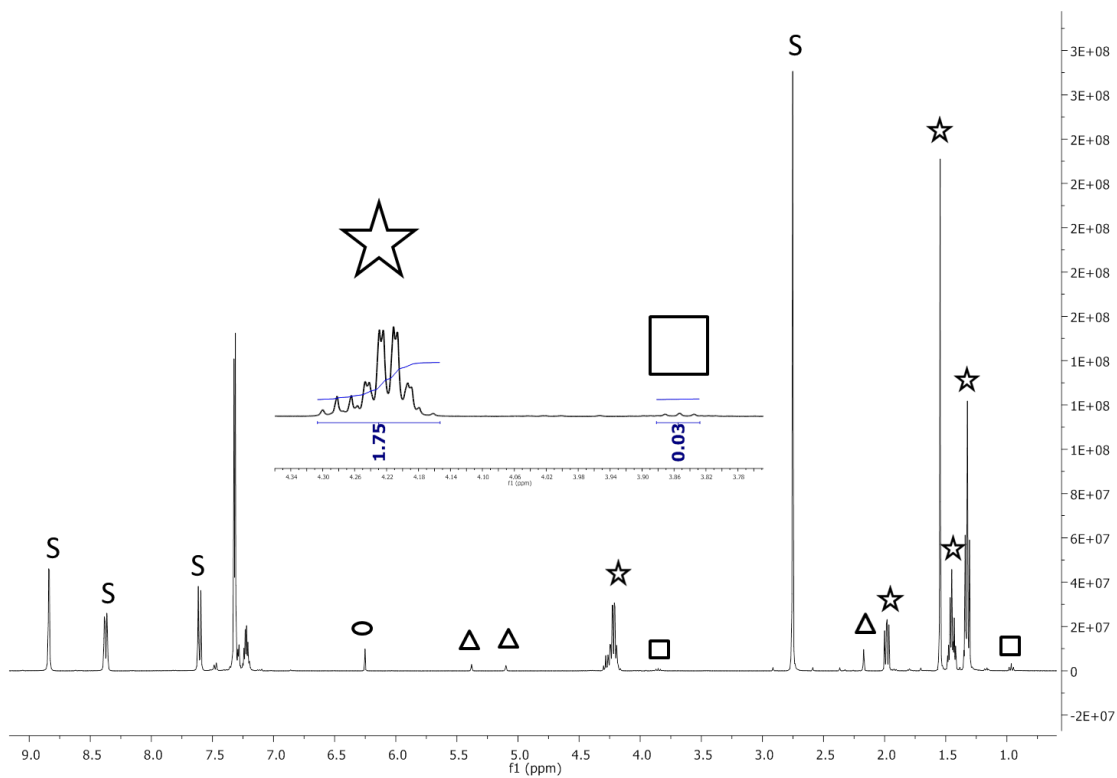


HPLC spectrum of entry 4, Table 2.7.

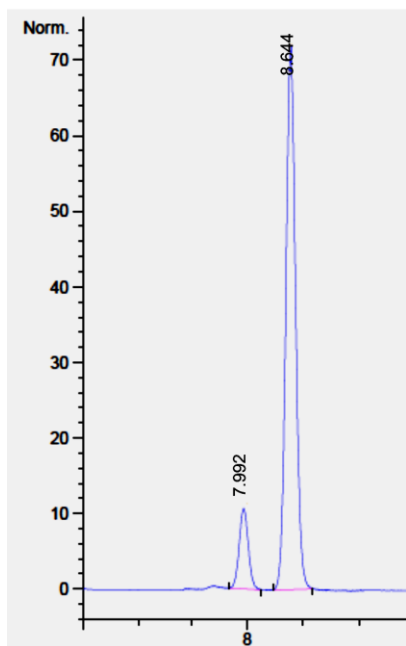
DAI-CEL CHRALCEL, IB, n-hexane/i-PrOH 99.5:0.5

peak	time (min)	area percent
1	7.998	30.381
2	8.549	69.919

100,000



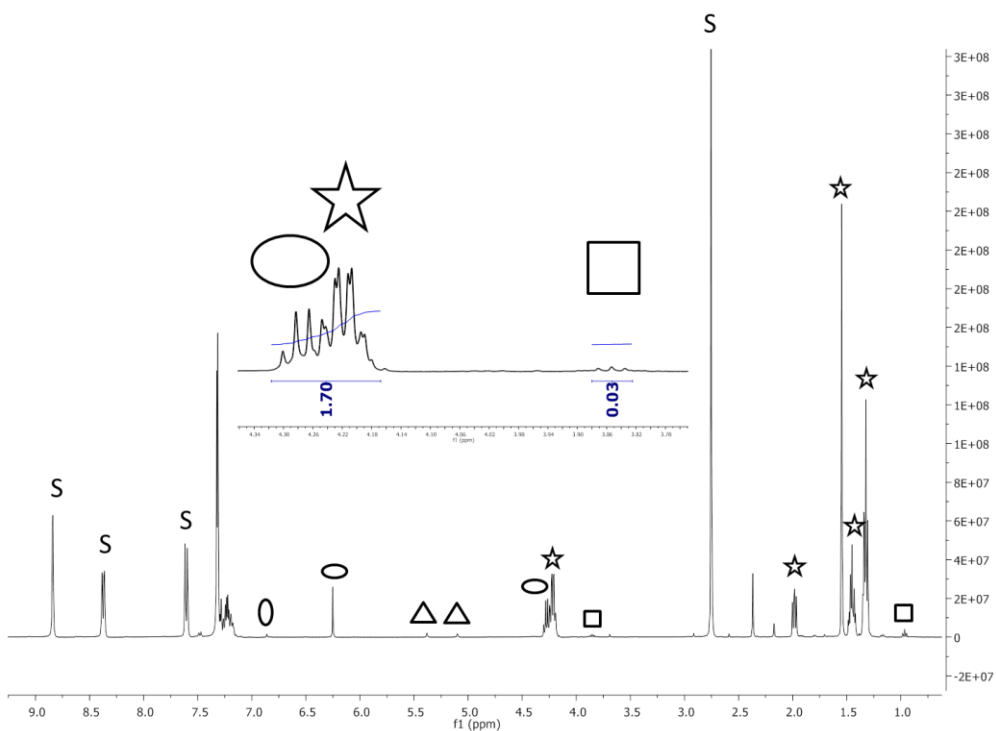
<sup>1</sup>H NMR (CDCl<sub>3</sub>) spectrum of entry 5, Table 2.7.



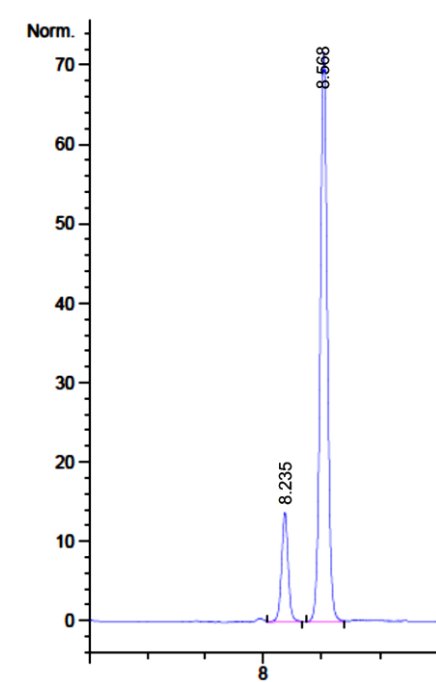
HPLC spectrum of entry 5, Table 2.7.

DAI-CEL CHRALCEL, IB, n-hexane/i-PrOH 99.5:0.5

peak	time (min)	area	percent
1	7.992	12,322	
2	8.644	87,678	
			100,000



<sup>1</sup>H NMR (CDCl<sub>3</sub>) spectrum of entry 1, Table 2.8.

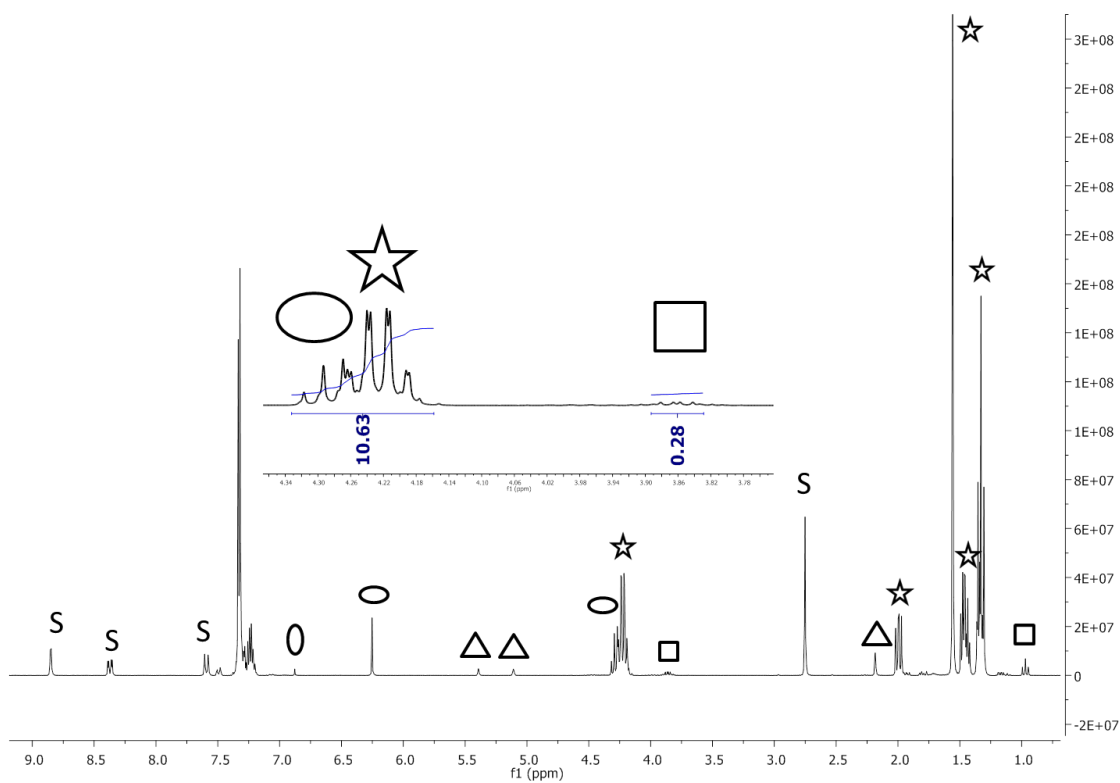


HPLC spectrum of entry 1, Table 2.8.

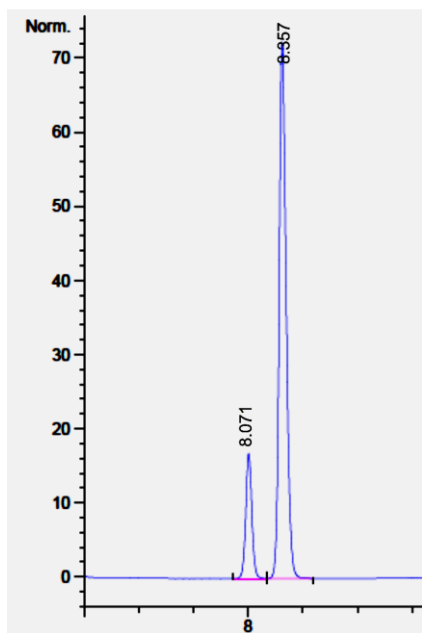
DAI-CEL CHRALCEL, IB, n-hexane/i-PrOH 99.5:0.5

peak	time (min)	area	percent
1	8.325	13,663	
2	8.568	86,337	
			100,000





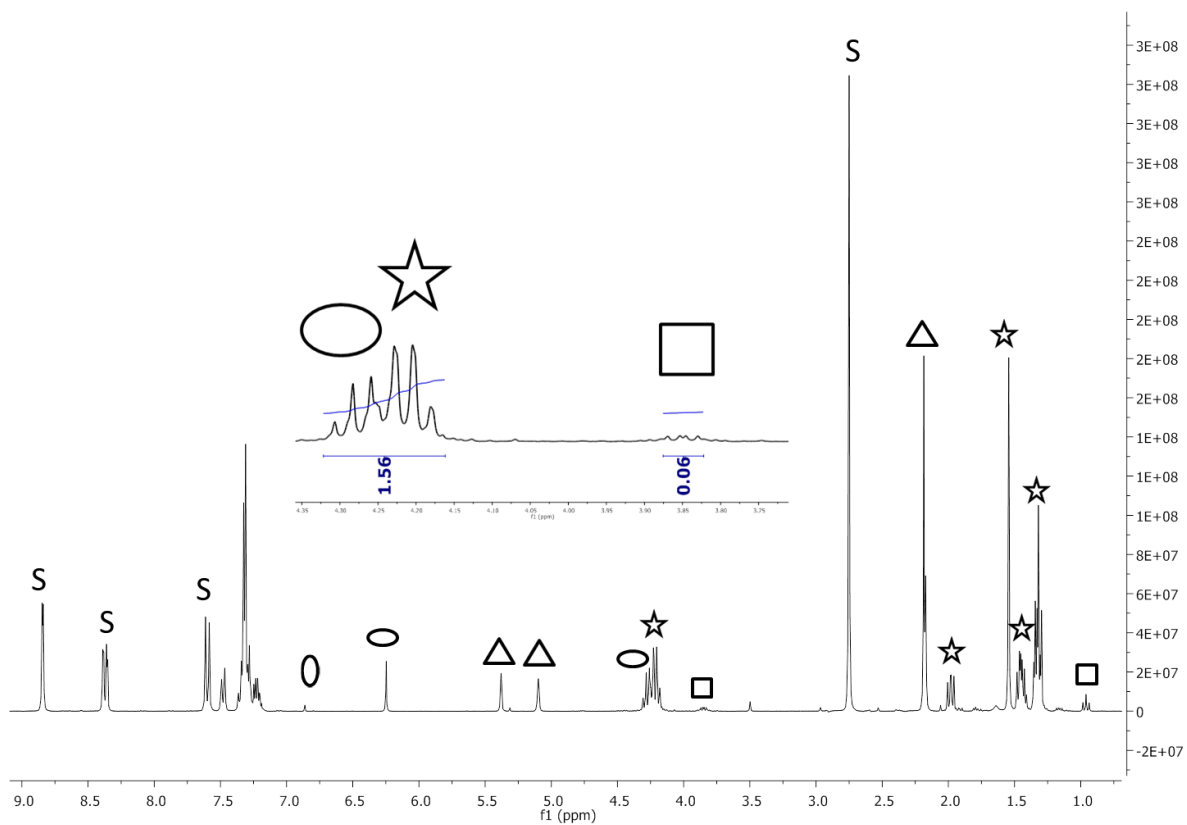
<sup>1</sup>H NMR (CDCl<sub>3</sub>) spectrum of entry 2, Table 2.8.



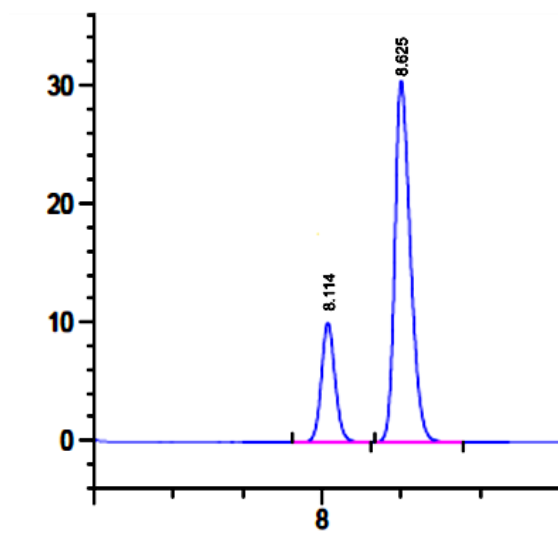
HPLC spectrum of entry 2, Table 2.8.

DAI-CEL CHRALCEL, IB, n-hexane/i-PrOH 99.5:0.5

peak	time (min)	area	percent
1	8.071	16,205	
2	8.357	83,795	
			100,000



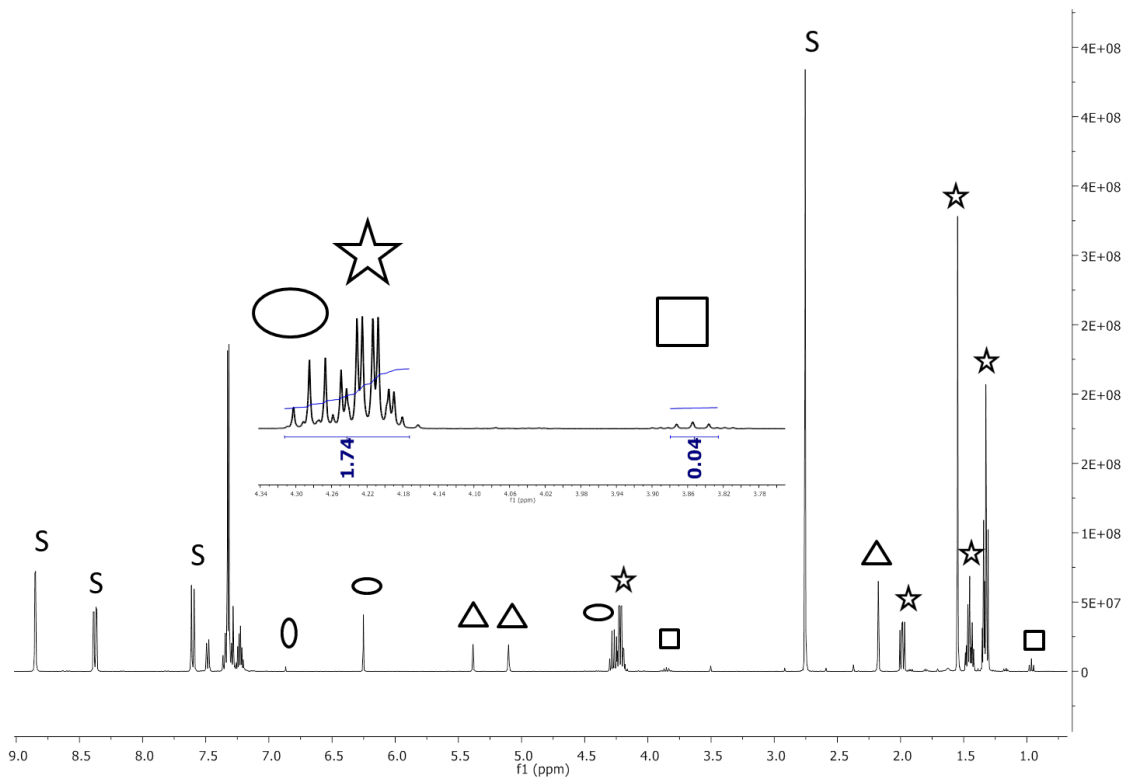
<sup>1</sup>H NMR (CDCl<sub>3</sub>) spectrum of entry 3, Table 2.8.



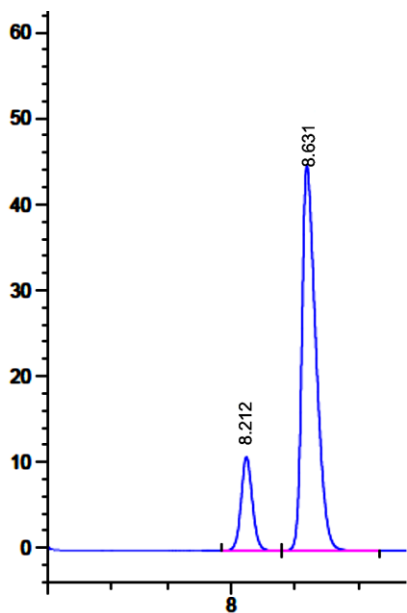
HPLC spectrum of entry 3, Table 2.8.

DAI-CEL CHRALCEL, IB, n-hexane/i-PrOH 99.5:0.5

peak	time (min)	area percent
1	8.114	20,998
2	8.625	79,002
		100,000



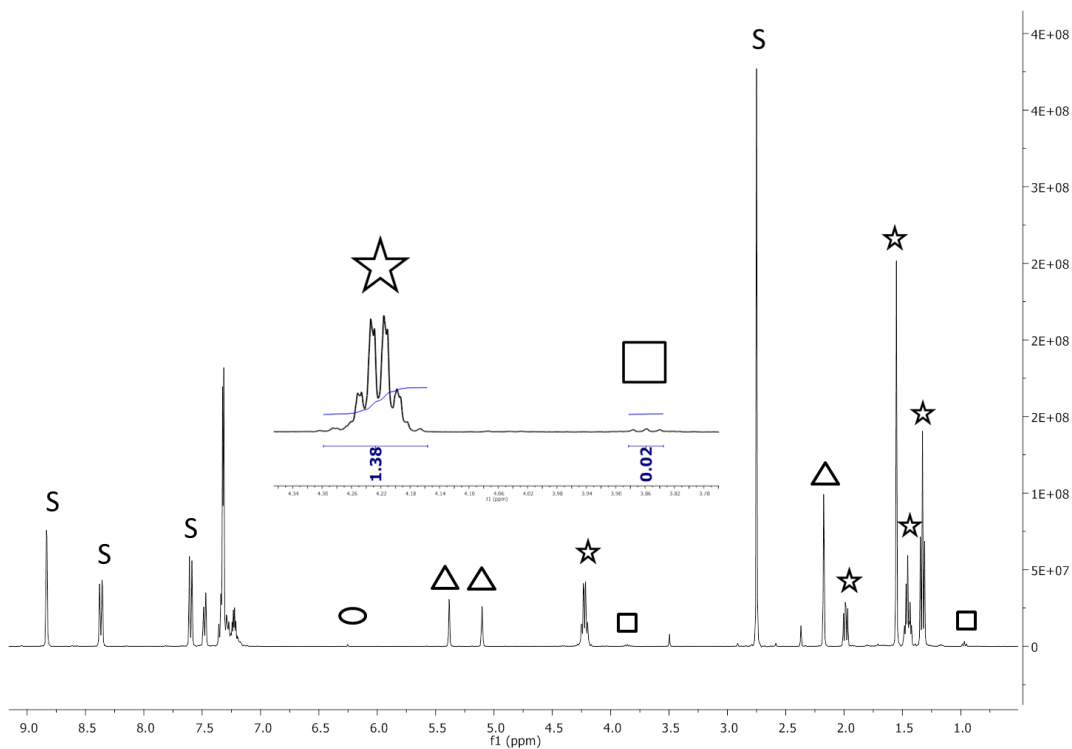
<sup>1</sup>H NMR (CDCl<sub>3</sub>) spectrum of entry 4, Table 2.8.



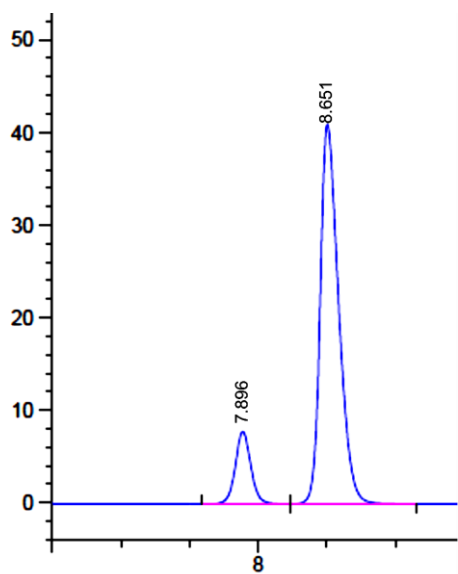
HPLC spectrum of entry 4, Table 2.8.

DAI-CEL CHRALCEL, IB, n-hexane/i-PrOH 99.5:0.5

peak	time (min)	area	percent
1	8.212	11,255	
2	8.631	88,745	
			100,000



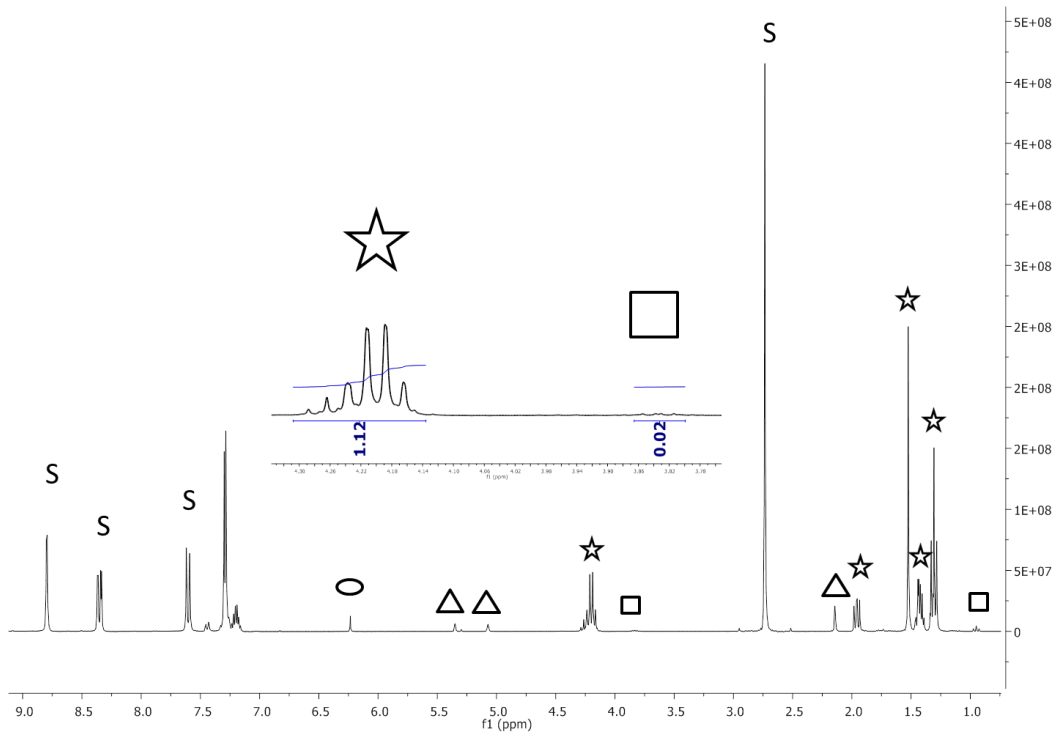
<sup>1</sup>H NMR (CDCl<sub>3</sub>) spectrum of entry 5, Table 2.8.



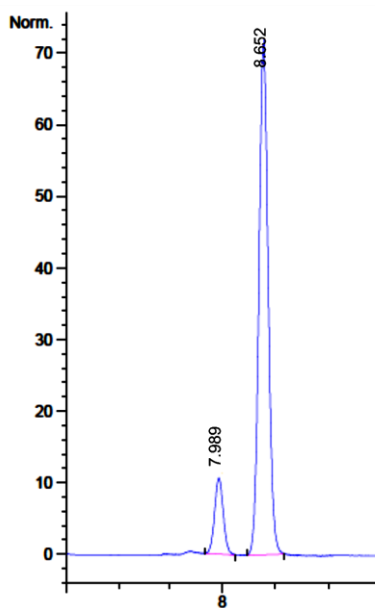
HPLC spectrum of entry 5, Table 2.8.

DAI-CEL CHRALCEL, IB, n-hexane/i-PrOH 99.5:0.5

peak	time (min)	area	percent
1	7.896	13,029	
2	8.651	86,971	
			100,000



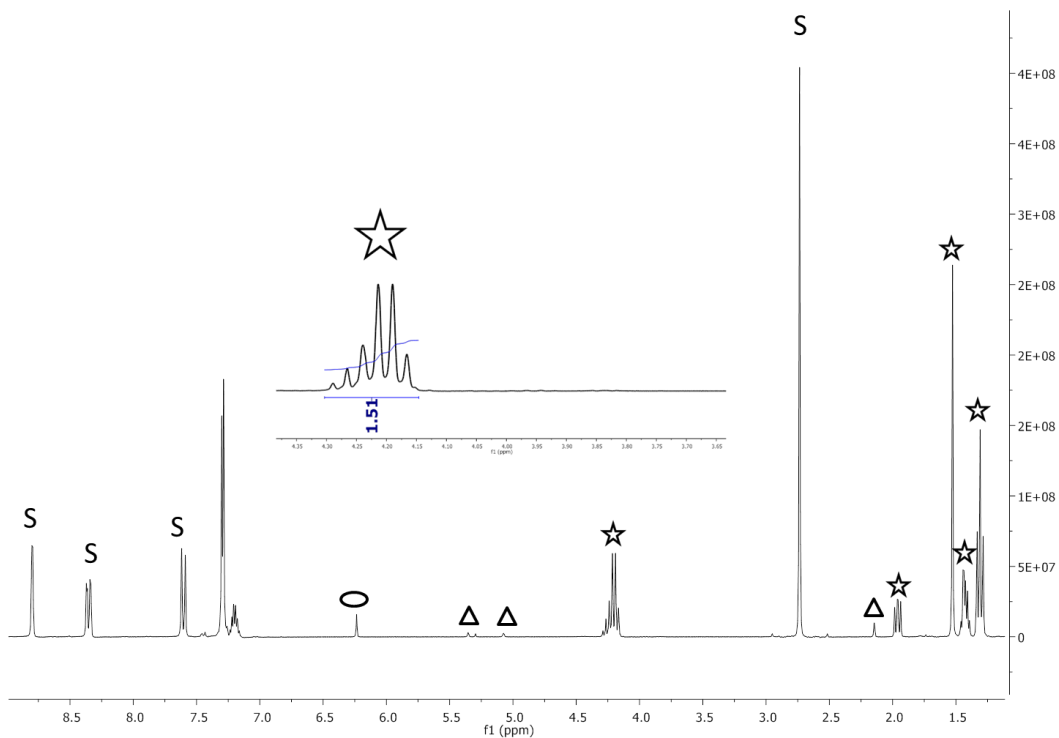
<sup>1</sup>H NMR (CDCl<sub>3</sub>) spectrum of entry 6, Table 2.8.



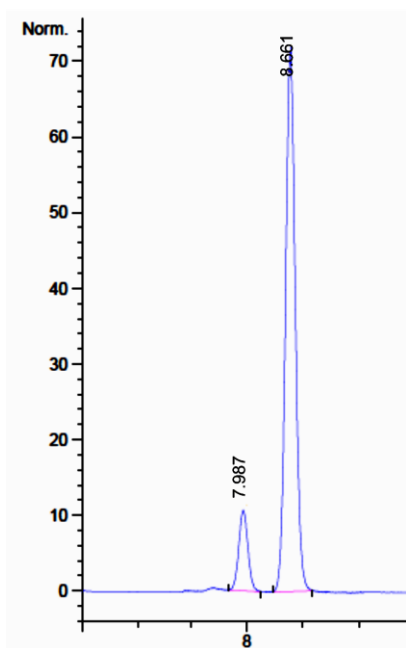
HPLC spectrum of entry 6, Table 2.8.

DAI-CEL CHRALCEL, IB, n-hexane/i-PrOH 99.5:0.5

peak	time (min)	area	percent
1	7.989	10,551	
2	8.652	89,449	
			100,000



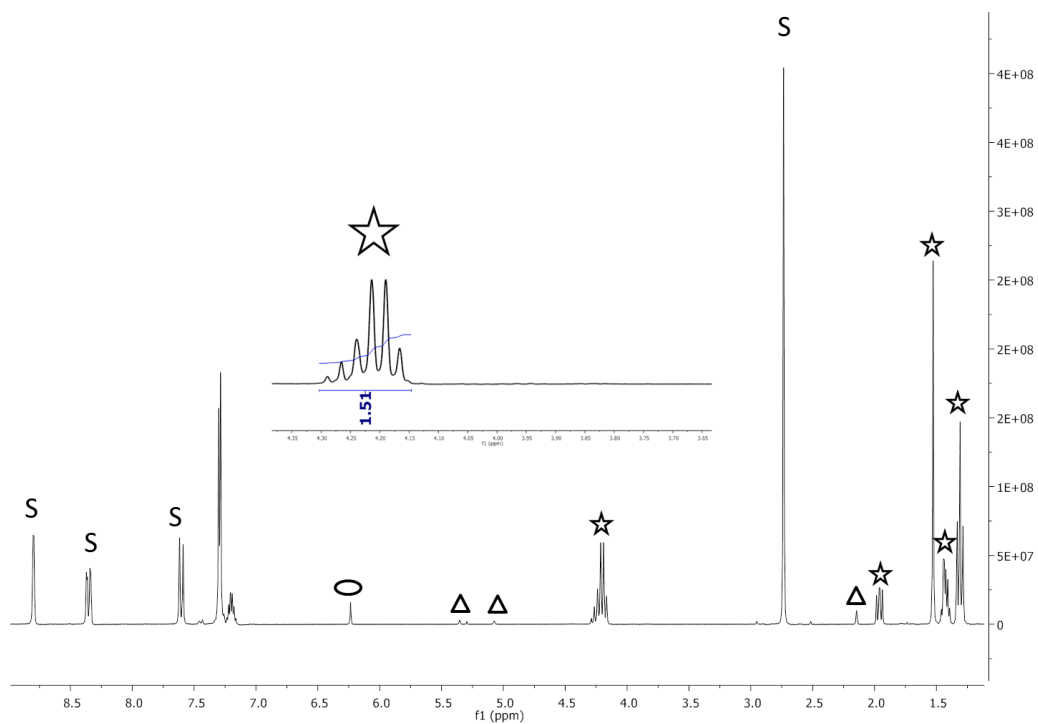
<sup>1</sup>H NMR (CDCl<sub>3</sub>) spectrum of entry 7, Table 2.8.



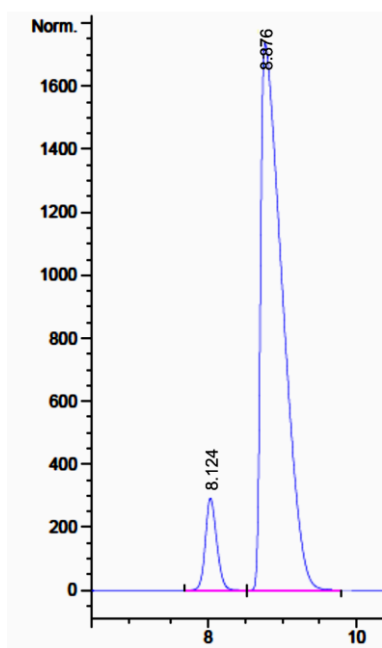
HPLC spectrum of entry 7, Table 2.8.

DAI-CEL CHRALCEL, IB, n-hexane/i-PrOH 99.5:0.5

peak	time (min)	area	percent
1	7.987	10,638	
2	8.661	89,362	
			100,000



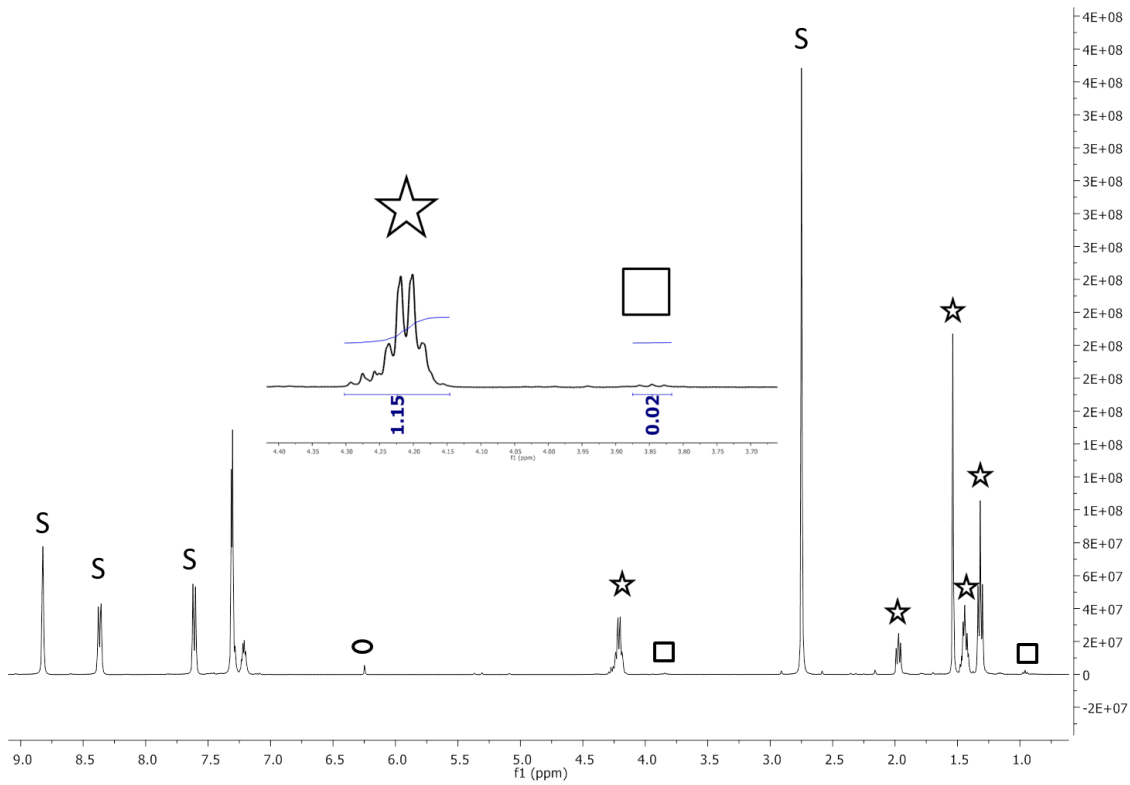
<sup>1</sup>H NMR (CDCl<sub>3</sub>) spectrum of entry 8, Table 2.8.



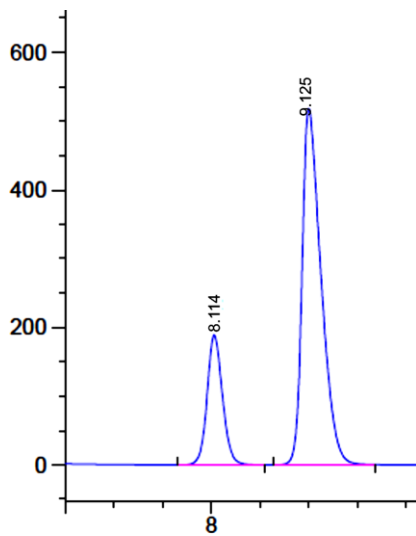
HPLC spectrum of entry 8, Table 2.8.

DAI-CEL CHRALCEL, IB, n-hexane/i-PrOH 99.5:0.5

peak	time (min)	area	percent
1	8.124	6,666	
2	8.876	93,334	
			100,000



<sup>1</sup>H NMR (CDCl<sub>3</sub>) spectrum of entry 9, Table 2.8.



HPLC spectrum of entry 9, Table 2.8.

DAI-CEL CHRALCEL, IB, n-hexane/i-PrOH 99.5:0.5

peak	time (min)	area	percent
1	8.114	21,743	
2	9.125	78,257	
			100,000



1. G. P. Moss, *Pure appl. Chem.*, 1987, **59**, 779-832.
2. F.-P. Montforts, B. Gerlach and F. Hoepfer, *Chem. Rev.*, 1994, **94**, 327-347.
3. B. Franck and A. Nonn, *Angew. Chem., Int. Ed. Engl.*, 1995, **34**, 1795-1811.
4. J. Halpern, *Science*, 1985, **227**, 869-875.
5. A. Battersby, *Science*, 1994, **264**, 1551-1557.
6. R. B. Woodward, W. A. Ayer, J. M. Beaton, F. Bickelhaupt, R. Bonnett, P. Buchschacher, G. L. Closs, H. Dutler, J. Hannah, F. P. Hauck, S. Itö, A. Langemann, E. Le Goff, W. Leimgruber, W. Lwowski, J. Sauer, Z. Valenta and H. Volz, *Tetrahedron*, 1990, **46**, 7599-7659.
7. K. C. S. E. J. E. V. W. Nicolaou, 1996, **Chap. 8**, 99-136.
8. H. W. Fisher, B., *Justus Liebigs Ann. Chem.*, 1926, **450**, 164-181.
9. A. D. Adler, Ed., *The Chemical and Physical Behavior of Porphyrin Compounds and Related Structure. Annales New York Accademy Science*, 1973, **206**.
10. D. E. Dolphin, *Biochemistry: The Porphyrin*, Academic Press: New York, **Vol. VI part A, Vol. VII part B**.
11. F. A. de Matteis, W. N. Ed.; , *Heme and Hemoproteins*, 1978.
12. CAS.
13. P. Rothmund, *J. Am. Chem. Soc.*, 1935, **57**, 2010-2011.
14. P. Rothmund, *J. Am. Chem. Soc.*, 1936, **58**, 625-627.
15. P. Rothmund, *J. Am. Chem. Soc.*, 1939, **61**, 2912-2915.
16. P. Rothmund and A. R. Menotti, *J. Am. Chem. Soc.*, 1941, **63**, 267-270.
17. S. Aronoff and M. Calvin, *J. Org. Chem.*, 1943, **08**, 205-223.
18. G. D. Dorough, J. R. Miller and F. M. Huennekens, *J. Am. Chem. Soc.*, 1951, **73**, 4315-4320.
19. G. D. Dorough and F. M. Huennekens, *J. Am. Chem. Soc.*, 1952, **74**, 3974-3976.
20. S. Silvers and A. Tulinsky, *J. Am. Chem. Soc.*, 1964, **86**, 927-928.
21. M. J. Hamor, T. A. Hamor and J. L. Hoard, *J. Am. Chem. Soc.*, 1964, **86**, 1938-1942.
22. E. B. Fleischer, C. K. Miller and L. E. Webb, *J. Am. Chem. Soc.*, 1964, **86**, 2342-2347.
23. L. E. Webb and E. B. Fleischer, *J. Chem. Phys.*, 1965, **43**, 3100-3111.
24. E. B. Fleischer, *Acc. Chem. Res.*, 1970, **3**, 105-112.
25. A. D. Adler, F. R. Longo and W. Shergalis, *J. Am. Chem. Soc.*, 1964, **86**, 3145-3149.
26. A. D. Adler, F. R. Longo, J. D. Finarelli, J. Goldmacher, J. Assour and L. Korsakoff, *The Journal of Organic Chemistry*, 1967, **32**, 476-476.
27. J. B. A. Kim, A. D.; Longo, F. R., *The Porphyrins*, 1978/79, **vols. 1-7**.
28. K. D. Rousseau, D., *Tetrahedron*, 1974, **48**, 4251-4254.
29. G. H. Barnett, M. F. Hudson and K. M. Smith, *J. Chem. Soc., Perkin Trans. 1*, 1975, 1401-1403.
30. S. M. S. Chauhan, B. B. Sahoo and K. A. Srinivas, *Synth. Commun.*, 2001, **31**, 33-37.
31. M. Radha Kishan, V. Radha Rani, M. R. V. S. Murty, P. Sita Devi, S. J. Kulkarni and K. V. Raghavan, *J. Mol. Catal. A: Chem.*, 2004, **223**, 263-267.
32. M. O. Liu, C.-H. Tai, W.-Y. Wang, J.-R. Chen, A. T. Hu and T.-H. Wei, *J. Organomet. Chem.*, 2004, **689**, 1078-1084.
33. M. O. Liu and A. T. Hu, *J. Organomet. Chem.*, 2004, **689**, 2450-2455.
34. J. S. Lindsey, H. C. Hsu and I. C. Schreiman, *Tetrahedron Lett.*, 1986, **27**, 4969-4970.
35. J. S. Lindsey, I. C. Schreiman, H. C. Hsu, P. C. Kearney and A. M. Marguerettaz, *The Journal of Organic Chemistry*, 1987, **52**, 827-836.
36. G. R. Geier Iii and J. S. Lindsey, *J. Chem. Soc., Perkin Trans. 2*, 2001, 677-686.
37. G. R. Geier Iii and J. S. Lindsey, *J. Chem. Soc., Perkin Trans. 2*, 2001, 687-700.
38. G. R. Geier Iii, B. J. Littler and J. S. Lindsey, *J. Chem. Soc., Perkin Trans. 2*, 2001, 701-711.
39. G. R. Geier Iii, B. J. Littler and J. S. Lindsey, *J. Chem. Soc., Perkin Trans. 2*, 2001, 712-718.
40. G. R. L. Geier Iii, J. S., *J. Porphyrins Phthalocyanines*, 2002, **6**, 159.
41. A. Ghosh, *Angew. Chem., Int. Ed. Engl.*, 2004, **43**, 1918-1931.
42. G. R. Geier Iii and J. S. Lindsey, *Tetrahedron*, 2004, **60**, 11435-11444.
43. R. A. W. N. Johnstone, M. L. P. G.; Pereira, M. M.; Rocha Gonzales, A. M. d'A.; Serra, A. C., *Heterocycles*, 1996, **43**, 1423-1437.
44. M. Gouterman, R. J. Hall, G. E. Khalil, P. C. Martin, E. G. Shankland and R. L. Cerny, *J. Am. Chem. Soc.*, 1989, **111**, 3702-3707.
45. S. S. Tsuchiya, M., *Chem. Lett.*, 1989, 263-266.
46. S. Tsuchiya, *J. Chem. Soc., Chem. Comm.*, 1992, 1475-1477.
47. P. G. Gassman, A. Ghosh and J. Almlof, *J. Am. Chem. Soc.*, 1992, **114**, 9990-10000.
48. J. F. Bartoli, P. Battioni, W. R. De Foor and D. Mansuy, *J. Chem. Soc., Chem. Comm.*, 1994, 23-24.

49. E. K. Woller and S. G. DiMugno, *J. Org. Chem.*, 1997, **62**, 1588-1593.
50. C. T. H. Chen, S. J., *J. Chin. Chem. Soc.*, 1997, **44**, 23-31.
51. K. Ozette, P. Leduc, M. Palacio, J.-F. Bartoli, K. M. Barkigia, J. Fajer, P. Battioni and D. Mansuy, *J. Am. Chem. Soc.*, 1997, **119**, 6442-6443.
52. C.-J. Liu, W.-Y. Yu, S.-M. Peng, T. C. W. Mak and C.-M. Che, *Journal of the Chemical Society, Dalton Transactions*, 1998, 1805-1812.
53. N. Ono, H. Miyagawa, T. Ueta, T. Ogawa and H. Tani, *Journal of the Chemical Society, Perkin Transactions I*, 1998, 1595-1602.
54. A. P. Nelson and S. G. DiMugno, *J. Am. Chem. Soc.*, 2000, **122**, 8569-8570.
55. G. J. Capitosti, C. D. Guerrero, D. E. Binkley, C. S. Rajesh and D. A. Modarelli, *J. Org. Chem.*, 2002, **68**, 247-261.
56. E. Annoni, M. Pizzotti, R. Ugo, S. Quici, T. Morotti, M. Bruschi and P. Mussini, *Eur. J. Inorg. Chem.*, 2005, **2005**, 3857-3874.
57. A. M. d. A. R. Gonsalves, J. M. T. B. Varejão and M. M. Pereira, *Journal of Heterocyclic Chemistry*, 1991, **28**, 635-640.
58. G. R. Geier, Y. Ciringh, F. Li, D. M. Haynes and J. S. Lindsey, *Org. Lett.*, 2000, **2**, 1745-1748.
59. H. Sharghi and A. H. Nejad, *Helvetica Chimica Acta*, 2003, **86**, 408-414.
60. H. Sharghi and A. HassaniNejad, *Tetrahedron*, 2004, **60**, 1863-1868.
61. M. Onaka, T. Shinoda, Y. Izumi and E. Nolen, *Tetrahedron Lett.*, 1993, **34**, 2625-2628.
62. P. Laszlo and J. Luchetti, *Chem. Lett.*, 1993, **22**, 449-452.
63. T. Shinoda, Y. Izumi and M. Onaka, *J. Chem. Soc., Chem. Comm.*, 1995, 1801-1802.
64. P. J. Brothers, in *Advances in Organometallic Chemistry*, Academic Press, 2001, vol. Volume 48, pp. 289-342.
65. A. D. L. Adler, F. R.; Kampas, F.; Kim, J., *J. Inorg. Nucl. Chem.*, 1970, **32**, 2443-2445.
66. J. P. Collman, C. E. Barnes, P. N. Swepston and J. A. Ibers, *J. Am. Chem. Soc.*, 1984, **106**, 3500-3510.
67. J. P. Collman, C. E. Barnes, P. J. Brothers, T. J. Collins, T. Ozawa, J. C. Gallucci and J. A. Ibers, *J. Am. Chem. Soc.*, 1984, **106**, 5151-5163.
68. M. Tsutsui, D. Ostfeld and L. M. Hoffman, *J. Am. Chem. Soc.*, 1971, **93**, 1820-1823.
69. D. P. Rillema, J. K. Nagle, L. F. Barringer and T. J. Meyer, *Journal of the American Chemical Society*, 1981, **103**, 56-62.
70. C. M. Che, C. K. Poon, W. C. Chung and H. B. Gray, *Inorg. Chem.*, 1985, **24**, 1277-1278.
71. A. Antipas, J. W. Buchler, M. Gouterman and P. D. Smith, *J. Am. Chem. Soc.*, 1978, **100**, 3015-3024.
72. P. Le Maux, H. Bahri and G. Simonneaux, *J. Chem. Soc., Chem. Comm.*, 1991, 1350-1352.
73. P. Le Maux, H. Bahri and G. Simonneaux, *Tetrahedron*, 1993, **49**, 1401-1408.
74. B. C. Chow and I. A. Cohen, *Bioinorganic Chemistry*, 1971, **1**, 57-63.
75. B. Meunier, *Chem. Rev.*, 1992, **92**, 1411-1456.
76. R. A. Sheldon, Ed.; Marcel Dekker: New York, *Metalloporphyrins in Catalytic Oxidations*, 1994.
77. F. C. Montanari, L., Ed; Kluwer Academic: Dordrecht (The Netherlands), *Metalloporphyrins Catalyzed Oxidations*.
78. P. R. Ortiz de Montellano, *Cytochrome P450: Structures, Mechanism and Biochemistry*, 2nd ed., 1995, pp.3-48.
79. R. H. Holm, P. Kennepohl and E. I. Solomon, *Chem. Rev.*, 1996, **96**, 2239-2314.
80. J. P. Klinman, *Chem. Rev.*, 1996, **96**, 2541-2562.
81. E. I. Solomon, U. M. Sundaram and T. E. Machonkin, *Chem. Rev.*, 1996, **96**, 2563-2606.
82. L. Que and R. Y. N. Ho, *Chem. Rev.*, 1996, **96**, 2607-2624.
83. B. J. Wallar and J. D. Lipscomb, *Chem. Rev.*, 1996, **96**, 2625-2658.
84. M. Sono, M. P. Roach, E. D. Coulter and J. H. Dawson, *Chem. Rev.*, 1996, **96**, 2841-2888.
85. H. S. Shimada, S.G.; Yeom, H.; Ishimura, Y., *Oxygenases abd Model System*, 1997, pp. 195-221.
86. J. L. L. McLain, J.; Groves, J. T., *Biomimetic Oxidations Catalyzed by Transition Metal Complexes*, 2000, pp 91-169.
87. J. T. S. Groves, K.; Lee, J., *The Porphyrin Handbook; Biochemistry and Binding: Action of Small Molecules*, 2000, **vol. 4**, pp 17-40.
88. B. R. Meunier, A; Pratviel, G.; Bernadou, J., *The Porphyrin Handbook*, 2000, **vol. 4**.
89. M. B. J. Erzhova, B. R., *Catalyzed O2-oxidations*, 2002, pp 1-77.
90. P. Hlavica, *European Journal of Biochemistry*, 2004, **271**, 4335-4360.
91. B. Meunier, S. P. de Visser and S. Shaik, *Chem. Rev.*, 2004, **104**, 3947-3980.
92. T. Punniyamurthy, S. Velusamy and J. Iqbal, *Chem. Rev.*, 2005, **105**, 2329-2364.
93. T. G. Traylor, C. Kim, W.-P. Fann and C. L. Perrin, *Tetrahedron*, 1998, **54**, 7977-7986.
94. W. Nam, H. J. Han, S.-Y. Oh, Y. J. Lee, M.-H. Choi, S.-Y. Han, C. Kim, S. K. Woo and W. Shin, *J. Am. Chem. Soc.*, 2000, **122**, 8677-8684.

95. W. Nam, S. W. Jin, M. H. Lim, J. Y. Ryu and C. Kim, *Inorg. Chem.*, 2002, **41**, 3647-3652.
96. W. Nam, S.-Y. Oh, Y. J. Sun, J. Kim, W.-K. Kim, S. K. Woo and W. Shin, *J. Org. Chem.*, 2003, **68**, 7903-7906.
97. J. Collman, X. Zhang, V. Lee, E. Uffelman and J. Brauman, *Science*, 1993, **261**, 1404-1411.
98. P. E. Ellis Jr and J. E. Lyons, *Coord. Chem. Rev.*, 1990, **105**, 181-193.
99. D. Mansuy, *Coord. Chem. Rev.*, 1993, **125**, 129-141.
100. J. T. Groves, T. E. Nemo and R. S. Myers, *J. Am. Chem. Soc.*, 1979, **101**, 1032-1033.
101. J. R. L. Smith and P. R. Sleath, *J. Chem. Soc., Perkin Trans. 2*, 1982, 1009-1015.
102. J. T. Groves and R. S. Myers, *J. Am. Chem. Soc.*, 1983, **105**, 5791-5796.
103. J. P. Collman, R. R. Gagne, C. Reed, T. R. Halbert, G. Lang and W. T. Robinson, *Journal of the American Chemical Society*, 1975, **97**, 1427-1439.
104. P. S. Traylor, D. Dolphin and T. G. Traylor, *J. Chem. Soc., Chem. Comm.*, 1984, 279-280.
105. E. B. Fleischer, R. Thorp and D. Venerable, *Journal of the Chemical Society D: Chemical Communications*, 1969, 475a-475a.
106. J. W. Faller and J. W. Sibert, *J. Organomet. Chem.*, 1971, **31**, C5-C8.
107. S. S. Eaton, G. R. Eaton and R. H. Holm, *J. Organomet. Chem.*, 1971, **32**, C52-C54.
108. D. Cullen, E. Meyer, T. S. Srivastava and M. Tsutsui, *J. Chem. Soc., Chem. Comm.*, 1972, 584-585.
109. S. S. Eaton, G. R. Eaton and R. H. Holm, *J. Organomet. Chem.*, 1972, **39**, 179-195.
110. J. J. Bonnet, S. S. Eaton, G. R. Eaton, R. H. Holm and J. A. Ibers, *J. Am. Chem. Soc.*, 1973, **95**, 2141-2149.
111. R. G. Little and J. A. Ibers, *J. Am. Chem. Soc.*, 1973, **95**, 8583-8590.
112. F. R. Hopf, T. P. O'Brien, W. R. Scheidt and D. G. Whitten, *J. Am. Chem. Soc.*, 1975, **97**, 277-281.
113. G. R. Eaton and S. S. Eaton, *J. Am. Chem. Soc.*, 1975, **97**, 235-236.
114. S. S. Eaton and G. R. Eaton, *Inorg. Chem.*, 1977, **16**, 72-75.
115. J. W. Faller, C. C. Chen and C. J. Malerich, *J. Inorg. Biochem.*, 1979, **11**, 151-170.
116. J. P. Collman, A. O. Chong, G. B. Jameson, R. T. Oakley, E. Rose, E. R. Schmittou and J. A. Ibers, *J. Am. Chem. Soc.*, 1981, **103**, 516-533.
117. K. M. Kadish and D. Chang, *Inorg. Chem.*, 1982, **21**, 3614-3618.
118. N. Farrell, D. H. Dolphin and B. R. James, *J. Am. Chem. Soc.*, 1978, **100**, 324-326.
119. D. R. Paulson, A. W. Addison, D. Dolphin and B. R. James, *Journal of Biological Chemistry*, 1979, **254**, 7002-7006.
120. D. Dolphin, B. R. James and T. Leung, *Inorg. Chimica Acta*, 1983, **79**, 25-27.
121. T. Leung, B. R. James and D. Dolphin, *Inorg. Chimica Acta*, 1983, **79**, 180-181.
122. J. T. Groves and R. Quinn, *Inorg. Chem.*, 1984, **23**, 3844-3846.
123. J. T. Groves and R. Quinn, *J. Am. Chem. Soc.*, 1985, **107**, 5790-5792.
124. J. T. Groves and K. H. Ahn, *Inorg. Chem.*, 1987, **26**, 3831-3833.
125. M. J. Camenzind, B. R. James and D. Dolphin, *J. Chem. Soc., Chem. Comm.*, 1986, 1137-1139.
126. J.-C. Marchon and R. Ramasseul, *J. Chem. Soc., Chem. Comm.*, 1988, 298-299.
127. T.-S. Lai, H.-L. Kwong, R. Zhang and C.-M. Che, *Journal of the Chemical Society, Dalton Transactions*, 1998, 3559-3564.
128. R. Zhang, W.-Y. Yu, H.-Z. Sun, W.-S. Liu and C.-M. Che, *Chem. Eur. J.*, 2002, **8**, 2495-2507.
129. W. C. Still, *J. Am. Chem. Soc.*, 1979, **101**, 2493-2495.
130. W. H. Pirkle and P. L. Rinaldi, *J. Org. Chem.*, 1979, **44**, 1025-1028.
131. J. Marco-Contelles, M. T. Molina and S. Anjum, *Chem. Rev.*, 2004, **104**, 2857-2900.
132. T.-S. Lai, R. Zhang, K.-K. Cheung, C.-M. Che and H.-L. Kwong, *Chem. Commun.*, 1998, 1583-1584.
133. R. Zhang, W.-Y. Yu, T.-S. Lai and C.-M. Che, *Chem. Commun.*, 1999, 1791-1792.
134. A. Berkessel, P. Kaiser and J. Lex, *Chem. Eur. J.*, 2003, **9**, 4746-4756.
135. M. Momenteau and C. A. Reed, *Chem. Rev.*, 1994, **94**, 659-698.
136. A. D. E. J. W. a. S. L. N. Y. Hamilton, *Suptamolecular Control of Structure and Reactivity*, 1996.
137. J. Froidevaux, P. Ochsenein, M. Bonin, K. Schenk, P. Maltese, J. P. Gisselbrecht and J. Weiss, *J. Am. Chem. Soc.*, 1997, **119**, 12362-12363.
138. J. P. Collman, Z. Wang and A. Straumanis, *J. Org. Chem.*, 1998, **63**, 2424-2425.
139. N. Jux, *Org. Lett.*, 2000, **2**, 2129-2132.
140. D. Jokic, Z. Asfari and J. Weiss, *Org. Lett.*, 2002, **4**, 2129-2132.
141. E. Rose, A. Lecas, M. Quelquejeu, A. Kossanyi and B. Boitrel, *Coord. Chem. Rev.*, 1998, **178-180, Part 2**, 1407-1431.
142. J. T. S. Groves, K.; Lee, J., *The Porphyrin Handbook*, 2000, **vol. 4**, pp 17-39.
143. K. S. Suslick, *The Porphyrin Handbook*, 2000, **vol. 4**, 41-63.
144. J. C. R. Marchon, R., *The Porphyrin Handbook*, 2003, **vol. 11**, pp. 75-132.
145. E. Rose, B. Andrioletti, S. Zrig and M. Quelquejeu-Etheve, *Chem. Soc. Rev.*, 2005, **34**, 573-583.

146. S. O'Malley and T. Kodadek, *J. Am. Chem. Soc.*, 1989, **111**, 9116-9117.
147. L. K. Gottwald and E. F. Ullman, *Tetrahedron Lett.*, 1969, **10**, 3071-3074.
148. T. G. Traylor, H. Diekmann and C. K. Chang, *J. Am. Chem. Soc.*, 1971, **93**, 4068-4070.
149. J. P. Collman, V. J. Lee, C. J. Kellen-Yuen, X. Zhang, J. A. Ibers and J. I. Brauman, *J. Am. Chem. Soc.*, 1995, **117**, 692-703.
150. J. P. Collman, X. Zhang, P. C. Herrmann, E. S. Uffelman, B. Boitrel, A. Straumanis and J. I. Brauman, *J. Am. Chem. Soc.*, 1994, **116**, 2681-2682.
151. J. P. Collman, B. Boitrel, L. Fu, J. Galanter, A. Straumanis and M. Rapta, *J. Org. Chem.*, 1997, **62**, 2308-2309.
152. D. Ricard, B. Andrioletti, B. Boitrel and M. L'Her, *Chem. Commun.*, 1999, 1523-1524.
153. A. Didier, L. Michaudet, D. Ricard, V. Baveux-Chambenoît, P. Richard and B. Boitrel, *Eur. J. Org. Chem.*, 2001, **2001**, 1927-1926.
154. B. Boitrel, V. Baveux-Chambenoît, P. Richard, C. Ruzié and A. Didier, *J. Porphyrins Phthalocyanines*, 2005, **09**, 82-88.
155. L. Michaudet, P. Richard and B. Boitrel, *Tetrahedron Lett.*, 2000, **41**, 8289-8292.
156. L. Michaudet, P. Richard and B. Boitrel, *Chem. Commun.*, 2000, 1589-1590.
157. E. Rose, B. Boitrel, M. Quelquejeu and A. Kossanyi, *Tetrahedron Lett.*, 1993, **34**, 7267-7270.
158. S. Licoccia, M. Paci, P. Tagliatesta, R. Paolesse, S. Antonaroli and T. Boschi, *Magnetic Resonance in Chemistry*, 1991, **29**, 1084-1091.
159. E. Rose, A. Kossanyi, M. Quelquejeu, M. Soleilhavoup, F. Duwavran, N. Bernard and A. Lecas, *J. Am. Chem. Soc.*, 1996, **118**, 1567-1568.
160. S. Vilain-Deshayes, P. Maillard and M. Momenteau, *J. Mol. Catal. A: Chem.*, 1996, **113**, 201-208.
161. E. Rose, M. Soleilhavoup, L. Christ-Tommasino, G. Moreau, J. P. Collman, M. Quelquejeu and A. Straumanis, *J. Org. Chem.*, 1998, **63**, 2042-2044.
162. B. Andrioletti, E. Rose and M. Etheve-Quelquejeu, *J. Porphyrins Phthalocyanines*, 2003, **07**, 375-381.
163. B. Boitrel and V. Baveux-Chambenoit, *New J. Chem.*, 2003, **27**, 942-947.
164. J. A. Dale and H. S. Mosher, *J. Am. Chem. Soc.*, 1973, **95**, 512-519.
165. A. I. Meyers and K. A. Lutomski, *J. Am. Chem. Soc.*, 1982, **104**, 879-881.
166. S. O'Malley and T. Kodadek, *Organometallics*, 1992, **11**, 2299-2302.
167. G. Reginato, Lorenzo D. Bari, P. Salvadori and R. Guillard, *Eur. J. Org. Chem.*, 2000, **2000**, 1165-1171.
168. R. L. Halterman and S. T. Jan, *J. Org. Chem.*, 1991, **56**, 5253-5254.
169. R. L. Halterman, S.-T. Jan, A. H. Abdulwali and D. J. Standlee, *Tetrahedron*, 1997, **53**, 11277-11296.
170. M. Frauenkron and A. Berkessel, *Tetrahedron Lett.*, 1997, **38**, 7175-7176.
171. W.-C. Lo, C.-M. Che, K.-F. Cheng and T. C. W. Mak, *Chem. Commun.*, 1997, 1205-1206.
172. C.-M. Che, J.-S. Huang, F.-W. Lee, Y. Li, T.-S. Lai, H.-L. Kwong, P.-F. Teng, W.-S. Lee, W.-C. Lo, S.-M. Peng and Z.-Y. Zhou, *J. Am. Chem. Soc.*, 2001, **123**, 4119-4129.
173. T.-S. Lai, C.-M. Che, H.-L. Kwong and S.-M. Peng, *Chem. Commun.*, 1997, 2373-2374.
174. X.-G. Zhou, X.-Q. Yu, J.-S. Huang and C.-M. Che, *Chem. Commun.*, 1999, 2377-2378.
175. J.-L. Liang, J.-S. Huang, X.-Q. Yu, N. Zhu and C.-M. Che, *Chem. Eur. J.*, 2002, **8**, 1563-1572.
176. J. F. Barry, L. Campbell, D. W. Smith and T. Kodadek, *Tetrahedron*, 1997, **53**, 7753-7776.
177. H. Nakagawa, Y. Sei, K. Yamaguchi, T. Nagano and T. Higuchi, *J. Mol. Catal. A: Chem.*, 2004, **219**, 221-226.
178. Y. Ferrand, P. Le Maux and G. Simonneaux, *Tetrahedron: Asymmetry*, 2005, **16**, 3829-3836.
179. J. P. Collman, Z. Wang, A. Straumanis, M. Quelquejeu and E. Rose, *J. Am. Chem. Soc.*, 1998, **121**, 460-461.
180. J. P. Collman, Z. Wang, C. Linde, L. Fu, L. Dang and J. I. Brauman, *Chem. Commun.*, 1999, 1783-1784.
181. B. Boitrel, V. Baveux-Chambenoît and P. Richard, *Eur. J. Inorg. Chem.*, 2002, **2002**, 1666-1672.
182. G. Du, B. Andrioletti, E. Rose and L. K. Woo, *Organometallics*, 2002, **21**, 4490-4495.
183. E. Rose, Q.-Z. Ren and B. Andrioletti, *Chem. Eur. J.*, 2004, **10**, 224-230.
184. H. M. L. Davies and J. R. Manning, *Nature*, 2008, **451**, 417-424.
185. M. M. Diaz-Requejo and P. J. Perez, *Chem. Rev.*, 2008, **108**, 3379-3394.
186. I. D. G. Watson, L. Yu and A. K. Yudin, *Acc. Chem. Res.*, 2006, **39**, 194-206.
187. Z. Li and C. He, *Eur. J. Org. Chem.*, 2006, 4313-4322.
188. J. A. Halfen, *Curr. Org. Chem.*, 2005, **9**, 657-669.
189. P. Mueller and C. Fruit, *Chem. Rev.*, 2003, **103**, 2905-2919.
190. P. Dauban and R. H. Dodd, *Synlett*, 2003, 1571-1586.
191. Y. Yamada, T. Yamamoto and M. Okawara, *Chem. Lett.*, 1975, 361-362.
192. D. A. Evans, M. M. Faul and M. T. Bilodeau, *J. Org. Chem.*, 1991, **56**, 6744-6746.
193. D. A. Evans, M. M. Faul, M. T. Bilodeau, B. A. Anderson and D. M. Barnes, *J. Am. Chem. Soc.*, 1993, **115**, 5328-5329.
194. D. A. Evans, M. T. Bilodeau and M. M. Faul, *J. Am. Chem. Soc.*, 1994, **116**, 2742-2753.
195. R. Breslow and S. H. Gellman, *J. Chem. Soc., Chem. Commun.*, 1982, 1400-1401.

196. J. P. Mahy, G. Bedi, P. Battioni and D. Mansuy, *Tetrahedron Lett.*, 1988, **29**, 1927-1930.
197. J. Yang, R. Weinberg and R. Breslow, *Chem. Commun.*, 2000, 531-532.
198. J. P. Mahy, G. Bedi, P. Battioni and D. Mansuy, *New J. Chem.*, 1989, **13**, 651-657.
199. J. P. Mahy, P. Battioni and D. Mansuy, *J. Am. Chem. Soc.*, 1986, **108**, 1079-1080.
200. J. P. Mahy, P. Battioni, G. Bedi, D. Mansuy, J. Fischer, R. Weiss and I. Morgenstern-Badarau, *Inorg. Chem.*, 1988, **27**, 353-359.
201. X. Q. Yu, J. S. Huang, X. G. Zhou and C. M. Che, *Org. Lett.*, 2000, **2**, 2233-2236.
202. J.-L. Liang, S.-X. Yuan, J.-S. Huang, W.-Y. Yu and C.-M. Che, *Angew. Chem., Int. Ed. Engl.*, 2002, **41**, 3465-3468.
203. J.-L. Liang, S.-X. Yuan, J.-S. Huang and C.-M. Che, *J. Org. Chem.*, 2004, **69**, 3610-3619.
204. X. Lin, C.-M. Che and D. L. Phillips, *J. Org. Chem.*, 2008, **73**, 529-537.
205. L. He, P. W. H. Chan, W.-M. Tsui, W.-Y. Yu and C.-M. Che, *Organic Letters*, 2004, **6**, 2405-2408.
206. J. W. W. Chang and P. W. H. Chan, *Angew. Chem., Int. Ed. Engl.*, 2008, **47**, 1138-1140.
207. S.-M. Au, W.-H. Fung, M.-C. Cheng, C.-M. Che and S.-M. Peng, *Chem. Commun.*, 1997, 1655-1656.
208. S.-M. Au, J.-S. Huang, W.-Y. Yu, W.-H. Fung and C.-M. Che, *J. Am. Chem. Soc.*, 1999, **121**, 9120-9132.
209. C.-M. Che and W.-Y. Yu, *Pure Appl. Chem.*, 1999, **71**, 281-288.
210. S. K.-Y. Leung, W.-M. Tsui, J.-S. Huang, C.-M. Che, J.-L. Liang and N. Zhu, *J. Am. Chem. Soc.*, 2005, **127**, 16629-16640.
211. J. B. Sweeney, *Chem. Soc. Rev.*, 2002, **31**, 247-258.
212. D. Mansuy, J. P. Mahy, A. Dureault, G. Bedi and P. Battioni, *J. Chem. Soc., Chem. Commun.*, 1984, 1161-1163.
213. J. P. Mahy, G. Bedi, P. Battioni and D. Mansuy, *J. Chem. Soc., Perkin Trans.*, 1988, 1517-1524.
214. J.-P. Simonato, J. Pecaut, J.-C. Marchon and W. Robert Scheidt, *Chem. Commun.*, 1999, 989-990.
215. D. H. R. Barton, R. S. Hay-Motherwell and W. B. Motherwell, *J. Chem. Soc., Perkin Trans.*, 1983, 445-451.
216. R. Fructos Manuel, S. Trofimenko, M. M. Diaz-Requejo and J. Perez Pedro, *J. Am. Chem. Soc.*, 2006, **128**, 11784-11791.
217. D. P. Albone, S. Challenger, A. M. Derrick, S. M. Fillery, J. L. Irwin, C. M. Parsons, H. Takada, P. C. Taylor and D. J. Wilson, *Org. Biomol. Chem.*, 2005, **3**, 107-111.
218. T. Ando, S. Minakata, I. Ryu and M. Komatsu, *Tetrahedron Lett.*, 1998, **39**, 309-312.
219. H. Wu, L.-W. Xu, C.-G. Xia, J. Ge, W. Zhou and L. Yang, *Catal. Commun.*, 2005, **6**, 221-223.
220. B. M. Chanda, R. Vyas and A. V. Bedekar, *J. Org. Chem.*, 2001, **66**, 30-34.
221. J. U. Jeong, B. Tao, I. Sagasser, H. Henniges and K. B. Sharpless, *J. Am. Chem. Soc.*, 1998, **120**, 6844-6845.
222. L. Simkhovich and Z. Gross, *Tetrahedron Lett.*, 2001, **42**, 8089-8092.
223. S. Cenini, A. Penoni and S. Tollari, *J. Mol. Catal. A*, 1997, **124**, 109-113.
224. R. Vyas, G.-Y. Gao, J. D. Harden and X. P. Zhang, *Org. Lett.*, 2004, **6**, 1907-1910.
225. G.-Y. Gao, J. D. Harden and X. P. Zhang, *Org. Lett.*, 2005, **7**, 3191-3193.
226. J. D. Harden, J. V. Ruppel, G.-Y. Gao and X. P. Zhang, *Chem. Commun.*, 2007, 4644-4646.
227. S. Braese, C. Gil, K. Knepper and V. Zimmermann, *Angew. Chem., Int. Ed. Engl.*, 2005, **44**, 5188-5240.
228. S. Cenini, E. Gallo, A. Caselli, F. Ragaini, S. Fantauzzi and C. Piangiolino, *Coord. Chem. Rev.*, 2006, **250**, 1234-1253.
229. K. R. Henery-Logan and R. A. Clark, *Tetrahedron Lett.*, 1968, 801-806.
230. W. Broeckx, N. Overbergh, C. Samyn, G. Smets and G. L'Abbe, *Tetrahedron*, 1971, **27**, 3527-3534.
231. B. C. G. Soderberg, *Curr. Org. Chem.*, 2000, **4**, 727-764.
232. H. Kwart and A. A. Khan, *J. Am. Chem. Soc.*, 1967, **89**, 1950-1951.
233. H. Kwart and A. A. Khan, *J. Am. Chem. Soc.*, 1967, **89**, 1951-1953.
234. T. Katsuki, *Chem. Lett.*, 2005, **34**, 1304-1309.
235. H. Kawabata, K. Omura, T. Uchida and T. Katsuki, *Chem. Asian J.*, 2007, **2**, 248-256.
236. J. T. Groves and T. Takahashi, *J. Am. Chem. Soc.*, 1983, **105**, 2073-2074.
237. G.-Y. Gao, J. E. Jones, R. Vyas, J. D. Harden and X. P. Zhang, *J. Org. Chem.*, 2006, **71**, 6655-6658.
238. J. V. Ruppel, J. E. Jones, C. A. Huff, R. M. Kamble, Y. Chen and X. P. Zhang, *Org. Lett.*, 2008, **10**, 1995-1998.
239. J. E. Jones, J. V. Ruppel, G.-Y. Gao, T. M. Moore and X. P. Zhang, *J. Org. Chem.*, 2008, **73**, 7260-7265.
240. S. Fantauzzi, E. Gallo, A. Caselli, C. Piangiolino, F. Ragaini and S. Cenini, *Eur. J. Org. Chem.*, 2007, 6053-6059.
241. A. Caselli, E. Gallo, F. Ragaini, F. Ricatto, G. Abbiati and S. Cenini, *Inorg. Chimica Acta*, 2006, **359**, 2924-2932.
242. J. Bourgois, M. Bourgois and F. Texier, *Bull. Chem. Soc. Fr.*, 1978, 485-527.
243. P. Scheiner, *Tetrahedron*, 1968, **24**, 2757-2766.
244. P. Scheiner, *J. Org. Chem.*, 1965, **30**, 7-10.

245. S. Fantauzzi, E. Gallo, A. Caselli, F. Ragaini, P. Macchi, N. Casati and S. Cenini, *Organometallics*, 2005, **24**, 4710-4713.
246. V. Di Bussolo, M. R. Romano, M. Pineschi and P. Crotti, *Org. Lett.*, 2005, **7**, 1299-1302.
247. R. L. O. R. Cunha, D. G. Diego, F. Simonelli and J. V. Comasseto, *Tetrahedron Lett.*, 2005, **46**, 2539-2542.
248. U. M. Lindstrom and P. Somfai, *Chem. Eur. J.*, 2001, **7**, 94-98.
249. B. M. Trost and D. R. Fandrick, *Org. Lett.*, 2005, **7**, 823-826.
250. J. Aahman, T. Jarevaang and P. Somfai, *J. Org. Chem.*, 1996, **61**, 8148-8159.
251. J. Aahman and P. Somfai, *J. Am. Chem. Soc.*, 1994, **116**, 9781-9782.
252. C. Piangiolino, E. Gallo, A. Caselli, S. Fantauzzi, F. Ragaini and S. Cenini, *Eur. J. Org. Chem.*, 2007, 743-750.
253. S. Fantauzzi, E. Gallo, A. Caselli, C. Piangiolino, F. Ragaini, N. Re and S. Cenini, *Chem. Eur. J.*, 2009, **15**, 1241-1251.
254. M. G. Buonomenna, E. Gallo, F. Ragaini, A. Caselli, S. Cenini and E. Drioli, *Appl. Catal., A: General*, 2008, **335**, 37-45.
255. E. Gallo, M. G. Buonomenna, L. Vigano, F. Ragaini, A. Caselli, S. Fantauzzi, S. Cenini and E. Drioli, *J. Mol. Catal. A*, 2008, **282**, 85-91.
256. S. Cenini, E. Gallo, A. Penoni, F. Ragaini and S. Tollari, *Chem. Commun.*, 2000, 2265-2266.
257. F. Ragaini, A. Penoni, E. Gallo, S. Tollari, C. L. Gotti, M. Lapadula, E. Mangioni and S. Cenini, *Chem. Eur. J.*, 2003, **9**, 249-259.
258. E. S. Lewis and L. Funderburk, *J. Am. Chem. Soc.*, 1967, **89**, 2322-2327.
259. B. T. Farrer and H. H. Thorp, *Inorg. Chem.*, 1999, **38**, 2497-2502.
260. A. Caselli, E. Gallo, S. Fantauzzi, S. Morlacchi, F. Ragaini and S. Cenini, *Eur. J. Inorg. Chem.*, 2008, 3009-3019.
261. A. Reichelt and S. F. Martin, *Acc. Chem. Res.*, 2006, **39**, 433-442.
262. D. Zhang, H. Song and Y. Qin, *Acc. Chem. Res.*, 2011, **44**, 447-457.
263. H. Nozaki, S. Moriuti, H. Takaya and R. Noyori, *Tetrahedron Lett.*, 1966, 5239-5244.
264. H. Lebel, J.-F. Marcoux, C. Molinaro and B. Charette Andre, *Chem. Rev.*, 2003, **103**, 977-1050.
265. A. Caballero, A. Prieto, M. M. Diaz-Requejo and P. J. Perez, *Eur. J. Inorg. Chem.*, 2009, 1137-1144.
266. C.-Y. Zhou, J.-S. Huang and C.-M. Che, *Synlett*, 2010, 2681-2700.
267. B. Morandi and E. M. Carreira, *Angew. Chem., Int. Ed. Engl.*, 2010, **49**, 938-941.
268. I. Nicolas, T. Roisnel, P. Le Maux and G. Simonneaux, *Tetrahedron Lett.*, 2009, **50**, 5149-5151.
269. M. P. Le, T. Roisnel, I. Nicolas and G. Simonneaux, *Organometallics*, 2008, **27**, 3037-3042.
270. C.-M. Che and J.-S. Huang, *Coord. Chem. Rev.*, 2002, **231**, 151-164.
271. G. Simonneaux and P. Le Maux, *Coord. Chem. Rev.*, 2002, **228**, 43-60.
272. C. G. Hamaker, G. A. Mirafzal and L. K. Woo, *Organometallics*, 2001, **20**, 5171-5176.
273. A. J. Hubert, A. J. Noels, A. J. Anciaux and P. Teyssie, *Synthesis*, 1976, 600-602.
274. A. J. Anciaux, A. J. Hubert, A. F. Noels, N. Petiniot and P. Teyssie, *J. Org. Chem.*, 1980, **45**, 695-702.
275. M. P. Doyle, W. H. Tamblin and V. Bagheri, *J. Org. Chem.*, 1981, **46**, 5094-5102.
276. M. P. Doyle, L. D. Van and W. H. Tamblin, *Synthesis*, 1981, 787-789.
277. R. Paulissen, H. Reimlinger, E. Hayez, A. J. Hubert and P. Teyssié, *Tetrahedron Lett.*, 1973, **14**, 2233-2236.
278. A. Ghanem, M. G. Gardiner, R. M. Williamson and P. Mueller, *Chem. Eur. J.*, 2010, **16**, 3291-3295.
279. H. M. L. Davies and S. J. Hedley, *Chem. Soc. Rev.*, 2007, **36**, 1109-1119.
280. M. P. Doyle, *J. Org. Chem.*, 2006, **71**, 9253-9260.
281. H. M. L. Davies and S. A. Panaro, *Tetrahedron*, 2000, **56**, 4871-4880.
282. M. P. Doyle, *Chem. Rev.*, 1986, **86**, 919-939.
283. H. M. L. Davies, M. G. Coleman and D. L. Ventura, *Org. Lett.*, 2007, **9**, 4971-4974.
284. M. P. Doyle, J. H. Griffin, V. Bagheri and R. L. Dorow, *Organometallics*, 1984, **3**, 53-61.
285. J. A. S. Howell, *Dalton Trans.*, 2007, 3798-3803.
286. J. A. S. Howell, *Dalton Trans.*, 2007, 1104-1114.
287. H. J. Callot and C. Piechocki, *Tetrahedron Lett.*, 1980, **21**, 3489-3492.
288. K. C. Brown and T. Kodadek, *J. Am. Chem. Soc.*, 1992, **114**, 8336-8338.
289. P. Tagliatesta and A. Pastorini, *J. Mol. Catal. A: Chem.*, 2002, **185**, 127-133.
290. J. R. Wolf, C. G. Hamaker, J.-P. Djukic, T. Kodadek and L. K. Woo, *J. Am. Chem. Soc.*, 1995, **117**, 9194-9199.
291. T. Niino, M. Toganoh, B. Andrioletti and H. Furuta, *Chem. Commun.*, 2006, 4335-4337.
292. H. J. Callot and E. Schaeffer, *J. Chem. Soc., Chem. Commun.*, 1978, 937-938.
293. J. Maxwell and T. Kodadek, *Organometallics*, 1991, **10**, 4-6.
294. J. L. Maxwell, K. C. Brown, D. W. Bartley and T. Kodadek, *Science*, 1992, **256**, 1544-1547.
295. D. W. Bartley and T. Kodadek, *J. Am. Chem. Soc.*, 1993, **115**, 1656-1660.

296. L. Zhang and K. S. Chan, *Organometallics*, 2007, **26**, 679-684.
297. A. G. M. Barrett, D. C. Braddock, I. Lenoir and H. Tone, *J. Org. Chem.*, 2001, **66**, 8260-8263.
298. J. L. Maxwell, S. O'Malley, K. C. Brown and T. Kodadek, *Organometallics*, 1992, **11**, 645-652.
299. P.-F. Teng, T.-S. Lai, H.-L. Kwong and C.-M. Che, *Tetrahedron: Asymmetry*, 2003, **14**, 837-844.
300. Y. Tatsuno, A. Konishi, A. Nakamura and S. Otsuka, *J. Chem. Soc., Chem. Commun.*, 1974, 588-589.
301. A. Nakamura, A. Konishi, Y. Tatsuno and S. Otsuka, *J. Am. Chem. Soc.*, 1978, **100**, 3443-3448.
302. A. Nakamura, *Pure Appl. Chem.*, 1978, **50**, 37-42.
303. G. Jommi, R. Pagliarin, G. Rizzi and M. Sisti, *Synlett*, 1993, 833-834.
304. W. Hess, J. Treutwein and G. Hilt, *Synthesis*, 2008, 3537-3562.
305. T. Niimi, T. Uchida, R. Irie and T. Katsuki, *Tetrahedron Lett.*, 2000, **41**, 3647-3651.
306. T. Fukuda and T. Katsuki, *Tetrahedron*, 1997, **53**, 7201-7208.
307. T. Fukuda and T. Katsuki, *Synlett*, 1995, 825-826.
308. T. Uchida and T. Katsuki, *Synthesis*, 2006, 1715-1723.
309. T. Katsuki, *Adv. Synth. Catal.*, 2002, **344**, 131-147.
310. H. Shitama and T. Katsuki, *Chem. Eur. J.*, 2007, **13**, 4849-4858.
311. T. Niimi, T. Uchida, R. Irie and T. Katsuki, *Adv. Synth. Catal.*, 2001, **343**, 79-88.
312. T. Yamada, T. Ikeno, Y. Ohtsuka, S. Kezuka, M. Sato and I. Iwakura, *Sci. Technol. Adv. Mater.*, 2006, **7**, 184-196.
313. T. Ikeno, M. Sato and T. Yamada, *Chem. Lett.*, 1999, 1345-1346.
314. T. Yamada, T. Ikeno, H. Sekino and M. Sato, *Chem. Lett.*, 1999, 719-720.
315. T. Ikeno, I. Iwakura, S. Yabushita and T. Yamada, *Org. Lett.*, 2002, **4**, 517-520.
316. T. Ikeno, I. Iwakura and T. Yamada, *Bull. Chem. Soc. Jpn.*, 2001, **74**, 2151-2160.
317. A. Caselli, M. G. Buonomenna, B. F. de, L. Laera, S. Fantauzzi, F. Ragaini, E. Gallo, G. Golemme, S. Cenini and E. Drioli, *J. Mol. Catal. A: Chem.*, 2010, **317**, 72-80.
318. I. Shepperson, S. Quici, G. Pozzi, M. Nicoletti and D. O'Hagan, *Eur. J. Org. Chem.*, 2004, 4545-4551.
319. B. Morandi, B. Mariampillai and E. M. Carreira, *Angew. Chem., Int. Ed. Engl.*, 2011, **50**, 1101-1104.
320. C.-T. Yeung, K.-C. Sham, W.-S. Lee, W.-T. Wong, W.-Y. Wong and H.-L. Kwong, *Inorg. Chim. Acta*, 2009, **362**, 3267-3273.
321. J. Gao, F. R. Woolley and R. A. Zingaro, *Org. Biomol. Chem.*, 2005, **3**, 2126-2128.
322. B. K. Langlotz, H. Wadepl and L. H. Gade, *Angew. Chem., Int. Ed. Engl.*, 2008, **47**, 4670-4674.
323. I. Boldini, G. Guillemot, A. Caselli, A. Proust and E. Gallo, *Adv. Synth. Catal.*, 2010, **352**, 2365-2370.
324. L. Huang, Y. Chen, G.-Y. Gao and X. P. Zhang, *J. Org. Chem.*, 2003, **68**, 8179-8184.
325. A. Penoni, R. Wanke, S. Tollari, E. Gallo, D. Musella, F. Ragaini, F. Demartin and S. Cenini, *Eur. J. Inorg. Chem.*, 2003, 1452-1460.
326. J. P. Collman, E. Rose and G. D. Venburg, *J. Chem. Soc., Chem. Comm.*, 1993, 934-935.
327. Y. Chen and X. P. Zhang, *J. Org. Chem.*, 2004, **69**, 2431-2435.
328. Y. Chen, G.-Y. Gao and X. Peter Zhang, *Tetrahedron Lett.*, 2005, **46**, 4965-4969.
329. Y. Chen, K. B. Fields and X. P. Zhang, *J. Am. Chem. Soc.*, 2004, **126**, 14718-14719.
330. S. Zhu, J. V. Ruppel, H. Lu, L. Wojtas and X. P. Zhang, *J. Am. Chem. Soc.*, 2008, **130**, 5042-5043.
331. Y. Chen and X. P. Zhang, *Synthesis*, 2006, 1697-1700.
332. Y. Chen and X. P. Zhang, *J. Org. Chem.*, 2007, **72**, 5931-5934.
333. Y. Chen, J. V. Ruppel and X. P. Zhang, *J. Am. Chem. Soc.*, 2007, **129**, 12074-12075.
334. S. Zhu, J. A. Perman and X. P. Zhang, *Angew. Chem., Int. Ed. Engl.*, 2008, **47**, 8460-8463.
335. J. V. Ruppel, T. J. Gauthier, N. L. Snyder, J. A. Perman and X. P. Zhang, *Org. Lett.*, 2009, **11**, 2273-2276.
336. S. Zhu, X. Xu, J. A. Perman and X. P. Zhang, *J. Am. Chem. Soc.*, 2010, **132**, 12796-12799.
337. M. P. Doyle, *Angew. Chem., Int. Ed. Engl.*, 2009, **48**, 850-852.
338. M. Veyrat, O. Maury, F. Faverjon, D. E. Over, R. Ramasseul, J.-C. Marchon, I. Turowska-Tyrk and W. R. Scheidt, *Angew. Chem., Int. Ed. Engl.*, 1994, **33**, 220-223.
339. E. Rose, M. Quelquejeu, R. P. Pandian, A. Lecas-Nawrocka, A. Vilar, G. Ricart, J. P. Collman, Z. Wang and A. Straumanis, *Polyhedron*, 2000, **19**, 581-586.
340. E. Rose, Q.-z. Ren and B. Andrioletti, *Chem. Eur. J.*, 2004, **10**, 224-230.
341. S. Fantauzzi, E. Gallo, E. Rose, N. Raoul, A. Caselli, S. Issa, F. Ragaini and S. Cenini, *Organometallics*, 2008, **27**, 6143-6151.
342. A. W. Johnson, D. Ward, P. Batten, A. L. Hamilton, G. Shelton and C. M. Elson, *J. Chem. Soc., Perkin Trans 1*, 1975, 2076-2085.
343. H. J. Callot and E. Schaeffer, *J. Organomet. Chem.*, 1978, **145**, 91-99.
344. H. J. Callot and E. Schaeffer, *Nouv. J. Chim.*, 1980, **4**, 307-309.
345. P. Chattopadhyay, T. Matsuo, T. Tsuji, J. Ohbayashi and T. Hayashi, *Organometallics*, 2011, **30**, 1869-1873.
346. I. Iwakura, H. Tanaka, T. Ikeno and T. Yamada, *Chem. Lett.*, 2004, **33**, 140-141.

347. E. Rose, E. Gallo, N. Raoul, L. Bouche, A. Pille, A. Caselli and O. Lequin, *J. Porphyrins Phthalocyanines*, 2010, **14**, 646-659.
348. H. Lu, W. I. Dzik, X. Xu, L. Wojtas, B. de Bruin and X. P. Zhang, *J. Am. Chem. Soc.*, 2011, **133**, 8518-8521.
349. W. I. Dzik, X. Xu, X. P. Zhang, J. N. H. Reek and B. B. de, *J. Am. Chem. Soc.*, 2010, **132**, 10891-10902.
350. J. L. Belof, C. R. Cioce, X. Xu, X. P. Zhang, B. Space and H. L. Woodcock, *Organometallics*, 2011, **30**, 2739-2746.
351. A. Bury, S. T. Corker and M. D. Johnson, *J. Chem. Soc., Perkin Trans. 1*, 1982, 645-651.
352. W. I. Dzik, J. N. H. Reek and B. B. de, *Chem. Eur. J.*, 2008, **14**, 7594-7599.
353. S. Kanchiku, H. Suematsu, K. Matsumoto, T. Uchida and T. Katsuki, *Angew. Chem., Int. Ed. Engl.*, 2007, **46**, 3889-3891.
354. H. Suematsu, S. Kanchiku, T. Uchida and T. Katsuki, *J. Am. Chem. Soc.*, 2008, **130**, 10327-10337.
355. M. Ichinose, H. Suematsu and T. Katsuki, *Angew. Chem., Int. Ed. Engl.*, 2009, **48**, 3121-3123.
356. H. Zhai, A. Bunn and B. Wayland, *Chem. Commun.*, 2001, 1294-1295.
357. W. Cui, S. Li and B. B. Wayland, *J. Organomet. Chem.*, 2007, **692**, 3198-3206.
358. D. Mansuy, M. Lange, J.-C. Chottard, P. Guerin, P. Morliere, D. Brault and M. Rougee, *J. Chem. Soc., Chem. Comm.*, 1977, 648-649.
359. C. J. Ziegler and K. S. Suslick, *J. Am. Chem. Soc.*, 1996, **118**, 5306-5307.
360. Z. Gross, N. Galili and L. Simkhovich, *Tetrahedron Lett.*, 1999, **40**, 1571-1574.
361. E. Dux, *Chem. Rev. (Deddington, U. K.)*, 2009, **19**, 11-15.
362. J. C. Lewis, R. G. Bergman and J. A. Ellman, *Acc. Chem. Res.*, 2008, **41**, 1013-1025.
363. M. Minozzi, D. Nanni and P. Spagnolo, *Chem. Eur. J.*, 2009, **15**, 7830-7840.
364. W. G. Shou, J. Li, T. Guo, Z. Lin and G. Jia, *Organometallics*, 2009, **28**, 6847-6854.
365. B. J. Stokes, B. Jovanovic, H. J. Dong, K. J. Richert, R. D. Riell and T. G. Driver, *J. Org. Chem.*, 2009, **74**, 3225-3228.
366. M. Shen, E. Leslie Brooke and G. Driver Tom, *Angew. Chem., Int. Ed. Engl.*, 2008, **47**, 5056-5059.
367. B. J. Stokes, H. Dong, B. E. Leslie, A. L. Pumphrey and T. G. Driver, *J. Am. Chem. Soc.*, 2007, **129**, 7500-7501.
368. K. Sun, R. Sachwani, K. J. Richert and T. G. Driver, *Org. Lett.*, 2009, **11**, 3598-3601.
369. M. Shen and T. G. Driver, *Org. Lett.*, 2008, **10**, 3367-3370.
370. J. V. Ruppel, R. M. Kamble and X. P. Zhang, *Org. Lett.*, 2007, **9**, 4889-4892.
371. H. Lu, J. Tao, J. E. Jones, L. Wojtas and X. P. Zhang, *Org. Lett.*, 2010, **12**, 1248-1251.
372. H.-J. Lu, V. Subbarayan, J.-R. Tao and X. P. Zhang, *Organometallics*, 2010, **29**, 389-393.
373. J.-L. Liang, S.-X. Yuan, J.-S. Huang and C.-M. Che, *J. Org. Chem.*, 2004, **69**, 3610-3619.
374. R. F. Yoshimura, D. J. Hogenkamp, W. Y. Li, M. B. Tran, J. D. Belluzzi, E. R. Whittimore, F. M. Leslie and K. W. Gee, *J. Pharmacol. Exp. Ther.*, 2007, **323**, 907-915.
375. S. Minakata, *Acc. Chem. Res.*, 2009, **42**, 1172-1182.
376. S. Cenini, F. Ragaini, E. Gallo and A. Caselli, *Curr. Org. Chem.*, 2011, **15**, 1578-1592.
377. B. J. Stokes and T. G. Driver, *Eur. J. Org. Chem.*, 2011, **2011**, 4071-4088.
378. K. Sun, S. Liu, P. M. Bec and T. G. Driver, *Angew. Chem., Int. Ed. Engl.*, 2011, **50**, 1702-1706.
379. B. J. Stokes, S. Liu and T. G. Driver, *J. Am. Chem. Soc.*, 2011, **133**, 4702-4705.
380. H. Lu, H. Jiang, Y. Hu, L. Wojtas and X. P. Zhang, *Chem. Sci.*, 2011, **2**, 2361-2366.
381. H. Lu, H. Jiang, L. Wojtas and X. P. Zhang, *Angew. Chem., Int. Ed. Engl.*, 2010, **49**, 10192-10196.
382. M. A. Lynch, O. Duval, A. Sukhanova, J. Devy, S. P. MacKay, R. D. Waigh and I. Nabiev, *Bioorg. Med. Chem. Lett.*, 2001, **11**, 2643-2646.
383. R. T. McBurney, A. M. Z. Slawin, L. A. Smart, Y. Yu and J. C. Walton, *Chem. Commun.*, 2011, **47**, 7974-7976.
384. A. M. Linsenmeier, C. M. Williams and S. Brase, *J. Org. Chem.*, 2011, **76**, 9127-9132.
385. M. E. Buden, V. B. Dorn, M. Gamba, A. B. Pierini and R. A. Rossi, *J. Org. Chem.*, 2010, **75**, 2206-2218.
386. G. Smolinsky, *J. Am. Chem. Soc.*, 1961, **83**, 2489-2493.
387. G. Smolinsky, *J. Am. Chem. Soc.*, 1960, **82**, 4717-4719.
388. D. Intriери, A. Caselli, F. Ragaini, P. Macchi, N. Casati and E. Gallo, *Eur. J. Inorg. Chem.*, 2011, **2012**, 569-580.
389. D. Intriери, A. Caselli, F. Ragaini, S. Cenini and E. Gallo, *J. Porphyrins Phthalocyanines*, 2010, **14**, 732-740.
390. S. Fantauzzi, E. Gallo, A. Caselli, F. Ragaini, N. Casati, P. Macchi and S. Cenini, *Chem. Commun.*, 2009, 3952-3954.
391. S. Fantauzzi, A. Caselli and E. Gallo, *Dalton Trans.*, 2009, 5434-5443.
392. Q.-A. Chen, K. Gao, Y. Duan, Z.-S. Ye, L. Shi, Y. Yang and Y.-G. Zhou, *J. Am. Chem. Soc.*, 2012, **134**, 2442-2448.
393. R. Sanz, Y. Fernández, M. P. Castroviejo, A. Pérez and F. J. Fañanás, *Eur. J. Org. Chem.*, 2007, 62-69.



394. M. Ethirajan, Y. Chen, P. Joshi and R. K. Pandey, *Chem. Soc. Rev.*, 2011, **40**, 340-362.
395. C.-J. Liu, W.-Y. Yu, C.-M. Che and C.-H. Yeung, *J. Org. Chem.*, 1999, **64**, 7365-7374.
396. J. A. Smieja, K. Shirzad, M. Roy, K. Kittilstved and B. Twamley, *Inorg. Chim. Acta*, 2002, **335**, 141-146.
397. J.-L. Liang, J.-S. Huang, X.-Q. Yu, N. Zhu and C.-M. Che, *Chem. Eur. J.*, 2002, **8**, 1563-1572.
398. E. Gonzalez, P. J. Brothers and A. Ghosh, *J. Phys. Chem. B*, 2010, **114**, 15380-15388.
399. M. J. Zdilla and M. M. Abu-Omar, *Inorg. Chem.*, 2008, **47**, 10718-10722.
400. M. J. Zdilla, J. L. Dexheimer and M. M. Abu-Omar, *J. Am. Chem. Soc.*, 2007, **129**, 11505-11511.
401. V. Lyaskovskyy, A. I. O. Suarez, H. Lu, H. Jiang, X. P. Zhang and B. de Bruin, *J. Am. Chem. Soc.*, 2011, **133**, 12264-12273.
402. H. Stamm and H. Jaeckel, *J. Am. Chem. Soc.*, 1989, **111**, 6544-6550.
403. K. Nikki, H. Inakura, L. Wu, N. Suzuki and T. Endo, *J. Chem. Soc., Perkin Trans. 2*, 2001, 2370-2373.
404. D. Intriери, A. Caselli, F. Ragaini, P. Macchi, N. Casati and E. Gallo, *Eur. J. Inorg. Chem.*, 2012, 569-580.
405. P. Zardi, D. Intriери, A. Caselli and E. Gallo, *J. Organomet. Chem.*, 2012, **716**, 269-274.
406. A. K. Kumar, *Int. J. Pharm. Pharm. Sci.*, 2013, **5**, 467-472.
407. B. Castano, S. Guidone, E. Gallo, F. Ragaini, N. Casati, P. Macchi, M. Sisti and A. Caselli, *Dalton Trans.*, 2013, **42**, 2451-2462.
408. D. Intriери, M. Mariani, A. Caselli, F. Ragaini and E. Gallo, *Chem. Eur. J.*, 2012, **18**, 10487-10490.
409. J.-P. Djukic, D. A. Smith, V. G. Young, Jr. and L. K. Woo, *Organometallics*, 1994, **13**, 3020-3026.
410. L. K. Woo and D. A. Smith, *Organometallics*, 1992, **11**, 2344-2346.
411. M. P. Doyle, R. Duffy, M. Ratnikov and L. Zhou, *Chem. Rev.*, 2010, **110**, 704-724.
412. A. Klose, E. Solari, C. Floriani, N. Re, A. Chiesi-Villa and C. Rizzoli, *Chem. Commun.*, 1997, 2297-2298.
413. H. M. L. Davies and C. Venkataramani, *Org. Lett.*, 2003, **5**, 1403-1406.
414. N. Li, Z. Su, P. Coppens and J. Landrum, *J. Am. Chem. Soc.*, 1990, **112**, 7294-7298.
415. R. Guilard, B. Boisselier-Cocolios, A. Tabard, P. Cocolios, B. Simonet and K. M. Kadish, *Inorg. Chem.*, 1985, **24**, 2509-2520.
416. X.-W. Zou, L.-F. Zheng, L.-L. Wu, L.-L. Zong and Y.-X. Cheng, *Chinese Journal of Chemistry*, 2008, **26**, 373-378.
417. J.-L. Zhang, P. W. H. Chan and C.-M. Che, *Tetrahedron Lett.*, 2003, **44**, 8733-8737.
418. S. B. Z. Halime, B. Najjari, M. Lachkar, T. Roisnel and B. Boitrel, *J. Porphyrins Phthalocyanines*, 2010, **14**, 412-420.
419. H. M. L. Davies, T. Hansen and M. R. Churchill, *J. Am. Chem. Soc.*, 2000, **122**, 3063-3070.
420. M. L. Rosenberg, K. Vlasana, G. N. Sen, D. Wragg and M. Tilset, *J. Org. Chem.*, 2011, **76**, 2465-2470.
421. Y. Li, J.-S. Huang, Z.-Y. Zhou, C.-M. Che and X.-Z. You, *J. Am. Chem. Soc.*, 2002, **124**, 13185-13193.
422. I. Artaud, N. Gregoire, P. Leduc and D. Mansuy, *J. Am. Chem. Soc.*, 1990, **112**, 6899-6905.
423. Y. Li, J.-S. Huang, G.-B. Xu, N. Zhu, Z.-Y. Zhou, C.-M. Che and K.-Y. Wong, *Chem. Eur. J.*, 2004, **10**, 3486-3502.
424. Y. Q. Pei Tang, *Synthesis*, 2012, **44**, 2969-2984.
425. S. Zhu, X. Cui and X. P. Zhang, *Eur. J. Inorg. Chem.*, 2012, **2012**, 430-434.
426. M. P. Doyle, *Angew. Chem., Int. Ed. Engl.*, 2009, **48**, 850-852.
427. D. A. Smith, D. N. Reynolds and L. K. Woo, *J. Am. Chem. Soc.*, 1993, **115**, 2511-2513.
428. W. A. Donaldson, *Tetrahedron*, 2001, **57**, 8589-8627.
429. R. G. Salomon and J. K. Kochi, *J. Amer. Chem. Soc.*, 1973, **95**, 3300-3310.
430. 0.143 mL of a Fe<sub>2</sub> toluene solution (3.81x10<sup>-3</sup> mol/L) was added to 2.0 mL of a toluene solution containing α-methylstyrene/EDA= 1000:1100. The reaction was run at RT for 5 minutes. Then the NMR analysis revealed 85% yield, trans/cis ratio = 98:2 and a ee (trans isomer) = 70%
431. A. D. Becke, *J. Chem. Phys.*, 1993, **98**, 5648-5652.
432. V. Barone and M. Cossi, *J. Phys. Chem. A*, 1998, **102**, 1995-2001.
433. M. Cossi, N. Rega, G. Scalmani and V. Barone, *J. Comput. Chem.*, 2003, **24**, 669-681.
434. M. Dolg, H. Stoll, H. Preuss and R. M. Pitzer, *J. Phys. Chem.*, 1993, **97**, 5852-5859.
435. C. Mealli and D. M. Proserpio, *J. Chem. Educ.*, 1990, **67**, 399.
436. T. Imamoto, N. Iwadata and K. Yoshida, *Org. Lett.*, 2006, **8**, 2289-2292.
437. F. Ragaini, S. Cenini, F. Turra and A. Caselli, *Tetrahedron*, 2004, **60**, 4989-4994.
438. Y.-C. Hsu, K.-H. Gan and S.-C. Yang, *Chem. Pharm. Bull.*, 2005, **53**, 1266-1269.
439. O. Lober, M. Kawatsura and J. F. Hartwig, *J. Am. Chem. Soc.*, 2001, **123**, 4366-4367.